The Adiabatic Theory of the Linear Hose Instability of a Relativistic Electron Beam Propagating in Resistive Plasma

K.J. O'Brien

September 1985

UWFDM-650

Ph.D. thesis.

FUSION TECHNOLOGY INSTITUTE

UNIVERSITY OF WISCONSIN

MADISON WISCONSIN

The Adiabatic Theory of the Linear Hose Instability of a Relativistic Electron Beam Propagating in Resistive Plasma

K.J. O'Brien

Fusion Technology Institute
University of Wisconsin
1500 Engineering Drive
Madison, WI 53706

http://fti.neep.wisc.edu

September 1985

UWFDM-650

Ph.D. thesis.

THE ADIABATIC THEORY OF THE LINEAR HOSE INSTABILITY OF A RELATIVISTIC ELECTRON BEAM PROPAGATING IN RESISTIVE PLASMA

by

KEVIN JOSEPH O'BRIEN

A thesis submitted in partial fulfillment of the
requirements for the degree of

Doctor of Philosophy
(Nuclear Engineering)

at the
University of Wisconsin-Madison
1985

THE ADIABATIC THEORY OF THE LINEAR HOSE INSTABILITY OF A RELATIVISTIC ELECTRON BEAM PROPAGATING IN RESISTIVE PLASMA

Kevin Joseph O'Brien

Under the supervision of Professor Gregory Allen Moses

In this thesis we demonstrate that the cold Vlasov beam, the circle-limit of the warm Vlasov beam, the spread-mass model, and the energy-group model of a relativistic electron beam undergoing linear hose instability, are all formally equivalent. Therefore, the circle-orbit beam is the natural starting point for a higher order theory. Introducing the next order in non-circularity we make contact with the adiabatic theory for warm beams. The adiabatic theory is founded upon the existence of transverse action invariants which remain sufficiently well-defined, despite the nonaxisymmetric potential and the coupling resonances driven by linear hose instability. The existence of action invariants enables the elimination of a fast variable, analogous to gyro-motion, called vortex-gyration. One problem with adiabatic beam theory is that coupling resonances between the degrees of freedom could destroy the adiabatic invariants upon which the theory rests. In this thesis we employ KAM theory to study the destruction of action invariants

due to linear hose instability. We define nonaxisymmetric adiabatic beams to be those for which KAM tori exist in the transverse phase space. For hose deflections of the magnitude considered in linear theory we find that KAM tori persist, preventing the destruction of the invariants.

Approved:

Professor Gregory Allen Moses
Nuclear Engineering

ACKNOWLEDGEMENTS

There are a number of people who have contributed in their own way to the work presented in this thesis. I dedicate this thesis to both of my parents, James and Katie O'Brien; thank you for your continued faith in my abilities and your constant support of my decision to continue my education.

I wish to thank my thesis advisor, Professor Gregory A. Moses, for providing the technical guidance which has shaped my career and research interests. Thanks are also due to Professor James D. Callen for his constant interest in my research and his interest in the theoretical ideas which have been applied in this thesis. Particularly, I wish to thank him for his implicit moral support at a crucial time in my graduate career.

My colleagues, fellow graduate students, have also had, during the long course of our daily interactions, a beneficial effect upon my personal development as well as my technical development. I wish to thank Dennis Croessmann for sharing with me various of his insights into the problem of doing engineering research. Also, I would like to express my affection and admiration for Joseph Johnson, Bruce Glasgow, Douglass Henderson, Jack Watrous, Micheal Wehner, and Mark Carter.

Finally, I wish to thank Dennis Bruggink for his good humored interest in, and tolerance of, the graduate students domiciled on the third floor of the Engineering Research Building.

Contents

List of Figures

List of Tables

Chapter 1

Introduction

In recent years there has been a great deal of theoretical, numerical , and experimental work aimed at understanding, simulating, and preventing, respectively, the resistive hose instability of relativistic, high-current self-pinched electron beams propagating in resistive plasma.

Interest in the hose instability is concomitant with an ever widening appreciation that ultra-high-current relativistic electron beams have many exciting applications, from food preservation, to controlled nuclear fusion, to national defense, naming only a few for the moment. Ultra-high-current relativistic electron beams are generated in linear induction accelerators and in cyclic induction accelerators [1.1]. Many applications of these electron beams involve stable propagation through ambient gas subsequent to exiting the accelerator. The resistive hose instability is often the major impediment to such stable propagation. A beam is also subject to a related instability, called the beam breakup instability,

even before it leaves the accelerator [1.2].

Applications of ultra-high-current ($\sim 10-100$ kAmp) relativistic ($\gamma \sim 10-100$) electron beams are diverse [1]. Such beams will provide a means of collectively accelerating heavy ions for inertial confinement fusion [1.3]. In a magnetic confinement fusion device, plasma may be heated directly by a beam or indirectly through the generation of intense microwave radiation. Electron beams can produce intense x-ray pulses of short duration. These pulses may be used in flash radiography to provide short-time-resolution x-ray photographs of materials which are changing on a short time scale. In the area of radiation simulation, relativistic electron beams may be applied to the study of electro-magnetic pulses and their effects upon materials. Free electron lasers may be driven by ultra-high-current relativistic electron beams. These lasers in turn have many applications which include : isotope separation, controlled thermonuclear fusion, material processing, communications, and national defense. Concerning the latter, electron beam physics comprises an important component of directed energy technology.

[1] cf., Table 1.

Applications of Electron Beams

Application	Energy (MEV)	Peak Power (MW)	Average Power (MW)	Pulse Duration (NSEC)	Rep-Rate
Environmental					
Sludge disinfection	1-5	-	0.1-0.5	cw	cw
Waste-water disinfection	10	-	2-10	cw	cw
Drinking-water purification	10	-	2-10	cw	cw
Cellulose degradation	-	-	2-10	cw	cw
Flue-gas cleanup	0.5-2	-	3-30	cw	cw
Radiative Processing					
Food preservation	5-10	-	0.1-0.5	cw	cw
Polymerization	0.3-3.0	-	1-10	cw	cw
Radiation Sources					
Synchrotron	700-3000	-	10^4	-	-
Free-electron lasers	1-1000	-	-	-	-
Diagnostics					
Radiography	20	10^6	-	30-100	-
Defense					
Nuclear-effects simulation	0.1-15	10^4-10^7	-	30-100	1/hr
Directed-energy technology	10^3	-	-	-	-

Table 1.1: Some of the many applications of ultra-high- current relativistic electron beams [1.1].

Ultra-High-Electron-Current Induction Accelerators

Device	Laboratory	Energy (MeV)	Current (kAmp)	Duration (nsec)	Rep-Rate (Hz)
Astron Type					
Astron	LLNL(US)(1963)*	4	0.2	300	60
Astron	LLNL(US)(1968)	6	0.8	300	5
FXR	LLNL(US)(1982)	20	4	75	0.1
ERA	Berkeley(US)(1971)	4	0.9	2-45	0.2
NEP-2	Dubna(USSR)(1971)	30	0.25	500	50
NBS	NRL(US)(1973)	0.8	1.0	2000	S.P.
ATA	LLNL(US)(1984)	50	10	50	1-10
Radlac Type					
LIU-10	(USSR)(1977)	13.5	50	20 or 40	?
Radlac-1	Sandia/AFWL(US)(1980)	9	25	12	S.P.
MABE	Sandia(US)(1983)	8	80	40	S.P.
Auto-Accelerators					
Auto-Accelerator	(USSR)(1974)	1.0	5-15	?	S.P.
Auto-Accelerator	NRL(US)(1962)	7.3	70	10	S.P.
Cyclic Type					
Betatron	(USSR)(1964)	100	0.1	†	S.P.
Modified Betatron	Irvine(US)(1983)	(10)‡	(1)	†	S.P.
Modified Plasma Betatron	Cornell(US)(1984)	3	2	†	S.P.
Modified Betatron	NRL(US)(1985)	(50)	(5-10)	†	S.P.

* Year machine was completed
? Parameter not known
† Depends upon extraction scheme
‡ Parenthesis indicate design value
S.P. Single-Pulse

Table 1.2: Important parameters of some ultra-high-electron- current induction accelerators[1.1].

1.1 Resistive Hose Instability

Upon exiting the accelerator, many applications of high-current relativistic electron beams involve subsequent propagation of the beam through an ambient gas. Such transport must be efficient and reliable. Both efficiency and reliability depend upon maintaining stability of the beam. However, such beams are known to be subject to a wide array of destructive instabilities, the importance of any one depending upon the particular circumstances. Generally, beam instabilities divide into two classes: microinstabilities driven by nonequilibrium momentum distributions, and macroinstabilites driven by nonequilibrium spatial distributions. In this thesis we shall be interested only in the latter class of macroinstabilites, otherwise known as fluid instabilities.

It is generally believed that the $m = 1$ "dipole moment" is the most deleterious of the lowest few (m=0 sausage, m=1 hose, and $m \geq 2$ filamentation) macroscopic multipole modes. Hose instability results in beam destruction through gross sideways deflection of the beam current and need not involve appreciable internal deformation of the beam. In contrast to sausage and filamentation, a hosing beam may displace laterally more or less rigidly.

Three distinct types of hose instability may be distinguished. In each the background plasma plays an important role. First, in absence of any monopole plasma return current, a fixed plasma channel acts kinematically by determining the important monopole and dipole decay time scales associated with free decay of monopole or dipole excitations. If the beam current is displaced the magnetic field axis may only follow diffusively, on the dipole decay time scale. Instability

is due to the phase difference between the lateral displacements of the beam and field axes. Second, in presence of monopole plasma return current, a more dangerous "self-hose" mechanism comes into play. The plasma now participates dynamically as well as kinematically since it supports an axial monopole current of its own. Lateral offset of these currents with respect to one another results in absolute instability due to magnetic repulsion. Third, due to creation of the plasma channel by the beam, the plasma channel may tend to follow a slow beam displacement at fixed z ; this is a coupled beam-channel mode.

Ideally, as the beam exits the accelerator port, beam current should be carried entirely in the monopole equilibrium $J_{bo}(r)$, independent of θ, z, t, where (r, θ) are coordinates transverse to the axial flow along z , and t is the time. Expressing the beam current in terms of multipole moments

$$J_b(r, \theta, z, t) = \sum_{m=0}^{\infty} J_{bm}(r, z, t) e^{im\theta} \tag{1.1}$$

the objective of any propagation experiment is to create the beam in the monopole equilibrium and prevent any unstable excitation of the $m \geq 0$ states. Through the self-consistent field and source equations the multipole moments are coupled together. These equations are nonlinear, due to the beam-current- dependent generation of plasma conductivity σ , and the plasma Ohm's law $J_p = \sigma E$. An emittance mismatch between the accelerator and the gas into which the beam is injected may trigger an $m = 0$ sausage mode. Even if this mode damps, the nonlinearity allows it to set off the $m = 1$ moment which may in turn trigger the $m = 2$ and so forth. If these nonaxisymmetric excitations are unstable they destroy the beam by feeding upon free kinetic energy in the $m = 0$ axial flow.

Experimentally, one considers a relativistic electron beam injected at $z = 0$ into a tank $z > 0$ containing gas or plasma [2]. Assuming a well formed axisymmetric equilibrium within the accelerator, a natural situation to consider is that of deflection, either intentionally for experimental purposes, or unintentionally due to stray fields, emittance mismatch, or geometrical irregularities, of the beam as it passes $z = 0$. This lateral deflection or modulation of the beam occurs with phase $k\beta c - \omega t$ in the accelerator reference frame, where ω is the frequency and k is the axial wave-number of the disturbance, $\beta = v_z/c$ is the "fluid- beta" of the beam, and c is the speed of light in vacuo. It is customary, and useful, to employ "beam variables" (z, ς) where $\varsigma = \beta ct - z$ is the "slice-variable", in place of (z, t). For ultra-relativistic beams the slice variable, which describes the position of a particle with respect to the head of the beam, is a single particle constant of motion. Physically, axial acceleration of an ultra-relativistic beam particle involves the effective mass [3] $\gamma^3 m \gg m$, where m is the particle rest mass and $\gamma^{-2} = 1 - \beta^2$.

Transforming the phase, by elimination of t, results in $k\beta c - \omega t \longrightarrow -\Omega z/\beta c - \omega\varsigma/\beta c$, the "Doppler- shifted" phase. Here $\Omega = \omega - k\beta c$ is the "Doppler-shifted" hose frequency, the frequency experienced by a moving segment, as viewed in the accelerator rest frame. Since Ω describes the z response of a slice at fixed ς it scales with the characteristic single particle frequency Ω_β of transverse betatron oscillation of the particles within the particular ς disk. The frequency ω describes

[2] cf. Fig. 1.1

[3] This point is made explicit in Chapter 3

the axial structure of the hose pattern within the beam frame. Since ω describes how the disturbance changes from slice to slice, at fixed z , it scales with the characteristic dipole decay time τ_1 governing the dipole fields which couple each slice to its neighbors. Therefore, the dispersion relation is couched mainly in terms of dimensionless "frequencies" Ω/Ω_β and $\omega\tau_1$; however, monopole plasma current brings in explicit ω dependence as well.

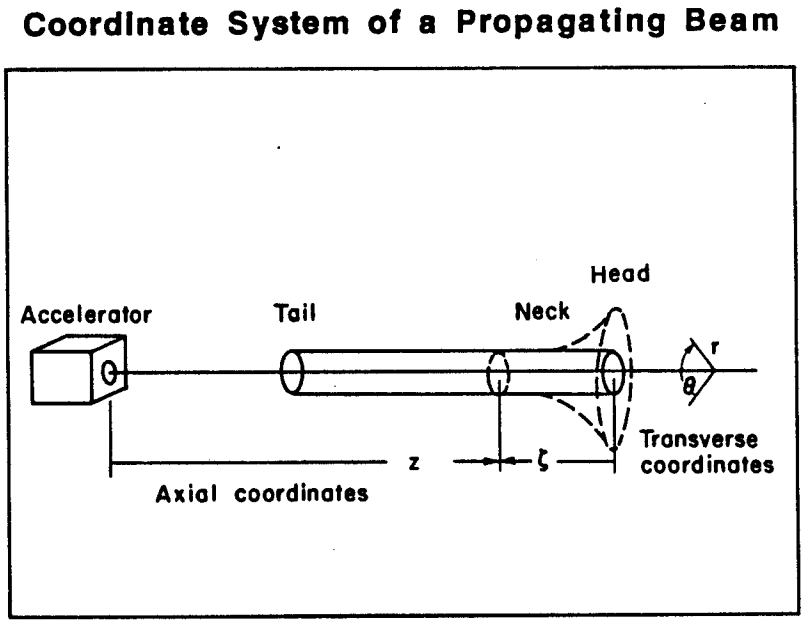

Figure 1.1: Basic geometry of a typical beam experiment. Note conventional definition of the beam variables z and ς . Also shown are the physically important distinctions between various regions of the beam.

1.2 Previous Theories of Hose Instability

Various models of linear hose instability of a relativistic electron beam have been developed since the original (unpublished) ground breaking work of C.Longmire in the 1950's. The first published work (1960) was Rosenbluth's "nonrigid" treatment of the low frequency $\Omega/\Omega_{\beta o} \ll 1$ limit. Rosenbluth started with the relativistic Vlasov equation and ultimately considered the fluid moments thereof to arrive at a mode which was essentially a rigid lateral displacement on a hydrodynamic time scale [1.4]. Following this was a period of unpublished work [4] which centered around the important "rigid-beam" model of Lewis. When extended to higher driver frequencies the rigid-beam model does not yield a high-frequency cutoff and exhibits an infinite resonance. A rigid-beam model (1964), valid only in the low-frequency limit, was developed by Weinberg for a modulated or "chopped" beam. The motivation being to allow any convective instability to convect out the tailend of the short pulse before growing to appreciable amplitude [1.5] . Following this Weinberg developed a "nonrigid-beam" model (1967), valid for all driver frequencies but utilizing idealized circular transverse orbits (as opposed to precessing ellipses) [1.6]. This theory was developed for general rounded profiles and all values of m. Calculated growth rates did not include phase mixing effects since for these calculations specialization to a harmonic pinch potential was employed.

[4] We refer to work of M.Rosenbluth, N.Christofilos, H.W.Lewis, K.Brueckner, G.Ascoli, H.Chang, S.Yadavalli, H.Singhaus, A.Sessler and R.Briggs. We do not have access to all of this work but surmise its existence from references in the literature.

It has often been stated that a cold beam, that is, a beam with circular transverse orbits [5] , will not yield phase mix damping. One purpose of the present work is to demonstrate that circle orbits do yield phase mix damping in beams with anharmonic pinch potentials. The lack of phase mixing in the growth rates calculated in [1.6] had nothing to do with the use of circle orbits.

Anharmonic phase mixing effects significantly influence the evolution of non-axisymmetric beam phenomena such as hose deflections. Mixing arises due to radially dependent betatron frequencies of transverse particle orbits in the pinch potential well. The pinch potential is defined as $\psi = \beta A_z - \phi$ where A_z is the axial component of the vector potential and ϕ is the scalar potential. The pinch potential completely describes transverse dynamics, in absence of collisional effects. In terms of ψ the betatron frequency is

$$\Omega_\beta^2(r) = \frac{q}{\gamma m}\left(-\frac{1}{r}\frac{d\psi}{dr}\right) . \tag{1.2}$$

Imagining the beam to be composed of a sequence of slices, labeled by ς, as the hose disturbance develops, a given slice experiences a shaking back and forth. Because of the spread in betatron frequency each slice responds as if it were a collection of oscillators, each of different frequency, coupled to the perturbation. We propose to call models which explicitly treat each disk as a collection of oscillators "multiple-oscillator" models. Multiple-oscillator models include the "spread-mass" [1.7], the "energy-group" [1.8], and the "multi-component" models [1.9].

[5] As far as we are aware H.Lewis first employed the idealization of circular helices in a treatment of the $m = 0$ sausage instability.

The first multiple-oscillator model, the "spread-mass" model [1.4] (1978), exploited the known damping and convection due to relativistic mass spread, by introducing an artificial mass spread. A distribution of particle masses, chosen to recover the correct low and high-frequency results of perturbative kinetic theory for the Bennett [1.10] beam, are introduced to yield finite resonance and cutoff. In the spread-mass model each slice is resolved into a superposition of disks. Each disk is defined by the particular mass of the individual particles in it. The partial current profile associated with each disk is that of the equilibrium beam. Each disk undergoes rigid harmonic oscillations in response to the linearized $J \times B$ force, averaged over the radial profile of the disk. Phase mixing arises due to the differing shaking frequencies of each oscillator. The spread-mass model agrees well with the rigid-beam model for low-frequencies and yields a cutoff frequency. Since each disk has the same radial structure the spread-mass model does not include any radial localization of the response. Physically, one expects that particles for which $\Omega \sim \bar{\Omega}_\beta$, where $\bar{\Omega}_\beta$ denotes the orbit average betatron frequency, should couple maximally to the perturbation.

Subsequently the "energy-group" model (1980) was developed [1.8]. In the energy-group model the slice is resolved into disks each of which is comprized of particles having a particular range of transverse energy. Each energy group has a partial profile which is flat out to an energy dependent radius beyond which it vanishes. The energy- group model purports [6] to incorporate radial structure

[6] We prove in Chapter 8 that the energy-group model is in fact perfectly equivalent to the spread-mass model, and also to the circle-orbit Vlasov theory, therefore the claim that radial

but does not have the proper analytical properties revealed in an Ampère-Vlasov treatment [1.6].

Formal solution of the linearized Ampère and Vlasov equations results in an integro-differential equation for the vector potential. Analysis of the analytical properties of the perturbed current indicates a radially localized resonance which gives a logarithmic singularity.

Recognizing the clues provided by the formal Vlasov result the "multi- component" model [1.9] was developed (1982). In the multi-component model each slice is resolved into disks according to the azimuthal frequency of the particles. Each component is localized within a frequency dependent radius. Selection of the radial profile of the disks is effected by requiring the correct logarithmic singularity and results in parabolic profiles. This model has the powerful advantage of successfully duplicating the important analytical properties deduced from the, formal, linearized Ampère-Vlasov theory [7].

effects are treated more carefully than in the spread-mass model is illusory.

[7]The Vlasov theory is not, however, the final word either. In Vlasov calculations the evolution operator is inverted upon the unperturbed orbits; therefore, any effects due to orbit perturbations are lost. A superior method of calculation consists in computing the first-order orbit perturbations and building the perturbed current as an integral over all initial positions that "launch" particles which arrive at a given time, at a given space point, on the *perturbed* orbits. We use this method for the circle-orbit equilibrium beam in Chapter 7.

1.3 Adiabatic Theory

In this thesis we demonstrate that the cold Vlasov beam, the circle-limit of the warm Vlasov beam, the spread-mass, and the energy-group models are all formally equivalent (they differ only in the underlying physical interpretation as to the meaning of the calculation, the final results are all the same) therefore, logically, the circle-orbit beam, or, as we shall say, the "circular-helix beam" is the natural starting point for the development of a "higher-order" theory.

Introducing the next order, in non-circularity, we make contact with the "adiabatic" theory for warm beams [1.13,1.14]. Adiabatic beam theory provides the framework within which a drift-kinetic treatment of charged particle beams is constructed. The drift-kinetic equation is used to compute the reduced single particle distribution function from which the pressure tensor is computed by moments. This pressure tensor is used to close the exact fluid continuity and momentum equations [8].

The adiabatic theory is founded upon the fact that there exist transverse action invariants which remain sufficiently well defined despite the nonaxisymmetric potential and the coupling resonances driven by the linear hose instability. The existence of action invariants enables the elimination of a fast variable, analogous to gyro-motion, here called "vortex gyration", and the reduced description of the particle orbit as a circular orbit [9], here called "circular-drift". Particle orbits in a

[8] This procedure follows long traditions in fluid dynamics in that the appropriate physical approximations are incorporated in the closure relations.

[9] For a radially expanding beam the drift is in reality a "spiraling-helix".

general charged particle beam resemble precessing ellipses in the transverse (r, θ) plane. The basic idea is to resolve the ellipse into a circle and an epicycle, then the epicyclic vortex gyration is averaged out of the problem [10].

One major problem with an adiabatic, drift-kinetic treatment, however, is the fact that resonances between the different degrees of freedom may destroy the adiabatic invariants upon which the theoretical foundation rests. In this thesis we employ methods of Hamiltonian mechanics (KAM theory) to study the resonance properties of the beam orbits and to investigate the validity of the drift-kinetic theory.

Transverse dynamics in an axisymmetric equilibrium constitutes an integrable nonlinear Hamiltonian system. This thesis is concerned however with $m = 1$ non-axisymmetric phenomena. We *define* nonaxisymmetric adiabatic charged particle beams to be those for which KAM tori exist in the transverse phase space. The drift-kinetic treatment is justified in situations for which the KAM structure is well enough preserved. We have investigated stochastic effects of linear hose perturbations upon the transverse dynamics. Utilizing section maps we have studied the transverse orbit structure due to coupling resonances, between harmonics of circular drift and vortex gyration, driven by linear hose perturbations.

The Hamiltonian of a particle in a beam undergoing a linear hose instability is

$$H = H_{\perp} + \delta H \tag{1.3}$$

[10] This procedure is essentially a small gyro-radius expansion where the vortex gyration radius plays the role of gyro-radius.

where the unperturbed Hamiltonian for a Bennett beam is

$$H_\perp = \frac{1}{2m}\left(p_r^2 + \frac{P_\theta^2}{\rho^2 a^2}\right) + 2T\log(1+\rho^2) \tag{1.4}$$

with $T = q\beta I_b(1 - 1/\beta^2(1+f_c)/(1+f_m))/2c$ the Bennett temperature, a the Bennett radius, and $\rho = r/a$ the dimensionless radial position of a particle in the beam. The hose perturbation δH is given in detail in Chapter 9.

Expanding $H_\perp$ about a reference circle orbit to lowest order yields a system of harmonic oscillators

$$H_\perp = \Omega_\theta J_\theta + \epsilon^2 \Omega_r J_r + \cdots \tag{1.5}$$

where J_θ is the action of the circular drift, J_r is the action of the vortex-gyration, Ω_θ is the circular-drift frequency, and Ω_r is the vortex-gyration frequency. The system is inherently nonlinear so we expand to higher order to expose the lowest order nonlinearity. Expanding to fourth order in the small parameter $\epsilon \equiv \delta\rho/\rho_o$ we get the transverse Hamiltonian

$$H_\perp = \Omega_\theta J_\theta + \epsilon^2 \Omega_r J_r + \epsilon^3 \Omega_3 J_r^{\frac{3}{2}} sin^3\xi + \epsilon^4 \Omega_4 J_r^2 sin^4\xi + \cdots \tag{1.6}$$

for a particle on a near-circle orbit at reference radius ρ_o . We employ Deprit's [1.15] version of canonical Lie transform perturbation theory to get the action-angle variables and Hamiltonian to the requisite order in ϵ . The azimuthal contribution is already in its exact action-angle variables. Performing the Lie transform calculation [1.16] we get the "near-circle" Hamiltonian

$$H_\perp = \Omega_\theta \hat{J}_\theta + \epsilon^2 \Omega_r \hat{J}_r + \epsilon^4 \Omega_2 \hat{J}_r^2 + \cdots . \tag{1.7}$$

Particles on orbits of high eccentricity, small angular momentum J_θ, are not realistically included in this theory. In a well mixed beam however the fraction of particles on such orbits is negligible. One should also note that the theory here is order ϵ^4 so particles on orbits of substantial "gyro-radius" are consistently included so that really only a small class of particles is left out.

The introduction of a nonaxisymmetric potential δH due to a linear hose instability couples the two oscillators nonlinearly. The result of this interaction is coupling resonance between the vortex gyration and the circular drift. The anisotropy engendered by the lateral hose deflection can result in transfer of energy between these two degrees of freedom thereby destroying the action invariants. In our investigation of this phenomenon we have discovered that for lateral deflections of the order typically considered in the context of linear instability [11], that is $\delta y/a \sim 10^{-6} - 10^{-4}$, well preserved KAM tori prevent excessive modification of the invariants. Even though the transverse orbits undergo stochastisation, due to resonance overlap, the vortex gyration invariant is bounded by KAM tori. This means that radial diffusion, due to energy transfer between the two degrees of freedom, is bounded as well, therefore, particles remain within a well-defined ring even in the nonintegrable situation of linear hose instability. We view this as justification for the adiabatic model in the linear regime.

[11] Lateral displacement amplitudes for beam breakup instability, for example, are typically $\delta y/a \sim 10^{-4}$ (beam breakup instability is essentially hose instability of a beam inside the accelerator). Beam breakup is trigged by beam coupling to dipole cavity modes [1.2].

1.4 Synopsis of Thesis and Original Contributions

This thesis deals with a constellation of problems centered upon the basic question of whether or not a reduced "fluid-kinetic" model of electron beam propagation can be used to study nonaxisymmetric instabilities such as the linear hose instability. Our main results are concerned with the modification of transverse action invariants, due to the coupling resonances driven by the nonaxisymmetric pinch potential of a hosing beam. In the course of this investigation we have also developed formalism, and have clarified essential points of previous theory. Not a small part of our work has been in the nature of logical organization of the development and presentation of the subject, and in the refinement and illumination of the interrelations between various different approaches to the subject.

In Chapter 2 the basic physical concepts underlying electron beam theory are presented. The basic scaling parameters: charge neutralization time, monopole decay time, dipole decay time, and charge and current neutralization factors, are discussed. We point out the fact that an ultra-relativistic electron beam has a magnetic Reynold's number $S \sim 10^{-2}$, which is to be contrasted with a typical magnetic Reynold's number in a magnetic fusion plasma, a tokamak for example has $S \sim 10^{6}$.

In Chapter 3 we discuss relativistic beam equilibria. In Section 3.2, starting with the Boltzmann H-theorem, we derive the single-particle phase-space momentum distribution for a spatially uniform beam. We discover the important fact that the effective mass for axial dynamics is $\sim \gamma^3 m$. Therefore, for paraxial ultra-relativistic electron beams, the axial degree of freedom is effectively cold. In

Section 3.3, using the relativistically covariant Maxwell-Boltzmann distribution, we derive the single-particle phase-space distribution in terms of the covariant pinch-potential. Using a relativistically covariant formulation of the Maxwell-Boltzmann distribution, combined with the inhomogeneous Maxwell equation, we carefully reduce the problem of specifying the equilibrium of two superimposed particle streams, by means of an ansatz concerning the pinch-potentials of the streams, to the classical Poisson-Boltzmann equation. We determine the conditions under which a beam is in a pure-pinch. In Section 3.4 we carefully derive the class of Bennett equilibria which are self-similar solutions of the Poisson-Boltzmann equation. Having gotten the pinch-potential we compute the important properties of the classical Bennett equilibrium. Using the virial of Clausius we calculate the Bennett temperature. Also, in Section 3.5 we derive the paraxial Hamiltonian for an electron in a beam and introduce the concept of near-circularity of the transverse betatron motion. We show that for near-circle particles in a Bennett equilibrium the transverse motion resolves into circular-drift and vortex-oscillation. A graphical result shows that the frequency of the vortex-oscillation is greater than the circular-drift (betatron) frequency. This is our first contact with the important fact that the circle-orbits are crucial to the theory; the fast vortex-gyration may be averaged out of the problem.

In Chapter 4 we present, primarily in the interest of completeness and to foster a correct perspective, a brief discussion of the subtle issue of beam driven generation of free electrons in the ambient gas through which it propagates. Many, perhaps not dominant, interesting effects are *known* to be associated with con-

ductivity generation. For example, in low density gas, the head of the beam may not be charge neutralized quickly enough to short out the radial electric field. Beam generated free electrons therefore accelerate radially under the influence of large E_r; the Lorentz force $qv_r \times B_\theta$ due to the magnetic field B_θ accelerates the free electrons axially. The result is that in the head of a beam propagating in low density gas the *net current* may actually *exceed* the beam current. We argue in Chapter 4 that the dominant conductivity generating effect in the body of a beam propagating in atmospheric air is direct beam-driven collisional ionization.

In Chapter 5 we present a careful, and original, derivation of the EMPULSE field equations describing the electromagnetic fields of an ultra-relativistic, paraxial electron beam propagating in resistive plasma. We point out the fact that all hose models differ primarily only in the recipe for computing the perturbed beam current J_{b1} . We also derive the field equation for a charge neutral beam with self-consistent conductivity generation by impact ionization, and for a charge neutral beam with conductivity generation neglected, the "pure-pinch" field equation.

In Chapter 6 we present an original, and complete, account of the important rigid-beam theory. Rigid-beam theory is less a single, coherent formalism, than it is a loose collection of ideas and concepts. Rigid-beam theory originated in the work of pioneers in the field of electron beam propagation, and in work on the hose instability in particular. We have tried to develop the whole theory logically, from first principles, and with only the important ideas emphasised. In Section 6.2 we derive the "hose equation" and dispersion relation for the continuous rigid beam, and compare the predictions of theory with old (available) data from the

Astron accelerator. We point out the failure of the rigid beam theory to produce a high-frequency cutoff and the importance of phase mixing effects in this regard. We extend the continuous rigid beam theory to the case of a beam propagating in a powerful B_z guide-field. Stabilization of lateral beam displacements is possible with the guide-field. We treat only the case of circular polarization of the beam displacement. In Section 6.4 we introduce the key idea of beam chopping. Chopping a beam into short segments is one natural way to limit destructiveness of the convective hose instability. In Section 6.5 we present an original, and general, Green function treatment of the chopped rigid beam hose equations which brings to the forefront the overall structure of the theory of chopped rigid beams. One result of this work is the realization that, for thin beams in particular, simple monopole and dipole decay lengths may not be sufficient to describe the decay of the fields.

In Chapter 7 we investigate Vlasov or "nonrigid" treatments of linear hose instability. In Section 7.2 a general warm-Vlasov theory is presented for the case of a beam whose transverse orbits are precessing ellipses. The circle-orbit limit of the final result is also calculated. A beam with circular transverse orbits is a cold beam. Utilizing the result of the circle-orbit limit, we employ a variational principle to estimate the growth rate and compute an approximate dispersion relation. We prove in subsequent work that this result, the circle-limit of the warm Vlasov theory, is identical to the cold Vlasov theory, the energy-group model, and the spread-mass model. In Section 7.3 we compute the perturbed current J_{b1} *including* orbit perturbations (which are absent in a Vlasov calculation).

The resulting current perturbation differs substantially from the circle-limit of the warm Vlasov beam. We suggest that the rigorous method of computing the perturbed current for the warm beam with precessing elliptical transverse orbits is to carry out a similar calculation including orbit perturbations. Such a calculation will be very involved technically however. In Section 7.4 we specialize to a radially uniform beam, in order to bring more emphasis to the boundary conditions, and study a cold beam propagating in a plasma channel surrounded by cold gas, and in a plasma surrounded by a steel tank. Again, we use a general Green function approach. One interesting result which we obtain involves stabilization of hose instability by the image currents in the steel tank wall.

In Chapter 8 we study, what we propose calling, "multiple-oscillator" models of hose instability. In Section 8.1 we introduce the basic physical and mathematical ideas. In Section 8.2 we look at the spread-mass model. In Section 8.2 we develop the general multiple-oscillator equations and specialize to the energy-group model. In Section 8.3 we specialize the general multiple-oscillator equations to the multicomponent model. Our treatment makes it clear that it is *only* the choice of oscillator component radial profile which distinguishes the energy-group from the multicomponent model. We clarify and deepen the understanding of the relationship between these two models.

In Chapter 9 we shift gears and discuss fluid, and fluid-kinetic models. In Section 9.1 we introduce the motivation for developing reduced descriptions. In Section 9.2 we present an original, careful, and complete formalism for an ultra-relativistic *fluid* electron beam. We start with the coupled, *covariant* Maxwell

and Vlasov equations, in four-vector notation, and derive the resulting fluid hierarchy by computing moments of the Vlasov equation. Discarding a third order cumulant we close the cumulant hierarchy. We discuss an apparent discrepancy between the number of unknowns and the number of equations in terms of gauge-fixing. We methodically introduce a series of four *natural* approximations which build into the hierarchy a "beamlike" character. Finally, we arrive at a tractable set of 8 fluid plus EMPULSE equations. We argue that, albeit useful, a fully fluid approach does not build into the theory enough of the important kinetic features of a *beam* . In particular, phase-mix damping is not included *a priori* . In Section 9.3 we come to the point and derive an adiabatic, or drift-kinetic, or fluid-kinetic hybrid, theory. We reduce the transverse dynamics to that of a spiral and a vortex oscillation. We average out the oscillation to arrive at a picture of the beam as a superposition of two counter rotating fluids. This treatment is formulated in terms of action-angle variables. We compare the conditions for the beam to be isothermal and find they differ from the predictions of Section 9.2. This point constitutes a definite disagreement between the fluid and the adiabatic theories. In Section 9.4 we investigate the modification of the transverse invariants, upon which the adiabatic theory is founded. We render the equilibrium Hamiltonian in action-angle variables, using the method of Lie transforms, and compute the perturbation due to the hose instability. We consider a low-frequency hose instability. After computing the perturbed Hamiltonian, which involves a double Fourier series of terms coupling the circular and the vortex ocsillations, we use Poincaré section mappings to graphically study the coupling resonances. Hamil-

ton's equations of motion are integrated around the phase space torus and the point of intersection with a "section" recorded each pass.

In Chapter 10 we present the conclusions we have drawn from this work. The main conclusion, regarding the adiabatic theory, is that the coupling resonances, while they definitely modify the actions, do not totally undercut the foundations of the theory. Well enough preserved KAM tori apparently persist, bounding the actions, and preventing excessive transfer of energy between the circular-drift and the vortex-gyration.

By demonstrating that the cold Vlasov (circle-orbit) dispersion relation is the same as *both* the spread-mass and the energy-group models, we have also shown that circle-orbits *do* yield phase mix damping. This fact has been of some confusion in the literature.

We believe that our investigation of the foundations of adiabatic theory in the context of beams undergoing nonaxisymmetric perturbations is the first of its kind. Also, the methods we have employed are novel. Our detailed treatment of the covariant fluid hierarchy for a beam is also, to our knowlege, unique. These facets of our work, plus those original contributions delineated in the synopsis in Section 1.4, and mentioned earlier in Chapter 1, form the core of this thesis.

1.5 References

1.1 C.A.Kapetanakos, P.Sprangle, "Ultra-High Current Electron Induction Accelerators", Phys. Today, Page 58, Feb. 1985

1.2 G.J.Caporaso, W.A.Barletta, D.L.Birx, R.J.Briggs, Y.P.Chong, A.G.Cole, T.J.Fessenden, R.E.Hester, E.J.Lauer, V.K.Neil, A.C.Paul, D.S.Prono, and K.W.Struve, "Beam Dynamics in the Advanced Test Accelerator", Proceeding of the Fifth International Conference on High-Power Particle Beams, San Francisco, September 1983

1.3 G.A.Moses, Private communication

1.4 M.N.Rosenbluth, "Long-Wavelength Beam Instability", Phys. Fluids 3,932 (1960)

1.5 S.Weinberg, "The Hose Instability Dispersion Relation", J. Math. Phys. 5,1371 (1964)

1.6 S. Weinberg, "General Theory of Resistive Beam Instabilities", J. Math. Phys. 8,614 (1967)

1.7 E.P.Lee, "The Hose Instability of a Beam With the Bennett Profile", Phys. Fluids 21,1327 (1978)

1.8 H.S.Uhm, M.Lampe, "Theory of Resistive Hose Instability in Relativistic Electron Beams", Phys. Fluids 23,1574 (1980)

1.9 W.Sharp, M.Lampe, H.S.Uhm, "Multicomponent Model of the Resistive Hose Instability", Phys. Fluids 25,1456 (1982)

1.10 W.H.Bennett, "Self-Focussing Streams", Phys. Rev. 98,1584 (1954)

1.11 E.P.Lee, L.D.Pearlstein, "Hollow Equilibrium and Stability of a Relativistic Electron Beam Propagating in a Preionized Channel", Phys. Fluids 16, 904 (1973)

1.12 G.Joyce, M.Lampe, "Numerical Simulation of the Axisymmetric Hollowing Instability of a Propagating Beam", Phys. Fluids 26, 3377 (1983)

1.13 J.Mark, "Plasmas in Particle Accelerators: Adiabatic Theories for Bunched Beams", SIAM J. Appl. Math. 42, 914 (1982)

1.14 J.Mark, S.Yu, "Dynamically Consistent Closure Equations for Hydrodynamic Models of Pinched Beams", Phys. Lett. 92A, 903 (1982)

1.15 A.Deprit, "Canonical Transformations Depending Upon a Small Parameter", Cel. Mech. 1, 12 (1969)

1.16 K.J.O'Brien, G.A.Moses, "Adiabatic Beam Theory: Resonant Modification of Transverse Invariants", UW-FDM 601 (1984)

Chapter 2

Basic Physical Assumptions

In this thesis we are concerned with a well collimated electron beam with $\gamma \gg 1$ and $v_\perp/v_z \ll 1$, such a beam is called an ultra-relativistic ($\gamma \gg 1$) paraxial ($v_\perp/v_z \ll 1$) beam. The paraxiality may be expressed formally by

$$a\tilde{\Omega}_\beta \sim \left(\frac{I_{net}}{I_A}\right)^{\frac{1}{2}} \sim \frac{v_\perp}{v_z} \ll 1 \tag{2.1}$$

$$v_z = c - O\left(\tilde{\Omega}_\beta^2 a^2\right) \tag{2.2}$$

where I_A is the Alfvén current, $I_{net} = I_b + I_p$ the net current and $\tilde{\Omega}_\beta$ is the transverse betatron wavenumber.

To order the fields E_z , $\mathbf{E}_\perp$, B_z , and $\mathbf{B}_\perp$ we introduce the charge neutralization parameter $c/(4\pi\sigma a)$ which relates fundamental periods of interest $\sim a/c$ to the basic time scale $1/(4\pi\sigma)$ upon which the ambient plasma electrons rearrange themselves so as to charge neutralize the primary beam electrons. In this thesis, for reasons given in detail later, we shall always assume that $a/(4\pi\sigma c) \ll 1$. The

charge neutrality parameter and the paraxiality parameter are sufficient to order the fields and various derivatives. Formally the order scheme is

$$\mathbf{B}_\perp \sim \frac{4\pi a}{c} J_{bz} \sim a\frac{\partial}{\partial r} \sim 1 \tag{2.3}$$

$$B_z \sim \frac{4\pi a}{c} J_{b\perp} \sim a\left(\frac{\partial}{\partial z}\right)_\varsigma \sim \frac{v_\perp}{v_z} \tag{2.4}$$

$$\mathbf{E}_\perp \sim \frac{c}{4\pi\sigma a}\frac{v_\perp}{v_z} \tag{2.5}$$

$$E_z \sim a\left(\frac{\partial}{\partial \varsigma}\right)_z \sim \frac{c}{4\pi\sigma a}\,. \tag{2.6}$$

Notice that the orderings of $a\partial/\partial r$ and $a\partial/\partial z$ result in

$$\left(\frac{\partial J_b}{\partial z}\right)_\varsigma \sim a\tilde{\Omega}_\beta \nabla_\perp J_b \tag{2.7}$$

which indicates stronger radial gradients than the "time" evolution in z .

The region of the beam under consideration in this work is the "beam body" [1]. The beam body is the region beginning just behind the "pinch-point" (where the E_z spike initiates avalanche [2] ionization), and extending back to a point in the "tail" of the beam. In the tail recombination and plasma cooling establish a balance with beam driven ionization and heating. Self-consistent conductivity generation by beam impact ionization is included in our model. The conductivity therefore increases linearly in the slice-variable ς.

The slice variable is not an ignorable coordinate when conductivity generation is included. A related ignorable coordinate is $\eta = \log(\varsigma/\varsigma_o)$ where ς_o is a reference

[1] cf. Fig. 2.1.

[2] See Chapter 4

slice just behind the pinch point. Fourier components are therefore given in terms of $\exp(-i\omega\eta - i\Omega z/\beta c)$ where ω is a *dimensionless* frequency. Exponential growth in η corresponds to power law growth in ς .

Conventional hose theory is primarily formulated in terms of the following dimensionless parameters

- monopole current neutralization fraction $f_m = J_p/J_b$ where J_p and J_b are plasma and beam current density respectively, $-1 \leq f_m \leq 0$ (physically $f_m = f_m(r, \theta, \varsigma, z)$ but it is usual and useful to approximate f_m as a constant)

- charge neutralization fraction $f_c = \rho_p/\rho_b$ where ρ_p and ρ_b are plasma and beam charge densities respectively, $-1 \leq f_c \leq 0$ (physically $f_c = f_c(r, \theta, \varsigma, z)$ but it is usual and useful to approximate f_c as a constant)

- paraxiality $(I_b/I_A)(1 + f_m)$ where $((I_b/I_A)(1 + f_m) \ll 1$ implies $v_z \gg v_\perp)$, where $I_A = \beta\gamma mc^3/q = 17\beta\gamma$ kAmp is the Alfvén current

Conventional hose theory also depends upon the following dimensional scale factors

- charge neutralization time scale τ_c(sec)

- monopole decay time $\tau_o(sec)$

- dipole decay time τ_1(sec)

- betatron wavenumber $\tilde{\Omega}_\beta(cm^{-1}) = \Omega_\beta/\beta c$

- Bennett radius a(cm)

In terms of the slice variable ς the decay times become lengths $\varsigma_c, \varsigma_0, \varsigma_1$.

An approximate charge neutralization time scale τ_c for neutralization of the beam charge by ambient plasma electrons (they are radially expelled from the beam region, leaving behind a core of stationary positive ions) may be derived by combining charge continuity, Poisson's equation, and the plasma Ohm's law

$$\beta c \frac{\partial}{\partial \varsigma} \delta\rho + \nabla \cdot \delta J = 0 \tag{2.8}$$

$$\nabla \cdot \delta E = 4\pi \delta\rho \tag{2.9}$$

$$\delta J = \delta(\sigma E) \tag{2.10}$$

where δ denotes an excitation away from charge, current, and field free (plasma) equilibrium. Neglecting conductivity gradients and perturbations yields the approximate free decay of charge excitations

$$\left(\beta c \frac{\partial}{\partial \varsigma} + 4\pi\bar{\sigma}\right) \delta\rho = 0 \tag{2.11}$$

where $\bar{\sigma}$ is a radially averaged conductivity, hence $\delta\rho \approx \delta\rho_o \exp(-\varsigma/\varsigma_c)$ where $\varsigma_c = \beta c \tau_c = \beta c / 4\pi\bar{\sigma}$ is the charge decay length. In this work good charge neutrality ($4\pi\bar{\sigma} \gg c/a$) is assumed, therefore $f_c \sim -1$. For example, a 100 Amp beam of 300 nsec duration propagating in 1 Torr H_2 produces $\sigma \sim 10^{12}\ sec^{-1}$ with electron temperatures $\sim$ 1 eV, for a 1 cm beam $4\pi\sigma \sim 10^{13}$ whereas $c/a \sim 10^9$. For higher current beams ($I_b \sim$ 100 kAmp) in 760 Torr air the situation regarding charge neutralization is even more favorable.

An approximate decay length ς_o for free decay of monopole excitations may be derived by looking at the beam (of radius a) within a plasma region (of radius $b \gg a$) as a coaxial cable. The inductance per unit length of such a coaxial cable is $L = (4/c^2)\log(b/a)$. A radially averaged "Lenz law" reads

$$\delta\epsilon = -L\beta c\frac{\partial}{\partial\varsigma}\delta I \approx -L\beta c\frac{\partial}{\partial\varsigma}\pi a^2\bar{\sigma}\delta\epsilon \tag{2.12}$$

where $\delta\epsilon$ is the induced emf due to a monopole current excitation δI. The emf is $\delta\epsilon \approx \delta\epsilon_o \exp(-\varsigma/\varsigma_o)$ where $\varsigma_o = L\beta c\pi a^2\bar{\sigma} = (\beta 4\pi a^2\bar{\sigma}/c)\log(b/a)$. Typically $\log(b/a) \sim 10$, so for the parameters above $\varsigma_o \sim 300$ cm, whereas the beam pulse length is $\varsigma_b \sim 10^4$ cm. In general the monopole decay length is $\beta 4\pi a^2\bar{\sigma}/c$ times a dimensionless geometrical factor (a "form factor").

An approximate dipole decay length ς_1 (also known as the resistive skin depth) is derived from the source-free (for free decay) linearized Ampère equation

$$\left(\frac{d}{dr}\frac{1}{r}\frac{d}{dr}r - \beta\frac{4\pi}{c}\sigma_o\frac{\partial}{\partial\varsigma}\right)A_1 = 0 \tag{2.13}$$

where σ_o is the conductivity monopole, and A_1 the axial vector potential dipole. The fundamental radial mode is

$$A_1 \sim \frac{dA_o}{dr}\exp\left(-\frac{\varsigma}{\varsigma_1}\right) + \cdots \tag{2.14}$$

where A_o is the axial vector potential monopole. With the help of the monopole Ampère equation the dipole equation becomes

$$\frac{dJ_o}{dr} - \beta\sigma_o\frac{1}{\varsigma_1}\frac{dA_o}{dr} = 0\,. \tag{2.15}$$

Writing $\sigma_o(r) = \sigma_o \times$ (function of r) and noting that , dimensionally, $A_o \sim (\pi a^2/c)J_o$,a radial average of the dipole equation yields $\varsigma_1 = \beta\pi a^2\sigma_o/c$ times a form factor.

An important scaling conclusion is that dipole fields decay much more rapidly than monopole fields $\tau_o \sim (\log b/a)\tau_1 \gg \tau_1$ since, generally $b \gg a$. For the Bennett beam $\tau_o = (4\log(b/a))\tau_1$ where $4\log(b/a) \sim 10$ typically. Considering dipole perturbations, the monopole fields remain unchanged on the relevant dipole time scale. These decay lengths apply only for a "fat" beam which fills its plasma channel the conductivity of which is peaked on axis and decreases monotonically with radius. Thin beams in unusual plasma conductivity profiles cannot realistically be described in terms of the simple decay rates [3] .

Finite plasma conductivity is crucial to the rapid growth (on the dipole time scale) of the hose instability. If $\sigma \sim \infty$ monopole and dipole fields are "frozen" in the plasma. Growth periods scale not with τ_1 but with the Alfvén time $\tau_A \sim a\sqrt{n_p}/B_\theta \gg \tau_1$ (where n_p is the plasma density, B_θ the magnetic field strength) which governs magneto-hydrodynamic motion. For example, with $I_b = 100$ amp, $a = 1$ cm, $\varsigma_b = 10^4$ cm, and $n_p = 10^{12}$ cm^{-3} , using $v_A \approx 2.2 \times 10^{11} B_\theta/\sqrt{n_p}$ where for a beam $B_\theta = 0.2I_b/a$ we have $\tau_A = 1/k_\perp v_A \sim a/v_A = 2.3 \times 10^{-11} a^2\sqrt{n_p}/I_b$; therefore $\tau_A = 10^{-7}$ sec whereas $\tau_1 = 10^{-9}$ sec. For a beam- plasma system the magnetic Reynolds number is $S = \tau_1/\tau_A \ll 1$ which puts this system in quite a different regime than, for example, a tokamak with $S = 10^6$.

Resistivity enables fields to decouple from plasma motion partially by "field-

[3] This point is made explicit in Chapter 6

slippage". It is just this slippage that causes the first type of hose instability. As for the second, the magnetic repulsion of two current filaments is apparently not dependent upon resistivity.

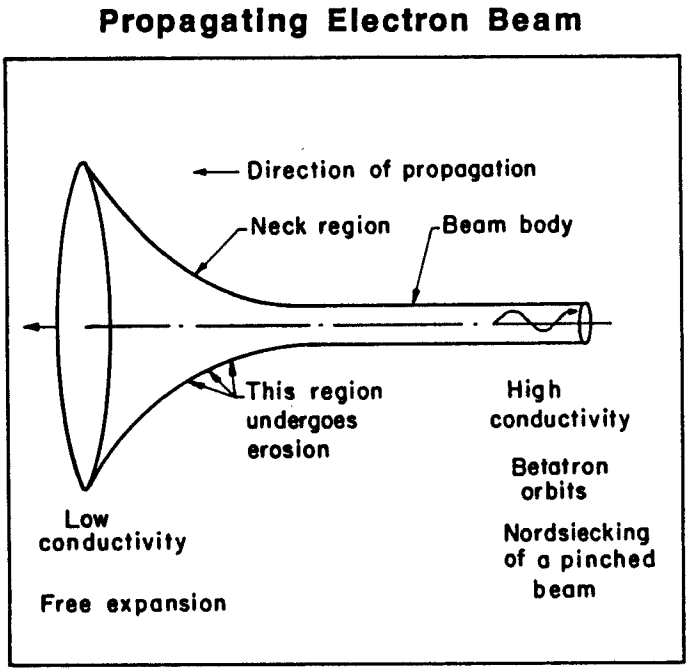

Figure 2.1: The region of the beam under consideration in this work is the "beam body". This figure depicts a beam along with the usual terminology used to describe the physically distinct regions of the beam.

Chapter 3

Relativistic Beam Equilibrium

3.1 Introduction

An electron beam will always have a spread in particle momentum, due to random fluctuations in the forces that accelerated the beam. Further randomizing effects are particle collisions with ambient plasma electrons, ions, and molecules. Generally collisions between beam electrons are not a dominant effect since the beam is comparatively sparse.

Dispersion of the phase space distribution f will arise from cumulative random events. Statistically we anticipate an evolution to a "quasi- steady" state f_o . Over and above the secular development of the distribution, small, rapid variations away from the mean will exhibit the Gaussianity typical of such fluctuations. We may safely assume that the time scale of fluctuations due to scattering is short compared to the secular scale over which large changes in the mean occur. The

natural formalism to apply to such a system is the Boltzmann H-theorem [3.1].

3.2 Momentum Distribution

Before considering the general case it is interesting to look at a spatially uniform situation for which the distribution is of momentum only. Denoting by f the single-particle momentum distribution function, the H-function is defined as

$$h(f) = \int d^3p f \log f \ . \tag{3.1}$$

This functional of f has the well-known property $dh/dt < 0$ as time evolves. Quasi-steady-state f_o is such that variation $f_o + \delta f$ yields a first order variation $\delta h = 0$. This variation must be carried out subject to $\delta U = \delta \mathbf{G} = \delta n = 0$ where U , $\mathbf{G}$, and n are the mean energy, momentum, and number densities respectively. Carrying out this constrained variation by means of Lagrange multipliers α and $1/T$ yields

$$f_o = \exp\left(\alpha - \frac{1}{T}\left(H - \mathbf{v}_o \cdot \mathbf{p}\right)\right) \tag{3.2}$$

where $H = \gamma mc^2$ is the Hamiltonian and $\mathbf{v}_o = v_o \mathbf{z}$ the beam electron fluid velocity.

To bring out the spectrum of small, rapid fluctuations away from quasi-steady state we expand to second order in the fluctuation amplitude. Expanding $\mathbf{p} = p_o \mathbf{z} + q_{\|}\mathbf{z} + \mathbf{q}_{\perp}$, where $\mathbf{q}$ denotes a rapid, small, random fluctuation away from $\mathbf{p}_o$, yields a Maxwellian

$$f_o = n_o \left(2\pi\gamma_o mT\right)^{-2} \left(2\pi\gamma_o^3 mT\right)^{-1} \exp\left(-\frac{1}{2T}\left(\frac{q_{\perp}^2}{\gamma_o m} + \frac{q_{\|}^2}{\gamma_o^3 m}\right)\right) + O\left(q^3\right) \tag{3.3}$$

where $\gamma_o^{-2} = 1 - v_o^2/c^2$. An important result is that the effective axial mass is $\gamma_o^3 m$, therefore we may neglect axial single particle dynamics. Furthermore, the large axial energy results in a microcanonical distribution

$$\left(2\pi\gamma_o^3 mT\right)^{-1} \exp\left(-\frac{q_\parallel^2}{2T\gamma_o^3 m}\right) \sim \delta\left(q_\parallel\right) \tag{3.4}$$

which means physically that the axial degree of freedom is effectively cold.

3.3 Phase Space Distribution

Having examined the momentum distribution now we consider the entire phase space distribution. We consider a superposition of two charged particle streams, electron and ion, each with fluid velocity directed along the z-axis of the accelerator frame. It is useful to rewrite the Maxwell-Boltzmann distribution in the relativistically covariant form

$$f_\sigma = N_\sigma \exp(-a_\mu^\sigma P_\sigma^\mu) \tag{3.5}$$

which in fact is a Lorentz scalar. The label σ denotes particle species and will be omitted upon occasion. In the lab frame the four-vectors a and P have contravariant components

$$a_\sigma^\mu = (\frac{c}{T_\sigma}, 0, 0, \frac{v_\sigma}{T_\sigma}) \tag{3.6}$$

$$P_\sigma^\mu = (\frac{H_\sigma}{c}, 0, 0, P_z^\sigma) \tag{3.7}$$

where T is the temperature, v the fluid velocity, $H = \gamma mc^2 + q\phi$ the Hamiltonian, and $P^\mu = p^\mu + (q/c)A^\mu$ the canonical momentum. The vector a is timelike (with

metric convention $g = diag(1, -1, -1, -1)$) in the lab frame:

$$a_\mu a^\mu = \left(\frac{c}{\gamma T}\right)^2 \tag{3.8}$$

and is thus timelike in any frame.

The distribution 3.5 may be explicitly factored in Maxwell and Boltzmann components (momentum and spatial distributions respectively). To accomplish this we note that $P^\mu = p^\mu + (q/c)A^\mu$ thus

$$f = N \exp\left(-a_\mu p^\mu\right) \exp\left(-\frac{q}{c} a_\mu A^\mu\right) \tag{3.9}$$

where the first factor is the momentum distribution and the second the spatial distribution. To see this explicitly we use $p^\mu = (\gamma mc, \mathbf{p})$ and $A^\mu = (\phi, \mathbf{A})$ to calculate the exponents

$$a_\mu p^\mu = \frac{1}{T}\left(\gamma mc^2 - \mathbf{v}_o \cdot \mathbf{p}\right) \tag{3.10}$$

$$\frac{q}{c} a_\mu A^\mu = \frac{q}{T}\left(\phi - \frac{\mathbf{v}_o}{c} \cdot \mathbf{A}\right) \tag{3.11}$$

therefore $\exp\left(-a_\mu p^\mu\right)$ is the distribution we previously considered, while the Boltzmann factor is $\exp\left(-(q/c)a_\mu A^\mu\right)$. The total phase space distribution may be written, making use of the results 3.3 and 3.4 as

$$f_o = n_o \delta\left(P_z - \gamma_o mc\beta_o\right)\left(2\pi\gamma_o mT\right)^{-1} \exp\left(-\frac{p_\perp^2}{2\gamma_o mT}\right) \exp\left(-\frac{q}{c} a_\mu A^\mu\right) . \tag{3.12}$$

The contraction of a_μ with the four-vector potential A^μ we call the covariant pinch potential Ψ

$$\Psi_\sigma = \frac{q_\sigma}{c} A_\mu a^\mu . \tag{3.13}$$

Note that Ψ is $-q_\sigma/T_\sigma$ times the pinch potential $\psi = \beta A_z - \phi$ which we ordinarily use. The determination of the equilibrium phase space distribution now devolves to calculation of the covariant pinch potential.

In the fluid rest frame of the species labeled by σ the vector a^μ_σ has no spacelike components and the covariant pinch potential is

$$\Psi_\sigma = \frac{q_\sigma}{T_\sigma}\phi \, . \tag{3.14}$$

Contrariwise, in a frame for which $\phi = 0$ the beam is said to be in a "pure pinch"

$$\Psi_\sigma = -\frac{q_\sigma}{T_\sigma}\beta_\sigma A_z \, . \tag{3.15}$$

Doubtlessly both of these conventions are frame dependent, nevertheless, we shall be interested ultimately in the case for which the beam is a pure pinch with respect to the accelerator rest frame.

Calculation of the covariant pinch potential is accomplished by solving the self-consistent field and source problem for the inhomogeneous Maxwell equation. The current density four vector for the sigma species is defined as

$$j^\mu = (n_\sigma c q_\sigma, \mathbf{J}_\sigma) \tag{3.16}$$

$$n_\sigma = \int d^3p f_\sigma \tag{3.17}$$

$$\mathbf{J}_\sigma = q_\sigma c \int d^3p f_\sigma \mathbf{p}(p^2 + m_\sigma^2 c^2)^{-\frac{1}{2}} \, . \tag{3.18}$$

Calculating j^μ explicitly yields the result

$$j^\mu_\sigma = c q_\sigma N_\sigma Q_\sigma a^\mu_\sigma e^{-\Psi_\sigma} \, . \tag{3.19}$$

$$Q_\sigma = \frac{4\pi m_\sigma^2 c^2}{a_\mu^\sigma a_\sigma^\mu} K_2 \left(m_\sigma c \sqrt{a_\mu^\sigma a_\sigma^\mu} \right) \tag{3.20}$$

where K_2 is the modified Bessel function of the second order. In this formula all terms are manifestly covariant and one therefore writes the total current in an arbitrary frame (with z axis along that of the lab and streams) as

$$j^\mu = \sum_\sigma j_\sigma^\mu \, . \tag{3.21}$$

The total current provides the source in the inhomogeneous Maxwell equation:

$$(\partial^\lambda \partial_\lambda g_\nu^\mu - \partial^\mu \partial_\nu) A^\nu = \frac{4\pi}{c} j^\mu \, . \tag{3.22}$$

If we contract the inhomogeneous Maxwell equation (in the Lorentz gauge) with the four vector $\frac{q_\sigma}{c} a_\mu^l$ we get a nonlinear equation for the pinch potential

$$\frac{1}{r} \frac{d}{dr} r \frac{d}{dr} \Psi_l = -\frac{4\pi}{c} \sum_\sigma q_\sigma q_l N_\sigma Q_\sigma a_\mu^\sigma a_l^\mu e^{-\Psi_\sigma} \tag{3.23}$$

where we assume an axisymmetric ground state and treat the hypothetical case of a long beam so that $\partial/\partial z = 0$. To get Bennett equilibria we invoke an ansatz which converts this equation into the Poisson-Boltzmann equation. To this end let us force the covariant pinch potentials of the streams to be related to one another by

$$e^{-\Psi_\sigma} = b_\sigma e^{-\Psi_0} \tag{3.24}$$

where b_σ is to be determined by forcing self-consistency, that is, forcing Ψ_0 to solve the Poisson-Boltzmann equation

$$\frac{1}{r} \frac{d}{dr} r \frac{d}{dr} \Psi_0 - 2e^{-\Psi_0} = 0 \, . \tag{3.25}$$

This equation results only if we have

$$\frac{2\pi}{c}\sum_{\sigma} q_\sigma q_l N_\sigma Q_\sigma b_\sigma a^\sigma_\mu a^\mu_\sigma = -1 \tag{3.26}$$

so that if we define the matrix m

$$m_{l\sigma} = -\frac{2\pi}{c} q_\sigma q_l N_\sigma Q_\sigma a^\sigma_\mu a^\mu_l \tag{3.27}$$

we may solve for the unknown coefficients by inversion of the system of linear equations

$$b_\sigma = (m^{-1})_{\sigma l} 1_l \, . \tag{3.28}$$

The vector potential A_μ is gotten by inverting the system

$$\Psi_\sigma = \frac{q_\sigma}{c} a^\sigma_\mu A^\mu \, . \tag{3.29}$$

If we explicitly refer to ions and electrons $\sigma = (i, e)$ we arrive at the following formulæ for the scalar and vector potentials:

$$A_0 = \frac{c}{q_i q_e}\left(\frac{q_i a^i_3 - q_e a^e_3}{a^e_0 a^i_3 - a^i_0 a^e_3}\right)\Psi_0 = \phi \tag{3.30}$$

$$A_3 = \frac{c}{q_i q_e}\left(\frac{q_e a^e_0 - q_i a^i_0}{a^e_0 a^i_3 - a^i_0 a^e_3}\right)\Psi_0 = -A_z \, . \tag{3.31}$$

From the relation 3.30 for the scalar potential we can see under what conditions a pure pinch ($\phi = 0$) results in the frame with respect to which this formula is defined, namely

$$\frac{v_e q_e}{T_e} = \frac{q_i v_i}{T_i} \tag{3.32}$$

in terms of physical variables. This is the same as the condition one arrives at in a nonrelativistic treatment. Notice that a pure pinch involves counter- streaming of

the ion and electron beams. Nonrelativistically one can show that the pure pinch results in the same three-vector current density in all three frames of reference, lab, ion fluid, and electron fluid rest frames; it is of course this net current which provides the pinch force. If the second particle stream is also an electron beam then the pure pinch occurs when

$$\frac{v_{e1}}{v_{e2}} = \frac{T_{e1}}{T_{e2}} \tag{3.33}$$

where beam 1 is the primary electron beam and beam 2 is the plasma return current which partially current neutralizes the primary current. In this case the two beams are co-streaming.

3.4 Bennett Equilibrium

The Poisson-Boltzmann equation 3.25 is a "classical" equation of mathematical physics [3.2] and admits a class of self-similar solutions [3.3] which are invariant under the one parameter (α) Lie group of transformations

$$r' = \exp(-\frac{1}{2}\alpha)r \tag{3.34}$$

$$\Psi_0' = \Psi_0 + \alpha\,. \tag{3.35}$$

Here we find the mathematical basis for the self-similar expansion, that is, the Nordsiéck expansion, of self-pinched particle beams [3.4]. The most general solution yielding a positive density $n = n_0 e^{-\Psi_0}$ is

$$\Psi_0 = 2\log\left(\frac{\Re^2\chi + \Im^2\chi + 1}{\sqrt{\nabla_\perp \Re\chi \cdot \nabla_\perp \Re\chi}}\right) \tag{3.36}$$

where χ is an arbitrary harmonic function $\nabla^2\chi = 0$, with $\Re$ and $\Im$ denoting the real and imaginary parts respectively. Generalized Bennett solutions, gotten by taking the most general case of axisymmetry

$$\Re\chi = \left(\frac{r}{a}\right)^n \cos n\theta \tag{3.37}$$

$$\Im\chi = \left(\frac{r}{a}\right)^n \sin n\theta \tag{3.38}$$

are given by

$$\Psi_o = 2\log\frac{a}{2n}\left(\left(\frac{a}{r}\right)^{n-1} + \left(\frac{r}{a}\right)^{n+1}\right) \tag{3.39}$$

where a and n are arbitrary positive real numbers. The self-similarity is apparent, providing the scale radius a scales as r, since r scales as $\exp(-\alpha/2)$ under the invariance group, the Nordsiéck expansion of a with time preserves the group invariance.

Taking $n = 1$ we get the "classical" Bennett solution (dropping constants)

$$\Psi_o = 2\log\left(1 + \frac{r^2}{a^2}\right) . \tag{3.40}$$

Taking $n > 1$ yields hollow equilibria [3.7]; however in this thesis we are only concerned with the classical Bennett distribution.

Given the pinch potential for the Bennett distribution we may easily compute the important properties of the equilibrium. The current density of the Bennett equilibrium is

$$J_{bo}(r) = \frac{I_b}{\pi a^2}\exp\left(-\Psi\right) = \frac{I_b}{\pi a^2}\left(1 + \frac{r^2}{a^2}\right)^{-2} \tag{3.41}$$

and the vector potential is

$$A_{zo}(r) = -(1+f_m)\frac{I_b}{c}\log\left(1+\frac{r^2}{a^2}\right) \tag{3.42}$$

while the squared betatron wavenumber is

$$\tilde{\Omega}_\beta^2(r) = \tilde{\Omega}_{\beta o}^2\left(1+\frac{r^2}{a^2}\right)^{-1} . \tag{3.43}$$

The squared betatron wavenumber has a mean value $\tilde{\Omega}_\beta^2 = \tilde{\Omega}_{\beta o}^2/2$ and is distributed uniformly on the interval $(0, \tilde{\Omega}_{\beta o}^2)$; in this sense the Bennett potential is maximally anharmonic. The Bennett equilibrium has the property that one half the total current is carried within one Bennett radius. Also, the wings of the distribution are wider than a Gaussian; in fact, the mean square radius is infinite, Fig. 3.1.

The Bennett equilibrium is the natural quasi-equilibrium to which a beam will evolve. Experimentally this is found to be true to a high degree of accuracy, as shown in Fig. 3.2 with depicts results for a 5.2 MeV, 220 Amp electron beam after propagation through 2 meters of 40 Torr nitrogen gas. Apparently the Bennett equilibrium is attained very rapidly.

The Bennett temperature, which physically is a condition for radial force balance between expansive thermal pressure and compressive magnetic pinch, may easily be computed by means of the virial theorem of Clausius [3.7]

$$T = \frac{1}{2}\gamma mc^2\beta^2\langle\tilde{\Omega}_\beta^2 r^2\rangle = \frac{1}{2}\gamma mc^2\beta^2\int d^2r J_{bo}(r)\tilde{\Omega}_\beta^2 r^2 . \tag{3.44}$$

In terms of the current and charge neutralization factors f_m , f_c , with the help of the Poisson and Ampère equations, we may express the equilibrium pinch

potential ψ_o solely in terms of the axial vector potential A_{zo}

$$\nabla_r^2 \phi_o = -4\pi (1 + f_c) \rho_{bo} \tag{3.45}$$

$$\nabla_r^2 A_{zo} = -\frac{4\pi}{c} (1 + f_m) J_{bo} \tag{3.46}$$

combining these equations we arrive at

$$\nabla_r^2 \psi_o = -\frac{4\pi}{c} (1 + f_m) \left(1 - \frac{1}{\beta^2} \frac{1 + f_c}{1 + f_m}\right) J_{bo} \tag{3.47}$$

therefore $\psi_o = \beta\lambda A_{zo}$ where $\lambda = 1 - 1/\beta^2(1 + f_c)/(1 + f_m)$, so that the squared betatron wavenumber is

$$\tilde{\Omega}_\beta^2(r) = -\frac{q\lambda}{\gamma m \beta^2 c^2} \frac{1}{r} \frac{dA_{zo}}{dr} . \tag{3.48}$$

From this, using the result 3.42 for A_{zo} , the squared betatron wavenumber on axis is

$$\tilde{\Omega}_{\beta o}^2 = \frac{2qI_b\lambda(1 + f_m)}{\gamma m c^3 \beta a^2} . \tag{3.49}$$

Computing the virial moment in terms of this expression yields the Bennett temperature

$$T = \frac{q\beta I_b \lambda (1 + f_m)}{2c} . \tag{3.50}$$

A fully current neutral equilibrium exists only if $f_c = -1$ since otherwise $T < 0$, therefore the $f_m = -1$ equilibrium is cold $T = 0$.

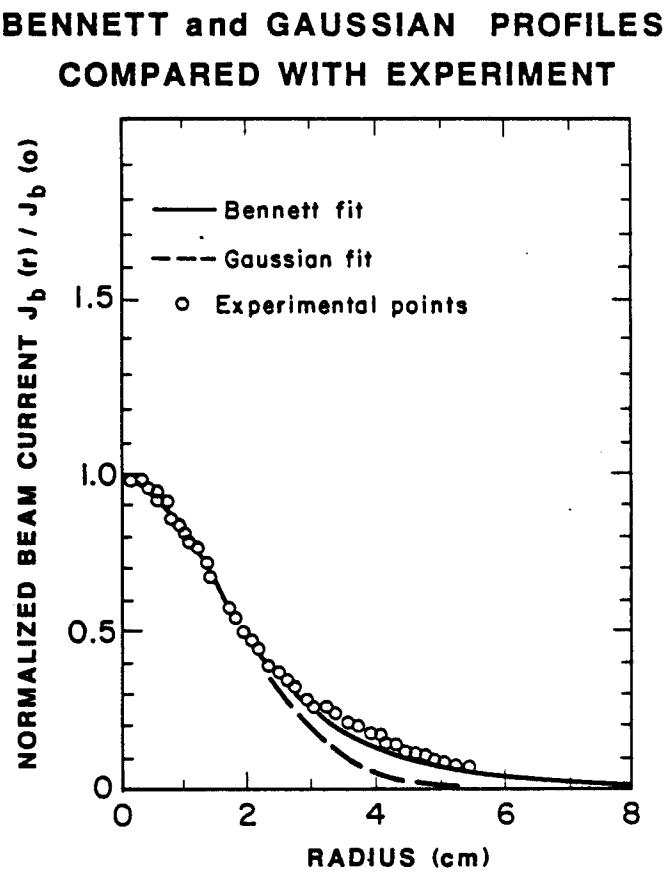

Figure 3.1: Radial profile of a 5.2 MeV, 220 Amp electron beam after propagating 2 meters through 40 Torr N_2 gas, data from the Astron accelerator (1974) [3.5,3.6].

3.5 Paraxial Transverse Hamiltonian

The paraxial nature of our electron beam may be exploited to derive a useful form for the Hamiltonian. The single particle Hamiltonian for a particle in the beam (not just an equilibrium beam) is

$$H = \gamma mc^2 + q\phi = \left((mc^2)^2 + (\mathbf{p}c)^2\right)^{\frac{1}{2}} + q\phi \,. \tag{3.51}$$

Introducing the canonical momentum $\mathbf{P} = \mathbf{p} + \frac{q}{c}\mathbf{A}$ we may expand the Hamiltonian as follows

$$H = \gamma_o mc^2 + \frac{1}{2\gamma_o m}\left(p_r^2 + \frac{P_\theta^2}{r^2}\right) - \frac{qA_z P_z}{\gamma_o mc} + q\phi + \cdots \tag{3.52}$$

where the "fluid gamma" γ_o is defined as $(\gamma_o mc^2)^2 = (mc^2)^2 + (P_z c)^2$ and terms of order $A_z^2/(\gamma_o mc)^2$ have been dropped. Noting that $P_z = \gamma_o mc\beta_o$ and introducing the pinch potential $\psi_o = \beta_o A_z - \phi$ the Hamiltonian becomes

$$H = \gamma_o mc^2 + \frac{1}{2\gamma_o m}\left(p_r^2 + \frac{P_\theta^2}{r^2}\right) - q\psi_o \,. \tag{3.53}$$

In the remainder of the thesis we shall only be interested in the transverse Hamiltonian $H_\perp = H - \gamma mc^2$ which reads

$$H_\perp = \frac{1}{2\gamma m}\left(p_r^2 + \frac{P_\theta^2}{r^2}\right) - q\psi \tag{3.54}$$

where we have dropped the subscript o from γ_o.

Hamilton's equations yield the equation of motion for the transverse variables (r, θ)

$$\frac{d}{dt}\left(\gamma m \frac{d\mathbf{r}}{dt}\right) = q\frac{\partial \psi}{\partial \mathbf{r}} \,. \tag{3.55}$$

If scattering is considered to be important, then a small-angle scattering term $\delta\mathbf{F}$ should really be present on the right hand side of the 3.55. We may neglect the axial dynamics so that $d\gamma/dt = 0$ on the time scale of propagation for several betatron wavelengths. In terms of beam variables the force law becomes

$$\frac{\partial^2 \mathbf{r}}{\partial z^2} = \frac{q}{\gamma m \beta^2 c^2} \frac{\partial \psi}{\partial \mathbf{r}} \tag{3.56}$$

which, written out explicitly is just

$$\frac{d^2 r}{dz^2} - r\left(\frac{d\theta}{dz}\right)^2 = \frac{q}{\gamma m c^2 \beta^2} \frac{\partial \psi}{\partial r} \tag{3.57}$$

$$r\frac{d^2\theta}{dz^2} + 2\frac{dr}{dz}\frac{d\theta}{dz} = \frac{q}{\gamma m c^2 \beta^2} \frac{1}{r} \frac{\partial \psi}{\partial \theta} \,. \tag{3.58}$$

Anticipating more detailed work, presented in Chapter 9, on the single particle dynamics in the Bennett equilibrium, here some simple results concerning the transverse orbits and the concept of near-circularity will be discussed.

For the axisymmetric equilibrium $\psi = \psi(r)$ 3.56 reduces to

$$\frac{\partial^2 \mathbf{r}}{\partial z^2} + \tilde{\Omega}_\beta^2(r)\mathbf{r} = 0 \tag{3.59}$$

which corresponds to

$$\frac{d^2 r}{dz^2} - r\left(\frac{d\theta}{dz}\right)^2 + \tilde{\Omega}_\beta^2(r) r = 0 \tag{3.60}$$

$$r\frac{d^2\theta}{dz^2} + 2\frac{dr}{dz}\frac{d\theta}{dz} = 0 \,. \tag{3.61}$$

Equations 3.60 and 3.61 admit two integrals of motion, that is, the axisymmetric transverse Hamiltonian is a nonlinear integrable system; it is in fact just motion in a central potential. For the Bennett equilibrium the energy and angular

momentum integrals are ($\rho = r/a$)

$$H_\perp = \frac{1}{2}\gamma mc^2\beta^2 a^2\left(\frac{d\rho}{dz}\right)^2 + \frac{1}{2}\frac{P_\theta^2}{\gamma ma^2}\frac{1}{\rho^2} + \frac{1}{2}\gamma mc^2\beta^2 a^2\tilde{\Omega}_{\beta o}^2 \log\left(1+\rho^2\right) \qquad (3.62)$$

$$P_\theta = \gamma m\beta ca^2\rho^2\tilde{\Omega}_\beta(\rho)\ . \qquad (3.63)$$

The effective potential for radial motion is

$$\tilde{V} = \frac{1}{2}\gamma mc^2\beta^2 a^2\tilde{\Omega}_{\beta o}^2\left(\frac{l}{\rho^2} + \log\left(1+\rho^2\right)\right) \qquad (3.64)$$

where $l = P_\theta^2/(\gamma mc\beta a^2\tilde{\Omega}_{\beta o})^2$. The potential-minimum radius ρ_o upon which circle orbits revolve and about which near-circle orbits oscillate, for particles with $P_\theta = \gamma m\beta ca^2\rho_o^2\tilde{\Omega}_\beta(\rho_o)$, is given by

$$\rho_o^2 = \frac{1}{2}l\left(1+\sqrt{1+\frac{4}{l}}\right) \qquad (3.65)$$

and the squared ratio of the angular to radial frequencies for near-circle orbits centered at ρ_o is

$$\frac{\Omega_\theta^2}{\Omega_r^2} = \frac{1}{2\left(1+2\rho_o^2\right)} \qquad (3.66)$$

where we have used $\Omega_r^2(\rho_o) = (1/\gamma ma^2)d^2\tilde{V}/d\rho_o^2$ and $\Omega_\theta^2(\rho_o) = \beta^2c^2\tilde{\Omega}_\beta^2(\rho_o)$. Fig. 3.3 depicts Ω_θ/Ω_r and $\pi a^2 J_{bo}(\rho_o)/I_b$ plotted versus ρ_o . According to this plot most particles on near-circle orbits have $\Omega_\theta/\Omega_r \ll 1$, which means that the radial "vortex gyration" may be treated as a high frequency degree of freedom and averaged out of the problem. What will be missing are various high frequency effects.

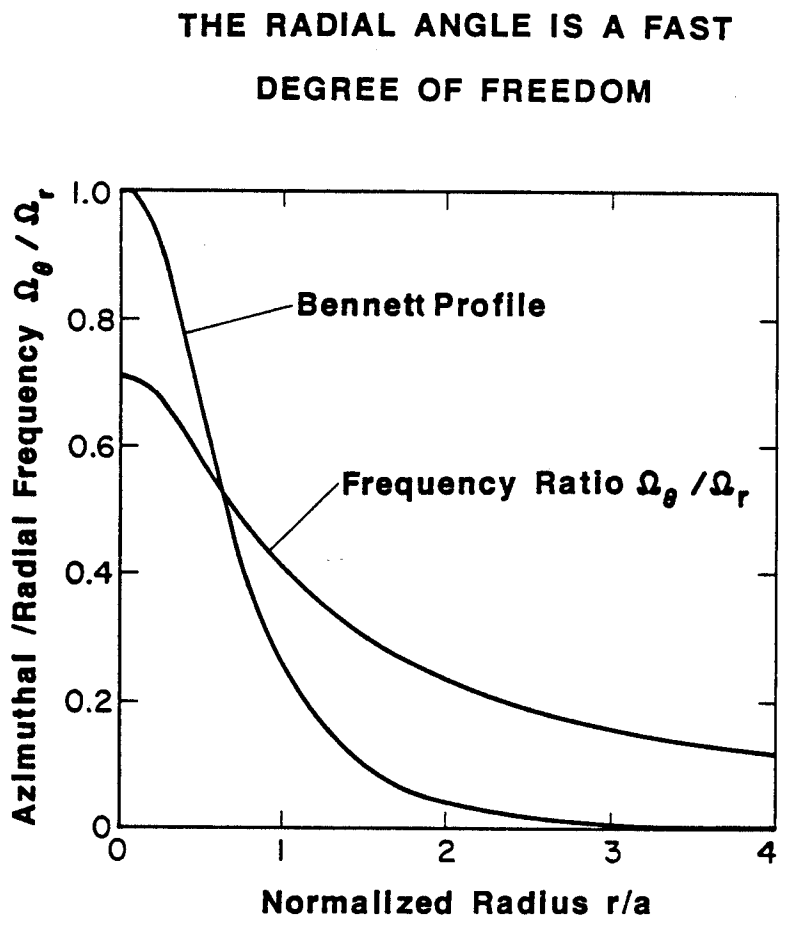

Figure 3.2: Most particles on near-circle orbits have $\Omega_\theta/\Omega_r \ll 1$ as depicted in this plot of Ω_θ/Ω_r and $\pi a^2 J_{bo}(\rho_o)/I_b$ plotted versus ρ_o .

3.6 References

3.1 L.D.Landau, E.M.Lifshitz, Statistical Physics , Volume 5 Course of Theoretical Physics, Pergamon Press (1980)

3.2 G.W.Walker, "Some Problems Illustrating the Forms of Nebulae", Proc. Roy. Soc. A41, 410 (1915)

3.3 L.Dresner, "Phase-Plane Analysis of Nonlinear, Second-Order, Ordinary Differential Equations", J. Math. Phys. 12, 1339 (1970)

4.4 Nordseick reference

3.5 E.P.Lee, "Kinetic Theory of a Relativistic Beam", Phys. Fluids 19, 60 (1976)

3.6 R.J.Briggs, R.E.Hester, E.J.Lauer, E.P.Lee, R.L.Spoerlein, "Radial Expansion of Self-Focused, Relativistic Electron Beams", Phys. Fluids 19, 1007 (1976)

3.7 G.Benford, D.L.Book, R.N.Sudan, "Relativistic Beam Equilibria with Back Currents", Phys. Fluids 13, 2621 (1970)

3.8 H.Goldstein, Classical Mechanics , Addison-Wesley Publishing Company (1950)

Chapter 4

Conductivity Generation

4.1 Introduction

Intricate and subtle effects are likely associated with the details of conductivity generation in the ambient gas during passage of the beam. Careful treatment of conductivity generation is necessary to correctly understand the physics of beam propagation. The problem is to accurately account for the interactions of relativistic electrons with the ambient molecules, ions, electrons, and photons as well as the subsequent interactions amongst the molecules, ions, electrons, and photons themselves.

Conductivity is determined by the free electron distribution in the gas. The evolution of the non-equilibrium electron energy distribution results from interaction of electrons with other electrons, gas molecules, ions, and the fields generated by the primary beam current as well as the beam electrons themselves. This de-

scription may be formalized by a Boltzmann equation [4.1]. In a gaseous media many different atomic and molecular processes contribute to the collision operator in the Boltzmann equation. We shall have to content ourselves with a simple thermally averaged model. Detailed "gas chemistry" can hardly be incorporated within the simple framework of an analytical model such as developed in this thesis. For a comprehensive discussion of air chemistry in relation to electron beam propagation a good source, with many references, is [4.2].

4.2 Phenomenological Conductivity Model

A phenomenological model of conductivity evolution at fixed z due to passage of the beam is [4.3]

$$\frac{\partial \sigma}{\partial \zeta} = \kappa J_b + \frac{\alpha_E}{c}\sigma - \beta_r \sigma^2 \tag{4.1}$$

which accounts for beam-driven impact ionization κ , avalanche ionization α_E , and recombination β_r . These production and loss mechanisms are the dominant physical processes for creating and destroying *free* electrons. Physically, κ, α_E and β_r depend upon plasma electron temperature T_e. One may neglect this temperature dependence and consider the coefficients to be thermally averaged.

4.3 Impact Ionization

The impact ionization coefficient κ is

$$\kappa = \frac{q^2}{m\nu_m}\frac{\partial n_e}{\partial \zeta}\frac{1}{J_b} \tag{4.2}$$

where ν_m is the effective plasma electron-molecule collision frequency, n_e is the plasma (free) electron number density, q is the electron charge, and m the electron rest mass. In air, for plasma temperatures $0.5eV \leq T_e \leq 1.0eV$, $\kappa = 8.5 \times 10^{-4}$ cm/statcoulomb [4.3].

4.4 Avalanche Ionization

The avalanche coefficient is

$$\alpha_E = \frac{A\rho_g S^3}{1 + BS + CS^2 + DS^3}(sec^{-1}) \tag{4.3}$$

where $S = E_z^2/\rho_g^2$, ρ_g is the air density in atmospheres, and E_z (statcoulomb) is the inductively generated axial electric field. The *experimentally* determined constants are $A = 1.42 \times 10^{-4}$, $B = 9.18 \times 10^{-6}$, $C = 2.66 \times 10^{-10}$, $D = 2.82 \times 10^{-17}$ [4.3].

4.5 Recombination

The recombination coefficient is $\beta_r = 7.1 \times 10^{-15}\rho_g/\rho_o$ (sec/cm) where ρ_o is the STP density of air and ρ_g is the air density in the experiment [4.3].

4.6 Local Conductivity Approximation

Within the beam body we neglect avalanche ionization (which is important only near the pinch point E_z spike) and plasma electron-ion recombination (which depends quadratically upon n_e). Conductivity generation is due only to direct

beam-driven impact ionization. Nonlocal impact ionization (knock-on effects of high-energy secondary electrons) which causes spatial spreading of conductivity is not considered either. Such a "local conductivity approximation" is generally valid above a threshold gas pressure and is certainly reasonable in STP air. The conductivity equation is therefore

$$\frac{\partial \sigma}{\partial \varsigma} = \kappa J_b \, . \tag{4.4}$$

This may be integrated simply

$$\sigma(r, \theta, \varsigma, z) = \kappa \int_0^{\varsigma} d\varsigma' \, J_b(r, \theta, \varsigma', z) + \tilde{\sigma}(r, \theta, z) \tag{4.5}$$

where $\tilde{\sigma}$ is conductivity due to any residual plasma electrons generated by previous pulses, or intentionally by a laser, prior to injection of the lead pulse. Usually it is a reasonable to assume, for widely spaced pulses, that the gas is fully relaxed and $\tilde{\sigma} \sim 0$. In any case, residual conductivity will be important only for the head of the pulse since the pulse will rapidly generate a plasma electron density far in excess of any residual free electrons due to pre-excited air. If the time spread between pulses is long compared to the de-excitation period then even for the head $\tilde{\sigma} \sim 0$. To quantify these simple arguments requires detailed investigation of relaxation rates for de-excitation of air after passage of a pulse of electrons.

4.7 References

4.1 S.S.Yu, "Boltzmann Approach to Conductivity Calculations", UCID-17907 (1978)

4.2 A.W.Ali, "On Electron Beam Ionization of Air and Chemical Reactions for Disturbed Air Deionization", NRL-Report No. 4619 (1981)

4.3 M.Lampe, W.Sharp, R.F.Hubbard, E.P.Lee, R.J.Briggs, "Current and Conductivity Effects on Hose Instability", Phys. Fluids 27,2921 (1984)

Chapter 5

Field Equations

5.1 Introduction

It is the purpose of Chapter 5 to present a derivation of the basic field equation we use to describe the dipole fields generated by a linear hose instability of an ultra-relativistic, paraxial electron beam immersed in an Ohmic plasma. Our starting point is with the full Maxwell equations

$$-\partial^2 \mathbf{A} + \nabla\left(\nabla\cdot\mathbf{A} + \frac{1}{c}\frac{\partial\phi}{\partial t}\right) = \frac{4\pi}{c}\mathbf{J} \tag{5.1}$$

$$-\partial^2\phi + \frac{1}{c}\frac{\partial}{\partial t}\left(\nabla\cdot\mathbf{A} + \frac{1}{c}\frac{\partial\phi}{\partial t}\right) = 4\pi\rho \tag{5.2}$$

where $\partial^2 = 1/c^2\partial^2/\partial t^2 - \nabla^2$ and the fields $\mathbf{E}$ and $\mathbf{B}$ are given by

$$\mathbf{E} = -\nabla\phi - \frac{1}{c}\frac{\partial\mathbf{A}}{\partial t} \tag{5.3}$$

$$\mathbf{B} = \nabla\times\mathbf{A}\,. \tag{5.4}$$

The plasma is treated as a simple Ohmic medium so the induced plasma current is $\mathbf{J}_p = \sigma\mathbf{E}$. In the Maxwell equations $\mathbf{J}$ and ρ are the total current and charge densities respectively.

A relativistic transformation from the accelerator rest frame into the beam rest frame is not useful since the plasma, which is at rest in the accelerator rest frame, would become a relativistic entity. Although it is possible to transform conductivity relativistically, we do not find such a transformation to be necessary. Beam variables are used instead:$(z,t) \longrightarrow (z,\varsigma)$ defined by $\varsigma = \beta ct - z$. The partial derivatives transform according to

$$\frac{1}{c}\left(\frac{\partial}{\partial t}\right)_z = \beta\left(\frac{\partial}{\partial \varsigma}\right)_z \tag{5.5}$$

$$\left(\frac{\partial}{\partial z}\right)_t = \left(\frac{\partial}{\partial z}\right)_\varsigma - \left(\frac{\partial}{\partial \varsigma}\right)_z . \tag{5.6}$$

It is important to clearly understand that this transformation is not a relativistic transformation to the beam frame; in fact, all equations are written for an observer in the accelerator rest frame. In this thesis we will work in the Lorentz gauge $\nabla \cdot \mathbf{A} + 1/c\partial\phi/\partial t = 0$. In this gauge, with the beam variables, the full set of equations reads

$$\partial^2 A_z = -\frac{4\pi}{c} J_z \tag{5.7}$$

$$\partial^2 \mathbf{A}_\perp = -\frac{4\pi}{c} \mathbf{J}_\perp \tag{5.8}$$

$$\partial^2 \phi = -4\pi\rho \tag{5.9}$$

$$\beta\frac{\partial\phi}{\partial\varsigma} + \beta\frac{\partial A_z}{\partial z} - \frac{\partial A_z}{\partial\varsigma} + \nabla_\perp \cdot \mathbf{A}_\perp = 0 \tag{5.10}$$

$$\beta c\frac{\partial \rho}{\partial \varsigma}+\nabla_{\perp}\cdot\mathbf{J}_{\perp}+\frac{\partial J_z}{\partial z}-\frac{\partial J_z}{\partial \varsigma}=0 \tag{5.11}$$

$$J_z=J_b-\sigma\frac{\partial \phi}{\partial z}+\sigma\frac{\partial \phi}{\partial \varsigma}-\beta\sigma\frac{\partial A_z}{\partial \varsigma} \tag{5.12}$$

$$\mathbf{J}_{\perp}=-\sigma\nabla_{\perp}\phi-\sigma\beta\frac{\partial \mathbf{A}_{\perp}}{\partial \varsigma}\,. \tag{5.13}$$

5.2 EMPULSE Field Equations

A key approximation facilitating rigorous derivation of useful field equations is the decoupling of the transverse vector potential $\mathbf{A}_{\perp}$ from the determination of the scalar potential ϕ and axial vector potential A_z by setting $\partial\mathbf{A}_{\perp}/\partial\varsigma$ to zero in the transverse induced current $\mathbf{J}_{\perp}$. It is important to note that simply setting $\mathbf{A}_{\perp}$ to zero is much too strong since this implies $\sigma\nabla_{\perp}\phi=0$ which leaves in fact little physics. Also notice that the transverse vector potential is still coupled to the axial vector and scalar potentials through the Lorentz gauge condition. Single particle dynamics will turn out not to depend upon the transverse vector potential for a paraxial beam so we need never actually compute $\mathbf{A}_{\perp}$.

Combining the equations with incorporation of this approximation yields

$$\beta\partial^2\frac{\partial \psi}{\partial \varsigma}=\frac{4\pi}{c}\left(\nabla_{\perp}\cdot(\sigma\nabla_{\perp}\phi)-\frac{\partial}{\partial z}J_z+\frac{1}{\gamma^2}\frac{\partial}{\partial \varsigma}J_z\right) \tag{5.14}$$

$$\beta\partial^2\frac{\partial \phi}{\partial \varsigma}=-\frac{4\pi}{c}\left(\nabla_{\perp}\cdot(\sigma\nabla_{\perp}\phi)-\frac{\partial}{\partial z}J_z+\frac{\partial}{\partial \varsigma}J_z\right) \tag{5.15}$$

$$J_z=J_b-\sigma\frac{\partial \phi}{\partial z}-\sigma\frac{\partial \psi}{\partial \varsigma} \tag{5.16}$$

$$\frac{\partial}{\partial \varsigma}\left(\psi+\frac{1}{\gamma^2}\phi\right)-\frac{\partial}{\partial z}(\psi+\phi)+\beta\nabla_{\perp}\cdot\mathbf{A}_{\perp}=0\,. \tag{5.17}$$

A second key approximation, the "frozen field" approximation, concerns the relative magnitudes of $\partial/\partial\varsigma$ and $\partial/\partial z$. We assume that the z dependence is much weaker than the ς dependence. Physically this is reasonable since the fields are expected to look like fixed patterns translating in the z direction, evolving only slowly in the "time" variable z, whereas the dependence upon the "slice" variable ς may be strong if there is axial field structure in the beam frame. Our assumption is that

$$\left(\frac{\partial}{\partial z}\right)_{\varsigma} \ll \left(\frac{\partial}{\partial \varsigma}\right)_{z} \tag{5.18}$$

and we will set $\partial/\partial z = 0$ in the field equations, therefore $\partial^2 = \nabla_\perp^2 + 1/\gamma^2 \partial^2/\partial\varsigma^2$.

As we are interested only in low frequency modes we drop displacement terms $\partial^2/\partial\varsigma^2 \ll \nabla_\perp^2 \sim 1/a^2$ also. The field equations are therefore

$$\nabla_\perp^2 (\psi + \phi) = -\beta \frac{4\pi}{c} J_z \tag{5.19}$$

$$\beta \nabla_\perp^2 \frac{\partial}{\partial \varsigma}\psi = \frac{4\pi}{c}\left(\nabla_\perp \cdot (\sigma \nabla_\perp \phi) + \frac{1}{\gamma^2}\frac{\partial}{\partial \varsigma} J_z\right) . \tag{5.20}$$

Finally, we drop $1/\gamma^2$ terms for ultra-relativistic beams (we keep β displayed even though $\beta \sim 1$). The result is the well known EMPULSE equations of Lee [5.1].

$$\nabla_\perp^2 (\psi + \phi) - \frac{4\pi}{c}\sigma \frac{\partial \psi}{\partial \varsigma} = -\frac{4\pi}{c} J_b \tag{5.21}$$

$$\nabla_\perp^2 \frac{\partial \psi}{\partial \varsigma} = \frac{4\pi}{c} \nabla_\perp \cdot (\sigma \nabla_\perp \phi) . \tag{5.22}$$

Note that one cannot set $\phi \equiv 0$ in these equations consistently; however one may have $\phi \sim 0$ as an approximation.

5.3 Linearized EMPULSE Field Equations

In order to study the linear hose instability, which is an $m = 1$ nonaxisymmetric mode, we expand J_b , σ , ϕ and ψ up to dipole terms

$$J_b = J_b(r) + J_{b1}(r, \varsigma, z)cos\theta \tag{5.23}$$

$$\sigma = \sigma_o(r) + \sigma_1(r, \varsigma, z)cos\theta \tag{5.24}$$

$$\psi = \psi_o(r) + \psi_1(r, \varsigma, z)cos\theta \tag{5.25}$$

$$\phi = \phi_o(r) + \phi_1(r, \varsigma, z)cos\theta \tag{5.26}$$

and linearize the field equations to arrive at

$$\frac{1}{r}\frac{\partial}{\partial r}r\frac{\partial}{\partial r}(\psi_o + \phi_o) = -\frac{4\pi}{c}\left(J_{bo} - \sigma\frac{\partial\psi_o}{\partial\varsigma}\right) \tag{5.27}$$

$$\frac{1}{r}\frac{\partial}{\partial r}r\frac{\partial}{\partial r}\frac{\partial\psi_o}{\partial\varsigma} = \frac{4\pi}{c}\frac{1}{r}\frac{\partial}{\partial r}r\sigma_o\frac{\partial\phi_o}{\partial\varsigma} \tag{5.28}$$

$$\frac{\partial}{\partial r}\frac{1}{r}\frac{\partial}{\partial r}r(\psi_1 + \phi_1) - \frac{4\pi}{c}\sigma_o\frac{\partial\psi_o}{\partial\varsigma} = -\frac{4\pi}{c}J_{b1} + \frac{4\pi}{c}\sigma_1\frac{\partial\psi_o}{\partial\varsigma} \tag{5.29}$$

$$\frac{\partial}{\partial r}\frac{1}{r}\frac{\partial}{\partial r}r\frac{\partial\psi_1}{\partial\varsigma} = \frac{1}{r}\frac{\partial}{\partial r}r\left(\frac{4\pi}{c}\sigma_o\frac{\partial\phi_1}{\partial r} + \frac{4\pi}{c}\sigma_1\frac{\partial\phi_o}{\partial r}\right) - \frac{4\pi}{c}\sigma_o\frac{\phi_o}{r^2}\,. \tag{5.30}$$

Physically meaningful solutions are selected by appropriate boundary conditions. These conditions are: regularity at the origin $r = 0$ and vacuum boundary conditions at $r = R$. By vacuum boundary conditions we mean boundary conditions linking the solution in the plasma to the solution in the cold gas surrounding the plasma. This gas is considered to resist breakdown for the field strengths of interest and therefore acts electromagnetically as a vacuum (the dielectric constant and magnetic permeability are those of vacuum).

We could also use infinite conductivity conditions at $r = R$, in which case the potentials vanish at $r = R$. This is the case for propagation in a tank with a stainless steel wall, the conductivity of which is typically six to ten orders of magnitude greater than that of a plasma [5.2].

Boundary conditions for the vacuum case are

$$\frac{\partial \psi_o}{\partial r}(0) = \frac{\partial \phi_o}{\partial r}(0) = 0 \tag{5.31}$$

$$\psi_1(0) = \phi_1(0) = 0 \tag{5.32}$$

$$\psi_o(R) = \phi_o(R) = 0 \tag{5.33}$$

$$\frac{1}{r}\frac{\partial}{\partial r} r \left(\psi_1 + \phi_1\right)(R) = 0 \tag{5.34}$$

$$\left(\frac{\partial}{\partial \varsigma}\frac{1}{r}\frac{\partial}{\partial r} r \psi_1 - \frac{4\pi}{c}\sigma_o \frac{\partial \phi_1}{\partial r} - \frac{4\pi}{c}\sigma_1 \frac{\partial \phi_o}{\partial r}\right)(R) = 0 \,. \tag{5.35}$$

In the vacuum region the scalar and pinch potentials have the simple forms

$$\psi_o = 0 \tag{5.36}$$

$$\psi_1 \propto \frac{1}{r} \tag{5.37}$$

$$\phi_o \propto log\left(\frac{r}{R}\right) \tag{5.38}$$

$$\phi_1 \propto \frac{1}{r} \tag{5.39}$$

where the constant coefficients are gotten by matching with the solutions for $r < R$ by means of the jump conditions at $r = R$

$$[\psi_o] = 0 \tag{5.40}$$

$$[\psi_1] = 0 \tag{5.41}$$

$$[\frac{\partial \psi_o}{\partial r} + \frac{\partial \phi_o}{\partial r}] = 0 \tag{5.42}$$

$$[\frac{1}{r}\frac{\partial}{\partial r} r\,(\psi_1 + \phi_1)] = 0\,. \tag{5.43}$$

5.4 Pure Pinch Field Equations

If we are considering a well charge-neutralized beam for which $f_c \sim -1$ then $\lambda \sim 1$ and $\phi \sim 0$. Such a beam equilibrium is said to be a "pure pinch"; for this situation the full field equations simplify considerably. The field equations collapse to Ampère's equation

$$\left(\nabla_\perp^2 - \frac{4\pi}{c}\beta\sigma\frac{\partial}{\partial\varsigma}\right) A_z = -\frac{4\pi}{c} J_b\,. \tag{5.44}$$

Employing the dipole expansions as before we may linearize the Ampère equation

$$\left(\nabla_r^2 - \frac{4\pi}{c}\beta\sigma_o\frac{\partial}{\partial\varsigma}\right) A_o = -\frac{4\pi}{c} J_{bo} \tag{5.45}$$

$$\left(\nabla_r^2 - \frac{1}{r^2} - \frac{4\pi}{c}\beta\sigma_o\frac{\partial}{\partial\varsigma}\right) A_1 = -\frac{4\pi}{c} J_{b1} + \frac{4\pi}{c}\beta\frac{\partial A_o}{\partial\varsigma}\sigma_1\,. \tag{5.46}$$

We employ a few simple tricks to eliminate the dipole conductivity σ_1 . First, notice that $\beta\partial A_o/\partial\varsigma = -E_{zo} = -J_{po}/\sigma_o = -J_{po}/J_{bo}/\varsigma = -f_m/\varsigma$, where we have made use of the conductivity law $\partial\sigma/\partial\varsigma = \kappa J_b$ which results in $\sigma_o = \kappa\varsigma J_{bo}$ for the monopole if we neglect any conductivity present prior to passage of the pulse under consideration. Next, apply $1 + \partial/\partial\varsigma$ to the dipole equation to get

$$\left(1+\varsigma\frac{\partial}{\partial\varsigma}\right)\left(\frac{\partial}{\partial r}\frac{1}{r}\frac{\partial}{\partial r} r - \frac{4\pi}{c}\beta J_{bo}(r)\kappa\varsigma\frac{\partial}{\partial\varsigma}\right) A_1 = -\frac{4\pi}{c}\left(1 + f_m + \varsigma\frac{\partial}{\partial\varsigma}\right) J_{b1} \tag{5.47}$$

which is the basic field equation employed in subsequent work work involving plasma current and conductivity generation.

For various hose models which neglect conductivity generation effects the appropriate field equation is just

$$\left(\frac{\partial}{\partial r}\frac{1}{r}\frac{\partial}{\partial r}r - \frac{4\pi}{c}\beta\sigma_o\frac{\partial}{\partial\varsigma}\right)A_1 = -\frac{4\pi}{c}J_{b1} \tag{5.48}$$

where $\sigma_o = \sigma_o(r)$ is independent of slice position in the beam, perhaps even interpreted as a radial average, or radially uniform profile.

There are essentially as many distinct models of linear hose instability as distinct methods of computing the perturbed current source J_{b1} which appears in the basic field equations 5.47 and 5.48.

5.5 References

5.1 E.P.Lee, "The New Field Equations", UCID-17286 (1976)

5.2 E.P.Lee, "Hose Theory", Lawrence Livermore National Laboratory, UCID-16268 (1973)

Chapter 6

Rigid-Beam Model

6.1 Introduction

Early work on the hose instability exploited the fact that a great deal of the relevant physics is contained in the simple picture of the beam bending as an internally rigid rod. Since the rigid-beam hose model is historically the first treatment of linear hose instability, and since the development of this theory is not readily available in the literature, we will present an original and fairly complete account here. Rigid-hose ideas form the basis for much of our subsequent work and a full understanding of these ideas will prove beneficial later.

As implied by the name, in rigid-beam theory the fundamental assumption is that particles maintain the same relative positions with respect to one another in the hosing beam as in the unperturbed beam. The beam undergoes hose instability as a single entity, with a single response frequency, since the particles

all respond identically.

The basic mechanism for the hose instability, in the context of rigid-beam theory, may be described as follows. (i) The electron beam suffers a lateral displacement with respect to its equilibrium position; (ii) As a result, dipole fields are induced in the plasma; (iii) Dipole fields result in a restoring force the strength of which is proportional to the relative displacement between the beam current and the monopole field axes; (iv) The monopole field axis tries to rejoin the beam current axis, but may only do so on a resistive monopole decay time scale; (v) By the time the field axis has diffused towards the displaced current axis, the current is already responding to the restoring force and is swinging back; (vi) The current and field displacements get out of phase and the result is an underdamped oscillation, or, in the case of instability, an overstable oscillation in which the beam is always drawn back to the axis but overshoots with a greater amplitude each swing.

Without loss of any key physics we will investigate a charge neutral $f_c = -1$ beam with no plasma current $f_m = 0$. For this situation plasma generation effects play no part in the description of the instability. The equations which form the basis of the rigid-beam model are the single particle force equation and the Ampère monopole and dipole equations with constant conductivity

$$\frac{\partial^2 \mathbf{r}}{\partial z^2} = \frac{q}{\gamma m c^2 \beta} \frac{\partial A}{\partial \mathbf{r}} \tag{6.1}$$

$$\left(\frac{1}{\rho} \frac{\partial}{\partial \rho} \rho \frac{\partial}{\partial \rho} - \frac{4\pi a^2 \sigma_o}{c} \frac{\partial}{\partial \zeta} \right) A_o = -\frac{4\pi}{c} J_{bo} \tag{6.2}$$

$$\left(\frac{\partial}{\partial\rho}\frac{1}{\rho}\frac{\partial}{\partial\rho}\rho - \frac{4\pi a^2\sigma_o}{c}\frac{\partial}{\partial\zeta}\right)A_1 = -\frac{4\pi}{c}a^2 J_{b1}\ . \tag{6.3}$$

In general a hosing beam will displace transversely in two directions in a complicated pattern. For simplicity we will consider a plane polarized hose instability. For this case it suffices to consider lateral displacement in the x direction. To get the x displacement of the beam center of mass we must ensemble average the x component of the force equation 6.1 over the distribution J_b of particles in the beam, this yields

$$\frac{\partial^2 y}{\partial z^2} = \frac{1}{2}\frac{q}{\gamma mc^2\beta a}\frac{2\pi a^2}{I_b}\int_0^\infty d\rho\rho\left(J_{b1}\frac{dA_o}{d\rho} - A_1\frac{dJ_{bo}}{d\rho}\right) \tag{6.4}$$

where we have defined y to be the center of mass of the beam. This is the basic force equation we will use. This equation is not specific to the rigid-beam model; in fact it is quite generic, having no particular assumptions built into it at this point in the development. The model specificity enters in the calculation of A_1 and J_{b1} .

Now we must incorporate the crucial assumption of rigid-beam theory, that the beam displaces laterally as an internally rigid but bendable rod. Mathematically, a rigid displacement of a function $f(\mathbf{r})$ in the direction $\mathbf{x}$ is described by $f(\mathbf{r}) \longrightarrow f(\mathbf{r}-\mathbf{x}) \equiv f^*(\mathbf{r})$ which, when linearized yields

$$f^*(\mathbf{r}) = f(\mathbf{r}) - \mathbf{x}\cdot\frac{\partial f}{\partial \mathbf{r}} + \cdots\ . \tag{6.5}$$

By means of this formula the perturbed current for a rigid beam displacement is

$$J_{b1} = -y(\zeta, z)\frac{1}{a}\frac{dJ_{bo}}{d\rho} \tag{6.6}$$

where y is the lateral displacement of the beam center of mass in the x direction.

6.2 Continuous Rigid Beam

In Section 6.2 we will consider the case of a continuous, rigid beam. A continuous beam is one for which the current is independent of ς . Such a beam is a long continuous current pulse. The distinction here is between a single long pulse and a sequence of short pulses.

The simplest method of computing A_1 is to assume that the field undergoes a rigid displacement also

$$A_1 = -d(\varsigma, z)\frac{1}{a}\frac{dA_o}{d\rho} \tag{6.7}$$

where d is the lateral displacement of the field axis. It is not necessary to model A_1 in this fashion for a rigid beam displacement and we will ultimately calculate A_1 from J_{b1} ; however, this simple fundamental mode expression has been used and yields several interesting results. This model should rightly be called the "Lewis model" since it was developed by H.W.Lewis in unpublished work. Historically, this is probably the first model of hose instability. Despite its inherent simplicity the Lewis model contains much of the relevant physics. Aside from its simple structure the main importance of the Lewis model is that an initial value problem may be easily posed which is immediately applicable to experiment [6.1].

Introducing the expression 6.7 for A_1 in 6.4 yields the rigid beam 6.7 force equation

$$\frac{\partial^2 y}{\partial z^2} + \tilde{\Omega}_s^2 (y - d) = 0 \tag{6.8}$$

where Ω_s denotes the rigid-beam "shaking" frequency and $\tilde{\Omega}_s$ the corresponding

wavenumber defined by

$$\tilde{\Omega}_s^2 = \frac{1}{2}\frac{q}{\gamma mc^2\beta a}\frac{2\pi a^2}{I_b}\int_0^\infty d\rho\rho\frac{dJ_{bo}}{d\rho}\frac{dA_o}{d\rho}\,. \tag{6.9}$$

Likewise, in terms of the assumed forms for J_{b1} and A_1 the field equation 6.3 becomes

$$\frac{\partial d}{\partial \varsigma} + \frac{1}{\varsigma_1}(d-y) = 0 \tag{6.10}$$

where ς_1 is the "rigid-beam dipole decay length", defined by

$$\frac{1}{\varsigma_1} = \frac{2\pi a^2}{I_b}\frac{1}{\sigma_o}\int_0^\infty d\rho\rho J_{bo}\frac{dJ_{bo}}{d\rho}\frac{d\rho}{dA_o}\,. \tag{6.11}$$

Specializing to the Bennett equilibrium we have the shaking wavenumber $\tilde{\Omega}_s^2 = \tilde{\Omega}_{\beta o}^2/3$ and the rigid dipole decay length $\varsigma_1 = (3\pi a^2\sigma_o)/c$. In terms of these quantities the rigid-beam hose equations are

$$\frac{\partial^2 y}{\partial z^2} + \tilde{\Omega}_s^2(y-d) = 0 \tag{6.12}$$

$$\frac{\partial d}{\partial \varsigma} + \frac{1}{\varsigma_1}(d-y) = 0\,. \tag{6.13}$$

These equations have an immediate physical interpretation. The force equation 6.12 states that the beam center of mass undergoes driven harmonic oscillations with restoring force proportional to the relative displacement of the current and field axes; when $y - d = 0$ the beam axis is unaccelerated. The field equation 6.13 states that the field axis tries to follow the current axis but may only do so diffusively.

Integrating the field equation for d and substituting in the force equation results in the "hose equation" for a continuous rigid beam

$$\frac{\partial^2 y}{\partial z^2} + \tilde{\Omega}_s^2 y = \tilde{\Omega}_s^2\int_0^\varsigma d\varsigma'\frac{1}{\varsigma_1}e^{\frac{1}{\varsigma_1}(\varsigma'-\varsigma)}y(\varsigma') \tag{6.14}$$

where the term on the right side is a defocussing term due to the induced dipole field and the term $\tilde{\Omega}_s^2 y$ on the left hand side is a focussing term due to the monopole fields.

We may easily solve the hose equation 6.14 by means of Laplace transforms for a situation of experimental interest. Consider modulating the beam at $z = 0$ as it streams past. Suppose that the ends of the beam not displaced. Then the correct initial conditions are easily seen to be $y(\varsigma, 0) = \exp(-i\omega_f \varsigma/\beta c)$ where ω_f is the forcing (driving) frequency, $y(\varsigma, z) = 0$ for $\varsigma < 0$ (since the beam head is $\varsigma = 0$), and $y(0, z) =$ constant . The solution satisfying these initial and boundary conditions is

$$y(\varsigma, z) = \exp\left(-i\tilde{\omega}_f \varsigma + i\left(1 + \frac{i}{\tilde{\omega}_f \varsigma_1}\right)^{-\frac{1}{2}}\right) \tag{6.15}$$

for $\varsigma/\varsigma_1 \gg \tilde{\Omega}_\beta z$ which means physically that enough of the beam has streamed past the point z that any transients have died out. This result was apparently first derived, but never published, by Lewis. Mathematically detailed results [1] concerning the solutions of the hose equation 6.14 were obtained by Yadavalli [6.2].

Introducing the Fourier dependence $y \sim d \sim \exp\left(-i\tilde{\omega}\varsigma - i\tilde{\Omega} z\right)$ equation 6.14 yields the rigid-beam dispersion relation

$$-i\tilde{\omega}\varsigma_1 = \frac{\Omega^2}{\Omega_s^2 - \Omega^2} \,. \tag{6.16}$$

This dispersion relation is plotted in Fig. 6.1 for real Ω . A more usual experimental situation to consider is that of a beam which is modulated at a fixed position

[1] cf. also [6.10], [6.11] , and [6.12].

z in the laboratory as it streams past. The driver frequency is ω which is real and the growth in z as a given slice streams away from the point of modulation is determined by $Im\left(k(\omega)\right)$. Since k always occurs in conjugate pairs we always consider the root with $Im\left(k(\omega)\right) < 0$ since this root yields growth for $z > 0$. Solving 6.16 for $Im^2\left(k(\omega)\right) = Im^2\left(\tilde{\Omega}\right)$ results in

$$Im^2\tilde{\Omega} = \frac{1}{2}\tilde{\Omega}_s^2\left(\sqrt{\frac{\omega^2\tau_1^2}{1+\omega^2\tau_1^2}} - \frac{\omega^2\tau_1^2}{1+\omega^2\tau_1^2}\right) . \tag{6.17}$$

From this equation we may compute the driver frequency ω_s which yields the maximum growth in z . Setting $\mathrm{dIm(k)/d}\omega_s = 0$ results in $\omega_s\tau_1 = \pm\sqrt{1/3}$. The corresponding growth rate is $\mathrm{max(Im(k))}=\sqrt{1/8}\tilde{\Omega}_s$. In Fig. 6.2 is plotted $\mathrm{Im}\Omega/\Omega_{\beta o}$ versus $\omega\tau_1$, where, recall that $\Omega_{\beta o}^2 = 3\Omega_s^2$. Notice that the growth rate approaches zero asymptotically as the driver frequency is increased. On physical grounds, one expects there to be high frequency cutoff, a driver frequency beyond which the positive growth becomes negative (damped). Such a cutoff was first predicted theoretically by Lee [6.3], and was first experimentally discovered in a series of experiments with Astron in 1976 [6.4]. It is a major failing of the rigid-beam model that no such cutoff is predicted.

In Figs. 6.2,6.3, and 6.4 experimental data from the Astron [2] experiment is

[2] Astron was a controlled nuclear fusion program conceived by N.C.Cristofilos [6.5] in 1958. The key idea of Astron was the creation of a cylidrical layer of relativistic electrons by injecting long pulses into a tank with a strong solenoidal field B_z . The injection was to be tangential to the circumference of a cylinder plus a slight axial component. The beam would therefore wrap itself around in a cylinder. The axial motion of the rotating cylinder of electrons was to be slowed by a system of resistors. Mirror trapping of the electrons would be accomplished and

compared with the rigid-beam model predictions. In the experiments a 300 nsec 6 MeV electron pulse was modulated sinusoidally as it passed through a 30 cm parallel-plate transmission line. The electric and magnetic fields of the electromagnetic wave deflected the beam to a maximum amplitude of 0.2 mradians. The resulting response of the beam as it streamed through a 12 meter tank filled with H_2 was analyzed to determine the growth rate dependence upon driver frequency (10's of MHz).

The dispersion relation 6.16 predicts infinite resonance as $\Omega \longrightarrow \Omega_s$ from below as indicated in Fig. 6.1. This is an unfortunate state of affairs since one never expects infinite resonance in a real system, such resonance would predict infinite growth rates. Another consequence of the infinite resonance is the prediction of absolute instability in the beam frame of reference, experimentally the growth is known to be convective [6.4]. Physically, the source of the infinite resonance may be traced to the fact that in the rigid-beam theory all particles respond at the rigid response frequency. It is the prediction of a unique response frequency that mathematically results in infinite resonance. M.N.Rosenbluth realized [3] that a

the electron current would provide magnetic field reversal. Plasma could be trapped within the cylinder and be heated to thermonuclear energies by Coulomb collisions with the relativistic electrons. Field reversal with high efficiency was never attained and this fusion concept was eventually superceded by others. The Astron-I accelerator however operated many years 1963-1968 at which time an upgraded Astron-II came on line which in turn operated many years 1968-1978 at which time Astron was finally dismantled. Astron paved the way for the current state-of-the-art induction linac the ATA (Advanced Test Accelerator) [6.6].

[3] Unpublished

spread in betatron frequency would have the effect of resolving the infinite resonance. Physically such a frequency spread may arise due to relativistic mass spread amongst the particles of the beam, or due to anharmonicity of the pinch potential. Assuming, for simplicity, that the betatron frequency is spread with a half-width $\Delta\Omega_s$ the dispersion relation should more properly read

$$-i\tilde{\omega}\varsigma_1 = \frac{\Omega^2}{(\Omega_s + \Delta\Omega_s)^2 - \Omega^2} \tag{6.18}$$

so that, as $\Omega \longrightarrow \Omega_s$ we have $-i\tilde{\omega}\varsigma_1 \leq \Omega_s/2\Delta\Omega_s$. This translates into a minimum growth length of order $(2\Delta\Omega_s/\Omega_s)\pi a^2\sigma_o/c$ as indicated in Fig. 6.6 which depicts qualitatively what the dispersion relation should look like with phase mixing effects included.

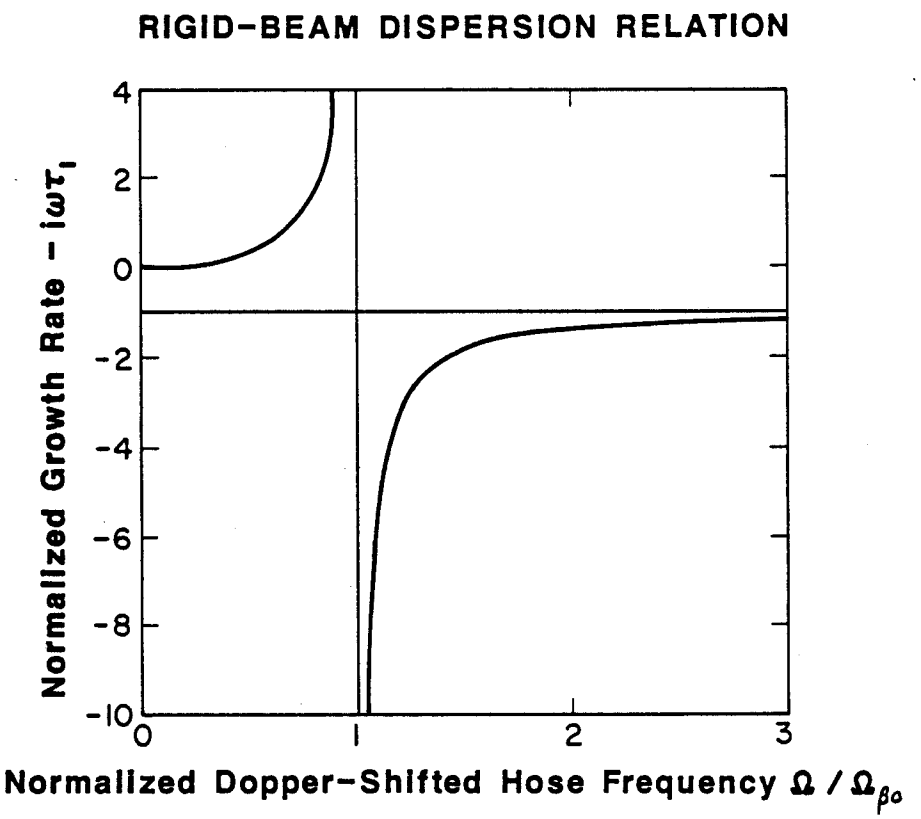

Figure 6.1: Dispersion relation for the continuous rigid beam. This result is dependable only in the low frequency limit $\Omega/\Omega_{\beta o} \ll 1$.

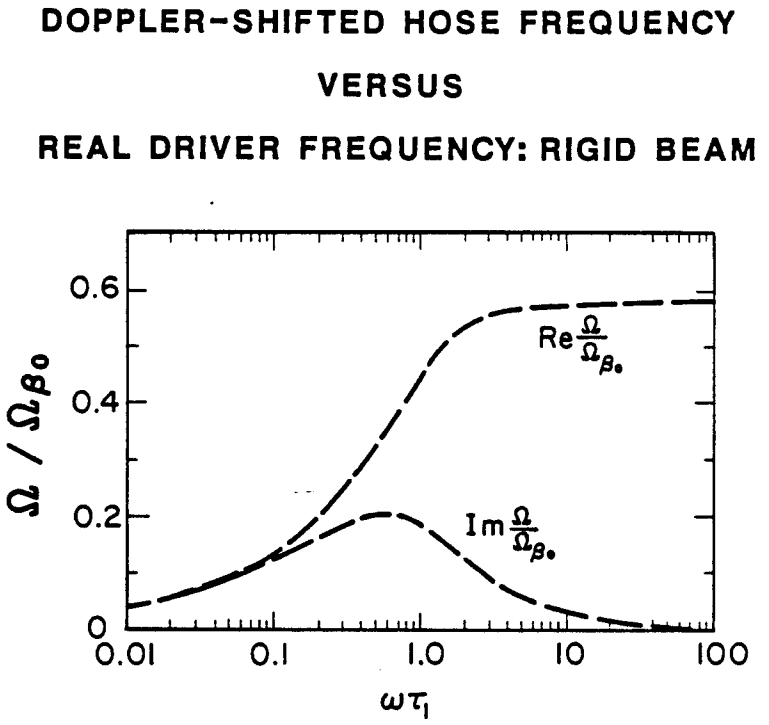

Figure 6.2: Normalized growth rate $\mathrm{Im}(\Omega/\Omega_{\beta c})$ plotted versus normalized driver frequency $\omega\tau_1$.

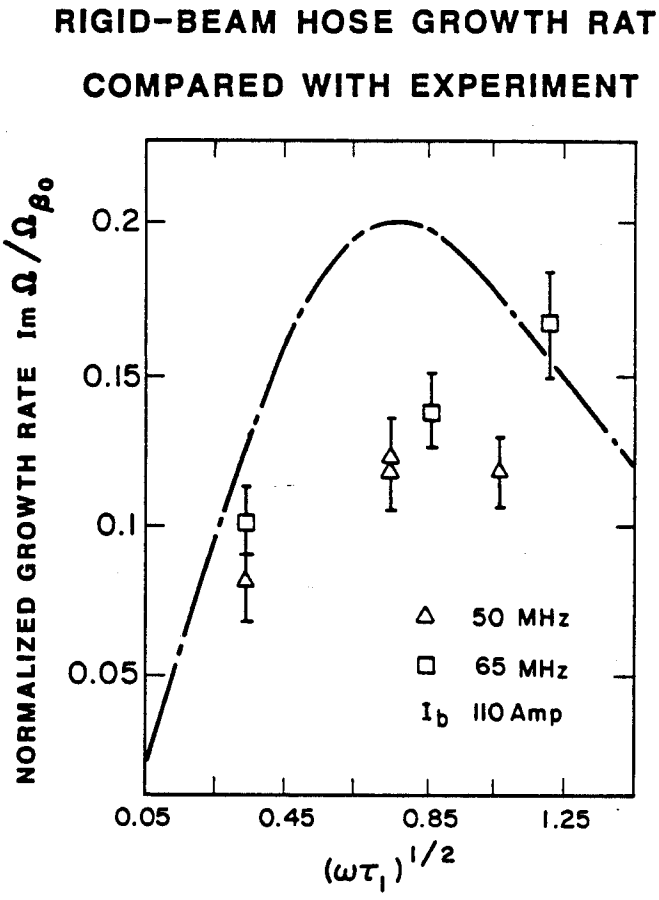

Figure 6.3: Comparison of Astron data with rigid-beam theory: A 6 MeV 110 Amp electron beam propagating in H_2 gas was sinusoidally perturbed with a driver frequency of 50 MHz and 65 MHz as it streamed through a 30 cm long parallel-plate transmission line. Maximum deflection amplitude was 0.2 mradian. Gas pressure was 1-2 Torr [6.1].

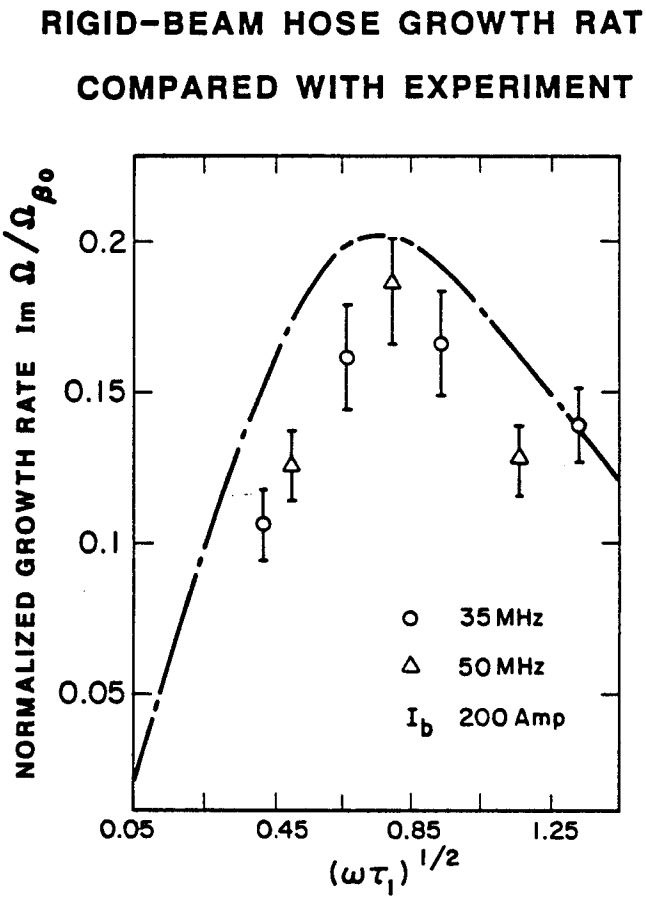

Figure 6.4: Comparison of Astron data with rigid-beam theory: A 6 MeV 200 Amp electron beam propagating in H_2 gas was sinusoidally perturbed with a driver frequency of 35 MHz and 50 MHz as it streamed through a 30 cm long parallel-plate transmission line. Maximum deflection amplitude was 0.2 mradian. Gas pressure was 1-2 Torr [6.1].

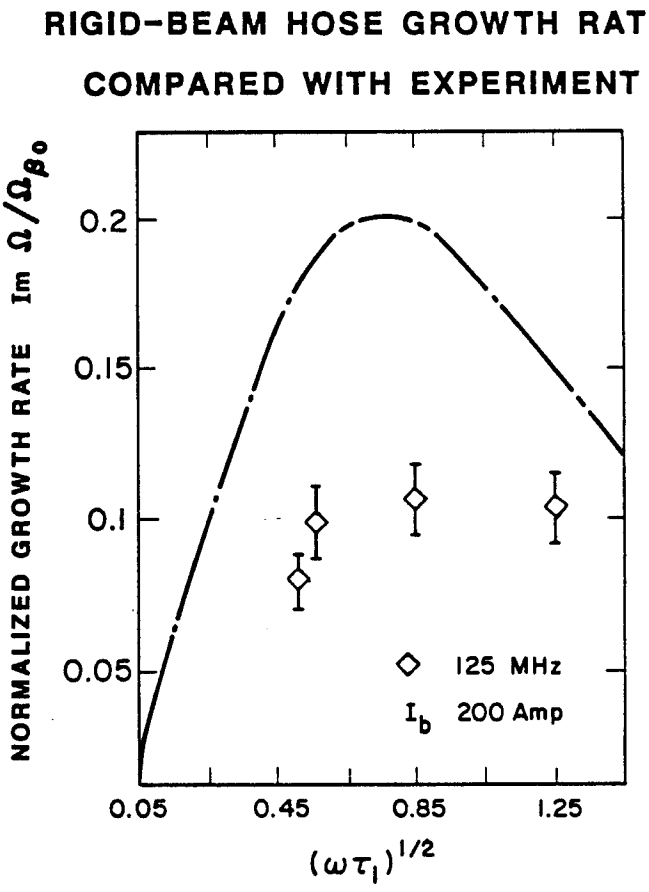

Figure 6.5: Comparison of Astron data with rigid-beam theory: A 6 MeV 200 Amp electron beam propagating in H_2 gas was sinusoidally perturbed with a driver frequency of 125 MHz as it streamed through a 30 cm long parallel-plate transmission line. Maximum deflection amplitude was 0.2 mradian. Gas pressure was 1-2 Torr [6.1].

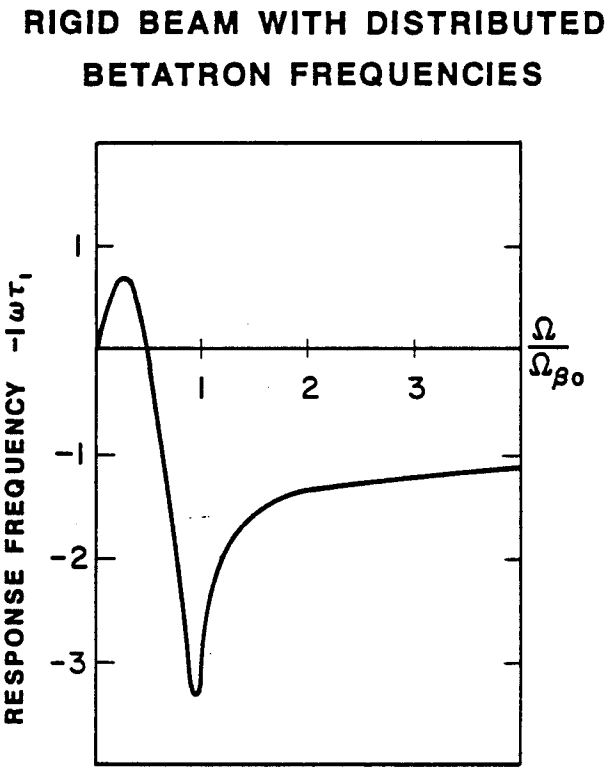

Figure 6.6: Dispersion relation for a continuous rigid beam with distributed betatron frequencies. Note the cutoff frequency beyond which the growth is damped.

6.3 Rotating Rigid Beam

The formalism developed in Section 6.2 may easily be generalized to include the effects of an applied solenoidal magnetic field B_z . This is important for several reasons. First, it is sometimes advantageous to apply a strong magnetic field in the accelerator to help overcome space charge effects which would otherwise destroy the beam [4]. Second, it is found that a strong solenoidal field can considerably lessen the severity of hose instability. Experimentally, one is interested in injecting the beam into a gas region which does not contain a B_z field. Conservation of canonical θ momentum shows that the beam must begin rotating as it leaves the accelerator [6.7]. It is for this reason that we refer here to rotating beams. The beam is not necessarily rotating within the accelerator, although with B_z a natural equilibrium does involve rotation.

The basic field equation 6.13 is unchanged by the presence of the applied magnetic field. The force equation 6.12 however must be changed to include the force due to B_z . Also, whereas we considered a plane polarized hose in Section 6.2, which was justifiable since the two transverse directions were not coupled in that case, now we cannot do this. We need to consider a general hose displacement in the transverse plane.

The main effect of the solenoidal field is to introduce another frequency into the problem. This frequency is related to the cyclotron frequency of the electrons

[4] A solenoidal field within the accelerator is also used to limit the destructiveness of the beam breakup instability. Beam breakup in the accelerator is caused by beam coupling to dipole cavity modes which impart a lateral displacement to the beam, cf. Chapter 1.

spiraling around the B_z field lines. We assume that the field strength B_z is uniform across the beam cross-section. This is reasonable since B_z is applied by a magnet structure the characteristic scale length of which is much greater than the beam radius. We also consider a charge neutral beam, as in Section 6.2, therefore the beam is in a pure magnetic pinch. Hence the Lorentz force is

$$\frac{\partial^2 \mathbf{r}}{\partial z^2} = \frac{q}{\gamma m \beta^2 c^3} (\mathbf{v}_\perp + \mathbf{v}_z) \times \mathbf{B} \tag{6.19}$$

where $\mathbf{B} = \mathbf{B}_\theta + \mathbf{B}_z$. The perpendicular velocity $\mathbf{v}_\perp$ is now of consequence due to the strong field B_z . Obviously the ensemble averaged force equation is the same as in Section 6.2 with the addition of a term due to the cyclotron force

$$\frac{\partial^2 \mathbf{R}}{\partial z^2} + \tilde{\Omega}_s^2 (\mathbf{R} - \mathbf{d}) + \frac{\partial \mathbf{R}}{\partial z} \times \tilde{\mathbf{\Omega}}_c = 0 \tag{6.20}$$

where the cyclotron vector $\tilde{\mathbf{\Omega}}_c$ is defined by

$$\tilde{\mathbf{\Omega}}_c = \frac{qB_z}{\gamma mc} \mathbf{z} \tag{6.21}$$

and the vector $\mathbf{R}$ is the centroid of the beam in the transverse plane. In place of the real vector $\mathbf{R}$ we prefer, following Lee [6.7], to introduce a complex scalar called a phasor, $y = y_x + iy_y$ where y denotes the centroid of the beam in the complex plane. The use of a phasor implies circular polarization, which is general enough for our immediate purposes. In terms of this phasor, after integrating the field equation for d as in Section 6.2, we get the rotating beam hose equation

$$\frac{\partial^2 y}{\partial z^2} - i\tilde{\Omega}_c \frac{dy}{dz} + \tilde{\Omega}_s^2 y = \tilde{\Omega}_s^2 \int_0^\varsigma d\varsigma' \frac{1}{\varsigma_1} e^{(\varsigma' - \varsigma)/\varsigma_1} y(\varsigma', z) \ . \tag{6.22}$$

Introducing the Fourier dependence $y \sim d \sim \exp\left(-i\tilde{\omega}\varsigma - i\tilde{\Omega}z\right)$ we arrive at the rigid beam dispersion relation for a rotating beam

$$-i\omega\tau_1 = \frac{\Omega^2 + \Omega\Omega_c}{\Omega_s^2 - \Omega^2 - \Omega\Omega_c} \,. \tag{6.23}$$

This dispersion relation is plotted in Fig. 6.7 for real Ω/Ω_c . Again, a more useful point of view is to consider real ω . Solving for k yields

$$\beta ck = \omega + \frac{1}{2}\left(\Omega_c \pm \sqrt{\Omega_c^2 - \frac{4\Omega_s^2 i\omega\tau_1}{1 - i\omega\tau_1}}\right) \,. \tag{6.24}$$

Considering the limit $\Omega_s/\Omega_c \ll 1$ we expand this result getting

$$\beta ck \approx \omega + \frac{1}{2}\left(\Omega_c \pm \Omega_c\left(1 - \frac{2\Omega_s^2}{\Omega_c^2}\frac{i\omega\tau_1}{1 - i\omega\tau_1}\right)\right) \tag{6.25}$$

from which we identify the growth rate

$$Im(k) = -\frac{\Omega_c}{\beta c}\left(\frac{\Omega_s}{\Omega_c}\right)^2 \frac{\omega\tau_1}{1 + \omega^2\tau_1^2} \,. \tag{6.26}$$

Computing the maximum growth for real driver frequency ω_s as before we find $\omega_s\tau_1 = 1$ for which

$$Im(k) = -\frac{1}{2}\frac{\Omega_c}{\beta c}\left(\frac{\Omega_s}{\Omega_c}\right)^2 \,. \tag{6.27}$$

For the beam without B_z we found that the maximum growth rate was max(Im(k)) $= 0.35355\ \tilde{\Omega}_s$. Here we find that this growth rate has been reduced by the factor $\Omega_s/\Omega_c \ll 1$. This explains why an applied B_z field is interesting. By applying a large enough field one can assure that $\Omega_s/\Omega_c \ll 1$ and stabilize the hose considerably.

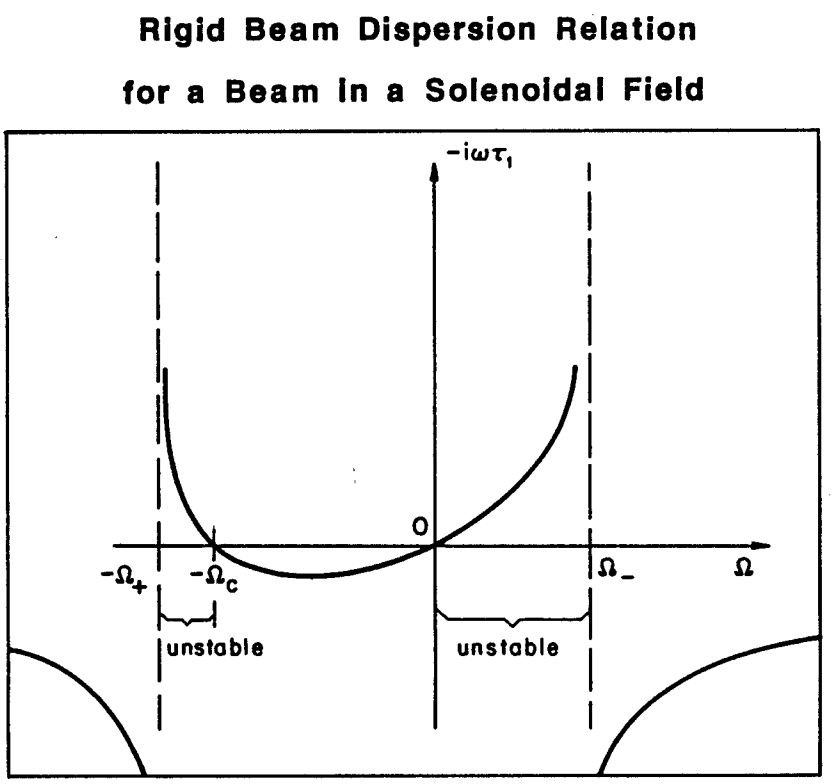

Figure 6.7: Dispersion relation for a rigid beam immersed in a solenoidal magnetic field B_z .

6.4 Chopped Rigid Beam

Experimentally it is observed that the hose instability is convective in nature. The maximum amplitude moves back from the head to the tail of the beam pulse, growing in amplitude and wavelength. A natural idea therefore is to attempt to limit the destructiveness of the mode by using pulses which are so short that appreciable growth cannot occur over the pulse length. There is no reflection of the hose "wave" at the beam tail so the instability is rendered harmless, it simply convects out of the beam before growing too large.

During early work attempting to understand the hose instability and to find techniques for curing it researchers conceived the idea of "chopping" the beam into short segments. Chopping a beam potentially cures the low frequency range of the hose spectrum. What chopping cannot cure is the short wavelength (high frequency) spectrum. Short wavelength growth may obviously destroy even a short pulse. Furthermore, chopping introduces some deleterious effects which are absent in a continuous beam, these include transmission of dipole fields from pulse to pulse, and low frequency resonant effects due to coupling between the pulses.

The continuous rigid-beam formalism may be easily modified to include beam chopping. We may consider a very long train made up of many short pulses. Fixing our attention upon a representative pulse somewhere in the train we must modify the formalism so that monopole and dipole fields from the pulses preceeding the pulse under observation are accounted for. It is usually [5] reasonable to assume that higher modes decay rapidly enough that only the monopole and

[5] cf., however, the result 6.60.

dipole fields from previous pulses are important.

Mathematically we may consider a chopped beam to be a very long continuous beam with current strongly modulated in ς . This modulation will be described by a function $f(\varsigma)$ called the "chopping function". For an evenly chopped beam the chopping function is periodic in the slice variable ς . We may be interested in chopping the beam in variable chop lengths to cure any resonant coupling effects between pulses due to steady periodicity. Physically, the accelerator may be operated with a random or programed variability in chop frequency.

Equilibrium beam current in a chopped beam is $J_{bo} = J_{bo}(r)f(\varsigma)$. Using this current the dipole field equation may easily be modified to include chopping. First notice that the perturbed current density J_{b1} is

$$J_{b1}(\rho, \varsigma, z) = -d(\varsigma, z)f(\varsigma)\frac{1}{a}\frac{dJ_{bo}}{d\rho} \tag{6.28}$$

therefore the field equation, following the argument used for the continuous beam, is replaced by

$$\frac{\partial d}{\partial \varsigma} + \frac{1}{\varsigma_1}(d - fy) = 0\,. \tag{6.29}$$

Integrating this equation for d yields

$$d = \int_{-\infty}^{\varsigma} d\varsigma' \frac{1}{\varsigma_1} e^{\frac{1}{\varsigma_1}(\varsigma' - \varsigma)} f(\varsigma') y(\varsigma') \tag{6.30}$$

where the integration runs to $-\infty$ as opposed to 0 in the continuous beam case.

In the force equation, the term $y\tilde{\Omega}_s^2$ on the left hand side is a focussing force due to the monopole fields. For a chopped beam the monopole fields at any (ς, z) will be those generated by the pulse at that location, plus any residual undecayed

fields from previous pulses. Formally, this means this term must be replaced according to

$$y\tilde{\Omega}_s^2 \longrightarrow y\tilde{\Omega}_s^2 \int_{-\infty}^{\varsigma} d\varsigma' \frac{1}{\varsigma_o} e^{\frac{1}{\varsigma_o}(\varsigma'-\varsigma)} f(\varsigma') \,. \tag{6.31}$$

Using the expressions 6.30 and 6.31 in the force equation 6.8 we get a heuristic form of the Weinberg equation [6.9] for a rigid chopped beam undergoing hose instability

$$\frac{\partial^2 y}{\partial z^2} + y\tilde{\Omega}_s^2 \int_{-\infty}^{\varsigma} d\varsigma' \frac{1}{\varsigma_o} e^{\frac{1}{\varsigma_o}(\varsigma'-\varsigma)} f(\varsigma') = \tilde{\Omega}_s^2 \int_{-\infty}^{\varsigma} d\varsigma' \frac{1}{\varsigma_1} e^{\frac{1}{\varsigma_1}(\varsigma'-\varsigma)} f(\varsigma') y(\varsigma') \,. \tag{6.32}$$

The structure of the rigid chopped beam force equation may be shown to be of this form, quite generally, without use of the assumed form 6.7 for A_1 . To accomplish this we will solve the monopole and dipole equations including the ς dependence directly.

6.5 General Structure of Chopped Rigid Beam Hose Equations

In order to bring out the overall structure of rigid-beam theory we have developed a Green function treatment to calculate $\partial A_o/\partial\rho$ and A_1 which are the necessary ingredients in the force equation. The basic set of equations which must be solved is

$$\left(\frac{1}{\rho}\frac{\partial}{\partial\rho}\rho\frac{\partial}{\partial\rho} - \frac{4\pi a^2\sigma_o}{c}\frac{\partial}{\partial\varsigma}\right) A_o = -\frac{4\pi}{c}a^2 f J_{bo} \tag{6.33}$$

$$\left(\frac{\partial}{\partial\rho}\frac{1}{\rho}\frac{\partial}{\partial\rho}\rho - \frac{4\pi a^2\sigma_o}{c}\frac{\partial}{\partial\varsigma}\right) A_1 = \frac{4\pi}{c}afy\frac{dJ_{bo}}{d\rho} \tag{6.34}$$

$$\frac{\partial^2 y}{\partial z^2} = -\frac{1}{2}\frac{q}{\gamma m c^2 \beta a}\frac{2\pi a^2}{I_b}\int_0^\infty d\rho\rho\left(A_1 + \frac{y}{a}\frac{\partial A_o}{\partial \rho}\right)\frac{dJ_{bo}}{d\rho}\,. \tag{6.35}$$

Notice that we really need to calculate not A_o but $\partial A_o/\partial\rho$. We will prove that A_1 and $\partial A_o/\partial\rho$ both have the same Green function. First, if we apply $\partial/\partial\rho$ to 6.33 we find that

$$\left(\frac{\partial}{\partial\rho}\frac{1}{\rho}\frac{\partial}{\partial\rho}\rho - \frac{4\pi a^2\sigma_o}{c}\frac{\partial}{\partial\varsigma}\right)\frac{\partial A_o}{\partial\rho} = -\frac{4\pi}{c}a^2 f\frac{dJ_{bo}}{d\rho} \tag{6.36}$$

therefore both A_1 and $\partial A_o/\partial\rho$ obey equations with the same partial differential operator. Notice that the independence of conductivity upon radius is crucial to this result. A solution, which we employed previously, is indeed that A_1 and $\partial A_o/\partial\rho$ are proportional to one another. In fact, a particular solution is simply $A_1 = -(y/a)\partial A_o/\partial\rho$, as can be seen by inspecting the source terms on the right hand sides of equations 6.34 and 6.36. This special solution corresponds to unaccelerated lateral displacement of the beam since the right hand side of the force equation 6.35 vanishes identically.

We have learned that the Green functions for A_1 and $\partial A_o/\partial\rho$ differ from one another, if at all, only because of differing boundary conditions. We will prove that A_1 and $\partial A_o/\partial\rho$ in fact have the same boundary conditions and therefore the same Green function $G(\rho,\rho';\varsigma,\varsigma')$ in a moment. For now let us assume this fact and complete the argument concerning the structure of the chopped hose equation.

In terms of the Green function the solutions for A_1 and $\partial A_o/\partial\rho$ are given by

$$\frac{y}{a}\frac{\partial A_o}{\partial\rho} = \frac{4\pi}{c}a\int_0^\infty d\rho'\rho'\int_0^\infty d\varsigma' G(\rho,\rho';\varsigma,\varsigma')\,f(\varsigma')y(\varsigma)\frac{dJ_{bo}}{d\rho'} \tag{6.37}$$

$$A_1 = -\frac{4\pi}{c} a \int_0^\infty d\rho' \rho' \int_0^\infty d\varsigma' G(\rho, \rho'; \varsigma, \varsigma') f(\varsigma') y(\varsigma') \frac{dJ_{bo}}{d\rho'} \tag{6.38}$$

where the crucial point to notice is the dependence upon $f(\varsigma)$ and $y(\varsigma)$, in fact, inserting these expressions into the force equation 6.35 we see that the overall structure is the same as the heuristic result 6.32. To see this explicitly we will define the current profile in terms of a dimensionless shape function $j_{bo}(\rho)$ by writing $J_{bo}(\rho) = (I_b/\pi a^2) j_{bo}(\rho)$, the resulting force equation reads

$$\frac{\partial^2 y}{\partial z^2} + y\tilde{\Omega}_s^2 \int_0^\infty d\rho\rho \frac{dj_{bo}}{d\rho} \int_0^\infty d\rho' \rho' \frac{dj_{bo}}{d\rho'} \int_0^\infty d\varsigma' G(\rho, \rho'; \varsigma, \varsigma') f(\varsigma') \,. \tag{6.39}$$

$$= \tilde{\Omega}_s^2 \int_0^\infty d\rho\rho \frac{dj_{bo}}{d\rho} \int_0^\infty d\rho' \rho' \frac{dj_{bo}}{d\rho'} \int_0^\infty d\varsigma' G(\rho, \rho'; \varsigma, \varsigma') f(\varsigma') y(\varsigma')$$

which displays the advertized structure.

To calculate the Green function, and prove the assertions above, let us now describe the types of boundary conditions of interest in more detail. As mentioned earlier, conductivity generation effects are not accounted for in rigid-beam theory. Certainly, to lowest order in theory, the dominant "term" is uniform conductivity out to some radius beyond which beam current is negligible. This is exactly the case for propagation in a plasma filled tank, and is quite reasonable even for propagation in gas since the conductivity will vanish at a radial position for which the beam current is insufficient to generate free electrons, and as this radius is larger than the radial extent within which the current is primarly carried the bulk of the beam current is exposed to conductivity which is, to a good approximation, radially uniform. On the basis of these arguments we may state that the generic situation of interest is that of a beam propagating in a

radially uniform conductivity channel which extends at least some distance beyond the bulk of the beam. It is only a slight idealization to model this as a beam propagating in a radially uniform conductivity channel which extends beyond the radius at which the beam current vanishes.

The question now is, what boundary conditions are to be placed upon the potentials at the edge of the conductivity channel? Three cases arise. First, for a plasma channel which fills a stainless steel tank, the potentials must vanish at the tank wall. Second, for a plasma channel surrounded by cold gas, the potentials must match by jump conditions with the vacuum solutions in the gas. Third, there is a possibility that the plasma region is effectively infinite, in which case the fields must behave properly at infinity. We will not deal with this case in this work.

For cases one and two we now discuss the boundary conditions and show that for A_1 and $\partial A_o/\partial\rho$ they are the same. For the conducting tank wall all potentials and their radial derivatives vanish on the wall. For this situation the boundary conditions are clearly the same for A_1 and $\partial A_o/\partial\rho$ since at the origin they both vanish also. For the second case, we need only show that the conditions at the plasma -gas interface are the same since again they clearly are at the origin. The azimuthal magnetic field must be continuous across the gas-plasma interface. In the gas the vacuum solution for the monopole magnetic field is $B_\theta = (2I_b/c)/r$ therefore the logarithmic derivative at the interface is $(1/B_\theta)dB_\theta/dR = -1/R$. Within the plasma the monopole field is $B_\theta = -\partial A_o/\partial r$ therefore the logarithmic derivative of $\partial A_o/\partial\rho$ at the interface is equal to $-a/R$. But this is the same as

the boundary condition on A_1 . Therefore, we have shown that A_1 and $\partial A_o/\partial\rho$ have the same boundary conditions for ρ.

To calculate the Green function we Laplace transform according to

$$\hat{f}(s) = \int_0^\infty ds e^{-s\varsigma} f(\varsigma) \tag{6.40}$$

whereupon the Laplace transform $\hat{G}$ of the Green function satisfies

$$\left(\frac{d}{d\rho}\frac{1}{\rho}\frac{d}{d\rho}\rho - q^2(s)\right)\hat{G} = -\frac{1}{\rho}\delta\left(\rho - \rho'\right) \tag{6.41}$$

where $q^2(s) = 4\pi a^2\sigma_o s/c$. The Green function may thus immediately be written as a product of the independent solutions ψ_1 and ψ_2 of the homogeneous equation

$$\left(\frac{d}{d\rho}\frac{1}{\rho}\frac{d}{d\rho}\rho - q^2(s)\right)\psi = 0 \tag{6.42}$$

with the result being of the form

$$\hat{G}\left(\rho, \rho'; s\right) = \psi_1\left(q(s)\rho_<\right)\psi_2\left(q(s)\rho_>\right) \tag{6.43}$$

where $\psi_1\left(q(s)\rho_<\right)$ satisfies the boundary condition for $\rho < \rho'$ and $\psi_2\left(q(s)\rho_>\right)$ satisfies the boundary condition for $\rho > \rho'$. The functions ψ_1 and ψ_2 must be normalized so that $\hat{G}$ exhibits the jump in derivative implied by 6.41

$$\left(\frac{d\hat{G}}{d\rho}\right)_{\rho+\epsilon} - \left(\frac{d\hat{G}}{d\rho}\right)_{\rho-\epsilon} = -\frac{1}{\rho}\,. \tag{6.44}$$

Specifically, we find that

$$\hat{G}\left(\rho, \rho'; s\right) = I_1\left(q(s)\rho_<\right)\left(K_1\left(q(s)\rho_>\right) - \alpha\left(q(s)\right)I_1\left(q(s)\rho_>\right)\right)\,. \tag{6.45}$$

where I_1 is the modified Bessel function of the first kind of order one, K_1 is the modified Bessel function of the second kind of order one, and $\alpha(q)$ must be chosen

so that the second factor in $\hat{G}$ satisfies the boundary condition at $\rho = a/R$. Here $\rho_<$ and $\rho_>$ refer to the lesser and greater of ρ and ρ' as usual.

In Chapter 6 we will only consider the case of propagation in a channel surrounded by cold gas, reserving for a discussion (in Chapter 7) of the effects of wall stabilization the case of a channel bounded by a conducting tank. For the case of plasma surrounded by gas, denoting by ψ_2 the second factor in $\hat{G}$, the boundary condition at $\rho = R/a$ is $\partial\psi_2/\partial\rho = -(a/R)\psi_2$. Using this to calculate α results in

$$\hat{G}\left(\rho,\rho';s\right) = I_1\left(q(s)\rho_<\right)K_1\left(q(s)\rho_>\right) + \frac{K_o\left(q(s)\frac{R}{a}\right)}{I_o\left(q(s)\frac{R}{a}\right)}I_1\left(q(s)\rho\right)I_1\left(q(s)\rho'\right) \ . \quad (6.46)$$

The Laplace transformed equations for $\hat{A}_1$ and $\partial\hat{A}_o/\partial\rho$ may now be solved in terms of the Laplace transformed Green function. These equations are

$$\left(\frac{d}{d\rho}\frac{1}{\rho}\frac{d}{d\rho}\rho - q^2(s)\right)\frac{d\hat{A}_o}{d\rho} = -\frac{4\pi}{c}a^2\hat{f}J_{bo} \quad (6.47)$$

$$\left(\frac{d}{d\rho}\frac{1}{\rho}\frac{d}{d\rho}\rho - q^2(s)\right)\hat{A}_1 = \frac{4\pi}{c}a\tilde{fy}\frac{dJ_{bo}}{d\rho} \ . \quad (6.48)$$

Solving these equations for $\hat{A}_1$ and $\partial\hat{A}_o/\partial\rho$ and formally inverting the Laplace transforms we arrive at

$$\frac{\partial A_o}{\partial\rho} = \frac{4\pi}{c}a^2\int_0^\infty d\rho'\rho'\frac{dJ_{bo}}{d\rho'}\int_0^\infty d\varsigma' f(\varsigma')\int_{s_o-i\infty}^{s_o+i\infty}\frac{ds}{2\pi i}e^{s(\varsigma-\varsigma')}\hat{G}\left(\rho,\rho';s\right) \quad (6.49)$$

$$A_1 = -\frac{4\pi}{c}a\int_0^\infty d\rho'\rho'\frac{dJ_{bo}}{d\rho'}\int_0^\infty d\varsigma' f(\varsigma')y(\varsigma')\int_{s_o-i\infty}^{s_o+i\infty}\frac{ds}{2\pi i}e^{s(\varsigma-\varsigma')}\hat{G}\left(\rho,\rho';s\right) \ . \quad (6.50)$$

From these we identify the Green function G

$$G\left(\rho,\rho';\varsigma-\varsigma'\right) = \int_{s_o-i\infty}^{s_o+i\infty}\frac{ds}{2\pi i}e^{s(\varsigma-\varsigma')}\hat{G}\left(\rho,\rho';s\right) \quad (6.51)$$

where $\hat{G}$ is given by 6.46. We may anticipate that this Laplace inversion will involve a sum over residues of poles of $\hat{G}$ in the complex s-plane. These poles will therefore appear in the theory as reciprocal decay lengths.

Physically, the response of a given beam slice cannot be influenced by following slices. This is because the slices do not interact with one another directly, only through the intermediary of the fields they generate. These fields remain in the plasma at the fixed position z where they were generated therefore they may influence succeeding slices which pass that z position but not preceeding slices. Eventually the fields at a given z excited by a given slice decay away, first the dipole field decays and then the monopole.

Mathematically, the response of a given beam slice will not be influenced by succeeding slices if $G(\rho, \rho'; \varsigma - \varsigma') = 0$ when $\varsigma - \varsigma' < 0$. When $\varsigma - \varsigma' < 0$ we may close the integration contour on the infinite half-circle in the positive real-s half-plane. The response is due to any singularities enclosed by the contour. Therefore, the constant s_o must be chosen so that there are no singularities to the right of $s_o \pm i\infty$.

When $\varsigma - \varsigma' > 0$ we may close the contour on the infinite half-circle in the negative real-s half-plane. Contributions from any poles and branches will contribute to the response according to the Cauchy residue theorem.

Mathematically, the operator in 6.41 is not self-adjoint, in the ς dependence it is anti-hermitian. The Green function therefore satisfies a reciprocity relation of the form

$$G(\rho, \rho'; \varsigma, \varsigma') = G(\rho', \rho; -\varsigma', -\varsigma) \tag{6.52}$$

which physically is a result of the fact that there is a preferred direction in ς as discussed above.

Let us now calculate the Green function. We define a new integration variable $w = s\varsigma_o$ where ς_o is the monopole decay length. In terms of w the Green function is

$$G\left(\rho,\rho';\varsigma-\varsigma'\right)=\frac{1}{\varsigma_o}\int_{w_o-i\infty}^{w_o+i\infty}\frac{dw}{2\pi i}e^{w(\varsigma-\varsigma')/\varsigma_o}\hat{G}\left(\rho,\rho';w\right) \tag{6.53}$$

where the Laplace transformed Green function $\hat{G}$ reads

$$\hat{G}\left(\rho,\rho';w\right)=I_1\left(\sqrt{w}\rho_<\right)K_1\left(\sqrt{w}\rho_>\right)+\frac{K_o\left(\sqrt{w}\frac{R}{a}\right)}{I_o\left(\sqrt{w}\frac{R}{a}\right)}I_1\left(\sqrt{w}\rho\right)I_1\left(\sqrt{w}\rho'\right)\ . \tag{6.54}$$

The functions I_o and I_1 are single valued and regular in the entire finite plane (they are entire functions) whereas both K_o and K_1 are multiple valued functions, which are single valued and regular on the entire plane cut from the branch point at the origin along the negative real axis. It is perhaps somewhat remarkable that although the functions K_o and K_1 are multiple valued the Laplace transformed Green function $\hat{G}$ is in fact single valued. This is due to a felicitous branch cancelation. On branch 1 $\hat{G}$ is just equation 6.54. To see what $\hat{G}$ looks like on branch 2 we use the analytic continuations of K_o and K_1 defined by

$$K_o\left(e^{2\pi i}w\right)=K_o\left(w\right)-2\pi i I_o\left(w\right) \tag{6.55}$$

$$K_1\left(e^{2\pi i}w\right)=K_1\left(w\right)+2\pi i I_1\left(w\right) \tag{6.56}$$

substituting these expressions into 6.54 we get back 6.54 unchanged. This proves the single valuedness of $\hat{G}$.

Since $\hat{G}$ is single valued the only contribution to the integral comes from residues of poles. Clearly the only poles are points w_n at which $I_o(\sqrt{w_n}R/a) = 0$ .Using the relation $I_o(w) = J_o(iw)$ where J_o is the Bessel function of the first kind of zeroth order, we find that the poles lie on the negative real axis in the w-plane and in terms of the zeros ν_n of J_o are given by

$$w_n = -\frac{a^2}{R^2}\nu_n^2 \,. \tag{6.57}$$

The residue of $1/I_o$ at w_n is

$$Res(w_n) = \frac{1}{I_1\left(\sqrt{w_n}\frac{R}{a}\right)}\frac{\sqrt{w_n}}{2}\frac{a}{R} \tag{6.58}$$

therefore, upon using some simple Bessel function identities and defining the higher order decay lengths ς_n

$$\varsigma_n = \frac{R^2}{a^2\nu_n^2}\varsigma_o \tag{6.59}$$

we arrive at the Green function G

$$G\left(\rho,\rho';\varsigma-\varsigma'\right) = \sum_{n=1}^{\infty}\frac{1}{\varsigma_n}e^{-(\varsigma-\varsigma')/\varsigma_n}\frac{2J_1\left(\nu_n\frac{a}{R}\rho\right)J_1\left(\nu_n\frac{a}{R}\rho'\right)}{(2\nu_n^2-1)J_1^2\left(\nu_n\right)} \tag{6.60}$$

where, for all practical purposes we may replace $2\nu_n^2 - 1$ with $2\nu_n^2$. This Green function may be constucted in a somewhat more direct fashion. Note that the eigenfunctions of the problem are of the form

$$u_n\left(\rho,\varsigma\right) = \exp\left(-\frac{a^2\nu_n^2}{\varsigma_o R^2}\varsigma\right)J_1\left(\nu_n\frac{a}{R}\rho\right) \tag{6.61}$$

therefore the Green function must be

$$G\left(\rho,\rho';\varsigma-\varsigma'\right) = \sum_{n=1}^{\infty} g_n u_n\left(\rho,\varsigma\right)u_n\left(\rho',-\varsigma'\right) \tag{6.62}$$

which, upon forcing the correct jump condition, yields 6.60.

One interesting result which we may deduce from the Green function 6.60 concerns the sufficiency of the monopole and dipole decay lengths to fully describe the field relaxation. According to 6.60 an infinite hierarchy of decay lengths $\varsigma_o > \varsigma_1 > \varsigma_2 > \cdots$ is necessary to describe the monopole and dipole vector potentials. Since ν_n is an increasing "function" of n the decay lengths ς_n decrease with n . Therefore, only those values of n for which ς_n is not too much smaller than ς_o are important. Examining the formula 6.59 for ς_n we find that for thin beams $a \ll R$ higher decay lengths may be very significant. This makes quite explicit the somewhat cryptic remark in Chapter 2 concerning the sufficiency of the monopole and dipole decay lengths. For thin beams they simply aren't sufficient.

6.6 References

6.1 K.G.Moses, R.W.Bauer, S.D.Winter, "Behavior of Relativistic Beams Undergoing Hose Motion in a Plasma Channel", Phys. Fluids **16**, 436 (1973)

6.2 S.V.Yadavalli, "Hose Instability of a Beam of Charged Particles Penetrating a Plasma", Z. Physik, **196**, 255 (1965)

6.3 E.P.Lee, "The Hose Instability of a Beam With the Bennett Profile", Phys. FLuids 21, 1327 (1978)

6.4 E.J.Lauer, R.J.Briggs, T.J.Fessenden, R.E.Hester, E.P.Lee, "Measurements of Hose Instability of a Relativistic Electron Beam", Phys. Fluids **21**, 1344 (1978)

6.5 N.Cristofilos, Proceedings of the Second United Nations Conference on the Peaceful Uses of Atomic Energy, Vol.32, P.279, Geneva (1958)

6.6 C.A.Kapetanakos, P.Sprangle, "Ultra-High-Current Electron Induction Accelerators", Phys. Today, Page 58, Feb. 1985

6.7 Private communication from J. R. Freeman, Sandia National Laboratories, concerning the RADLAC experiment.

6.8 E.P.Lee, "Hose Theory", Lawrence Livermore National Laboratory, UCID-16268 (1973)

6.9 S.Weinberg, "The Hose Instability Dispersion Relation", J. Math. Phys. 5,1371 (1964)

6.10 R.J.Briggs, R.E.Hester, "Beam Displacements Due to "Tickling" in the Astron Beam Experiments", UCID-5103 Lawrence Livermore Radiation Laboratory, Livermore CA, Feb. 1966

6.11 R.J.Briggs, "Propagation and Growth of the Hose Instability", UCID-5086 Lawrence Livermore Radiation Laboratory, Livermore CA, Jan. 1966

6.12 R.J.Briggs, "Transient Development of the Hose Instability", UCID-15127 Lawrence Livermore Radiation Laboratory, Livermore CA, Mar. 1967

Chapter 7

The Vlasov (Nonrigid) Beam

7.1 Introduction

Rigid-beam theory is based upon the fundamental assumption that all electrons respond to the transverse hose displacement the same. This means the electrons maintain the same position, relative to one another, in the displaced hosing beam as in the equilibrium.

On general physical grounds, however, one expects an electron to couple to the hose perturbation in a fashion which is dependent upon the relation between the characteristic frequency of the perturbation and the frequencies of the degrees of freedom of the electron. In particular, those electrons which have a frequency nearly in resonance with the perturbation will couple strongly and therefore respond greatly to the perturbation, those electrons whose frequencies are widely disparate from the perturbing frequency will not couple strongly and will there-

fore not respond greatly [1] . Physically, the response is dominated by the class of resonant electrons. One therefore expects a plastic deformation of the beam transversely as opposed to a rigid displacement.

In order to develop a more accurate treatment of the hose instability we shall have to approach the problem from a particle point of view, that is, we shall have to solve a Vlasov equation to determine the perturbed beam electron distribution function and then integrate over velocity to get the perturbed beam current source for the dipole field equation. This procedure, while seemingly straightforward, yields severe mathematical difficulties. It is the purpose of Chapter 7 to investigate various methods of coping with this problem. Emphasis is ultimately placed upon the circular helix model, a tractable and useful approach which leads naturally into the ideas of adiabatic beam theory.

In Chapter 7, as in Chapter 6, we shall not consider plasma current effects, therefore $f_m = 0$ throughout. This assumption is not made for technical reasons, we simply feel that the logical clarity of the entire development is superior if plasma effects are neglected until a point in the theory at which the essential relationships between the various models have been brought out [2]. In Section 8.4, the effects of plasma current and plasma conductivity generation will be introduced, and the results compared and contrasted with previous results.

[1] When we speak of the hose perturbation we are refering to the dipole fields in the plasma to which the electrons in a given slice are exposed as that slice streams past. The dipole fields are generated by previous slices of the beam.

[2] It turns out that "many" of the models are equivalent and our presentation of the current and conductivity effects thereby achieves a certain economy.

7.2 Elliptical Helices: General Profile

Transverse orbits in a general axisymmetric equilibrium beam resemble precessing ellipses ("rosettes") [7.1]. There are two isolating integrals of motion but the orbits cannot be characterized more precisely than rosettes without detailed solution of the orbit equations 3.60 and 3.61 . Here we do not need to actually compute the orbits and therefore will not.

The equilibrium phase space distribution function f_{bo} may be written as any normalizable function of the invariants of motion. As we consider only nonrotating beams ($B_z = 0$) the distribution depends only upon $H_\perp$ and P_z . The distribution function therefore reads $f_{bo} = f_{bo}(H_\perp, P_z)$. This f_{bo} is the general nonrotating, paraxial, axisymmetric equilibrium.

The equilibrium beam current $J_{bo}(r)$ is an integral over the momentum variables (p_r, p_θ)

$$J_{bo}(r) = q\beta c \int_0^\infty dp_r p_r \int_{-\infty}^\infty dp_\theta f_{bo}(r; p_r, p_\theta) \; . \tag{7.1}$$

It is more convenient to write this in terms of the invariants $H_\perp$ and P_θ . The Jacobian of the transformation $(p_r, p_\theta) \rightarrow (H_\perp, P_\theta)$ is easily computed to be $\gamma m / r p_r$, whence the current may be written as

$$J_{bo}(r) = q\beta c \frac{1}{r} \int_{-\infty}^\infty dP_\theta \int_{U(R;P_\theta)}^\infty dH_\perp \frac{1}{v_r(r; H_\perp, P_\theta)} f_{bo}(H_\perp) \tag{7.2}$$

where the radial velocity v_r is

$$v_r(r; H_\perp, P_\theta) = \pm \left(2(H_\perp - V(r)) - \frac{P_\theta^2}{\gamma m r^2} \right)^{\frac{1}{2}} \tag{7.3}$$

and $U(R, P_\theta)$ is defined to be effective radial potential evaluated at the radial turning point R where $v_r = 0$

$$U(R, P_\theta) = \frac{P_\theta^2}{2\gamma m R^2} - q\psi(R) \,. \tag{7.4}$$

The $H_\perp$ integral is over both branches of v_r , that is, we integrate from the minimum radius to the maximum and back to the minimum, this is twice the result of integration along one branch, therefore we have

$$J_{bo}(r) = 2q\beta c \frac{1}{r} \int_{-\infty}^{\infty} dP_\theta \int_{U(r,P_\theta)}^{\infty} dH_\perp \frac{1}{\mid v_r(r; P_\theta, H_\perp) \mid} f_{bo}(H_\perp) \,. \tag{7.5}$$

Since in linear theory we integrate along unperturbed orbits to invert the evolution operator the current perturbation J_{b1} is also given by this integral by replacing f_{bo} with f_{b1} .

The evolution of the phase space distribution function f_b is determined by the Vlasov equation, providing collisions are not a dominating effect, which reads

$$\left(\frac{\partial}{\partial t} + \frac{d\mathbf{r}}{dt} \cdot \frac{\partial}{\partial \mathbf{r}} + \frac{d\mathbf{p}}{dt} \cdot \frac{\partial}{\partial \mathbf{p}} \right) f_b = 0 \,. \tag{7.6}$$

Henceforth we will denote $\mathbf{v} = d\mathbf{r}/dt$ and $\mathbf{F} = d\mathbf{p}/dt$ where $\mathbf{F}$ is the Lorentz force. Equilibrium quantities will be denoted by a subscript 0 and linear perturbation terms by subscript 1. Writing $f_b = f_{bo} + f_{b1}$ and $\mathbf{F} = \mathbf{F}_o + \mathbf{F}_1$ and linearizing the Vlasov equation yields

$$\frac{df_{b1}}{dt} = -\mathbf{F}_o \cdot \frac{\partial f_{bo}}{\partial \mathbf{p}} \tag{7.7}$$

therefore, integrating upon the unperturbed orbits, we may write

$$f_{b1} = -\int_{-\infty}^{t} dt' \left(\mathbf{F}_o \cdot \frac{\partial f_{bo}}{\partial t} \right)' \tag{7.8}$$

where the prime denotes the unperturbed position at t' of a particle which reaches r, θ, z at time t.

The paraxiality of the beam results in a microcanonical axial momentum distribution $\delta(P_z - P_o)$ so the integration over p_z yields no contribution (due to the gradient of f_{bo}). This simplifies the problem somewhat, only the perpendicular component of $\mathbf{F}_o$ is needed, so the axial perturbed electric field E_{z1} does not appear. The perpendicular Lorentz force is $q\beta\hat{z} \times \mathbf{B}_1$. Recall that paraxial ordering also enables us to neglect B_z therefore the necessary fields are determined solely by the perturbed axial vector potential A_{z1} (henceforth we drop the z subscript and refer to A_1)

$$B_{r1} = \frac{1}{r}\frac{\partial A_1}{\partial \theta} \tag{7.9}$$

$$B_{\theta 1} = -\frac{\partial A_1}{\partial r} \, . \tag{7.10}$$

As usual we Fourier analyze in terms of the beam variables z, ς

$$A_1 = \hat{A}(r) \exp i\left(\theta - \frac{\Omega}{\beta c} z - \frac{\omega}{\beta c}\varsigma\right) \tag{7.11}$$

similarly for f_{b1} . The perturbed perpendicular Lorentz force thus reads

$$\mathbf{F}_\perp = \beta \frac{i}{r} A_1 \hat{\theta} + \beta \frac{\partial A_1}{\partial r}\hat{r} \, . \tag{7.12}$$

The perpendicular gradient of f_{bo} is

$$\frac{\partial f_{bo}}{\partial \mathbf{p}_\perp} = \mathbf{p}_\perp \frac{1}{p_\perp}\frac{\partial f_{bo}}{\partial p_\perp} \, . \tag{7.13}$$

Combining these results the perturbed f_{b1} reads

$$f_{b1} = -\frac{q}{c}\frac{1}{p_\perp}\frac{\partial f_{bo}}{\partial p_\perp}\int_{-\infty}^{z} dz' \left(p_r \frac{\partial A_1}{\partial r'} + \frac{i}{r'} p_\theta A_1\right) \tag{7.14}$$

where we have elected to work in terms of z in place of t . Introducing the Fourier components, taking cognizance of the fact that ς is a constant of motion in an ultra-relativistic beam, we have

$$\hat{f}_{b1} = -\frac{q}{c}\frac{1}{p_\perp}\frac{\partial f_{bo}}{\partial p_\perp}\int_{-\infty}^{z} dz' \left(p_r \frac{\partial \hat{A}}{\partial r'} + \frac{i}{r'} p_\theta \hat{A}\right) \exp i\left(\theta' - \theta - (z'-z)\frac{\Omega}{\beta c}\right) . \tag{7.15}$$

A simple subterfuge enables us to express the radial derivative of $\hat{A}$ along an orbit as a more convenient axial derivative by means of the chain rule

$$\frac{\partial \hat{A}}{\partial r'} = \beta c \frac{\gamma m}{p_r}\frac{d\hat{A}}{dz'} . \tag{7.16}$$

Using the fact that $p_z = \beta c \gamma m$ and $p_\theta = \gamma m r \Omega_\beta$ where Ω_β is the betatron frequency, and the previous result, we arrive at

$$\hat{f}_{b1} = -\frac{q}{c}\frac{p_z}{p_\perp}\frac{\partial f_{bo}}{\partial p_\perp}\int_{-\infty}^{z} dz' \left(\frac{d\hat{A}}{dz'} + i\frac{\Omega_\beta}{\beta c}\hat{A}\right) \exp i\left(\theta' - \theta - \frac{\Omega}{\beta c}(z'-z)\right) \tag{7.17}$$

here Ω_β has been pulled in front of the integral since on the unperturbed orbits it is an invariant $d\Omega_\beta/dz = -(1/p_z)\partial H_\perp/\partial p_\theta = 0$. Integrating the first term in 7.17 by parts cancels the second term and yields [3]

$$\hat{f}_{b1} = -\frac{q}{c}\frac{p_z}{p_\perp}\frac{\partial f_{bo}}{\partial p_\perp}\left(\hat{A} + i\frac{\Omega}{\beta c}\hat{I}\right) \tag{7.18}$$

where the orbit integral $\hat{I}$ is

$$\hat{I}\,(r; H_\perp, P_\theta) = \int_{-\infty}^{z} dz' \hat{A}(r') \exp i\left(\theta' - \theta - \frac{\Omega}{\beta c}(z'-z)\right) . \tag{7.19}$$

[3] For a rotating beam $p_\perp^2 = p_r^2 + (p_\theta - \gamma m r \omega_b)^2$ and tracing through the same argument as for the nonrotating beam yields the same result providing only that Ω is replaced with $\Omega - \omega_b$. Here ω_b is the Lagrange multiplier that appears in a calculation of the Maxwell-Boltzmann distribution involving P_θ dependence.

We may express the perpendicular momentum gradient of f_{bo} in terms of a gradient with respect to $H_\perp$. By use of the chain rule

$$\frac{\partial f_{bo}}{\partial p_\perp} = \frac{df_{bo}}{dH_\perp}\frac{\partial H_\perp}{\partial p_\perp} = \frac{df_{bo}}{dH_\perp}\beta c\frac{p_\perp}{p_z} \tag{7.20}$$

so that

$$\frac{p_z}{p_\perp}\frac{\partial f_{bo}}{\partial p_\perp} = \beta c\frac{df_{bo}}{dH_\perp} \ . \tag{7.21}$$

To get the current perturbation we integrate over the invariants $H_\perp$ and P_θ as follows

$$\hat{J}_{b1} = -2q^2\beta^2 c\frac{1}{r}\int_{-\infty}^{\infty} dP_\theta \int_U^{\infty} \frac{1}{\mid v_r \mid}\frac{df_{bo}}{dH_\perp}\left(\hat{A} + i\frac{\Omega}{\beta c}\hat{I}\right) \tag{7.22}$$

where now the orbit integral is written as an explicit sum over the two branches of v_r with an appropriate factor of $1/2$ to cancel the overall factor of 2 in 7.22

$$\hat{I} = \frac{1}{2}\sum_{\pm}\int_{-\infty}^{z} dz'\hat{A}(r'_\pm)\exp i\left(\theta'_\pm - \theta - \frac{\Omega}{\beta c}(z'-z)\right) \ . \tag{7.23}$$

To reiterate, the primed quantities $r'_\pm$ and $\theta'_\pm$ specify the unperturbed transverse location at $z' < z$ of a particle (with invariants $H_\perp$ and P_θ) that ends up at r and θ when $z' = z$. The subscript $\pm$ selects the branch of v_r , that is, $r'_\pm$ corresponds to the particle that started out on branch $v_r = \pm \mid v_r \mid$, likewise for $\theta'_\pm$.

The orbit integral may be reduced by exploiting the underlying periodicity of the integrand. Physically the orbit integral represents the accumulated effect of the perturbation upon particles with $H_\perp$ and P_θ . We expect however that the integral may be evaluated over one period of the motion.

We define the phase $\phi_\pm(z) = \theta_\pm(z) - (\Omega/\beta c)z$ in terms of which the orbit

integrals $\hat{I}_+$ and $\hat{I}_-$ read

$$\hat{I}_{\pm}(r)\exp\left(i\phi_{\pm}(z)\right) = \int_{-\infty}^{z} dz' \hat{A}(r'_{\pm})\exp\left(i\phi'_{\pm}\right) \ . \tag{7.24}$$

Now, for r_+ we have $v_r > 0$ and the particle is moving from r_{min} out to r_{max} , whereas, for r_- we have $v_r < 0$ and the particle is moving from r_{max} in to r_{min} . We should be able to relate the values of $\hat{I}_{\pm}(r,z)$ to their values at the previous radial turning points (the values at the turning points simply repeat themselves periodically in the integral from $-\infty$ to z). For $v_r > 0$ we write

$$\hat{I}_+(r)\exp\left(i\phi_+\right) = \hat{I}_+(r_{min})\exp\left(i\phi^+_{min}\right) + \int_{z_{min}}^{z} dz' \hat{A}(r'_+)\exp\left(i\phi'_+(z')\right) \tag{7.25}$$

and for $v_r < 0$

$$\hat{I}_-(r)\exp\left(i\phi_-\right) = \hat{I}_-(r_{max})\exp\left(i\phi^-_{max}\right) + \int_{z_{max}}^{z} dz' \hat{A}(r'_-)\exp\left(i\phi'_-(z')\right) \tag{7.26}$$

where $\phi^+_{min} \equiv \phi_+(r_{min})$ and $\phi^-_{max} \equiv \phi_-(r_{max})$. These equations give the values of $\hat{I}_{\pm}$ as their values at the previous turning points plus an increment attained during partial transit to the next turning point. It is convenient to change variables of integration to r' in place of z' , this is accomplished by

$$dz' = \beta c dr' \frac{1}{\pm v_r(r')} \ . \tag{7.27}$$

In terms of the variable of integration r' equations 7.25 and 7.26 read

$$\hat{I}_+(r)\exp\left(i\phi_+\right) = \hat{I}_+(r_{min})\exp\left(i\phi^+_{min}\right) + \beta c \int_{r_{min}}^{r} dr' \hat{A}(r'_+)\frac{1}{\mid v_r(r') \mid}\exp\left(i\phi'_+(z')\right) \tag{7.28}$$

$$\hat{I}_-(r)\exp\left(i\phi_-\right) = \hat{I}_-(r_{max})\exp\left(i\phi^-_{max}\right) - \beta c \int_{r_{max}}^{r} dr' \hat{A}(r'_-)\frac{1}{\mid v_r(r') \mid}\exp\left(i\phi'_-(z')\right) \ . \tag{7.29}$$

To save writing we will define dA' as follows

$$dA' = \beta c dr' \hat{A}(r') \frac{1}{\mid v_r(r') \mid} \tag{7.30}$$

in terms of which the orbit integrals read

$$\hat{I}_+(r) \exp(i\phi_+) = \hat{I}_+(r_{min}) \exp\left(i\phi^+_{min}\right) + \int_{r_{min}}^{r} dA' \exp(i\phi'_+(z')) \tag{7.31}$$

$$\hat{I}_-(r) \exp(i\phi_-) = \hat{I}_-(r_{max}) \exp(i\phi^-_{max}) - \int_{r_{max}}^{r} dA' \exp(i\phi'_-(z')) \ . \tag{7.32}$$

Explicitly, the phase may be written as

$$\phi_+(r) = \phi_+(r_{min}) + \int_{z_{min}}^{z} dz' \frac{d\phi_+}{dz'} \tag{7.33}$$

$$\phi_-(r) = \phi_-(r_{max}) + \int_{z_{max}}^{z} dz' \frac{d\phi_-}{dz'} \ . \tag{7.34}$$

Next we will demonstrate that the relative phase between ϕ_+ and ϕ_- is invariant. To see this notice that

$$\beta c \frac{d\phi_+}{dz'} = \beta c \left(\frac{d\theta_+}{dz'} - \frac{\Omega}{\beta c} \right) = \frac{d\theta_+}{dt'} - \Omega \tag{7.35}$$

$$\beta c \frac{d\phi_-}{dz'} = \beta c \left(\frac{d\theta_-}{dz'} - \frac{\Omega}{\beta c} \right) = \frac{d\theta_-}{dt'} - \Omega \tag{7.36}$$

hence we may write the phases as

$$\phi_+(r) = \phi_+(r_{min}) + \int_{r_{min}}^{r} dr' \frac{1}{\mid v_r(r') \mid} (\Omega_\beta(r') - \Omega) \tag{7.37}$$

$$\phi_-(r) = \phi_-(r_{max}) - \int_{r_{max}}^{r} dr' \frac{1}{\mid v_r(r') \mid} (\Omega_\beta(r') - \Omega) \ . \tag{7.38}$$

Replacing r_{max} with r_{min} in 7.38 and adding the result to 7.37 yields

$$\phi_+(r) + \phi_-(r) = \phi_+(r_{min}) + \phi_-(r_{min}) \tag{7.39}$$

this says that $\phi_+(r) - \phi_+(r_{min}) = -(\phi_-(r) - \phi_-(r_{min}))$. The conclusion we draw is that we are free to fix the relative phase between the two branches since it is invariant. Let us therefore write $\phi_-(r_{min}) = \phi_+(r_{min}) \equiv \phi_{min}$, with this convention we have $\phi_-(r) = 2\phi_{min} - \phi_+(r)$.

Now we will calculate the values $\hat{I}(r_{min})$ and $\hat{I}(r_{max})$, the values of the orbit integrals at the turning points r_{min} . These will enable us to compute $\hat{I}_-(r)$ and $\hat{I}_+(r)$ and therefore the orbit integral $\hat{I}$. First, notice that the continuity of the orbits implies

$$\lim_{r_- \to r_{min}} \hat{I}(r_-) = \lim_{r_+ \to r_{min}} \hat{I}(r_+) \equiv \hat{I}_{min} \tag{7.40}$$

$$\lim_{r_- \to r_{max}} \hat{I}(r_-) = \lim_{r_+ \to r_{max}} \hat{I}(r_+) \equiv \hat{I}_{max} \, . \tag{7.41}$$

Using these results, along with the result $\phi_-(r) = 2\phi_{min} - \phi_+(r)$, evaluating 7.31 and 7.32 at r_{max} and r_{min} respectively, yields

$$\hat{I}_{max} \exp i\,(\phi^+_{max} - \phi_{min}) = \hat{I}_{min} + \int_{r_{min}}^{r_{max}} dA' \exp i\,(\phi'_+ - \phi_{min}) \tag{7.42}$$

$$-\hat{I}_{max} \exp -i\,(\phi^+_{max} - \phi_{min}) = -\hat{I}_{min} + \int_{r_{min}}^{r_{max}} dA' \exp -i\,(\phi'_+ - \phi_{min}) \, . \tag{7.43}$$

Making the following definition

$$\Delta\phi \equiv \phi^+_{max} - \phi^+_{min} \tag{7.44}$$

let us explicitly compute $\Delta\phi$

$$\Delta\phi = \frac{1}{2} \oint dr' \frac{1}{v_r(r')} \left(\Omega_\beta(r') - \Omega\right) \tag{7.45}$$

which in turn, by direct calculation yields

$$\Delta\phi = \pi \frac{\bar{\Omega}_\beta - \Omega}{\bar{\Omega}_r} \tag{7.46}$$

where the orbit averaged radial frequency $\bar{\Omega}_r$ is

$$\bar{\Omega}_r = 2\pi \left(\oint \frac{dr}{v_r(r)} \right)^{-1} . \tag{7.47}$$

The orbit averaged betatron frequency $\bar{\Omega}_\beta$ is

$$\bar{\Omega}_\beta \equiv \oint \frac{\Omega_\beta(r)}{v_r(r)} dr \left(\oint \frac{dr}{v_r(r)} \right)^{-1} \tag{7.48}$$

in terms of $\bar{\Omega}_r$ and $P_\theta = \gamma m r^2 \Omega_\beta$ this becomes

$$\bar{\Omega}_\beta \equiv \frac{\bar{\Omega}_r}{2\pi} \frac{P_\theta}{\gamma m} \oint \frac{dr}{r^2 v_r(r)} . \tag{7.49}$$

Performing the algebra we may easily solve for the turning point values of the orbit integrals $\hat{I}_-$ and $\hat{I}_+$ from 7.42 and 7.43 and substitute the results in 7.31 and 7.32 to get

$$\hat{I}_+(r) = \int_{r_{max}}^{r} dA' \exp i\left(\phi'_+ - \phi_+\right) \tag{7.50}$$

$$+\frac{1}{2i \sin \Delta\phi} \int_{r_{min}}^{r_{max}} dA' \left(\exp i\left(\phi'_+ - \phi_+ - \Delta\phi\right) + \exp -i\left(\phi'_+ + \phi_+ - \Delta\phi\right)\right)$$

$$\hat{I}_-(r) = \int_{r_{max}}^{r} dA' \exp -i\left(\phi'_+ - \phi_+\right) \tag{7.51}$$

$$+\frac{1}{2i \sin \Delta\phi} \int_{r_{min}}^{r_{max}} dA' \left(\exp i\left(\phi'_+ + \phi_+ - \Delta\phi\right) + \exp -i\left(\phi'_+ - \phi_+ + \Delta\phi\right)\right) .$$

These may now be combined to yield the final result [7.2] for $\hat{I}$

$$\hat{I}(r) = -i\beta c \int_{r_{min}}^{r_{max}} \frac{dr'}{|\, v_r(r') \,|} \hat{A}(r') \left(\frac{\cos\phi \cos\phi'}{\tan \Delta\phi} \right. \tag{7.52}$$

$$\left. + H(r - r') \sin\phi \cos\phi' + H(r - r') \sin\phi' \cos\phi \right)$$

where

$$\phi(r) = \int_{r_{min}}^{r} dr' \frac{\Omega_\beta(r') - \Omega}{\mid v_r(r') \mid} \tag{7.53}$$

is the phase change in traveling from r_{min} to r and $H(r-r')$ is the usual Heaviside step function.

Having derived this result, for the orbit integral involving only one fundamental period of the motion, we may now determine which class of electrons contributes maximally to the perturbation. It will come as no surprise that those electrons having a frequency in resonance with the perturbation dominate the response.

Inspection of 7.52 indicates immediately that the major contribution will come from the term involving $1/\tan\Delta\phi$ in case $\tan\Delta\phi \approx 0$. This occurs when

$$\Delta\phi = \pi \frac{\bar{\Omega}_\beta - \Omega}{\bar{\Omega}_r} \approx n\pi \tag{7.54}$$

where n is an integer, solving the resonance condition we get $\Omega \approx \bar{\Omega}_\beta - n\bar{\Omega}_r$.

This result is of extreme significance in relation to the prominent theme of this thesis, as will become clearer as we proceed. Physically, one expects that a perturbation which drives a two degree of freedom dynamical system at a beat frequency will have a pronounced effect upon the evolution of the system.

We may approximate the orbit integral near the resonance by dropping the second and third terms. Approximating $\tan\Delta\phi \approx \Delta\phi \approx \pi(\bar{\Omega}_\beta - \Omega)/\bar{\Omega}_r$ the near resonance orbit integral reads

$$\hat{I}(r) \approx -i\beta c \frac{1}{\pi} \frac{\bar{\Omega}_r}{\bar{\Omega}_\beta - \Omega} \cos\phi(r) \int_{r_{min}}^{r_{max}} \frac{dr'}{\mid v_r(r') \mid} \hat{I}(r') \cos\phi(r') \ . \tag{7.55}$$

Next, we define the orbit average of $\hat{A}$ as

$$\bar{A} = \frac{\bar{\Omega}_r}{\pi} \int_{r_{min}}^{r_{max}} \frac{dr'}{\mid v_r(r') \mid} \cos\phi(r') \hat{A}(r') \ . \tag{7.56}$$

The orbit average $\bar{A}$ is a function only of the invariants $(H_\perp, P_\theta)$ of motion. In terms of $\bar{A}$ we have

$$\hat{I}(r) \approx -i\beta c \frac{1}{\bar{\Omega}_\beta - \Omega} \bar{A} \cos\phi(r) \ . \tag{7.57}$$

Since the betatron frequency is a function of the orbit invariants $(H_\perp, P_\theta)$ (the dependence upon the invariants is suppressed for notational convenience) the perturbed current has a logarithmic singularity due to the simple pole in the perturbed distribution (recall that $\hat{f}_{b1}$ is given by $\hat{f}_{b1} \sim \hat{A} + i(\Omega/\beta c)\hat{I}$ and the current is an integral of $\hat{f}_{b1}$ over $(H_\perp, P_\theta)$).

This thesis is concerned with a circle of questions surrounding the adiabatic approach to beam physics. The adiabatic approach is an extension for small "gyro-radius" of the cold laminar model, in which transverse orbits are circular. In adiabatic theory the orbits are near circular (vortex radius something less than half the circular drift radius). It is therefore of great interest to investigate the circle limit of the general elliptical theory just developed. To this end, let us return to our result for $\hat{f}_{b1}$ and determine what simplifications arise for circle orbits. For convenience we quote the result $\hat{f}_{b1}$ here

$$\hat{f}_{b1} = -\frac{q}{c}\beta c \frac{df_{bo}}{dH_\perp} \left(\hat{A} + i\frac{\Omega}{\beta c}\hat{I} \right) \ . \tag{7.58}$$

Suppose the orbits are circular, then $r'(z') = r$ is constant, therefore $\hat{A}(r')$ may

be removed from the orbit integral

$$\hat{I}(r;H_\perp,P_\theta)=\hat{A}(r)\int_{-\infty}^{z}dz'\exp i\left(\theta'-\theta-\frac{\Omega}{\beta c}(z'-z)\right)\ . \tag{7.59}$$

On the equilibrium orbits $\theta(z)=\Omega_\beta z/\beta c$ therefore, carrying out the orbit integral we arrive at

$$\hat{I}(r)=\hat{A}(r)\frac{-i\beta c}{\Omega_\beta-\Omega}\ . \tag{7.60}$$

Substituting this into $\hat{f}_{b1}$ yields the perturbed distribution for the cold beam

$$\hat{f}_{b1}=-\frac{q}{c}\beta c\frac{df_{bo}}{dH_\perp}\hat{A}\frac{\Omega_\beta}{\Omega_\beta-\Omega}\ . \tag{7.61}$$

Introducing $P_\theta=\gamma mr^2\Omega_\beta$ and integrating over the invariants to obtain the current perturbation we get

$$\hat{J}_{b1}=-2q^2\beta^2c\frac{1}{r}\int_{-\infty}^{\infty}dP_\theta\int_U^\infty dH_\perp\frac{1}{\mid v_r\mid}\frac{df_{bo}}{dH_\perp}\hat{A}\frac{P_\theta}{\gamma mr^2}\left(\frac{P_\theta}{\gamma mr^2}-\Omega\right)^{-1}\ . \tag{7.62}$$

For a nonrotating beam the equilibrium distribution f_{bo} is an even function of P_θ , therefore, multiplying the numerator and denominator of the integrand by $P_\theta/\gamma mr^2+\Omega$ and keeping only the term which is even in P_θ gives

$$\hat{J}_{b1}=-2q^2\beta^2c\frac{\hat{A}}{r}\frac{1}{\Omega_\beta^2-\Omega^2}\int_{-\infty}^{\infty}dP_\theta\int_U^\infty dH_\perp\frac{1}{\mid v_r\mid}\frac{df_{bo}}{dH_\perp}\left(\frac{P_\theta}{\gamma mr^2}\right)^2\ . \tag{7.63}$$

Now notice the following

$$\left(\frac{P_\theta}{\gamma mr^2}\right)^2\frac{df_{bo}}{dH_\perp}=-\frac{1}{\gamma mr}\frac{dH_\perp}{dr}\frac{df_{bo}}{dH_\perp}=-\frac{1}{\gamma mr}\frac{df_{bo}}{dr} \tag{7.64}$$

therefore, our result for the current perturbation in the laminar beam is

$$\hat{J}_{b1}=\frac{q\beta}{\gamma m}\frac{1}{\Omega_\beta^2-\Omega^2}\frac{1}{r}\frac{dJ_{bo}}{dr}\hat{A}\ . \tag{7.65}$$

Perhaps at this juncture it is well to remind the reader that the betatron frequency $\Omega_\beta(r)$ is given in terms of the equilibrium current J_{bo} by

$$\Omega_\beta^2(r) = \frac{4\pi}{c}\frac{q\beta}{\gamma m}\frac{1}{r^2}\int_0^r dr' r' J_{bo}(r') \tag{7.66}$$

which is easily derived from the definition 1.1 of Ω_β and the monopole Ampère equation. In terms of Ω_β the current perturbation reads

$$\frac{4\pi}{c}\hat{J}_{b1} = \frac{1}{r}\frac{d}{dr}\left(\frac{1}{r}\frac{d}{dr}\left(r^2\Omega_\beta^2\right)\right)\frac{1}{\Omega_\beta^2 - \Omega^2}\hat{A} \tag{7.67}$$

which is in a form useful for comparison with the results of the Section 7.3. Anticipating, we will show that the Vlasov calculation is incomplete, it does not yield the correct form of $\hat{J}_{b1}$ in the circle limit. This is because in a Vlasov calculation one inverts the partial differential operator on the unperturbed orbits. In Section 7.3 we will calculate the circle orbit current perturbation in a fashion which is superior in that it includes the orbit perturbations.

We may use our result 7.65 for the current perturbation $\hat{J}_{b1}$ to formulate an eigenvalue problem for $\omega(\Omega)$. Inserting 7.65 into the Ampère equation, including radially dependent conductivity $\sigma_o(\rho)$ ($\rho = r/a$) we have

$$\left(\frac{d}{d\rho}\frac{1}{\rho}\frac{d}{d\rho}\rho - \frac{4\pi i\omega}{c^2}\sigma_o(\rho)\right)\hat{A} = -\frac{4\pi}{c}\frac{q\beta}{\gamma m}\frac{1}{\Omega_\beta^2 - \Omega^2}\frac{1}{\rho}\frac{dJ_{bo}}{d\rho}\hat{A}\,. \tag{7.68}$$

We will use a variational technique to approximate the eigenvalue $\omega(\Omega)$ determined by this equation. To accomplish this we multiply the eigenequation by $\hat{A}$ and integrate over $\int_0^\infty d\rho\rho$

$$\int_0^\infty d\rho\hat{A}\frac{d}{d\rho}\frac{1}{\rho}\frac{d}{d\rho}\rho\hat{A} - \frac{4\pi}{c}i\omega\int_0^\infty d\rho\rho\sigma_o(\rho)\hat{A}^2 = \frac{-4\pi}{c}\frac{q\beta}{\gamma m}\int_0^\infty d\rho\frac{1}{\Omega_\beta^2 - \Omega^2}\frac{dJ_{bo}}{d\rho}\hat{A}^2\,. \tag{7.69}$$

Next, we insert a trial eigenfunction $\hat{A}$ and solve for ω . The difference between the exact eigenvalue $\tilde{\omega}$ and the approximate eigenvalue ω is $\delta\omega$ and is $O(\delta\hat{A}^2)$ where $\delta\hat{A}$ is the difference between the exact eigenfunction $\tilde{A}$ and the approximate eigenfunction $\hat{A}$. We use as a trial eigenfunction the rigid-beam fundamental mode $\hat{A} = dA_o/d\rho$. After integrating, with the fundamental mode, we find

$$\frac{i\omega}{c}\int_0^\infty d\rho\sigma_o(\rho)\left(\frac{dA_o}{d\rho}\right)^2 = \int_0^\infty d\rho\rho\frac{dA_o}{d\rho}\frac{dJ_{bo}}{d\rho}\frac{\Omega^2}{\Omega^2-\Omega_\beta^2} . \tag{7.70}$$

Let us specialize to the Bennett equilibrium

$$J_{bo}(\rho) = \frac{I_b}{\pi a^2}\left(1+\rho^2\right)^{-2} . \tag{7.71}$$

Assuming local conductivity generation ($\sigma_o(\rho) \sim J_{bo}(\rho)$)

$$A_o(\rho) = -\frac{I_b}{c}\log\left(1+\rho^2\right) \tag{7.72}$$

$$\sigma_o(\rho) = \sigma_o\left(1+\rho^2\right)^{-2} . \tag{7.73}$$

The dispersion relation now reads

$$i\omega\frac{\sigma_o\pi a^2}{2c^2}\int_0^\infty d\rho\frac{2\rho^3}{(1+\rho^2)^4} = \int_0^\infty d\rho\frac{2\rho^3}{(1+\rho^2)^4}\frac{\Omega^2}{\Omega^2-\Omega_\beta^2} . \tag{7.74}$$

If we define a new variable of integration $\nu = (1+\rho^2)^{-1}$ and introduce the dipole decay time $\tau = \sigma_o\pi a^2/2c^2$ we have the dispersion relation, as predicted by the circle-limit of the exact Vlasov theory

$$-i\omega\tau = \Omega^2\int_0^\infty d\nu 6\nu(1-\nu)\frac{1}{\nu\Omega_\beta^2-\Omega^2} . \tag{7.75}$$

We will prove in Section 7.4 that this is the same as the prediction of the cold-Vlasov theory. In Chapter 8 we will prove that this is also the same as the result predicted by the spread-mass and energy-group multiple-oscillator models.

7.3 Circular Helices: General Profile

In Section 7.1 we developed a general linearized Vlasov theory for the current perturbation $\hat{J}_{b1}$. We also investigated the circle orbit limit of the elliptical theory. In Section 7.4 we wish to examine the circle orbit case from a slightly different point of view [7.3] which will deepen our understanding of the significance of our results in Section 7.1.

An equilibrium beam with a cold transverse phase space has circular transverse orbits. When such a beam undergoes hose instability the orbits acquire a radial component. This means that although the equilibrium transverse distribution is one dimensional it is not sufficient to work with a one dimensional distribution. Since the current is a momentum integral of the distribution it is not necessary to work with a distribution in phase space at all. In Section 7.4 we will compute the current perturbation by computing the linearized perturbed orbits (that is, the linear differences between the exact orbits and the unperturbed orbits). We will then form the current by adding up all the orbits directly.

As usual for a paraxial beam we assume $d\gamma/dt = 0$ so, in component form, the orbit equations, as discussed in Chapter 3, read

$$\frac{d^2r}{dt^2} - \left(\frac{d\theta}{dt}\right)^2 r = \frac{q}{\gamma m}\frac{\partial \psi}{\partial r} \tag{7.76}$$

$$r\frac{d^2\theta}{dt^2} + 2\frac{dr}{dt}\frac{d\theta}{dt} = \frac{q}{\gamma m}\frac{1}{r}\frac{\partial \psi}{\partial \theta} \tag{7.77}$$

$$\frac{d^2z}{dt^2} = 0\,. \tag{7.78}$$

These equations will be linearized about circular helices. To this end we will write the exact orbit as $(\tilde{r}, \tilde{\theta}, \tilde{z})$ and the unperturbed helices as (r, θ, z) . The exact orbits are therefore

$$\tilde{r}(r, \theta, z; t) = r + D_r(r, \theta, z; t) \tag{7.79}$$

$$\tilde{\theta}(r, \theta, z; t) = \theta + \Omega_\beta(r)t + \frac{1}{r} D_\theta(r, \theta, z; t) \tag{7.80}$$

$$\tilde{z}(r, \theta, z; t) = z + \beta ct \tag{7.81}$$

where we have explicitly denoted the underlying variable t (we could express everything in terms of z by paraxiality but choose not to here). The terms D_r and D_θ are assumed small so we will neglect quadratic terms $O(D^2)$. The first time derivatives of $\tilde{r}, \tilde{\theta}, \tilde{z}$ are

$$\frac{d\tilde{r}}{dt} = \frac{dD_r}{dt} \tag{7.82}$$

$$\frac{d\tilde{\theta}}{dt} = \Omega_\beta + \frac{1}{r}\frac{dD_\theta}{dt} \tag{7.83}$$

$$\frac{d\tilde{z}}{dt} = \beta c \tag{7.84}$$

and the second time derivatives are

$$\frac{d^2\tilde{r}}{dt^2} = \frac{d^2 D_r}{dt^2} \tag{7.85}$$

$$\frac{d^2\tilde{\theta}}{dt^2} = \frac{1}{r}\frac{d^2 D_\theta}{dt^2} \tag{7.86}$$

$$\frac{d^2\tilde{z}}{dt^2} = 0\,. \tag{7.87}$$

Writing the equations of motion in terms of the exact orbits we have

$$\frac{d^2\tilde{r}}{dt^2} - \left(\frac{d\tilde{\theta}}{dt}\right)^2 \tilde{r} = -\tilde{r}\Omega_\beta^2(\tilde{r}) + \frac{1}{\gamma m} F_{r1}(\tilde{r}, \tilde{\theta}, \tilde{z}; t) \tag{7.88}$$

$$\frac{d^2\tilde{\theta}}{dt^2} + 2\frac{d\tilde{r}}{dt}\frac{d\tilde{\theta}}{dt} = \frac{1}{\gamma m}F_{\theta 1}(\tilde{r},\tilde{\theta},\tilde{z};t) \tag{7.89}$$

where the forces are defined $F_{r1} \equiv q\partial\psi/\partial\tilde{r}$ and $F_{\theta 1} \equiv (q/\tilde{r})\partial\psi/\partial\tilde{\theta}$. We have used the fact that the equilibrium ψ_o is axisymmetric $\partial\psi_o/\partial\tilde{\theta} = 0$. Introducing the derivatives listed above and linearizing the equations of motion yields

$$\frac{d^2D_r}{dt^2} - \Omega_\beta^2(r)D_r - 2\Omega_\beta(r)\frac{dD_\theta}{dt} = -\frac{d}{dr}\left(r\Omega_\beta^2(r)\right)D_r + \frac{1}{\gamma m}F_{r1}(r,\theta+\Omega_\beta t, z+\beta ct) \tag{7.90}$$

$$\frac{d^2D_\theta}{dt^2} + 2\frac{dD_r}{dt}\Omega_\beta(r) = \frac{1}{\gamma m}F_{\theta 1}(r,\theta+\Omega_\beta t, z+\beta ct)\ . \tag{7.91}$$

As usual we Fourier analyze the perturbed quantities according to

$$F_1(\tilde{r},\tilde{\theta},\tilde{z};t) = \hat{F}(\tilde{r})\exp i\left(i\tilde{\theta} + ik\tilde{z} - i\omega t\right)\ . \tag{7.92}$$

In the phase we replace the exact quantities by the unperturbed quantities as follows

$$\tilde{\theta} + k\tilde{z} - \omega t = \theta - (\Omega - \Omega_\beta(r))t + kz \tag{7.93}$$

where we have used $\tilde{\theta} = \theta + \Omega_\beta t + O(D)$ and $\tilde{z} = z + \beta ct$ and have recalled the definition of the Doppler-shifted hose frequency $\Omega \equiv \omega - k\beta c$. Henceforth, to save writing we will suppress the argument of Ω_β . The Fourier transform now reads

$$F(\tilde{r},\tilde{\theta},\tilde{z};t) = \hat{F}(r)\exp i\left(-(\Omega-\Omega_\beta)t + ikz + \theta\right) \tag{7.94}$$

where $\hat{F}$ may be $\hat{F}_r$, $\hat{F}_\theta$, $\hat{D}_r$, or $\hat{D}_\theta$ (we drop the subscript 1 on F). In terms of the Fourier transformed axial vector potential dipole $\hat{A}$ the force components read $\hat{F}_r = q\beta d\hat{A}/dr$ and $\hat{F}_\theta = q\beta(i/r)\hat{A}$ for a pure pinch. In terms of the Fourier

transformed quantities the equations of motion read

$$\left(\frac{d}{dr}\left(r\Omega_\beta^2\right) - (\Omega-\Omega_\beta)^2 - \Omega_\beta^2\right)\hat{D}_r + \left(2i\Omega_\beta\left(\Omega-\Omega_\beta\right)\right)\hat{D}_\theta = \frac{1}{\gamma m}\hat{F}_r \tag{7.95}$$

$$\left(-2i\Omega_\beta\left(\Omega-\Omega_\beta\right)\right)\hat{D}_r + \left(-i\left(\Omega-\Omega_\beta^2\right)^2\right)\hat{D}_\theta = \frac{1}{\gamma m}\hat{F}_\theta\,. \tag{7.96}$$

Solving these linear equations for $\hat{D}_r$ and $\hat{D}_\theta$ results in the following

$$\gamma m\hat{D}_r = \frac{1}{D}\left(\hat{F}_r + 2i\frac{\Omega_\beta}{\Omega-\Omega_\beta}\hat{F}_\theta\right) \tag{7.97}$$

$$\gamma m\hat{D}_\theta = \frac{1}{D}\left(-2i\frac{\Omega_\beta}{\Omega-\Omega_\beta}\hat{F}_r + \left(1 - \frac{1}{(\Omega-\Omega_\beta)^2}r\frac{d}{dr}\Omega_\beta^2\right)\hat{F}_\theta\right) \tag{7.98}$$

where the denominator D is

$$D = 4\Omega_\beta^2 - (\Omega-\Omega_\beta)^2 + r\frac{d}{dr}\Omega_\beta^2\,. \tag{7.99}$$

Now that we have computed the perturbed orbit components we may compute the current perturbation. Before carrying out the perturbed density calculation let us discuss the problem at hand in some generality.

Let $\mathbf{r}'$ be the position of a particle at $t=-\infty$. Denote by $\tilde{\mathbf{r}}(\mathbf{r}';t)$ the function which determines the *exact* position at time t of a particle which started at $\mathbf{r}'$ at $t=-\infty$. Denote by $\tilde{J}(\mathbf{r};t)$ the *exact* density at $\mathbf{r}$ at time t (here $\mathbf{r}$ is a point in space, not an orbit) and by $j(\mathbf{r})$ the unperturbed density. Clearly

$$\tilde{J}(\mathbf{r};t) = \int d\mathbf{r}' j(\mathbf{r}')\delta\left(\tilde{\mathbf{r}}(\mathbf{r}';t) - \mathbf{r}\right) \tag{7.100}$$

the density at $\mathbf{r},t$ is the integral of all the initial conditions which "launch" particles that arrive at $\mathbf{r}$ when the time is t. The Dirac delta says $\tilde{\mathbf{r}}(\mathbf{r}';t)-\mathbf{r}=0$

This determines a function $\mathbf{r}'(\mathbf{r};t)$. That is, the initial position as a function of the final position on the exact orbits. Recall that for a function f with a zero at x_o we have

$$\delta(f(x)) = \delta\left(f(x_o) + \frac{df}{dx_o}(x - x_o) + \cdots\right) \tag{7.101}$$
$$= \delta\left(\frac{df}{dx_o}(x - x_o) + \cdots\right) = \left(\frac{df}{dx_o}\right)^{-1} \delta(x - x_o) + \cdots$$

so for our problem (a vector function) we have

$$\delta(\tilde{\mathbf{r}}(\mathbf{r}';t) - \mathbf{r}) = \mid \frac{\partial \mathbf{r}'}{\partial \mathbf{r}} \mid \delta(\mathbf{r}' - \mathbf{r}'(\mathbf{r};t)) \tag{7.102}$$

and the exact density is

$$\tilde{J}(\mathbf{r};t) = \int d\mathbf{r}' j(\mathbf{r}') \mid \frac{\partial \mathbf{r}'}{\partial \mathbf{r}} \mid \delta(\mathbf{r}' - \mathbf{r}'(\mathbf{r};t)) \,. \tag{7.103}$$

This yields immediately the final result for the exact current density

$$\tilde{J}(\mathbf{r};t) = j(\mathbf{r}'(\mathbf{r};t)) \mid \frac{\partial \mathbf{r}'}{\partial \mathbf{r}} \mid \,. \tag{7.104}$$

The initial condition $\mathbf{r}'$ may be written as

$$\mathbf{r}'(\mathbf{r};t) = \mathbf{r} + \mathbf{v}(\mathbf{r})t + \delta\mathbf{r}'(\mathbf{r};t) \,. \tag{7.105}$$

This is substituted in the expression for the exact current $\tilde{J}$ which is then linearized, the current perturbation J_1 may then be identified as the term proportional to $\delta\mathbf{r}'$.

Having sketched the general procedure let us turn back to the specific problem at hand. Writing the exact current as an integral over initial conditions of all particles that make it to a given space point at a given time we have

$$r\tilde{J}_b(r,\theta,z;t) = \int dr' \int d\theta' \int dz' r' J_{bo}(r') \delta(\tilde{r} - r)\delta(\tilde{\theta} - \theta)\delta(\tilde{z} - z) \tag{7.106}$$

in this integral the arguments of the delta functions are explicitly $\tilde{r}(r',\theta',z';t)-r$ and similarly for $\tilde{\theta}$ and $\tilde{z}$. The Dirac delta functions say that

$$r' = r - D_r(r',\theta',z';t) \tag{7.107}$$

$$\theta' = \theta - \Omega_\beta(r')t - \frac{1}{r'}D_\theta(r',\theta',z';t) \tag{7.108}$$

$$z' = z - \beta ct \tag{7.109}$$

where, in linear theory we must expand $\Omega_\beta(r')$, $D_r(r',\theta',z';t)$, and $D_\theta(r',\theta',z';t)$ to order $O(D)$. Carrying out this Taylor expansion

$$r' = r - D_r(r,\theta,z;t) \tag{7.110}$$

$$\theta' = \theta - \Omega_\beta(r)t - \frac{1}{r}D_\theta(r,\theta,z;t) + tD_r(r,\theta,z;t)\frac{d}{dr}\Omega_\beta(r) \tag{7.111}$$

$$z' = z - \beta ct \tag{7.112}$$

from which we may compute the Jacobian $\mid \partial\mathbf{r}'/\partial\mathbf{r} \mid$, with the result being

$$\mid \frac{\partial\mathbf{r}'}{\partial\mathbf{r}} \mid = 1 - \frac{dD_r}{dr} + \frac{i}{r}D_\theta \; . \tag{7.113}$$

Linearizing the unperturbed current $J_{bo}(r')$ gives

$$r'J_{bo}(r') = rJ_{bo}(r) - D_r\frac{d}{dr}\left(rJ_{bo}(r)\right) \; . \tag{7.114}$$

Now that we have the linearized Jacobian determinant, and J_{bo} , we may linearize the exact current $\tilde{J}_{bo}$ as given by 7.104

$$\tilde{J}_b(r,\theta,z;t) = J_{bo}(r) - \frac{1}{r}D_r\frac{d}{dr}\left(rJ_{bo}(r)\right) - J_{bo}(r)\frac{d}{dr}D_r - \frac{i}{r}J_{bo}(r)D_\theta + \cdots \; . \tag{7.115}$$

The exact current is $\tilde{J}_b = J_{bo} + J_{b1} + \cdots$. We therefore identify the Fourier transformed current perturbation $\hat{J}_{b1}$ as

$$\hat{J}_{b1} = -\frac{1}{r}\frac{d}{dr}\left(r\hat{D}_r J_{bo}\right) - \frac{i}{r}\hat{D}_\theta J_{bo} \,. \tag{7.116}$$

It is convenient to express the equilibrium current J_{bo} in terms of the betatron frequency Ω_β as follows

$$J_{bo}(r) = \frac{\gamma m}{q\beta}\frac{c}{4\pi}\frac{1}{r}\frac{d}{dr}\left(r^2\Omega_\beta^2\right) \,. \tag{7.117}$$

The formula for $\hat{J}_{b1}$ now reads

$$\frac{4\pi}{c}\hat{J}_{b1}(r) = -\frac{\gamma m}{q\beta}\frac{1}{r}\left(\frac{d}{dr}\left(\hat{D}_r\frac{d}{dr}\left(r^2\Omega_\beta^2\right)\right) + \frac{i}{r}\hat{D}_\theta\frac{d}{dr}\left(r^2\Omega_\beta^2\right)\right) \,. \tag{7.118}$$

In terms of the Fourier amplitude $\hat{A}$, the results 7.98 and 7.97 for $\hat{D}_r$ and $\hat{D}_\theta$ read

$$\hat{D}_r = \frac{q\beta}{\gamma m}\frac{1}{D}\left(\frac{d\hat{A}}{dr} - 2\frac{\Omega_\beta}{\Omega-\Omega_\beta}\frac{\hat{A}}{r}\right) \tag{7.119}$$

$$\hat{D}_\theta = \frac{q\beta}{\gamma m}\frac{1}{D}\left(-2i\frac{\Omega_\beta}{\Omega-\Omega_\beta}\frac{d\hat{A}}{dr} + i\left(1 - \frac{1}{(\Omega-\Omega_\beta)^2}r\frac{d}{dr}\Omega_\beta^2\right)\frac{\hat{A}}{r}\right) \,. \tag{7.120}$$

Substituting these into the result for $\hat{J}_{b1}$ results in

$$\frac{4\pi}{c}\hat{J}_{b1} = -f\frac{d^2\hat{A}}{dr^2} - \left(\frac{f}{r} + \frac{df}{dr}\right)\frac{d\hat{A}}{dr} + \left(g + \frac{f}{r^2}\right)\hat{A} \tag{7.121}$$

where the coefficients are written in terms of $f(r)$ and $g(r)$

$$f(r) = \frac{1}{r}\frac{d}{dr}\left(r^2\Omega_\beta^2\right)\frac{D - 2\Omega\Omega_\beta}{D^2 - 8D\Omega\Omega_\beta} \tag{7.122}$$

$$g(r) = \frac{2}{\Omega^2 - \Omega_\beta^2}\frac{1}{r}\left(-2\Omega^2\frac{d}{dr}\left(\frac{\Omega_\beta^2}{D^2 - 8D\Omega\Omega_\beta}\right)\right. \tag{7.123}$$

$$+\Omega_\beta^2 \frac{d}{dr}\left(\frac{1}{r}\frac{d}{dr}\left(r^2\Omega_\beta^2\right)\right)\frac{D-2\Omega\Omega_\beta}{D^2-8D\Omega\Omega_\beta}\Bigg)$$

where

$$D = \Omega_\beta^2 - \Omega^2 + 2\Omega\Omega_\beta + \frac{1}{r}\frac{d}{dr}\left(r^2\Omega_\beta^2\right) . \tag{7.124}$$

The result 7.121 is to be contrasted and compared with the Vlasov result in the circle limit 7.67. Obviously something is missing in the Vlasov result. We believe that the rigorous approach in the general precessing elliptical helix case is to carry out a calculation analogous to the one we have just completed. Such a calculation presents mathematical complexities however due to the fact that the equilibrium orbits $r(t)$ and $\theta(t)$ must be determined by solving the orbit equations. Furthermore, the equilibrium radial motion will have nonzero time derivative resulting in a more cumbersome calculation.

Substituting 7.121 into the Ampère dipole equation results in the following eigen-equation for $\hat{A}$

$$\left(\frac{d}{dr}\frac{1}{r}\frac{d}{dr}r - q^2(\omega)\right)\hat{A} = f\frac{d^2\hat{A}}{dr^2} + \frac{1}{r}\frac{d}{dr}(rf)\frac{d\hat{A}}{dr} - \left(g + \frac{f}{r^2}\right)\hat{A} \tag{7.125}$$

where f and g are given above. Given the monopole equilibrium radial profile (that is, given $\Omega_\beta(r)$) this equation may be solved for $\hat{A}$ subject to the imposed boundary conditions. Generally, a solution satisfying the boundary conditions will exist only for a definite pair of frequencies Ω and ω . Therefore, given the real driver frequency ω the Doppler-shifted hose frequency $\Omega(\omega)$ determined by forcing satisfaction of the boundary condition constitutes the dispersion relation.

There is one case for which we may rightly expect the solution to be attainable by analytical means. In the low frequency limit $\Omega \to \omega \to 0$ this theory should

reduce to the rigid-beam theory. In rigid-beam theory the solution $\hat{A}$ is the fundamental radial mode $\hat{A} \sim dA_o/dr$. In terms of the equilibrium betatron frequency Ω_β this is $\hat{A} \sim r\Omega_\beta^2$. To verify that this is indeed a solution we investigate the low-frequency limit of the eigen-equation. Setting $\Omega = \omega = 0$ the functions f and g collapse to

$$f(r) = \frac{\chi}{\Omega_\beta^2 + \chi} \tag{7.126}$$

$$g(r) = -\frac{2}{r}\frac{d\chi}{dr}\frac{1}{\Omega_\beta^2 + \chi} \tag{7.127}$$

where the function χ is defined to be $\chi = (1/r)d(r^2\Omega_\beta^2)/dr$. The eigen-equation becomes

$$r^2(1-f)\frac{d^2\hat{A}}{dr^2} + r\left(1 - f - \frac{df}{dr}\right)\frac{d\hat{A}}{dr} - (1 - f - r^2 g)\hat{A} = 0\,. \tag{7.128}$$

From this equation it is a matter of algebra to demonstrate that $\hat{A} \sim r\Omega_\beta^2$ is a solution.

The low frequency solution $\hat{A} \sim r\Omega_\beta^2$ may be motivated from yet another point of view. Recall that in this limit the beam responds by undergoing a rigid lateral displacement. This means that the two linear perturbations $\hat{D}_r$ and $\hat{D}_\theta$ should be constants in this limit so that the displacement will be the same for all particles. It is easy enough to show that this is the case, in the zero frequency limit we have

$$\hat{D}_r = \frac{q\beta}{\gamma m}\frac{1}{D}\left(\frac{d\hat{A}}{dr} + 2\frac{\hat{A}}{r}\right) \tag{7.129}$$

$$\hat{D}_\theta = \frac{q\beta}{\gamma m}\frac{1}{D}\left(2i\frac{d\hat{A}}{dr} + i\left(1 - \frac{1}{\Omega_\beta^2}r\frac{d}{dr}\Omega_\beta^2\right)\frac{\hat{A}}{r}\right) \tag{7.130}$$

where

$$D = \Omega_\beta^2 + \frac{1}{r}\frac{d}{dr}(r^2\Omega_\beta^2) \,. \tag{7.131}$$

Upon substituting $\hat{A} \sim r\Omega_\beta^2$ into these equations we find that $\hat{D}_r \sim (q\beta/\gamma m)$ and $\hat{D}_\theta \sim i(q\beta/\gamma m)$. In terms of $\hat{D}_x$ and $\hat{D}_y$ we have $\hat{D}_y = \hat{D}_r \sin\theta + \hat{D}_\theta \cos\theta$ and $\hat{D}_x = \hat{D}_r \cos\theta - \hat{D}_\theta \sin\theta$, which is a rigid displacement in the direction $(1,1)$.

7.4 Circular Helices: Uniform Profile

In Section 7.1 we derived $\hat{J}_{b1}$ for a general beam on the basis of a Vlasov calculation, inverting the evolution operator on the *unperturbed* orbits. We also specialized to the circle limit (cold transverse phase space) and arrived at

$$\hat{J}_{b1}(r) = \frac{q\beta}{\gamma m}\frac{1}{\Omega_\beta^2(r) - \Omega^2}\frac{1}{r}\frac{dJ_{bo}}{dr}\hat{A}(r) \,. \tag{7.132}$$

In Section 7.4 we wish first to rederive this result from a slightly different perspective which will improve our understanding of its significance. Second, we will specialize to a beam with a uniform radial profile and sharp edge at $r = a$ propagating within a uniform conductivity channel. For this beam we will investigate two cases of boundary conditions

1. G: plasma surrounded by a cold gas

2. W: plasma surrounded by a steel tank

Case W is interesting because it involves the concept of wall stabilization.

Now, let us consider a cold laminar beam with arbitrary radial profile. Here, as opposed to Section 7.1, we will incorporate the assumption of a cold transverse

phase space at the outset (circle orbits). In this case the distribution is one dimensional in momentum space and reads

$$f_{bo} = f_{bo}(P_\theta)\delta(P_z - P_b) \tag{7.133}$$

where $P_\theta = \gamma m r^2 \Omega_\beta$ is the canonical angular momentum . The transverse particle energy $H_\perp$ is given in terms of P_θ by.

$$H_\perp = \frac{P_\theta^2}{\gamma m r^2} - q\beta A_o(r) \; . \tag{7.134}$$

As before, the distribution perturbation is determined by

$$f_{b1} = -q\beta \frac{df_{bo}}{dp_\theta} \int_{-\infty}^{t} dt' \, (\mathbf{z} \times \mathbf{B}_1)'_\theta \; . \tag{7.135}$$

By direct calculation $(\mathbf{z} \times \mathbf{B}_1)_\theta = (i/r)\hat{A}$ so that

$$\hat{f}_{b1} = -q\beta \frac{df_{bo}}{dp_\theta} \frac{i}{r} \hat{A} \int_{-\infty}^{t} dt' \exp i \left(\Omega_\beta(t'-t) + k\beta c(t'-t) - \omega(t'-t)\right) \tag{7.136}$$

which yields

$$\hat{f}_{b1} = -q\beta \frac{\hat{A}}{r} \frac{df_{bo}}{dp_\theta} \frac{1}{\Omega_\beta - \Omega} \; . \tag{7.137}$$

Integrating over p_θ to get $\hat{J}_{b1}$ yields

$$\hat{J}_{b1} = -q^2\beta^2 c \frac{\hat{A}}{r} \int_{-\infty}^{\infty} dp_\theta \frac{df_{bo}}{dp_\theta} \left(\Omega_\beta - \Omega\right)^{-1} \; . \tag{7.138}$$

The distribution f_{bo} for an unpolarized (nonrotating) beam is an even function of p_θ . Multiplying the numerator and denominator of the integrand by $\Omega_\beta + \Omega$ and keeping only the term which is even we have

$$\hat{J}_{b1} = -q^2\beta^2 c \frac{\hat{A}}{r} \frac{1}{\Omega_\beta^2 - \Omega^2} \int_{-\infty}^{\infty} dp_\theta \frac{df_{bo}}{dp_\theta} \left(\frac{p_\theta}{\gamma m r}\right) \tag{7.139}$$

finally, using $(p_\theta/r)\partial f_{bo}/\partial p_\theta = -\partial f_{bo}/\partial r$ we arrive at

$$\hat{J}_{b1} = -\frac{q\beta}{\gamma m}\frac{1}{\Omega_\beta^2 - \Omega^2}\frac{1}{r}\frac{dJ_{bo}}{dr}\hat{A} \tag{7.140}$$

or, entirely in terms of Ω_β

$$\frac{4\pi}{c}\hat{J}_{b1} = \frac{1}{\rho}\frac{d}{d\rho}\left(\frac{1}{\rho}\frac{d}{d\rho}\left(\rho^2\Omega_\beta\right)\right)\frac{1}{\Omega_\beta^2 - \Omega^2}\frac{\hat{A}}{a^2} \tag{7.141}$$

which is, naturally, the same as the result of Section 7.1 in the circle limit. This tells us that the circle limit of the warm Vlasov beam is the same as the cold Vlasov beam 7.65.

Let us now use our result for $\hat{J}_{b1}$ to investigate the dispersion relations for various boundary conditions at the plasma channel edge. We already treated the case of the fundamental mode $\hat{A} \sim dA_o/d\rho$, wherein boundary conditions were slighted, and we know that the cold-Vlasov beam will duplicate the previous results of the circle-limit of the warm- Vlasov beam.Therefore, let us now make different simplifying assumptions which will enable us to fully work out two examples involving boundary effects: we assume that the conductivity is radially uniform out to the gas-plasma interface. Recall that the Fourier transformed dipole Ampère equation is

$$\left(\frac{\partial}{\partial\rho}\frac{1}{\rho}\frac{\partial}{\partial\rho}\rho - q^2(\omega)\right)\hat{A} = -\frac{4\pi}{c}a^2\hat{J}_{b1} \tag{7.142}$$

where $q^2(\omega) = -i\omega\tau$ with $\tau = 4\pi\sigma_o a^2/\beta c^2$ an effective dipole decay constant. Since we consider only the case of uniform conductivity $\sigma_o \neq \sigma_o(r)$, hence, we may solve the field equation in terms of a Green function $\hat{G}(\rho, \rho'; q)$

$$\hat{A}(\rho) = \int_0^\infty d\rho' \rho' \hat{G}(\rho, \rho'; q)\frac{1}{\rho'}\frac{d}{d\rho'}\left(\frac{1}{\rho'}\frac{d}{d\rho'}(\Omega_\beta^2\rho'^2)\right)\frac{1}{\Omega_\beta^2(\rho') - \Omega^2}\hat{A}(\rho') \,. \tag{7.143}$$

This equation amounts to an eigen-equation for $\hat{A}$. At this point in the development only two major assumptions have been made

1. circular helices

2. uniform conductivity

Next, in order to facilitate working out some examples, we will specialize to a beam with a uniform radial profile out to radius $r = a$ at which point it has a sharp edge

3. uniform beam with sharp edge

For this beam the current density is $J_{bo} = (I_b/\pi a^2)H(\rho - 1)$ where H is the Heaviside step function. From the result 7.132 we calculate the following current perturbation for this beam

$$\frac{4\pi}{c}\hat{J}_{b1} = 2\frac{\Omega_\beta^2(1)}{\Omega_\beta^2(1) - \Omega^2}\frac{\hat{A}(1)}{a^2}\delta(\rho - 1) \; . \tag{7.144}$$

Hence, in terms of $\hat{G}$

$$\hat{A}(\rho) = 2\hat{A}(1)\frac{\Omega_\beta^2(1)}{\Omega_\beta^2(1) - \Omega^2}\int_0^\infty d\rho' \rho' \hat{G}(\rho, \rho'; q)\delta(\rho' - 1) \tag{7.145}$$

from which

$$\hat{A}(\rho) = 2\hat{A}(1)\frac{\Omega_\beta^2(1)}{\Omega_\beta^2(1) - \Omega^2}\hat{G}(\rho, 1; q) \; . \tag{7.146}$$

The dispersion relation is gotten by evaluating this at $\rho = 1$

$$1 = 2\frac{\Omega_\beta^2(1)}{\Omega_\beta^2(1) - \Omega^2}\hat{G}(1, 1; q) \tag{7.147}$$

which is our general dispersion relation for a uniform circular helix Vlasov beam propagating in a uniform conductivity channel.

Boundary condition effects are built into the Green function $\hat{G}(\rho, \rho'; q)$. Here we will investigate two special cases

G: uniform conductivity channel of radius $r = R$ surrounded by a cold gas

W: uniform conductivity channel of radius $r = R$ surrounded by a steel tank

For case G the Green function has already been derived in Chapter 6. Evaluating 6.46 at $\rho = \rho' = 1$ and substituting in 7.147 yields the dispersion relation

$$1 = 2\frac{\Omega_\beta^2}{\Omega_\beta^2 - \Omega^2}\left(I_1(q)K_1(q) + \frac{K_o(q\frac{R}{a})}{I_o(q\frac{R}{a})}I_1^2(q)\right) \tag{7.148}$$

where $q^2 = -i\omega\tau$. This is the dispersion relation for a circular helix beam with a uniform profile and sharp edge at radius a propagating in a uniform conductivity channel of radius R surrounded by cold gas.

For case W the potential vanishes at $r = R$, the Green function is easily computed from 6.45 for this boundary condition

$$\hat{G}(\rho, \rho'; q) = I_1(q\rho_<)K_1(q\rho_>) - \frac{K_1(q\frac{R}{a})}{I_1(q\frac{R}{a})}I_1(q\rho_<)I_1(q\rho_>) \; . \tag{7.149}$$

Evaluating this at $\rho = \rho' = 1$ and substituting in 7.147 yields

$$1 = 2\frac{\Omega_\beta^2}{\Omega_\beta^2 - \Omega^2}\left(I_1(q)K_1(q) - \frac{K_1(q\frac{R}{a})}{I_1(q\frac{R}{a})}I_1^2(q)\right) \; , \tag{7.150}$$

the dispersion relation for a circular helix beam with a uniform profile and a sharp edge at $r = a$ propagating in a uniform conductivity channel of radius $r = R$

surrounded by a steel tank (effectively infinite conductivity). The condition that $\hat{A} = 0$ at the wall means that an image current (of infinite density if $\sigma_{wall} = \infty$) is generated on the inner surface of the wall. This image current is equal and opposite to the net current I_b and reacts back upon the beam. This is a stabilizing effect (since opposite currents repel, the beam is pushed back towards the center of the tank). Notice that if $a = R$ then the dispersion relation 7.150 says that $\Omega = \pm\Omega_\beta$ so the oscillations are stable.

Generally, we expect that low frequency modes ($\Omega/\Omega_\beta \ll 1$) will be strongly affected by the wall when $a < R$, while the high frequency modes will be less affected.

Both cases G and W have a dispersion relation of the form

$$1 = \frac{\Omega_\beta^2}{\Omega_\beta^2 - \Omega^2}\hat{G}(q) \tag{7.151}$$

where $\hat{G}(q) \equiv 2\hat{G}(1,1;q)$. Solving for Ω^2 as a function of $q^2 = -i\omega\tau$ results in $\Omega^2 = \Omega_\beta^2(1 - \hat{G}(q))$ so that the normalized growth rate in z is $\mathrm{Im}(\Omega/\Omega_\beta) = -\mathrm{Im}\hat{G}(q)$ with growth occuring if $\mathrm{Im}(\Omega/\Omega_\beta) > 0$. Since in both cases G and W $\hat{G}$ involves the functions I_o , I_1 , K_o , and K_1 with argument $\sqrt{-i}\sqrt{\omega\tau}$ the imaginary part may be obtained through the use of the Kelvin functions [7.4] $ber(\sqrt{\omega\tau})$ and $bei(\sqrt{\omega\tau})$. In both cases G and W we will assume that the growth rate $-i\omega\tau$ as a function of Ω/Ω_β is less than one (this is linear theory after all) so we may expand $\hat{G}(q)$ in powers of $q^2 = -i\omega\tau$.

The functions $\hat{G}(q)$ for cases G and W respectively are

$$\hat{G}_G(q) = 2I_1^2(q)\left(\frac{K_1(q)}{I_1(q)} + \frac{K_o(q\frac{R}{a})}{I_o(q\frac{R}{a})}\right) \tag{7.152}$$

$$\hat{G}_W(q) = 2I_1^2(q)\left(\frac{K_1(q)}{I_1(q)} - \frac{K_1(q\frac{R}{a})}{I_1(q\frac{R}{a})}\right) . \tag{7.153}$$

Notice that in the limit $R/a \to \infty$ the two functions become one in the same

$$\hat{G}(q) = 2I_1(q)K_1(q) \tag{7.154}$$

since both K_o and K_1 vanish, while I_o and I_1 become infinite when $qR/a \to \infty$. If we expand the Bessel functions in powers of q to order q^2 we find $\hat{G} = 1 + q^2/8$ so that, to the same order in q , we have the dispersion relation

$$-i\omega\tau = 8\frac{\Omega^2}{\Omega_\beta^2 - \Omega^2} \tag{7.155}$$

where we have recalled that $q^2 = -i\omega\tau$. Redefining $\tau \to \tau/8$ we have arrived at the rigid-beam dispersion relation. Actually, this is as it should be since the boundary conditions have been moved off to infinity and we have assumed low frequency response.

To proceed in the bounded case $R/a < \infty$ we utilize the small argument expansions of the Bessel functions

$$I_o(q) = 1 + \frac{q^2}{4} + \cdots \tag{7.156}$$

$$K_o(q) = -\frac{q}{2}\left(1 + \frac{q}{2}\right)\log\frac{q}{2} - \frac{q}{2}\left(1 + \frac{q}{2}\right)\gamma + \frac{q^2}{4} + \cdots \tag{7.157}$$

$$I_1(q) = \frac{q}{2} + \frac{q^3}{16} + \cdots \tag{7.158}$$

$$K_1(q) = \frac{q}{2}\left(\gamma + \log\frac{q}{2}\right) + \frac{1}{q} - \frac{q}{4} + \cdots \tag{7.159}$$

where here $\gamma = 0.5772156646\cdots$ is the Euler-Macheroni number [7.4]. To order q^2 the functions $\hat{G}$ are

$$\hat{G}_G(q) = 1 - \frac{q^2}{2}\left(\log\frac{R}{a} + \frac{1}{4}\right) + O(q^4) \tag{7.160}$$

$$\hat{G}_W(q) = 1 - \frac{a^2}{R^2} - \frac{q^2}{2}\left(\log\frac{R^2}{a^2} - 1 + \frac{a^2}{R^2}\right) + O(q^4)\,. \tag{7.161}$$

Notice that the two functions $\hat{G}_G$ and $\hat{G}_W$ as expanded here do not become equal when $R/a \to \infty$. This is of course due to the fact that in this limit the expansion is invalid for the terms in each function $\hat{G}$ which involve R/a.

Solving for the growth rate to lowest order in q^2

$$-i\omega\tau_G = \frac{\Omega^2}{\Omega_\beta^2 - \Omega^2} \tag{7.162}$$

$$-i\omega\tau_W = \frac{\Omega^2 - (\frac{a}{R}\Omega_\beta)^2}{\Omega_\beta^2 - \Omega^2}\,, \tag{7.163}$$

where we have defined effective dipole decay constants τ_G and τ_W for the gas and wall cases

$$\tau_G = \frac{1}{2}\tau\left(\log\frac{R}{a} + \frac{1}{8}\right) \tag{7.164}$$

$$\tau_W = \frac{1}{2}\tau\left(\frac{2\log\frac{R}{a}}{1 - \frac{a^2}{R^2}} - 1\right)\,. \tag{7.165}$$

In the limit $R/a \to \infty$ the dispersion relations are the same except that the decay times do not properly agree with one another as we pointed out previously. Notice that for $\Omega^2 < (a^2/R^2)\Omega_\beta^2$ the wall stabilizes the hose mode [7.5]. Therefore, the low frequency spectrum is indeed stabilized by the conducting wall, as indicated in 7.163.

It is interesting to work backward from the dispersion relation 7.163 for the conducting wall case to the field and force equations that are implied. A moments contemplation reveals that the rigid-beam equations 6.12 and 6.13 need only be modified by adding a term $(a^2/R^2)d$ on the right-hand side of the force equation 6.12 in order to yield the dispersion relation 7.163 upon Fourier transforming. Specifically, the equations are

$$\frac{\partial^2 y}{\partial z^2} + \tilde{\Omega}_\beta^2(y-d) = \frac{a^2}{R^2}\tilde{\Omega}_\beta^2 d \tag{7.166}$$

$$\frac{\partial d}{\partial \varsigma} + \frac{1}{\varsigma_1}(d-y) = 0\,. \tag{7.167}$$

The wall effect therefore appears in the rigid-beam theory as a focussing force, the strength of which depends upon the ratio of the beam to the wall radius. If the beam is very thin (equivalently the tank is very large) then the effectiveness of the wall force is minimal. In the limit $a \to R$ the wall term just equals the focussing term $\tilde{\Omega}_\beta^2 d$ on the left-hand side of the force equation. Therefore in this limit the effectiveness of the fields is twice as great in focussing the beam as in the case without a wall.

7.5 References

7.1 J.Mark, L.Smith, "Plasmas in Particle Accelerators: The Warm-Beam Equilibria", SIAM J. APPL. MATH. **42**, 903 (1982)

7.2 W.M.Sharp, M.Lampe, H.S.Uhm, "Multicomponent Model of the Resistive Hose Instability", Phys. Fluids **25**, 1456 (1982)

7.3 S.Weinberg, "General Theory of Resistive Beam Instabilities", J. Math. Phys. **8**, 614 (1967)

7.4 M.Abramowitz, I.Stegun, Handbook of Mathematical Functions , Dover Publications Inc. (1970)

7.5 E.P.Lee, "Hose Theory", Lawrence Livermore National Laboratory, UCID-16268 (1973)

Chapter 8

Multiple-Oscillator Models

8.1 Introduction

Prior to investigating the adiabatic theory in detail it is useful to place this work in the perspective of the multiple-oscillator models: the spread-mass, energy-group, and multi-component models [8.1, 8.2, 8.3]. Multiple-oscillator models provide an efficient means of numerically simulating beams undergoing linear hose instability. If such an approach is not used then one has recourse to essentially two other methods. First, one may follow large ensembles of particles. Such particle following is used in several beam simulation computer programs in existence including Ringbearer-II, a linearized monopole/dipole hose simulator implemented at Lawrence Livermore National Laboratories [8.4, 8.5]. Second, one may use adiabatic theory to develop a fluid model of hose instability from which a "hydro-code" may be built.

Let us now discuss the physical motivation behind multiple-oscillator models. As indicated in Chapter 1, and proved in Chapter 3, the effective mass, as far as axial dynamics is concerned, is $m\gamma^3$. This means that the slice variable ς of a particle, at injection into the tank, is a single particle constant of motion. For this reason we may, conceptually, divide the beam into a succession of "slices" of width $\delta\varsigma \ll \beta c\tau_1 \equiv \varsigma_1$. Each such segment of the beam is comprized of particles undergoing transverse betatron oscillations. From the point of view of the rest frame of the slice the particles are axially at rest and are orbiting in the transverse plane, in general on precessing elliptical orbits. These transverse orbits have two important frequencies associated with them: radial frequency Ω_r and azimuthal frequency Ω_β . As shown in Chapter 3 [1] the radial frequency is typically larger than the azimuthal (betatron) frequency. Transverse dynamics in an axisymmetric paraxial beam equilibrium is completely determined (in absence of strong collisional effects) by the pinch potential ψ . If, as is usual, this potential is anharmonic, then frequencies Ω_r and Ω_β depend upon the instantaneous radial position of the particle. For such radially dependent frequencies one may define, as we did in Chapter 7, the orbit averaged frequencies $\bar{\Omega}_r$ and $\bar{\Omega}_\beta$, 7.47 and 7.48 respectively. Physically, any applied perturbation having a Fourier decomposition on the beam variables ς and z of the form $f(r,\theta,\varsigma,z) = \hat{f}(r)\exp i(\theta - \omega\varsigma/\beta c - \Omega z/\beta c)$ will couple maximally to those particles having $\bar{\Omega}_\beta \sim \Omega$. Under these circumstances one should expect the beam response to be dominated by the class of resonant particles resulting in a plastic deformation, as opposed to the

[1] cf. Fig. 3.2 for the particular case of a Bennett equilibrium

rigid displacement of the rigid-beam theory. This plastic deformation is more pronounced for high-frequency $\Omega \sim \Omega_\beta$ perturbations.

For an ultra-relativistic electron beam which is generated by a non-isoenergetic source, there will be a spread in axial energy of the particles within the beam. Consequently, the betatron frequencies will be spread, even in a beam with a harmonic pinch potential. Again, the beam segment resolves into classes of particles according to particle mass and certain particles may resonate with a perturbation by virtue of their particular relativistic mass.

The discussion above leads us to consider resolving the beam, for theoretical purposes, into distinct classes of particles; in fact each beam *segment* will be thought of as being composed of distinct classes of particles. Each class will have particles with a certain common property, that is : mass, transverse energy, or azimuthal frequency, as the case may be. In fact, we may further idealize in the following manner: let us think of each class of particles in the segment as a distinct entity with no internal "structure" of its own; then, the beam segment is composed not of particles but of some number N of sub-segments which we have proposed calling "oscillator components". On this line of thought we have arrived at the general "multiple-oscillator" approach to hose physics.

It is extremely useful to consider that each oscillator component responds linearly to a hose perturbation $\sim \exp i(\theta - \Omega z/\beta c - \omega\varsigma/\beta c)$. From this viewpoint let us now consider the following illuminating *gedanken* experiment. Suppose as the beam streams past a certain z position in the laboratory it is subjected to a so-called "tickling" perturbation. In this thought experiment let us further sup-

pose that the tickling is applied only to one thin segment of the beam. Since the segment thickness in ς is assumed much less than the monopole and dipole decay lengths the displacement of this slice transversely cannot affect the fields. Therefore, as the slice streams away from the point at which it was perturbed it will oscillate in some fashion in the unperturbed fields. Initially all sub-segments were displaced equally so the initial transverse displacement of the segment centroid was the same as the individual displacements of the sub-segments; that is, the segment was displaced rigidly. However, as the segment travels downstream the sub-segments oscillate harmonically at distinct fundamental frequencies. Therefore, the sub-segments, which were initially in phase, get out of phase with one another ; randomizing of the relative phases implies that the centroid of the segment damps back to the axis. This basic phenomenon is known as phase mix damping.

Mathematically, the preceeding ideas may be expressed as follows: we denote by $y(z)$ the transverse displacement in the direction $\mathbf{x}$ of the centroid of a given beam segment ς , the centroid displacement of the n^{th} oscillator component will be denoted y_n where $y_n = y^{(n)}\cos(\Omega_n z)$ with Ω_n the characteristic response frequency, the oscillator mass will be denoted m_n . The lateral displacement of the segment centroid is

$$y = \sum_{n=1}^{N} m_n y_n \left(\sum_{n=1}^{N} m_n \right)^{-1} . \tag{8.1}$$

At $z = 0$ the oscillators are therefore displaced by unity (since $y_n = y_{n'}$) . Subsequently the terms tend to cancel since the phases have randomized. Of

course, with a finite number of oscillators, the response $y(z)$ will be conditionally periodic; if the frequencies are rationally related there will be a long "time" periodicity in z ; if the frequencies are irrationally related then strictly speaking the system is aperiodic; however, certain clusters of oscillators may be nearly rationally related and again one may see a long term periodicity [2].

A dispersion relation for a beam with Ω_β variation may be gotten from any of the previous results for $\hat{J}_{b1}$ which we have derived, simply, by averaging over Ω_β weighted by a distribution which reflects the distribution of Ω_β over the particles in the beam. For example, the general result for the circular helix beam, with uniform radial profile, propagating in a uniform conductivity channel

$$1 = \frac{\Omega_\beta^2}{\Omega_\beta^2 - \Omega^2}\hat{G}(q) \tag{8.2}$$

may be modified to read

$$1 = \hat{G}(q)\int_0^\infty d\Omega_\beta g(\Omega_\beta)\frac{\Omega_\beta^2}{\Omega_\beta^2 - \Omega^2} \tag{8.3}$$

which form may be derived, by tracing through the arguments utilized in Chapter 7, for the extended single particle distribution $f_{bo}(P_\theta, \Omega_\beta)$. The function $g(\Omega_\beta)$ is the distribution of Ω_β amongst the particles of the beam. The distribution $g(\Omega_\beta)$ has a maximum at $\langle\Omega_\beta\rangle$ and half-width $\Delta\Omega_\beta$ assuming that the generic distribution g is a Gaussian or Lorentzian type function (bell shaped). Notice that if the width vanishes (so g is effectively a Dirac delta function $\delta(\Omega_\beta - \langle\Omega_\beta\rangle)$) then the dispersion relation 8.3 reduces to the rigid-beam model as it should.

[2]This periodicity is actually seen in numerical simulations, cf. [8.6].

Taking the limit $\Omega \to 0$ in the integral 8.3 results in

$$1 = \int_0^\infty d\Omega_\beta g(\Omega_\beta) \, . \tag{8.4}$$

Now, using

$$\frac{\Omega_\beta^2}{\Omega_\beta^2 - \Omega^2} = 1 + \frac{\Omega^2}{\Omega_\beta^2 - \Omega^2} \tag{8.5}$$

along with 8.4 we get

$$\hat{G}^{-1}(q) = 1 + \Omega^2 \int_0^\infty d\Omega_\beta g(\Omega_\beta) \frac{1}{\Omega_\beta^2 - \Omega^2} \, . \tag{8.6}$$

Recall that for both the cases G and W of Chapter 7 we had $\hat{G} = 1 + O(q^2)$, explicitly

$$\hat{G}_G = 1 - \frac{1}{2}\frac{\tau_G}{\tau} q^2 + \cdots \tag{8.7}$$

$$\hat{G}_W = \left(1 - \frac{a^2}{R^2}\right)\left(1 - \frac{1}{2}\frac{\tau_W}{\tau} q^2\right) + \cdots \tag{8.8}$$

where τ_G and τ_W are given by 7.164 and 7.165 respectively. Let us consider only the gas case. We have $\hat{G} = 1 + i\omega\tau_G/2$ so that $\hat{G}^{-1} = 1 - i\omega\tau_G/2$,and the dispersion relation 8.6 is

$$-i\omega\tau_G = \Omega^2 \int_0^\infty d\Omega_\beta g(\Omega_\beta) \frac{1}{\Omega_\beta^2 - \Omega^2} \, . \tag{8.9}$$

The integral may be written as a residue contribution plus a Cauchy principal value integral as follows

$$-i\omega\tau_G = i\frac{\pi}{2}\Omega g(\Omega) + P \int_0^\infty d\Omega_\beta g(\Omega_\beta) \frac{\Omega^2}{\Omega_\beta^2 - \Omega^2} \, . \tag{8.10}$$

For a $g(\Omega_\beta)$ of finite width, contemplation of the dispersion relation 8.10 convinces us there is a cutoff frequency at about $\langle \Omega_\beta \rangle$ and an upper bound on the growth rate of $\langle \Omega_\beta \rangle / 2\Delta\Omega_\beta$ as shown in Fig. 6.6.

8.2 Spread-Mass Model

Historically, the spread-mass (distributed-mass) model was the first multiple-oscillator model of an electron beam undergoing hose instability. The spread-mass model was developed, along with the basic multiple-oscillator concept, by E. P. Lee [8.1].

Physically, the motivation behind the spread-mass model is the fact that the betatron frequency, even in a harmonic pinch potential, will be distributed in some fashion if the beam has a γ variation [3]. This is because Ω_β depends directly upon the relativistic mass γm . In order to realistically treat hose instability, in a harmonic pinch potential, one should account for this spread in particle mass and the resulting spread in betatron frequency. This has the effect of eliminating the unique response frequency, and resulting infinite resonance, of the rigid-beam model.

For a beam with an anharmonic pinch potential a strong betatron frequency distributing effect is the nonlinearity of the potential. This spreading effect is completely independent of mass spread and will therefore occur even in a mono-energetic beam. However, even in a strongly anharmonic beam, with gamma variation, most of the particles may be located near the axis in a region which is locally radially uniform (and therefore harmonic) and here again the mass spread will be significant [4].

[3] M. N. Rosenbluth was the first to realize the importance of such betatron frequency spread in the context of hose instability.

[4] Private communication, M.N. Rosenbluth

Consider a thin segment of the beam. Suppose the segment is made up of overlapping wafers, each having the same radial profile as the unperturbed beam (Bennett profile) and each comprised of particles having a given mass. Let us denote the oscillator components (wafers) with a continuous subscript ν , where $0 \leq \nu \leq 1$; the lateral displacement of the ν oscillator is denoted $y_\nu(z,\varsigma)$. The rigid-response frequency of the ν oscillator is *assumed* to be

$$\Omega_\nu^2 = \nu\Omega_{\beta o}^2 \tag{8.11}$$

so that the response frequencies of the oscillators vary from 0 , corresponding to particles far from axis, to $\Omega_{\beta o}$ corresponding to particles on axis. In terms of the rigid-response "shaking" frequency Ω_s of the entire segment we define

$$\Omega_\nu^2 = \frac{m}{m_\nu}\Omega_s^2 \,. \tag{8.12}$$

These two equations may be combined to show that the wafer mass m_ν is related to the electron rest mass m by

$$m_\nu = \frac{1}{3\nu}m \,. \tag{8.13}$$

The basic equations we will use are the rigid-beam force and field equations, 6.12 and 6.13 respectively, written for each separate oscillator

$$\frac{\partial^2 y_\nu}{\partial z^2} + \tilde{\Omega}_\nu^2(y_\nu - d) = 0 \tag{8.14}$$

$$\frac{\partial d}{\partial \varsigma} + \frac{1}{\varsigma_1}(d - y) = 0 \tag{8.15}$$

where y is the average of y_ν over the distribution of oscillators. Introducing $\tilde{\Omega}_\nu^2 = \nu\tilde{\Omega}_{\beta o}^2$ and Fourier transforming results in

$$\left(\nu\tilde{\Omega}_{\beta o}^2 - \tilde{\Omega}^2\right) y_\nu - \nu\tilde{\Omega}_{\beta o}^2 d = 0 \tag{8.16}$$

$$(1 - i\omega\tau)d - y = 0\,. \tag{8.17}$$

Solving the force equation for y_ν and averaging over ν yields

$$y = d\int_0^1 d\nu g(\nu)\frac{\nu\Omega_{\beta o}^2}{\nu\Omega_{\beta o}^2 - \Omega^2} \tag{8.18}$$

where, here we have explicitly denoted the distribution of oscillators by $g(\nu)$ which is analogous to $g(\Omega_\beta)$ in the Section 8.1. Substituting into the field equation yields the dispersion relation

$$1 - i\omega\tau = \int_0^1 d\nu g(\nu)\frac{\nu\Omega_{\beta o}^2}{\nu\Omega_{\beta o}^2 - \Omega^2} \tag{8.19}$$

which bears a strong similarity to the dispersion relation 8.3 of Section 8.1.

So far, other than defining $\Omega_\nu^2 = \nu\Omega_{\beta o}^2$ and $\Omega_\nu^2 = (m/m_\nu)\Omega_s^2$, we have said little more than we did in Section 8.1. The essential theoretical content of the spread-mass model is introduced by selecting a specific form of the distribution function $g(\nu)$. Any such distribution must obey certain *natural* conditions, namely

$$\int_0^1 d\nu g(\nu) = 1 \tag{8.20}$$

$$g(0) = 0 \tag{8.21}$$

$$g(\nu) \geq 0 \tag{8.22}$$

$$\int_0^1 d\nu g(\nu) m_\nu = m \,. \tag{8.23}$$

The specific form for $g(\nu)$, chosen by Lee [8.1], is a quadratic polynomial, the lowest order polynomial with enough free constants to satisfy the conditions listed above. Lee uses

$$g(\nu) = 6\nu(1-\nu) \tag{8.24}$$

which is easily seen to be sufficient. The dispersion relation reads

$$-i\omega\tau = \Omega^2 \int_0^1 d\nu 6\nu(1-\nu) \frac{1}{\nu\Omega_{\beta o}^2 - \Omega^2} \tag{8.25}$$

which is in fact identical to the result 7.75 of the circle-limit of the warm-Vlasov beam, which result in turn is identical to the cold-Vlasov beam. In Section 8.3 we shall find that the energy-group model also yields the same dispersion relation. All of these identifications hold for the Bennett beam, which is our particular example in this thesis. In terms of the normalized frequency $\alpha = \Omega/\Omega_{\beta o}$, upon carrying out the integration, 8.25 yields $-i\omega\tau = F(\alpha)$ where

$$F(\alpha) = 6\alpha^2 \left(\frac{1}{2} - \alpha^2 + \alpha^2(1-\alpha^2) \left(\log \frac{1-\alpha^2}{\alpha^2} + \pi i \right) \right) \tag{8.26}$$

for $0 \leq \alpha \leq 1$ and α real. The real and imaginary parts of $F(\alpha)$ are plotted in Fig. 8.2; notice that there is a cutoff frequency [5].

[5]Note also that there is a zero frequency mode, that is, a nontrivial mode with both Ω and ω equal to zero. This zero frequency mode exists because the rigid-beam equations of motion have a symmetry (lateral displacement) which a particular solution does *not* share. Physically, the mode is a uniform lateral displacement of the beam (the beam remains straight) followed by propagation at the new (displaced) position. Mathematically, the existence of the mode is

It is interesting to consider the *gedanken* experiment again in terms of the spread-mass model. Suppose a single slice is perturbed at $z = 0$ such that the ν oscillator responds according to $y_\nu(z) = \cos(\Omega_\nu z/\beta c)$. The centroid (center of mass) of the disk is given by $y_{cm} = \langle (m_\nu/m) y_\nu \rangle$, which is $y_{cm} = \langle y_\nu/3\nu \rangle$, where $\langle\rangle$ denotes averaging over $g(\nu)$. Explicitly, the centroid response is

$$y_{cm}(z) = \int_0^1 d\nu 2(1-\nu) \cos\left(\sqrt{\nu}\frac{\Omega_{\beta o} z}{\beta c}\right) \tag{8.27}$$

which works out, in terms of the variable $\xi = \Omega_{\beta o} z/\beta c$ which measures axial distance in betatron wavelengths, to be

$$y_{cm}(\xi) = \frac{4}{\xi^2}\left(-\left(\frac{6}{\xi^2}+1\right) + \frac{6}{\xi}\sin\xi + \left(\frac{6}{\xi^2}-2\right)\cos\xi\right) . \tag{8.28}$$

Hence, for large ξ we find $y_{cm} \sim 1/\xi^2$ which indicates phase mix damping.

---

understood on the basis of the Goldstone theorem, cf. [8.7]. Plasma current $f_m \neq 0$ "breaks" the symmetry of the equations and the zero-frequency mode disappears, as we shall see in Section 8.5.

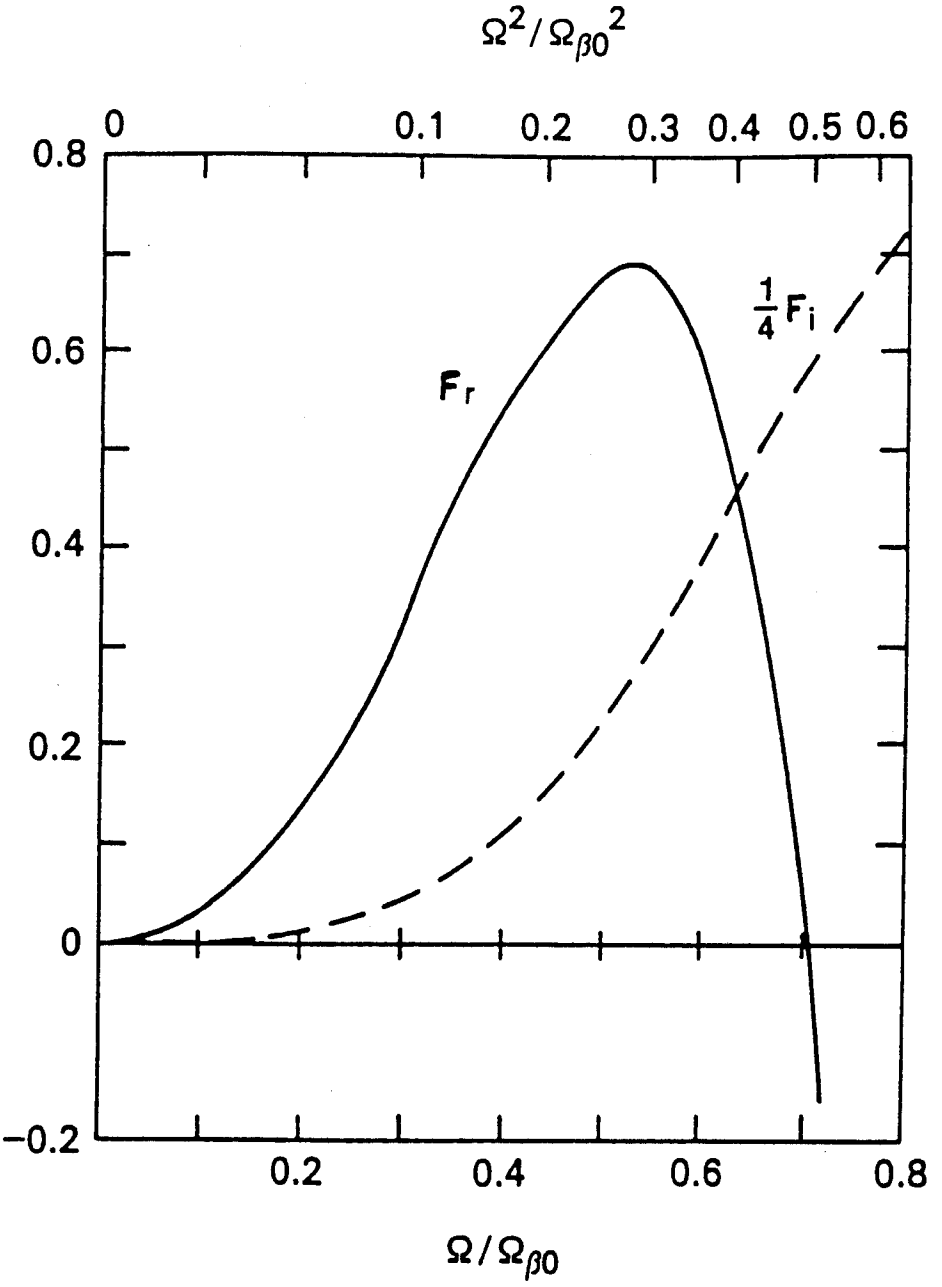

Figure 8.1: Real F_r and imaginary F_i parts of the spread-mass model dispersion relation $F(\alpha) = -i\omega\tau$. Note in particular the maximum growth-rate $F_r \approx 0.8$ and the high-frequency cutoff $F_r(\alpha) = 0$ at $\alpha \equiv \Omega/\Omega_{\beta o} \approx 0.7$.

8.3 Energy-Group Model

In Section 8.3 we wish to present an original, streamlined, development of the energy-group model of linear hose instability of an ultra-relativistic electron beam propagating in resistive plasma. The intention is to bring to the forefront the essential aspects of this model, emphasizing, in particular, the close formal similarity to the spread-mass model. The energy-group model was developed by H. S. Uhm and M. Lampe in 1980 [8.2]; their treatment included plasma current effects f_m and an applied axial magnetic guide field B_z . We will not consider either of these.

Before delving into the energy-group model in detail let us develop, in general, the basic multiple-oscillator equations which we will need. The starting point of the energy-group model, as with all hose models, is with the basic field and force equations

$$\left(\frac{\partial}{\partial r}\frac{1}{r}\frac{\partial}{\partial r}r - \frac{4\pi}{c}\beta\sigma(r)\frac{\partial}{\partial \varsigma}\right)A_1 = -\frac{4\pi}{c}J_{b1} \tag{8.29}$$

$$\frac{\partial^2 \mathbf{r}}{\partial z^2} = \frac{q\beta}{\gamma m}\frac{\partial A}{\partial \mathbf{r}} \,. \tag{8.30}$$

In multiple-oscillator models the current $J_{bo}(r)$ is considered to be a superposition of partial currents each associated with one of the oscillators. Generally, in order to resolve radially dependent resonances, the sub-segments will all have differing radii. Let us therefore denote the sub-segment label by R . This is meant to have underlying functional dependence upon the physical property [6] which dis-

[6] For the spread-mass, energy-group, and multi-component models, the physical properties are mass, transverse energy, and betatron frequency, respectively.

tinguishes one oscillator from another. Denoting the partial current by $J_b(r;R)$ (the current density at r due to the R oscillator) we may write the total current density $J_b(r)$ as an integral over the components

$$J_b(r) = \int_0^\infty dR J_b(r;R) \; . \tag{8.31}$$

Once again we define the lateral displacement of the R oscillator as $y(R)$, which obeys the linearized Newton's law, averaged over the component profile. Averaging the **x** component of 8.30 over the current $J_b(r,\theta;R) = J_{bo}(r;R) + J_{b1}(r;R)\cos\theta$ as we did in both the rigid-beam and spread-mass models, we have

$$\frac{\partial^2 y(R)}{\partial z^2} = \frac{q\beta}{\gamma m}\frac{\pi}{I(R)}\int_0^R drr\left(J_{b1}(r;R)\frac{dA_o}{dr} - A_1\frac{d}{dr}J_{bo}(r;R)\right) \tag{8.32}$$

where $I(R)$ is the total current due to the R component

$$I(R) = \int_0^R drr\int_0^{2\pi} d\theta J_b(r,\theta;R) \; . \tag{8.33}$$

Next, as always, we assume each component displaces rigidly, therefore

$$J_{b1}(r;R) = -y(R)\frac{d}{dr}J_{bo}(r;R) \; . \tag{8.34}$$

Inserting this into the linearized, averaged Newton's law we arrive at the generic multiple-oscillator equation

$$\left(\frac{\partial^2}{\partial z^2} + \Omega_c^2(R)\right) y(R) = -\frac{q\beta}{\gamma m}\frac{\pi}{I(R)}\int_0^R drrA_1\frac{d}{dr}J_{bo}(r;R) \tag{8.35}$$

where the oscillator-component frequency $\Omega_c(R)$ is

$$\Omega_c^2(R) = \frac{q\beta}{\gamma m}\frac{\pi}{I(R)}\int_0^R drr\frac{dA_o}{dr}\frac{d}{dr}J_{bo}(r;R) \; . \tag{8.36}$$

Fourier transforming 8.35 and solving for $y(R)$ yields

$$y(R) = -\frac{q\beta}{\gamma m}\frac{1}{\Omega_c^2(R) - \Omega^2}\frac{\pi}{I(R)}\int_0^R drr\hat{A}\frac{d}{dr}J_{bo}(r;R) \; . \tag{8.37}$$

At this point the development is completely general and any multiple- oscillator model may be constructed from this equation; model specificity consists in selecting the particular form of $J_{bo}(r;R)$, and of course, in the interpretation of the physical meaning of the oscillator component label R .

Now let us specialize to the energy-group model. The transverse energy of a particle in the beam is

$$H_\perp = \frac{1}{2\gamma m}\left(\frac{P_\theta^2}{r^2} + p_r^2\right) - q\beta A_o(r) \; . \tag{8.38}$$

In the energy-group model we divide a thin segment of the beam into sub-segments, each of which contains particles with a given transverse energy; the radial profile of each sub-segment is uniform out to a radius $R(H_\perp)$ which depends upon the energy of the particles in the sub-segment. Henceforth we will suppress the $H_\perp$ dependence of $R(H_\perp)$ for notational convenience. The radius R is the maximum radial turning point possible for a particle with transverse energy $H_\perp$ and is defined by

$$H_\perp = \frac{P_\theta^2}{2\gamma m R^2} - q\beta A_o(R) \; . \tag{8.39}$$

In the energy-group model each energy-group contributes a partial current density which is flat out to an energy-dependent radius $R(H_\perp)$

$$J_{bo}(r;R) = J_{bo}(0;R)H(R-r) \tag{8.40}$$

where $J_{bo}(0;R)$ is the partial density at the center of the beam. For this component shape $I(R)$ is

$$I(R) = \frac{\pi}{2} R^2 J_{bo}(0;R) \, . \tag{8.41}$$

Working out $\Omega_c(R)$ and $y(R)$ as given by 8.36 and 8.35 respectively, for the energy-group $J_{bo}(r;R)$ 8.40 , we find

$$y(R) = \frac{q\beta}{\gamma m} \frac{1}{\Omega_\beta^2(R) - \Omega^2} \frac{\hat{A}}{R} \tag{8.42}$$

$$\Omega_c^2(R) = -\frac{q\beta}{\gamma m} \frac{1}{R} \frac{dA_o}{dR} \, . \tag{8.43}$$

The source term J_{b1} in the dipole Ampère equation is now constructed, as usual in the rigid-beam theory, from 8.34 , so that in terms of our explicit form of $y(H_\perp)$ we have the current perturbation $\hat{J}_{b1}(r;R)$

$$\hat{J}_{b1}(r;R) = -\frac{q\beta}{\gamma m} \frac{1}{\Omega^2 - \Omega_\beta^2(R)} \frac{\hat{A}(R)}{R} \frac{dJ_{bo}}{dr}(r;R) \, . \tag{8.44}$$

The source term we need is $\hat{J}(r)$, the total perturbed current at the radius r . This current is the integral of $\hat{J}_{b1}(r;R)$ over R

$$\hat{J}(r) = \int_0^\infty dR \hat{J}_{b1}(r;R) \, . \tag{8.45}$$

In terms of the rigid-beam formula 8.34 this reads

$$\hat{J}_{b1}(r) = -\int_0^R dR y(R) \frac{dJ_{bo}}{dr}(r;R) \, . \tag{8.46}$$

Introducing 8.40 for $J_{bo}(r;R)$ and 8.42 for $y(R)$ results in

$$\hat{J}_{b1}(r) = \frac{q\beta}{\gamma m} \int_0^\infty J_{bo}(0;R) \frac{1}{\Omega^2 - \Omega_\beta^2(R)} \frac{\hat{A}}{R} \delta(R - r) \, . \tag{8.47}$$

To proceed we need to calculate $J_{bo}(0;R)$, this is accomplished with

$$J_{bo}(r) = \int_0^\infty dR J_{bo}(0;R) H(R-r) \tag{8.48}$$

which, after differentiating with respect to r once, yields upon evaluation at $r = R$

$$J_{bo}(0;R) = -\frac{dJ_{bo}}{dR} \ . \tag{8.49}$$

Substituting this in 8.47 and noting the Dirac delta function, we find

$$\hat{J}_{b1}(r) = -\frac{q\beta}{\gamma m} \frac{1}{\Omega^2 - \Omega_\beta^2(r)} \frac{1}{r} \frac{dJ_{bo}}{dr} \hat{A} \ . \tag{8.50}$$

Remarkably, this is the same as the circle-limit of the general Vlasov treatment, and also the same as the cold-Vlasov treatment.

Fourier transforming the field equation 8.29 , working in terms of the variable $\rho = r/a$, and inserting the perturbed current $\hat{J}_{b1}$ we have the eigen-equation

$$\left(\frac{d}{d\rho} \frac{1}{\rho} \frac{d}{d\rho} \rho + \frac{4\pi}{c^2} a^2 \sigma_o(\rho) i\omega \right) \hat{A} = -\frac{4\pi}{c} \frac{q\beta}{\gamma m} \frac{1}{\Omega^2 - \Omega_\beta^2} \frac{1}{\rho} \frac{dJ_{bo}}{d\rho} \hat{A} \ . \tag{8.51}$$

To approximate the eigenvalue ω we will use a variational technique. The method consists of multiplying the eigen-equation by $\hat{A}$ and integrating the resulting equation with $\int_0^\infty d\rho\rho$. A trial function $\hat{A}$ is then inserted to get the approximate eigenvalue. Multiplying by $\hat{A}$ and integrating yields

$$\int_0^\infty d\rho\rho \hat{A} \frac{d}{d\rho} \frac{1}{\rho} \frac{d}{d\rho} \rho \hat{A} + \frac{a^2 4\pi\omega}{c^2} \int_0^\infty d\rho\rho\sigma_o \hat{A}^2 = -\frac{4\pi}{c} \frac{q\beta}{\gamma m} \int_0^\infty d\rho \frac{1}{\Omega^2 - \Omega_\beta^2} \frac{dJ_{bo}}{d\rho} \hat{A}^2 \ . \tag{8.52}$$

A natural candidate for a trial eigenfunction is the fundamental mode $\hat{A} \sim dA_o/d\rho$ which we use in rigid-beam theory. Substituting this eigenfunction and integrat-

ing by parts results in the dispersion relation

$$\frac{i\omega}{c}\int_0^\infty d\rho\rho\sigma_o(\rho)\left(\frac{dA_o}{d\rho}\right)^2 = \int_0^\infty d\rho\rho\frac{dA_o}{d\rho}\frac{dJ_{bo}}{d\rho}\frac{\Omega^2}{\Omega^2-\Omega_\beta^2}\,. \tag{8.53}$$

This dispersion relation is good for any beam equilibrium J_{bo} and also allows for conductivity σ_o which is radially dependent and perhaps shaped differently than the current profile.

Now let us specialize to the Bennett distribution and assume that the conductivity is locally produced. Then the ingredients we need are

$$J_{bo}(\rho) = \frac{I_b}{\pi a^2}\left(1+\rho^2\right)^{-2} \tag{8.54}$$

$$A_o(\rho) = -\frac{I_b}{c}\log\left(1+\rho^2\right) \tag{8.55}$$

$$\sigma_o(\rho) = \sigma_o\left(1+\rho^2\right)^{-2}\,. \tag{8.56}$$

as derived in Chapter 3. Substituting these into the dispersion relation yields

$$i\omega\frac{\sigma_o\pi a^2}{2c^2}\int_0^\infty d\rho\frac{2\rho^3}{(1+\rho^2)^4} = \int_0^\infty d\rho\frac{2\rho^3}{(1+\rho^2)^4}\frac{\Omega^2}{\Omega^2-\Omega_\beta^2}\,. \tag{8.57}$$

Now, if we define a new variable of integration $\nu = (1+\rho^2)^{-1}$ and introduce the dipole decay time $\tau_1 = \sigma_o\pi a^2/2c^2$ we find

$$-i\omega\tau_1 = \Omega^2\int_0^1 d\nu 6\nu(1-\nu)\frac{1}{\nu\Omega_{\beta o}^2-\Omega^2} \tag{8.58}$$

which is the same as the spread-mass model 8.25 . We conclude, therefore, that the energy-group and spread-mass models are formally the same and differ essentially only in the physical interpretation which underlies them. Furthermore,

since we have shown that the energy-group prediction 8.50 for the perturbed current $\hat{J}_{b1}$ is the same as the circle-limit 7.65 of the exact Vlasov theory and also is the same as the cold-Vlasov theory 7.140, there appears to be a direct link between the spread-mass model and the circle-orbit model. This is an indication that the circle-orbit model contains the essential physics of the hose instability, at least, to the same extent that the spread-mass and energy-group models do. These interrelationships, between the various models, appear not to have been noticed prior to our work.

8.4 Multi-Component Model

Having resolved the beam into classes of particles according to mass, and then having resolved the beam into classes according to transverse energy, and having found that these two approaches are essentially the same, we now consider the resolution according to betatron frequency Ω_β . On the face of it, this seems as if it will be a more fruitful approach due to the fact that the betatron frequency determines the coupling of a particle to the hose perturbation. The multiple-oscillator model which results from dividing each beam segment into sub-segments according to betatron frequency is called the multi-component model. The multi-component model was developed by W. M. Sharp, M. Lampe, and H. S. Uhm in 1982 [8.3].

In the multi-component model we assume a component profile which is parabolic

$$J_{bo}(r;R) = J_{bo}(0;R)\left(1-\frac{r^2}{R^2}\right)H(R-r) \tag{8.59}$$

where H is the Heaviside step function. This particular shape is a special case of the more general shape

$$J_{bo}(r;R) = J_{bo}(0;R)\left(1-\frac{r^m}{R^m}\right)H(R-r) \tag{8.60}$$

which may range from a step function $m=\infty$ as in the energy-group model, to a triangle function $m=1$. The particular choice of $m=2$ is motivated by the fact that this choice gives an eigenequation with analytic properties close to those of the general Vlasov result [7].

Now that we have chosen a profile $J_{bo}(r;R)$ we may explicitly compute the perturbed total current $\hat{J}_{b1}(r)$. First, the quantity $I(R)$ turns out to be

$$I(R) = \frac{\pi}{2}R^2 J_{bo}(0;R) \tag{8.61}$$

next, to calculate $J_{bo}(0;R)$ we set up the total current

$$J_{bo}(r) = \int_0^\infty dR\left(1-\frac{r^2}{R^2}\right)J_{bo}(0;R)H(R-r) \tag{8.62}$$

[7] In this regard, it is *only* the choice of oscillator-component radial profile (which choice is actually quite *ad hoc* , aside from the *heuristic* arguments involving the analytic properties of the singularity predicted by the Vlasov theory, which, itself, is not the whole story) which makes the multi-component model differ at all from the energy-group model. In particular, nowhere does the distinction between classes of particles according to transverse energy (energy-group), and classes of particles according to angular momentum (multi-component), acquire an *operational* significance (the distinction never shows up in a calculational difference in the formalisms). It is, therefore, somewhat misleading to emphasize the underlying functional dependence of the oscillator-component label R ; all that really matters is the *shape* $J_{bo}(r;R)$.

from which, by differentiating twice with respect to r and then evaluating the result at $r = R$ yields

$$J_{bo}(0;R) = \frac{1}{4}\left(R\frac{d^2 J_{bo}}{dR^2} - \frac{dJ_{bo}}{dR}\right) . \tag{8.63}$$

Inserting $I(R)$ and $J_{bo}(r;R)$ into 8.36 and integrating by parts once we get

$$\Omega_c^2(R) = \frac{4\pi}{c}\frac{q\beta}{\gamma m}\frac{2}{R^2}\int_0^R drrJ_{bo}(r)\left(1 - \frac{r^2}{R^2}\right) \tag{8.64}$$

with the help of the Ampère monopole equation. Likewise, 8.35 becomes, after integrating by parts twice,

$$y(R) = -\frac{q\beta}{\gamma m}\frac{1}{\Omega_c^2(R) - \Omega^2}\frac{4}{R^2}\int_0^R dr r^2 \hat{A}(r) . \tag{8.65}$$

To calculate the total perturbed current density $\hat{J}_{b1}(r)$ we have

$$\hat{J}_{b1}(r) = \int_0^\infty dR\hat{J}_{b1}(r;R) \tag{8.66}$$

so, in terms of the rigid displacement 8.34

$$\hat{J}_{b1}(r) = -\int_0^\infty dRy(R)\frac{d}{dr}J_{bo}(r;R) . \tag{8.67}$$

Introducing the explicit form of $J_{bo}(r;R)$ this reduces to

$$\hat{J}_{b1}(r) = 2r\int_r^\infty dRy(R)J_{bo}(0;R)\frac{1}{R^2} . \tag{8.68}$$

Substituting our results 8.65 for $y(R)$ and 8.63 for $J_{bo}(o;R)$ we find the perturbed current $\hat{J}_{b1}(r)$ as predicted by the multi- component model, to be

$$\hat{J}_{b1}(r) = 2\frac{q\beta}{\gamma m}\int_r^\infty dR\frac{1}{R^4}\frac{d}{dR}\left(\frac{1}{R}\frac{dJ_{bo}}{dR}\right)\frac{1}{\Omega_c^2(R) - \Omega^2}\int_0^R dr' r'^2 \hat{A}(r') \tag{8.69}$$

where $\Omega_c^2(R)$ is given by 8.64. Substituting this in the Ampère dipole equation 8.29 we get the multi-component hose eigenvalue problem.

Up to this point our development has been for an arbitrary equilibrium beam $J_{bo}(r)$; now let us specialize to the Bennett equilibrium. As in Section 8.2, we will consider only local conductivity generation so that $\sigma_o(r)$ and $J_{bo}(r)$ have the same radial shape. For the Bennett profile the component frequency $\Omega_c(R)$ given by 8.64 works out to be

$$\Omega_c^2(R) = 2\Omega_{\beta o}^2 \frac{a^2}{R^2}\left(1 - \frac{a^2}{R^2}\log\left(1 + \frac{R^2}{a^2}\right)\right) , \tag{8.70}$$

where we have recalled that $\Omega_{\beta o}^2$ is

$$\Omega_{\beta o}^2 = \frac{2q\beta I_b}{a^2 c\gamma m} . \tag{8.71}$$

The perturbed current $\hat{J}_{b1}(r)$ given by 8.69 reduces to the integral

$$\hat{J}_{b1}(r) = 2\frac{q\beta}{\gamma m}\int_r^\infty dR \frac{24a^4}{R^3}\frac{1}{(a^2+R^2)^4}\frac{1}{\Omega_c^2(R) - \Omega^2}\int_0^R dr' r''\hat{A}(r') . \tag{8.72}$$

Next, assuming a test eigenfunction $\hat{A} = dA_o/dr$, the fundamental mode, we find that

$$\int_0^R dr r^2 \hat{A}(r) = -\frac{I_b}{c}\left(R^2 + a^2 \log\frac{a^2}{a^2+R^2}\right) . \tag{8.73}$$

Introducing the variable $\rho = r/a$ and inserting the previous result into $\hat{J}_{b1}$ we have

$$\hat{J}_{b1}(\rho) = -\frac{1}{a^2}\int_\rho^\infty dx \frac{12x}{(1+x^2)^4}\frac{\Omega_c^2(x)}{\Omega_c^2(x) - \Omega^2} . \tag{8.74}$$

From this equation we see that $\hat{J}_{b1}$ has a logarithmic singularity , not a pole as predicted by the Vlasov circle-orbit, spread-mass, or energy-group models.

A variational approximation for the eigenvalue, following the procedure employed previously, is

$$-i\omega\tau = -1 + 36\int_0^\infty d\rho \frac{\rho}{1+\rho^2}\int_\rho^\infty dx \frac{x}{(1+x^2)^4}\frac{\Omega_c^2(x)}{\Omega_c^2(x)-\Omega^2}\,. \tag{8.75}$$

8.5 Conductivity Effects On Multiple-Oscillator Models

In Section 8.5 we wish to investigate the modifications required of the previous work to account both for conductivity generation and for induced plasma current. Mathematically, this means that the field equation we must use is 5.47 , not 5.48 as we have been using. Field equation 5.47 is

$$\left(1+\frac{\partial}{\partial\eta}\right)\left(\frac{\partial}{\partial\rho}\frac{1}{\rho}\frac{\partial}{\partial\rho}\rho - \frac{4\pi}{c}a^2\beta J_{bo}(\rho)\kappa\frac{\partial}{\partial\eta}\right)A_1 = -\frac{4\pi}{c}a^2\left(1+f_m+\frac{\partial}{\partial\eta}\right)J_{b1} \tag{8.76}$$

where $\eta = \log(\varsigma/\varsigma_o)$ with ς_o a reference slice behind the pinch-point, and the Fourier phase is $\exp i\,(\theta - \omega\eta - \Omega z/\beta c)$ with ω being a *dimensionless* frequency, since η is *dimensionless*. Fourier transforming gives

$$\left(\frac{\partial}{\partial\rho}\frac{1}{\rho}\frac{\partial}{\partial\rho}\rho + \frac{4\pi}{c}a^2\beta J_{bo}(\rho)\kappa i\omega\right)\hat{A} = -\frac{4\pi}{c}a^2\left(1+\frac{f_m}{1-i\omega}\right)\hat{J}_{b1}\,. \tag{8.77}$$

Using a variational principle, now familiar, with test eigenfunction $\hat{A} = dA_o/d\rho$, we find the approximate eigenvalue for the Bennett beam

$$i\omega\tau = 1 + \left(1+\frac{f_m}{1-i\omega}\right)\int_0^\infty d\rho \frac{6\rho^2}{1+\rho^2}\frac{\hat{J}_{b1}(\rho)}{J_{bo}(0)} \tag{8.78}$$

where, here, $\tau \equiv I_b \kappa \beta / c$ is a *dimensionless* dipole decay "time". Inserting the Vlasov circle-orbit, spread-mass, and energy-group predictions of $\hat{J}_{b1}$ (all the same) the dispersion relation becomes

$$-i\omega\tau = F(\alpha) + \frac{f_m}{1 - i\omega}\left(1 + F(\alpha)\right) \tag{8.79}$$

where $\alpha = \Omega / \Omega_{\beta o}$ and $F(\alpha)$ is the function 8.26

$$F(\alpha) = 6\alpha^2 \left(\frac{1}{2} - \alpha^2 + \alpha^2(1 - \alpha^2) \left(\log \frac{1 - \alpha^2}{\alpha^2} + \pi i \right) \right) \tag{8.80}$$

which we first encountered in the spread-mass model [8].

[8] Notice that the plasma current $f_m \neq 0$ breaks the symmetry and eliminates the zero frequency mode. If $f_m \neq 0$ then as $\alpha \to 0$ we find that $-i\omega\tau = f_m/(1 - i\omega)$ instead of $-i\omega\tau = 0$.

8.6 References

8.1 E. P. Lee, "Resistive Hose Instability of a Beam With the Bennett Profile", Phys. Fluids **21** , 1327 (1978)

8.2 H. S. Uhm, M. Lampe, "Theory of the Resistive Hose Instability in Relativistic Electron Beams", Phys. Fluids **23** , 1574 (1980)

8.3 W. M. Sharp, M. Lampe, H. S. Uhm, "Multicomponent Model of the Resistive Hose Instability", Phys. Fluids **25** , 1456 (1982)

8.4 F. W. Chambers, "Mathematical Models for the Ringbearer Simulation Code", Lawrence Livermore National Laboratory, UCID-18302 (1979)

8.5 F. W. Chambers, J. A. Masamitsu, E. P. Lee, "Mathematical Models and Illustrative Results for the Ringbearer II Monopole/Dipole Beam Propagation Code" UCID-19494(1982)

8.6 E. P. Lee, "Gaussian-Profile Beam", UCID-19639 (1982)

8.7 S.Weinberg, "General Theory of Resistive Beam Instabilities", J. Math. Phys. **8** , 614 (1967)

Chapter 9

Adiabatic Beam Theory

9.1 Introduction

In Chapter 9 we are going to investigate fluid and drift-kinetic theories of hose instability in ultra-relativistic electron beams. Prior to this, all of our work has been essentially kinetic, that is, we have explicitly solved the Vlasov equation for the perturbed current, or have approximated or modeled the perturbed current based upon an underlying kinetic description. Now we wish to determine to what extent a reduced description, in terms of a moment hierarchy, is able to reproduce the important features of a fully kinetic treatment. Most importantly, a reduced treatment should not leave out the phase mixing effects.

Our reasons for studying reduced descriptions of relativistic particle beams are both academic and pragmatic. It is widely believed that fluid or fluid- kinetic treatments will provide more efficient methods for simulating beam propagation

over many betatron wavelengths. From a more theoretical perspective , however, it is of great interest to determine if a closure of the exact moment equations can be derived which incorporates into the hierarchy the salient kinetic features while providing a theoretically tractable and numerically efficient formalism. It is not at all clear, *a priori* , that the important kinetic properties, such as phase mix damping of nonaxisymmetric perturbations, will survive the"fluidizing" of *all* the degrees of freedom of the system, which results if one uses a fluid equation hierarchy with higher order moment discard closure, combined with assumptions concerning the pressure tensor. It is for this reason that we investigate a fluid-kinetic "hybrid" approach, that is, a drift-kinetic equation. We derive a drift kinetic equation which is gotten from the exact Vlasov equation by "fluidizing" two of the degrees of freedom, leaving one important kinetic degree of freedom intact. As we mentioned in Chapter 1, this procedure follows long traditions in fluid dynamics in that the exact moment equations are used and all approximations are built into the closure relation, the so-called equation of state.

9.2 Fluid Approach to Beam Simulation

The natural starting point for a development of the fluid equations for an ultra-relativistic electron beam is with the coupled covariant Vlasov and Maxwell equations

$$\left(v^\mu \frac{\partial}{\partial x^\mu} + \frac{q}{m} F^\mu_\nu v^\nu \frac{\partial}{\partial v^\mu}\right) f = 0 \tag{9.1}$$

$$\left(\partial^\alpha \partial_\alpha g^\mu_\nu - \partial^\mu \partial_\nu\right) A^\nu = \frac{4\pi}{c} q \int d^4 v f v^\mu \, . \tag{9.2}$$

where $v^\mu = (c\gamma, \mathbf{v}\gamma)$ is the single-particle four-velocity, $f = f(x, v)$ is the extended phase-space single-particle distribution function, $A^\mu = (\phi, \mathbf{A})$ is the four-vector potential, $g^\mu_\nu = diag(1, -1, -1, -1)$ is the metric tensor, and $F^\mu_\nu = \partial^\mu A_\nu - \partial^\nu A_\mu$ is the Faraday electromagnetic field tensor. In terms of the three-space electric field $\mathbf{E}$ and magnetic field $\mathbf{B}$ the components of the Faraday tensor are: $F^{0\nu} = -F^{\nu 0} = (0, \mathbf{E})$ and $F^{ij} = \epsilon^{ijk} B_k$ where ϵ is the Levi-Civita alternating tensor [1]. We have also defined the single-particle gamma $\gamma^{-2} = 1 - \mathbf{v} \cdot \mathbf{v}/c^2$ as usual. Transition between the cotangent and tangent bundles (raising and lowering of indices) is accomplished by means of the metric tensor: $v^\mu = g^{\mu\nu} v_\nu$, $v_\mu = g_{\mu\nu} v^\nu$ and $F_{\mu\nu} = g_{\mu\alpha} g_{\nu\beta} F^{\alpha\beta}$, with $g_{\nu\lambda} g^{\lambda\mu} = \delta^\mu_\nu$.

In order to construct a moment hierarchy we define the following four-velocity moments

$$j^\alpha = \int d^4v f v^\alpha \tag{9.3}$$

$$T^{\alpha\beta} = m \int d^4v f v^\alpha v^\beta \tag{9.4}$$

$$H^{\alpha\beta\gamma} = m \int d^4v f v^\alpha v^\beta v^\gamma \tag{9.5}$$

where j^α is the particle-current-density four-vector, $T^{\alpha\beta}$ is the stress-energy tensor, and $H^{\alpha\beta\gamma}$ is the heat-flow tensor. Next we apply $\int d^4v f$, $m \int d^4v f v^\alpha$, and $m \int d^4 f v^\alpha v^\beta$ to the covariant Vlasov equation 9.1 to get the first three moment equations

$$\frac{\partial}{\partial x^\alpha} j^\alpha = 0 \tag{9.6}$$

[1] We are using the convention that Greek indices run over 0,1,2,3, while Latin indices run over 1,2,3.

$$\frac{\partial}{\partial x^\alpha} T^{\alpha\beta} = q F^\beta_\alpha j^\alpha \tag{9.7}$$

$$\frac{\partial}{\partial x^\alpha} H^{\alpha\beta\gamma} = \frac{q}{m} F^\mu_\alpha \left(g^\alpha_\mu T^{\beta\gamma} + g^\beta_\mu T^{\alpha\gamma} \right) . \tag{9.8}$$

To proceed further we now define the fluid four-velocity $u^\mu = (c\Gamma, \mathbf{u}\Gamma)$ (not to be confused with the single-particle four-velocity v^μ). In terms of the fluid three-velocity $\mathbf{u}$ we define the fluid-gamma $\Gamma^{-2} = 1 - \mathbf{u}\cdot\mathbf{u}/c^2$. The proper-time τ of a fluid element is related to the laboratory time t by $\Gamma\tau = t$. There are two equivalent ways of defining the fluid four-velocity. First, it is the proper-time derivative of the fluid element position x^μ

$$\frac{\partial x^\mu}{\partial \tau} = u^\mu \tag{9.9}$$

and, second, it is related to the particle-current-density four-vector j^μ by

$$j^\mu = n u^\mu \tag{9.10}$$

where n is the proper fluid density. From the relation $g_{\mu\nu} j^\mu j^\nu = c^2$ we find $n^2 = g_{\mu\nu} j^\mu j^\nu / c^2$. Later on we shall need the following relation between the total time derivative in the laboratory d/dt , and the covariant derivative $\partial/\partial x^\mu$

$$\frac{d}{dt} = \frac{1}{\Gamma} u^\mu \frac{\partial}{\partial x^\mu} . \tag{9.11}$$

Analogous to the decomposition of the three-velocity into an ensemble average and a fluctuating part, we will now make what turns out to be an extremely useful decomposition of the single-particle four-velocity

$$v^\mu = \lambda u^\mu + \xi^\mu . \tag{9.12}$$

Pursuing the analogy with the three-velocity case, we will force the "thermal" term ξ^μ to average to zero

$$\int d^4v f \xi^\mu = 0 \,. \tag{9.13}$$

Applying $\int d^4v f$ to the velocity v^μ 9.12 we find that λ must satisfy

$$\lambda = n \left(\int d^4v f \right)^{-1} \tag{9.14}$$

where we have used the relation $j^\mu = nu^\mu$. Now that we have split v^μ into fluid and thermal components, let us write the moments j^α , $T^{\alpha\beta}$, and $H^{\alpha\beta\gamma}$ in terms of u^μ ,ξ^μ and λ . We find that

$$j^\alpha = nu^\alpha \tag{9.15}$$

$$T^{\alpha\beta} = mn\lambda u^\alpha u^\beta + P^{\alpha\beta} \tag{9.16}$$

$$H^{\alpha\beta\gamma} = \lambda T^{\alpha\beta} u^\gamma + \lambda \left(P^{\beta\gamma} u^\alpha + P^{\alpha\gamma} u^\beta \right) + m \int d^4v f \xi^\alpha \xi^\beta \xi^\gamma \tag{9.17}$$

where we have defined $P^{\alpha\beta}$, the "pressure tensor"

$$P^{\alpha\beta} = m \int d^4v f \xi^\alpha \xi^\beta \,. \tag{9.18}$$

In what amounts to, on the face of it, a seemingly innocuous approximation, we will employ a third order cumulant discard and drop the term

$$\int d^4v f \xi^\alpha \xi^\beta \xi^\gamma \tag{9.19}$$

from the heat tensor $H^{\alpha\beta\gamma}$.

Substituting the relations for j^{α} , $T^{\alpha\beta}$, and $H^{\alpha\beta\gamma}$ in terms of u^{α} , λ and $P^{\alpha\beta}$ into the moment equations, after a fair amount of algebra (in the case of the heat equation) we find

$$\frac{\partial}{\partial x^{\alpha}}(nu^{\alpha}) = 0 \tag{9.20}$$

$$\frac{\partial}{\partial x^{\alpha}}\left(P^{\alpha\beta} + \lambda mnu^{\alpha}u^{\beta}\right) = qnF^{\beta}_{\alpha}u^{\alpha} \tag{9.21}$$

$$\frac{\partial}{\partial x^{\alpha}}\left(\lambda u^{\alpha}P^{\beta\gamma}\right) = \frac{q}{m}F^{\mu}_{\nu}\left(g^{\gamma}_{\mu}P^{\beta\nu} + g^{\beta}_{\mu}P^{\nu\gamma}\right) - P^{\nu\gamma}\frac{\partial}{\partial x^{\nu}}\left(\lambda u^{\beta}\right) - P^{\nu\beta}\frac{\partial}{\partial x^{\nu}}\left(\lambda u^{\gamma}\right) \tag{9.22}$$

$$\left(\partial^{\alpha}\partial_{\alpha}g^{\mu}_{\nu} - \partial^{\mu}\partial_{\nu}\right)A^{\nu} = \frac{4\pi}{c}qnu^{\mu} \tag{9.23}$$

where we have now explicitly included the necessary Maxwell equation 9.23 in the system. These equations express conservation of mass, momentum, and energy of a relativistic fluid interacting with an electromagnetic field created by the fluid itself. At this point in the development the equations are completely general; later we will incorporate various assumptions which reflect the fact that we are studying a paraxial beam.

We wish now to briefly discuss an apparent discrepancy between the number of independent equations and the number of independent unknowns in our system. It is easy to see that the pressure tensor $P^{\alpha\beta}$ is symmetric; therefore, $P^{\alpha\beta}$ has 10 independent components. Counting the number of equations then we find 19. The quantities to be determined: λ , n , $P^{\alpha\beta}$, A^{α} , and u^{α} , are 20 in number. The apparent discrepancy between the number of equations and unknowns is resolved by noting that, as yet, we have not specified a gauge condition; that is, the Maxwell equation 9.23 is written for arbitrary gauge.

As written, the Maxwell equation 9.23 admits no solution. Since this fact is not widely appreciated we will prove it [9.1] and thereby deepen our understanding of the fluid equations. That no solution exists is shown if we demonstrate that the operator $\partial^\alpha \partial_\alpha g^\mu_\nu - \partial^\mu \partial_\nu$ is not invertible, that is, has no Green function. The Green function, supposed for the moment to exist, would satisfy

$$(\partial^\alpha \partial_\alpha g^\mu_\nu - \partial^\mu \partial_\nu)\, G^\nu_\alpha(x - x') = \delta^\mu_\alpha \delta(x - x') \tag{9.24}$$

where $x - x'$ is short for $(x - x')^\mu$. We Fourier analyze as follows

$$G^\nu_\alpha(x - x') = \int \frac{d^4k}{(2\pi)^4} G^\nu_\alpha(k) \exp -ik(x - x') \tag{9.25}$$

$$\delta^4(x - x') = \int \frac{d^4k}{(2\pi)^4} \exp -ik(x - x') \tag{9.26}$$

where $k(x - x') = k^\mu (x - x')_\mu$. Using these, the Maxwell equation 9.24 for the Green function becomes

$$\left(k^\mu k_\nu - k^2 g^\mu_\nu\right) G^\nu_\alpha(k) = \delta^\mu_\alpha \,. \tag{9.27}$$

We realize that there are only two independent two-tensors available in the space-time machinery, namely g^μ_ν and $x^\mu x_\nu$ and scalar multiples thereof, after Fourier transforming; therefore, we only have the tensors g^μ_ν and $k^\mu k_\nu$ from which to build $G^\mu_\nu(k)$. If for some $A(k)$ and $B(k)$ we are able to write

$$G^\nu_\alpha(k) = A(k) k^2 g^\nu_\alpha + B(k) k^\nu k_\alpha \tag{9.28}$$

(the factor k^2 in front of $A(k)$ is for convenience only) then we shall have found our Green function, *provided* it satisfies the Maxwell equation. Substituting G^ν_α

into the Maxwell equation 9.27 we find

$$\left(k^\mu k_\nu - k^2 g^\mu_\nu\right) G^\nu_\alpha = A(k)k^2\left(-k^2\delta^\mu_\alpha + k^\mu k_\alpha\right) \neq \delta^\mu_\alpha \,, \tag{9.29}$$

Therefore, we conclude that no such G^μ_α exists.

In this thesis we work in the Lorentz gauge $\partial_\mu A^\mu = 0$. This gauge condition provides the 20^{th} equation and, thereby, a well posed system. For the Lorentz gauge the Green function is easily shown to exist and is

$$G^\mu_\nu(k) = -\frac{g^\mu_\nu}{k^2} \tag{9.30}$$

which is the Feynman propagator. There is, however, another gauge which is particularly intriguing from the point of view of *plasma* physics, that is, the Landau gauge. In the Landau gauge the Green function works out to be

$$G^\mu_\nu(k) = -\frac{1}{k^2}\left(g^\mu_\nu - \frac{k^\mu k_\nu}{k^2}\right) \tag{9.31}$$

which is familiar, in structure, from the theory of the Landau collision operator, which involves the three-space version of the same tensor. This tensor is a "perpendicular projector"; that is, it projects a four-vector v^μ to its component which is perpendicular to k^μ . Note also that $k_\mu G^\mu_\nu = 0$ (k has no part perpendicular to itself) which is of the same form as the Lorentz gauge condition.

The system of fluid-Maxwell equations 9.20, 9.21, 9.22, and 9.23 which we have derived is fully general. The *only* approximation we made was the third order cumulant discard. Now we wish to incorporate the natural simplifying assumptions which derive from the fact that we are, after all, studying a beam

system. We shall be able, for an ultra-relativistic *beam*, to reduce the fluid equations to a very useful form by means of *natural* approximations.

Before reducing the equations for a beam, let us rewrite the energy equation using the following identity

$$\frac{\partial}{\partial x^\alpha}\left(\lambda u^\alpha P^{\alpha\beta}\right) = N\frac{d}{dt}\left(\frac{\lambda\Gamma}{N}P^{\beta\gamma}\right) \tag{9.32}$$

where $N = n\Gamma$ is the particle density in the laboratory frame [2]. The full set of fluid equations therefore reads

$$\frac{\partial}{\partial x^\alpha}\left(\frac{N}{\Gamma}u^\alpha\right) = 0 \tag{9.33}$$

$$\lambda mnu^\beta\frac{\partial u^\alpha}{\partial x^\alpha} + u^\alpha\frac{\partial}{\partial x^\alpha}(\lambda mu^\beta) + \frac{\partial}{\partial x^\alpha}P^{\alpha\beta} = qnF^\beta_\alpha u^\alpha \tag{9.34}$$

$$N\frac{d}{dt}\left(\frac{\lambda\Gamma}{N}P^{\alpha\beta}\right) = \frac{q}{m}F^\mu_\nu\left(g^\beta_\mu P^{\alpha\nu} + g^\alpha_\mu P^{\nu\beta}\right) - P^{\nu\alpha}\frac{\partial}{\partial x^\nu}\left(\lambda u^\beta\right) - P^{\nu\beta}\frac{\partial}{\partial x^\nu}\left(\lambda u^\alpha\right) . \tag{9.35}$$

The *first* important approximation we will make is that the relativistic fluid is *monoenergetic*; that is, the single-particle γ is the same for all particles. If we recall that $v^\mu = (c\gamma, \mathbf{v}\gamma)$ and $u^\mu = (c\Gamma, \mathbf{u}\Gamma)$ and also that $v^\mu = \lambda u^\mu + \xi^\mu$, then a moments contemplation reveals that $\xi^0 = 0$. This says that $c\gamma = \lambda c\Gamma + \xi^0 = \lambda c\Gamma$. Therefore, for a monoenergetic fluid $\gamma = \lambda\Gamma$. Also, the pressure tensor $P^{\mu\nu} = m\int dv^4 f\xi^\mu\xi^\nu$ vanishes for $\mu = 0$ or $\nu = 0$, that is $P^{0\nu} = 0$. The basic simplifications for a monoenergetic fluid are therefore

$$\gamma = \lambda\Gamma \tag{9.36}$$

[2]The proof of this identity involves the continuity equation 9.20 and the relation 9.11 between the total time derivative d/dt in the laboratory and the covariant derivative $\partial/\partial x^\mu$.

$$P^{0\nu} = 0\,. \tag{9.37}$$

These conditions reduce the fluid equations to the following

$$\frac{\partial}{\partial x^i}\left(Nu^i\right) = 0 \tag{9.38}$$

$$\frac{\partial}{\partial t}(\gamma m N u^i) + \frac{\partial}{\partial x^j}(\gamma m N u^i u^j) + \frac{\partial}{\partial x^j}P^{ji} = qN\left(cF_0^i + u^k F_k^i\right) \tag{9.39}$$

$$N\frac{d}{dt}(\gamma mc) = qF_i^0 u^i \tag{9.40}$$

$$N\frac{d}{dt}\left(\frac{\gamma}{N}P^{ij}\right) = \frac{q}{m}F_k^i P^{kj} + \frac{q}{m}F_k^j P^{ki} - P^{ki}\frac{\partial}{\partial x^k}\left(\gamma u^j\right) - P^{kj}\frac{\partial}{\partial x^k}\left(\gamma u^i\right)\,. \tag{9.41}$$

These are 11 equations for the 11 functions: γ , N , u^i , and P^{ij} [3].

To make subsequent simplifications easier to carry out it is worth the effort to write these fluid and field equations out in full component form in cylindrical (r, θ, z) coordinates. The monoenergetic relativistic fluid and field equations in cylindrical coordinates are

$$\frac{dN}{dt} + N\left(\frac{1}{r}\frac{\partial}{\partial r}(ru_r) + \frac{1}{r}\frac{\partial u_\theta}{\partial \theta} + \frac{\partial u_z}{\partial z}\right) = 0 \tag{9.42}$$

$$\frac{d}{dt}(\gamma mc) = q\left(u_r E_r + u_\theta E_\theta + u_z E_z\right) \tag{9.43}$$

$$N\frac{d}{dt}(\gamma m u_r) + \frac{1}{r}\frac{\partial}{\partial r}(rP_{rr}) + \frac{1}{r}\frac{\partial}{\partial \theta}P_{\theta r} + \frac{\partial}{\partial z}P_{zr} - \frac{1}{r}P_{\theta\theta} - \gamma m N\frac{u_\theta^2}{r} =$$
$$qN\left(E_r + \frac{u_\theta}{c}B_z - \frac{u_z}{c}B_\theta\right) \tag{9.44}$$

$$N\frac{d}{dt}(\gamma m u_\theta) + \frac{1}{r}\frac{\partial}{\partial r}(rP_{r\theta}) + \frac{1}{r}\frac{\partial}{\partial \theta}P_{\theta\theta} + \frac{\partial}{\partial z}P_{z\theta} + \frac{1}{r}P_{\theta r} + \gamma m N\frac{u_\theta u_r}{r} =$$

[3] The fields are gotten from the Maxwell equations $\frac{\partial}{\partial x^\alpha}F_\beta^\alpha = \frac{4\pi}{c}nqu_\beta$ (in the Lorentz gauge) which are a closed set themselves, given u_β .

$$qN\left(E_\theta + \frac{u_z}{c}B_r - \frac{u_r}{c}B_z\right) \tag{9.45}$$

$$N\frac{d}{dt}(\gamma m u_z) + \frac{1}{r}\frac{\partial}{\partial r}(rP_{rz}) + \frac{1}{r}\frac{\partial}{\partial \theta}P_{\theta z} + \frac{\partial}{\partial z}P_{zz} =$$
$$qN\left(E_z + \frac{u_r}{c}B_\theta - \frac{u_\theta}{c}B_r\right) \tag{9.46}$$

$$N\frac{d}{dt}\left(\frac{\gamma}{N}P_{rr}\right) = \frac{q}{m}(2B_\theta P_{rz} - 2B_z P_{r\theta})$$
$$-2P_{rr}\frac{\partial}{\partial r}(\gamma u_r) - 2P_{r\theta}\left(\frac{1}{r}\frac{\partial}{\partial \theta}(\gamma u_r) - \gamma\frac{u_\theta}{r}\right) - 2P_{rz}\frac{\partial}{\partial z}(\gamma u_r) \tag{9.47}$$

$$N\frac{d}{dt}\left(\frac{\gamma}{N}P_{r\theta}\right) = \frac{q}{m}(B_z P_{rr} - B_r P_{rz} - B_z P_{\theta\theta} + B_\theta P_{\theta z})$$
$$-P_{rr}\frac{\partial}{\partial r}(\gamma u_\theta) - P_{\theta r}\left(\frac{1}{r}\frac{\partial}{\partial \theta}(\gamma u_\theta) + \gamma\frac{u_r}{r}\right) - P_{rz}\frac{\partial}{\partial z}(\gamma u_\theta)$$
$$-P_{\theta r}\frac{\partial}{\partial r}(\gamma u_r) - P_{\theta\theta}\left(\frac{1}{r}\frac{\partial}{\partial \theta}(\gamma u_r) - \gamma\frac{u_\theta}{r}\right) - P_{\theta z}\frac{\partial}{\partial z}(\gamma u_r) \tag{9.48}$$

$$N\frac{d}{dt}\left(\frac{\gamma}{N}P_{rz}\right) = \frac{q}{m}(-B_\theta P_{rr} + B_r P_{r\theta} - B_z P_{\theta z} + B_\theta P_{zz})$$
$$-P_{rr}\frac{\partial}{\partial r}(\gamma u_z) - P_{r\theta}\frac{1}{r}\frac{\partial}{\partial \theta}(\gamma u_z) - P_{rz}\frac{\partial}{\partial z}(\gamma u_z)$$
$$-P_{zr}\frac{\partial}{\partial z}(\gamma u_r) - P_{z\theta}\left(\frac{1}{r}\frac{\partial}{\partial \theta}(\gamma u_r) - \gamma\frac{u_\theta}{r}\right) - P_{zz}\frac{\partial}{\partial z}(\gamma u_r) \tag{9.49}$$

$$N\frac{d}{dt}\left(\frac{\gamma}{N}P_{\theta\theta}\right) = \frac{q}{m}(2B_z P_{r\theta} - 2B_r P_{\theta z})$$
$$-2P_{\theta r}\frac{\partial}{\partial r}(\gamma u_\theta) - 2P_{\theta\theta}\left(\frac{1}{r}\frac{\partial}{\partial \theta}(\gamma u_\theta) + \gamma\frac{u_r}{r}\right) - 2P_{\theta z}\frac{\partial}{\partial z}(\gamma u_\theta) \tag{9.50}$$

$$N\frac{d}{dt}\left(\frac{\gamma}{N}P_{\theta z}\right) = \frac{q}{m}(B_z P_{rz} - B_r P_{zz} - B_\theta P_{r\theta} + B_r P_{\theta\theta})$$
$$-P_{\theta r}\frac{\partial}{\partial r}(\gamma u_z) - P_{\theta\theta}\frac{1}{r}\frac{\partial}{\partial \theta}(\gamma u_z) - P_{\theta z}\frac{\partial}{\partial z}(\gamma u_z)$$
$$-P_{zr}\frac{\partial}{\partial r}(\gamma u_\theta) - P_{z\theta}\left(\frac{1}{r}\frac{\partial}{\partial \theta}(\gamma u_\theta) + \gamma\frac{u_r}{r}\right) - P_{zz}\frac{\partial}{\partial z}(\gamma u_\theta) \tag{9.51}$$

$$N\frac{d}{dt}\left(\frac{\gamma}{N}P_{zz}\right) = \frac{q}{m}(-2B_\theta P_{rz} + 2B_r P_{\theta z})$$

$$-2P_{zr}\frac{\partial}{\partial r}(\gamma u_z) - 2P_{z\theta}\frac{1}{r}\frac{\partial}{\partial \theta}(\gamma u_z) - 2P_{zz}\frac{\partial}{\partial z}(\gamma u_z) \tag{9.52}$$

$$E_r = -\frac{\partial \phi}{\partial r} - \frac{1}{c}\frac{\partial A_r}{\partial t} \tag{9.53}$$

$$E_\theta = -\frac{1}{r}\frac{\partial \phi}{\partial \theta} - \frac{1}{c}\frac{\partial A_\theta}{\partial t} \tag{9.54}$$

$$E_z = -\frac{\partial \phi}{\partial z} - \frac{1}{c}\frac{\partial A_z}{\partial t} \tag{9.55}$$

$$B_r = \frac{1}{r}\frac{\partial A_z}{\partial \theta} - \frac{\partial A_\theta}{\partial z} \tag{9.56}$$

$$B_\theta = \frac{\partial A_r}{\partial z} - \frac{\partial A_z}{\partial r} \tag{9.57}$$

$$B_z = \frac{1}{r}\frac{\partial}{\partial r}(rA_\theta) - \frac{1}{r}\frac{\partial A_r}{\partial \theta} \tag{9.58}$$

$$\begin{aligned}
&\frac{1}{r}\frac{\partial}{\partial r}r\frac{\partial \phi}{\partial r} + \frac{1}{r^2}\frac{\partial^2 \phi}{\partial \theta^2} + \frac{\partial^2 \phi}{\partial z^2} - \frac{1}{c^2}\frac{\partial^2 \phi}{\partial t^2} \\
&4\pi\frac{1}{r}\frac{\partial}{\partial r}\left(r\sigma\frac{\partial \phi}{\partial r}\right) + 4\pi\frac{1}{r}\frac{\partial}{\partial \theta}\left(\sigma\frac{1}{r}\frac{\partial \phi}{\partial \theta}\right) + 4\pi\frac{\partial}{\partial z}\left(\sigma\frac{\partial \phi}{\partial z}\right) \\
&+\frac{4\pi}{c}\frac{1}{r}\frac{\partial}{\partial r}\left(r\sigma\frac{\partial A_r}{\partial t}\right) + \frac{4\pi}{c}\frac{1}{r}\frac{\partial}{\partial \theta}\left(\sigma\frac{\partial A_\theta}{\partial t}\right) + \frac{4\pi}{c}\frac{\partial}{\partial z}\left(\sigma\frac{\partial A_z}{\partial t}\right) \\
&= 4\pi q\frac{\partial}{\partial r}Nu_r + 4\pi q\frac{1}{r}\frac{\partial}{\partial \theta}Nu_\theta + 4\pi q\frac{\partial}{\partial z}Nu_z
\end{aligned} \tag{9.59}$$

$$\begin{aligned}
&\frac{1}{r}\frac{\partial}{\partial r}r\frac{\partial A_r}{\partial r} + \frac{1}{r^2}\frac{\partial^2 A_r}{\partial \theta^2} + \frac{\partial^2 A_r}{\partial z^2} - \frac{2}{r^2}\frac{\partial A_\theta}{\partial \theta} - \frac{A_r}{r^2} - \frac{1}{c^2}\frac{\partial^2 A_r}{\partial t^2} \\
&\qquad - \frac{4\pi}{c}\frac{\sigma}{c}\frac{\partial A_r}{\partial t} - \frac{4\pi}{c}\sigma\frac{\partial \phi}{\partial r} = 4\pi N q u_r
\end{aligned} \tag{9.60}$$

$$\frac{1}{r}\frac{\partial}{\partial r}r\frac{\partial A_\theta}{\partial r} + \frac{1}{r^2}\frac{\partial^2 A_\theta}{\partial \theta^2} + \frac{\partial^2 A_\theta}{\partial z^2} + \frac{2}{r^2}\frac{\partial A_r}{\partial \theta} - \frac{A_\theta}{r^2} - \frac{1}{c^2}\frac{\partial^2 A_\theta}{\partial t^2}$$

$$-\frac{4\pi}{c}\frac{\sigma}{c}\frac{\partial A_\theta}{\partial t}-\frac{4\pi}{c}\sigma\frac{1}{r}\frac{\partial\phi}{\partial\theta}=-\frac{4\pi}{c}Nqu_\theta \ . \tag{9.61}$$

$$\frac{1}{r}\frac{\partial}{\partial r}r\frac{\partial A_z}{\partial r}+\frac{1}{r^2}\frac{\partial^2 A_z}{\partial\theta^2}+\frac{\partial^2 A_z}{\partial z^2}-\frac{1}{c^2}\frac{\partial^2 A_z}{\partial t^2}-\frac{4\pi}{c}\frac{\sigma}{c}\frac{\partial A_z}{\partial t}-\frac{4\pi}{c}\sigma\frac{\partial\phi}{\partial z}=-Nqu_z \tag{9.62}$$

$$\frac{\partial\sigma}{\partial\varsigma}=\kappa qN\beta c \ . \tag{9.63}$$

These are the complete equations describing a collisionless [4] monoenergetic relativistic fluid interacting self-consistently with its own electromagnetic fields. The fluid is immersed in an Ohmic plasma, at rest with respect to the laboratory frame (in which the equations are written). Since the fluid is immersed in an Ohmic plasma there are fields generated by currents induced in the plasma by the fluid.

The equations listed above are too general to be of any practical use. We should rightly expect to be able to simplify the system by eliminating terms which are negligible for a *beam* ; that is, we can build into the equations a "beam-like" character. The most important, and obvious, feature of a beam is its directionality. The *second* important approximation we will make, therefore, is that we have an ultra-relativistic beam propagating in the z direction. In Chapter 3 we presented arguments, based upon the relativistic Maxwell-Boltzmann distribution, that the axial degree of freedom is effectively cold (due to the $\gamma^3 m$ effective axial mass) in an ultra-relativistic beam. Mathematically, that the beam is axially-cold

[4] Since local conductivity generation by direct beam impact ionization is occuring the fluid is not quite collisionless. There are, however, no self- collisions (beam-beam).

means that $\xi_z = 0$. This says that the pressure tensor simplifies further: $P^{ij} = 0$ for $i = 3$ or $j = 3$. Since the axial mass is effectively $\gamma^3 m$ we drop the axial dynamics as well:$\partial u_z/\partial z = 0$.

Dropping the z momentum equation and the P_{rz} , $P_{\theta z}$, and P_{zz} energy equations we have the "monoenergetic *axially-cold* fluid equations" [5] which are 7 in number, for the 7 functions: γ , N , u_r , u_θ , P_{rr} , $P_{r\theta}$, and $P_{\theta\theta}$.

Next, we shall build in the paraxial field ordering. With paraxial field ordering we also have the "frozen-field" approximation. Therefore, the field equations reduce to the EMPULSE equations which we derived in Chapter 5. In keeping with paraxial field ordering we will assume that all fields are obtainable from the scalar ϕ and pinch $\psi = \beta A_z - \phi$ potentials [6]. This is our *third* important approximation. Written in terms of beam variables $(z, \varsigma = \beta ct - z)$ with $u_z \equiv \beta c$

$$\left(\frac{\partial}{\partial t}\right)_z = \beta c \left(\frac{\partial}{\partial \varsigma}\right)_z \tag{9.64}$$

[5] Before, we used the appelation "monoenergetic fluid equations", now we further specialize , with the addition of another adjective, to "monoenergetic *axially-cold* fluid equations". Next we will incorporate the paraxial ordering of the fields and further specialize to the "monoenergetic, axially-cold *paraxial* fluid equations". Then, we will set $P_{r\theta} = 0$ to arrive at the "monoenergetic, axially-cold, paraxial *isotropic* fluid equations". Finally, we shall consider an axisymmetric $\partial/\partial\theta = 0$ irrotational $u_\theta = 0$ equilibrium $d/dt = 0$ and recover the Bennett equilibrium as the special *isothermal* ($P_{rr} = P_{\theta\theta}$) case. The Bennett equilibrium is therefore a "monoenergetic, axially-cold, paraxial, isotropic, axisymmetric, irrotational, isothermal" fluid beam (solution by means of "adjective increment".).

[6] Since any rotational current, due to u_θ, provides a source for B_z , strictly speaking, we should work with a radial vector potential A_r as well as A_z . We shall not do this since in this thesis we will assume that $B_z \ll B_\theta$.

$$\left(\frac{\partial}{\partial z}\right)_t = \left(\frac{\partial}{\partial z}\right)_\varsigma - \left(\frac{\partial}{\partial \varsigma}\right)_z \tag{9.65}$$

$$\beta c \frac{d}{dz} = \beta c \left(\frac{\partial}{\partial z}\right)_\varsigma + u_r \frac{\partial}{\partial r} + u_\theta \frac{1}{r}\frac{\partial}{\partial \theta} \tag{9.66}$$

the monoenergetic, axially-cold, paraxial fluid and field beam equations are

$$\beta c \frac{dN}{dz} + N\left(\frac{1}{r}\frac{\partial}{\partial r}(r u_r) + \frac{1}{r}\frac{\partial u_\theta}{\partial \theta}\right) = 0 \tag{9.67}$$

$$\beta c \frac{d}{dz}(\gamma m c) = -q\left(u_r \frac{\partial \phi}{\partial r} + \beta c \frac{\partial \psi}{\partial \varsigma}\right) \tag{9.68}$$

$$N\beta c \frac{d}{dz}(\gamma m u_r) + \frac{1}{r}\frac{\partial}{\partial r}(r P_{rr}) + \frac{1}{r}\frac{\partial}{\partial \theta}P_{\theta r} - \frac{1}{r}P_{\theta\theta} - \gamma m N \frac{u_\theta^2}{r} = qN\frac{\partial \psi}{\partial r} \tag{9.69}$$

$$N\beta c \frac{d}{dz}(\gamma m u_\theta) + \frac{1}{r}\frac{\partial}{\partial r}(r P_{r\theta}) + \frac{1}{r}\frac{\partial}{\partial \theta}P_{\theta\theta} + \frac{1}{r}P_{\theta r} + \gamma m N \frac{u_\theta u_r}{r} = qN\frac{1}{r}\frac{\partial \psi}{\partial \theta} \tag{9.70}$$

$$N\beta c \frac{d}{dz}\left(\frac{\gamma}{N}P_{rr}\right) = -2P_{rr}\frac{\partial}{\partial r}(\gamma u_r) - 2P_{r\theta}\left(\frac{1}{r}\frac{\partial}{\partial \theta}(\gamma u_r) - \gamma\frac{u_\theta}{r}\right) \tag{9.71}$$

$$N\beta c \frac{d}{dz}\left(\frac{\gamma}{N}P_{r\theta}\right) = -P_{rr}\frac{\partial}{\partial r}(\gamma u_\theta) - P_{\theta r}\left(\frac{1}{r}\frac{\partial}{\partial \theta}(\gamma u_\theta) + \gamma\frac{u_r}{r}\right) - P_{\theta r}\frac{\partial}{\partial r}(\gamma u_r) - P_{\theta\theta}\left(\frac{1}{r}\frac{\partial}{\partial \theta}(\gamma u_r) - \gamma\frac{u_\theta}{r}\right) \tag{9.72}$$

$$N\beta c \frac{d}{dz}\left(\frac{\gamma}{N}P_{\theta\theta}\right) = -2P_{\theta r}\frac{\partial}{\partial r}(\gamma u_\theta) - 2P_{\theta\theta}\left(\frac{1}{r}\frac{\partial}{\partial \theta}(\gamma u_\theta) + \gamma\frac{u_r}{r}\right) \tag{9.73}$$

$$\frac{1}{r}\frac{\partial}{\partial r}r\frac{\partial}{\partial r}(\phi + \psi) + \frac{1}{r^2}\frac{\partial^2}{\partial \theta^2}(\psi + \phi) - \frac{4\pi}{c}\sigma\frac{\partial \psi}{\partial \varsigma} = -4\pi q N \beta \tag{9.74}$$

$$\frac{1}{r}\frac{\partial}{\partial r}r\frac{\partial}{\partial r}\frac{\partial \psi}{\partial \varsigma} + \frac{1}{r^2}\frac{\partial^2}{\partial \theta^2}\frac{\partial \psi}{\partial \varsigma} = \frac{4\pi}{c}\frac{\partial}{\partial r}\sigma\frac{\partial \phi}{\partial r} + \frac{4\pi}{c}\frac{1}{r^2}\frac{\partial}{\partial \theta}\sigma\frac{\partial \phi}{\partial \theta} \tag{9.75}$$

$$\frac{\partial \sigma}{\partial \varsigma} = \kappa q N \beta c\,. \tag{9.76}$$

These equations, the monoenergetic, axially-cold, paraxial fluid, field, and conductivity equations, provide a quite rigorous [7] description of an ultra-relativistic

[7] Provided that the rotational current qNu_θ is small enough that B_z is still much weaker than B_θ and E_z .

electron *fluid* beam propagating in the z direction in an Ohmic plasma, generated locally through direct beam impact ionization.

Mathematically, the equations are a set of 10 coupled, nonlinear, partial differential equations for the 10 functions: γ , N , u_r , u_θ , P_{rr} , $P_{r\theta}$, $P_{\theta\theta}$, ψ , ϕ , and σ .

A set of equations which is general enough to use for hose instability problems, while being reasonable from the point of view of implementation as a numerical calculation, consists of the previous set of equations with $P_{\theta r} = 0$ which is our *fourth* important approximation. Furthermore, for propagation over a reasonably small number of betatron wavelengths, we may drop the secular evolution of γ as well, that is, $d\gamma/dz \approx 0$. Likewise, γ is taken to be independent of r and θ . The energy factor γ is therefore, with these approximations, a known constant. The set of equations reduces to 8, in number, for the 8 functions: u_r , u_θ , P_{rr} , $P_{\theta\theta}$, N , ψ , ϕ , and σ . At the risk of infuriating the reader, we will write out explicitly the fluid, field, and conductivity equations for the hose problem of a monoenergetic, axially-cold, paraxial, beam with diagonal pressure

$$\beta c\frac{dN}{dz} + N\frac{1}{r}\frac{\partial}{\partial r}(ru_r) + N\frac{1}{r}\frac{\partial u_\theta}{\partial \theta} = 0 \tag{9.77}$$

$$N\beta mc\gamma\frac{du_r}{dz} + \frac{\partial}{\partial r}(P_{rr}) - \frac{1}{r}(P_{rr} - P_{\theta\theta}) - \gamma mN\frac{u_\theta^2}{r} = qN\frac{\partial \psi}{\partial r} \tag{9.78}$$

$$N\beta mc\gamma\frac{d}{dz}(mu_\theta) + \frac{1}{r}\frac{\partial}{\partial \theta}P_{\theta\theta} + \gamma mN\frac{u_\theta u_r}{r} = qN\frac{1}{r}\frac{\partial \psi}{\partial \theta} \tag{9.79}$$

$$N\beta c\gamma\frac{d}{dz}\left(\frac{P_{rr}}{N}\right) + 2\gamma P_{rr}\frac{\partial u_r}{\partial r} = 0 \tag{9.80}$$

$$N\beta c\gamma\frac{d}{dz}\left(\frac{P_{\theta\theta}}{N}\right) + 2\gamma P_{\theta\theta}\frac{1}{r}\frac{\partial u_\theta}{\partial \theta} + 2\gamma P_{\theta\theta}\frac{u_r}{r} = 0 \tag{9.81}$$

$$\frac{1}{r}\frac{\partial}{\partial r}r\frac{\partial}{\partial r}(\phi+\psi)+\frac{1}{r^2}\frac{\partial^2}{\partial\theta^2}(\psi+\phi)-\frac{4\pi}{c}\sigma\frac{\partial\psi}{\partial\varsigma}=-4\pi qN\beta \tag{9.82}$$

$$\frac{1}{r}\frac{\partial}{\partial r}r\frac{\partial}{\partial r}\frac{\partial\psi}{\partial\varsigma}+\frac{1}{r^2}\frac{\partial^2}{\partial\theta^2}\frac{\partial\psi}{\partial\varsigma}=\frac{4\pi}{c}\frac{\partial}{\partial r}\sigma\frac{\partial\phi}{\partial r}+\frac{4\pi}{c}\frac{1}{r^2}\frac{\partial}{\partial\theta}\sigma\frac{\partial\phi}{\partial\theta} \tag{9.83}$$

$$\frac{\partial\sigma}{\partial\varsigma}=\kappa qN\beta c\,. \tag{9.84}$$

In Chapter 5 we presented the linearized version 5.27 , 5.28 ,5.29, and 5.30 of the EMPULSE field equations. If we expand the quantities N , u_r , u_θ , P_{rr} , and $P_{\theta\theta}$ up to dipole terms also and linearize the continuity equation 9.77, radial and angular momentum equations 9.78 and 9.79, and the two energy equations (equations of state) 9.80 and 9.81, then we will have a linearized monopole/dipole *fluid* model for the hose instability. However, there is a serious objection which we may raise at this point: namely, there is no way of knowing if the system will exhibit phase mix damping or not. Our approximations, while seemingly harmless enough, have not been of the type that would build into the system the important kinetic properties. We have simply discarded a third order cumulant [8], and made several cogent assumptions [9] about the pressure tensor. The question is: is this good enough? Even an irrotational beam will have two counter-rotating streams; hence there are two polarizations of u_θ . This means there will be a fluid stress between the two oppositely rotating fluid streams. Has our fluid hierarchy erased this feature? Let us defer these questions to Section 9.3. For now, we content ourselves with demonstrating that the Bennett equilibrium is contained in our system as a special case.

[8] Explicitly: $m\int dv^4 f\xi^\alpha\xi^\beta\xi^\gamma=0$.

[9] Explicitly: $P_{tt}=P_{rt}=P_{\theta t}=P_{zt}=P_{rz}=P_{\theta z}=P_{zz}=P_{r\theta}=0$.

The Bennett equilibrium, which we derived in Chapter 3, by means of the covariant Maxwell-Boltzmann distribution, is an axisymmetric ($\partial/\partial\theta = 0$),isothermal ($P_{rr} = P_{\theta\theta}$),irrotational ($u_\theta = 0$) equilibrium ($d/dz = 0$). In terms of the plasma neutralization fractions f_m , f_c , and $\lambda = 1 - 1/\beta^2(1+f_c)/(1+f_m)$ (this usage of the symbol λ is *not* as in the previous work in Chapter 9; it is the λ introduced in Chapter 3) the fluid and field equations reduce to

$$\frac{dP_{rr}}{dr} = qN\beta\lambda\frac{dA_o}{dr} \tag{9.85}$$

$$\frac{1}{r}\frac{d}{dr}r\frac{dA_o}{dr} = -\frac{4\pi}{c}(1+f_m)qN\beta c\ . \tag{9.86}$$

Introducing the kinetic transverse temperature by the relation $P_{rr} = NT$ and converting to the dimensionless variable $\rho = r/a$, integration of 9.85 yields

$$N = N_o \exp\left(\frac{q\beta\lambda}{T}A_o\right)\ . \tag{9.87}$$

Substituting this into 9.86 we find the Poisson-Boltzmann equation

$$\frac{1}{\rho}\frac{d}{d\rho}\rho\frac{df}{d\rho} = -\frac{4q\beta(1+f_m)\lambda I_b}{cT}e^f \tag{9.88}$$

where we have used $N_o = I_b/(\pi a^2 q\beta)$ and have defined $f = (q\beta\lambda/T)A_o$. By substitution we verify that the function $f = -2\log(1+\rho^2)$ solves this equation, *provided* that

$$T = \frac{q\beta(1+f_m)\lambda I_b}{2c}\ . \tag{9.89}$$

This is the Bennett temperature which we derived in Chapter 3 by means of the virial of Clausius. The temperature appears here as a condition that an isothermal, axisymmetric, radial equilibrium exists.

9.3 Drift-Kinetic Approach to Beam Simulation

Simulation of an ultra-relativistic electron beam undergoing linear hose instability must reproduce the essential phase mixing effects. Phase mixing damps the mode at a fixed slice postion, causing the mode be convective rather than absolute in character. A hose instability should convect from the head to the tail of the beam, growing in amplitude and in wavelength as it does. Experimentally, such convective behavior of small amplitude lateral displacements is well known. In the absence of phase mixing, due to the nonlinear pinch potential, theory predicts, in contrast to experiment, absolute growth in the beam slice rest frame.

In Section 9.2 we developed a fluid description of a paraxial monoenergetic electron beam; however, we did not build into the theory the important kinetic features associated with the details of single- particle orbits. We may say that the theory of Section 9.2 is not "beam-like" enough. It is the purpose of Section 9.3 to determine whether or not it is possible to do a little better. Generally, it isn't feasible to use a fully kinetic treatment since there are just too many variables, some of which are not crucial to the hose instability. On the other hand, a fully fluid model washes out too many of the specifically "beam-like" properties. Therefore, we wish to develop an intermediate, "hybrid", theory, wherein two degrees of freedom are washed out, that is, fluidized, while the degree of freedom of crucial importance to the hose instability is dealt with kinetically.

In the fluid theory the pressure tensor is determined by solving the second velocity moment equations. However, the definition of the pressure tensor suggests a slightly different method of computing the stresses. Suppose we use the exact

continuity and momentum equations, as in Section 9.2, but instead of using an approximate energy equation to determine the pressure, suppose we approximate the kinetic equation itself and determine the pressure as a second moment of the modified single particle distribution function? Such a modified distribution function is called a drift-kinetic distribution function, and the evolution equation which it obeys, a drift-kinetic equation.

Adiabatic beam theory is based upon an analogy with the adiabatic fluid-kinetic theory of Chew, Goldberger, and Low [9.2]. The gyration about field lines in the CGL theory is identified with the betatron vortex gyration of the transverse orbit in a beam. Contrary to the physical situation envisaged in the CGL theory, in a beam there is no strong field about which the particles gyrate [10].

The basic ideas of adiabatic beam theory were first worked out by J. Mark [9.3] in the context of heavy-ion beams. For certain applications of beams comprised of heavy ions, such as heavy-ion fusion, one is interested in axially bunching the beam by means of a gradient in beam energy from the head to the tail of the beam (the tail catches up with the head) which axially compresses the beam. For such applications the details of axial kinetics are more important than the details of transverse dynamics. For ultra-relativistic electron beams, however, axial dynamics drops out since the beams are usually, effectively, monoenergetic and axially-cold. In this case it is the transverse dynamics which is of primary interest. For purposes of numerical simulation it is still useful to develop an adiabatic theory for electron beams since by this means a drift-kinetic treatment

[10] Except in the case of a beam with a strong applied axial field B_z .

which reproduces the phase mix damping effects is possible.

To provide proper closure of the fluid equations it is not necessary to follow all of the transverse dynamics, only that part which is important for the hose instability. As we have demonstrated (abundantly, we hope) in previous Chapters the circle orbits are of extreme importance for the hose instability. In order to motivate the adiabatic beam theory let us consider the "near-circle" orbits, those orbits centered at r_o with small radial oscillations of amplitude δr , in an axisymmetric equilibrium. The orbit equations 3.60 and 3.61 may be combined to yield the radial equation

$$\ddot{r} = \frac{1}{r^3}\left(\frac{P_\theta}{\gamma m}\right)^2 + \frac{q}{\gamma m}\frac{d\psi_o}{dr} \tag{9.90}$$

where $P_\theta = \gamma m r^2 \Omega_\beta(r)$ with $\Omega_\beta^2(r) = (q/\gamma m)(-1/r)d\psi_o/dr$, and ψ_o is the equilibrium pinch potential. Expanding this equation about r_o with $r \to r_o + \delta r$ we find, to lowest order, the harmonic oscillator

$$\delta\ddot{r} + \Omega_r^2(r_o)\delta r = 0 \tag{9.91}$$

where the frequency $\Omega_r(r_o)$ is determined by

$$\Omega_r^2(r_o) = \frac{1}{r_o^3}\frac{d}{dr_o}\left(r_o^4\Omega_\beta^2(r_o)\right) . \tag{9.92}$$

The radial oscillation is therefore $\delta r = -(A/\Omega_r)\cos\xi$ where $\dot{\xi} = \Omega_r$. Associated with this oscillator is an *exact* invariant J_r defined by $J_r = (1/2\pi)\oint p_r dr$, which works out to be $J_r = (\gamma m/2)A^2/\Omega_r$. Using Hamilton's equations of motion it is easily proved that $\dot{J}_r = 0$ on the orbit. This means that we may use J_r to "eliminate" the radial oscillation from our considerations. Realize, however, that

any elliptical orbit may be thought of as a circular orbit, plus a radial (and perhaps angular) oscillation, providing only that the orbit is not too highly elliptical, that is, providing $\delta r/r_o \ll 1$.

Suppose now that the beam is expanding, or hosing in some fashion, such that the reference radius r_o has some underlying z dependence $r_o(z)$. In this case the frequency $\Omega_r(r_o(z))$ has a slow evolution in z (slow compared to the other slow frequency $\Omega_\beta(r_o)$). It is well known, however, that even for slowly varying frequencies, the quantity $J_r = (1/2\pi)\oint p_r dr$ is an "adiabatic" action invariant of motion. If the radius of the beam is expanding slowly, then the situation is exactly that of a *harmonic* pendulum, the length of the string of which is slowly varying. Our invariant $J_r = (\gamma m/2)A^2/\Omega_r$ is nothing but the energy of the radial oscillator divided by its frequency, which has been known since 1911 (when it was pointed out by Einstein [9.4]) to be an adiabatic invariant (think of $\frac{E}{\omega} = N\frac{h}{2\pi}$ where h is Planck's constant and N the number of quanta.)

In order to treat the general case of a particle in a nonaxisymmetric nonequilibrium beam undergoing a radial drift at velocity $u_r(r,\theta,z;\varsigma)$, an azimuthal drift with angular velocity $r\Omega_\theta(r,\theta,z;\varsigma)$, and radial and azimuthal oscillations superimposed upon the drifts, we transform to new momentum variables which are explicitly resolved into drift and oscillation components.

$$p_r = \gamma m u_r(r,\theta,z;\varsigma) + \gamma m \alpha_r(r,\theta,z;\varsigma)\sin\xi(r,\theta,z;\varsigma) \tag{9.93}$$

$$p_\theta = \gamma m r\Omega_\theta(r,\theta,z;\varsigma) + \gamma m\frac{1}{r}\alpha_\theta(r,\theta,z;\varsigma)\cos\xi(r,\theta,z;\varsigma) \tag{9.94}$$

where α_r is the linear momentum of the radial oscillator and α_θ is the angular

momentum of the azimuthal oscillator. In the following work, since we have a monoenergetic, axially-cold beam, we shall drop the slice label ς from the arguments of the various functions we are working with. In terms of these variables, the transverse Hamiltonian $H_\perp = (1/2\gamma m)(p_r^2 + p_\theta^2) - q\psi$ reads

$$H_\perp = \frac{1}{2}\gamma m\left(u_r^2 + r^2\Omega_\theta^2\right) + \gamma m u_r \alpha_r \sin\xi + \gamma m \Omega_\theta \alpha_\theta \cos\xi - q\psi \tag{9.95}$$

$$+\frac{1}{2}\gamma m \alpha_r^2 \sin^2\xi + \frac{1}{2}\gamma m \frac{\alpha_\theta^2}{r^2}\cos^2\xi \ .$$

From this Hamiltonian we compute the total time derivatives of p_r and $P_\theta = r p_\theta$ as $\dot{p_r} = -\partial H_\perp/\partial r$ and $\dot{P_\theta} = -\partial H_\perp/\partial\theta$ respectively, which yields explicitly

$$\dot{p_r} = q\frac{\partial\psi}{\partial r} - \gamma m r\Omega_\theta^2 + \frac{1}{r^3}\gamma m \alpha_\theta^2 \cos^2\xi \tag{9.96}$$

$$\dot{P_\theta} = q\frac{\partial\psi}{\partial\theta} \ . \tag{9.97}$$

There is another method of computing the derivatives as well. This involves the direct differentiation of the definitions of p_r and p_θ , 9.93 and 9.94 respectively, using the total derivative

$$\frac{d}{dt} = \beta c\frac{\partial}{\partial z} + u_r\frac{\partial}{\partial r} + \Omega_\theta\frac{\partial}{\partial\theta} \ . \tag{9.98}$$

Carrying out these differentiations we arrive at

$$\dot{p_r} = \gamma m\beta c\frac{\partial u_r}{\partial z} + \gamma m\left(u_r + \alpha_r\sin\xi\right)\frac{\partial u_r}{\partial r} + \gamma m\left(\Omega_\theta + \frac{\alpha_\theta}{r^2}\cos\xi\right)\frac{\partial u_r}{\partial\theta} \tag{9.99}$$

$$+\gamma m\dot{\alpha}_r\sin\xi + \gamma m\alpha_r\dot{\xi}\cos\xi$$

$$\dot{P_\theta} = \gamma m\beta c\frac{\partial}{\partial z}\left(r^2\Omega_\theta\right) + \gamma m\left(u_r + \alpha_r\sin\xi\right)\frac{\partial}{\partial r}\left(r^2\Omega_\theta\right) \tag{9.100}$$

$$+\gamma m\left(\Omega_\theta+\frac{\alpha_\theta}{r^2}\cos\xi\right)\frac{\partial}{\partial\theta}\left(r^2\Omega_\theta\right)+\gamma m\dot{\alpha}_\theta\cos\xi-\gamma m\alpha_\theta\dot{\xi}\sin\xi\ .$$

These derivatives will prove useful later on. In particular, we shall equate the corresponding results to obtain equations to determine α_r , α_θ , Ω_θ , and u_r .

The construction of an adiabatic beam theory is based fundamentally upon several important ordering assumptions. Underlying these ordering assumptions is the concept of near-circularity. We shall assume that the transverse orbits are near-circle, in the sense that $\delta r/r_o \sim \epsilon$ where $\epsilon \ll 1$ and r_o is the mean radius of the orbit. This assumption excludes orbits of near-zero angular momentum, that is, orbits which pass nearly through the origin on highly elliptical orbits. We shall argue that such orbits constitute a negligible fraction of the particles in the beam. Indeed, in thermal equilibrium, equipartition between the transverse degrees of freedom should obtain; therefore, most particles will have at least as much angular momentum as radial momentum. We will find that the requirement $\delta r/r_o \sim \epsilon$ is not really too demanding, in the sense that this ratio need only be something less than $1/2$.

By analogy with the simple near-circle case discussed above, wherein no radial drift was considered $u_r = 0$, we shall *require* that the oscillation angle ξ satisfy, for the case $u_r \sim \epsilon$,

$$\dot{\xi} = \Omega_r + O(\epsilon)\ . \tag{9.101}$$

We shall also assume, since we are dealing with near-circle orbits, that

$$\alpha_r \sim \alpha_\theta \sim \epsilon \tag{9.102}$$

$$\Omega_\theta \sim 1\ . \tag{9.103}$$

Clearly, in physical systems with large gradients, or with rapid variation of physical parameters with time, one cannot expect to find adiabatic invariants, therefore, we postulate the following (not severely restrictive) orderings of derivatives

$$\beta c \left(\frac{\partial}{\partial z}\right)_{\varsigma} \sim \frac{1}{r}\frac{\partial}{\partial \theta} \sim \epsilon \,. \tag{9.104}$$

In order to determine what the drift velocities u_r and $r\Omega_\theta$ are in terms of the pinch potential ψ , as well as determining the relation, if any, between α_r and α_θ we equate 9.96 with 9.99 , and equate 9.97 with 9.100 , and then solve for $\dot{\xi}$ to get

$$\dot{\xi} = \dot{\xi}_{-1}\epsilon^{-1} + \dot{\xi}_0\epsilon^0 + O(\epsilon) \tag{9.105}$$

where

$$\dot{\xi}_{-1} = \frac{1}{\alpha_r}\left(\frac{q}{\gamma m}\frac{\partial \psi}{\partial r} + r\Omega_\theta^2\right) \tag{9.106}$$

$$\dot{\xi}_0 = \frac{1}{\alpha_\theta}\left(\frac{d}{dt}(r^2\Omega_\theta) - \frac{q}{\gamma m}\frac{\partial \psi}{\partial \theta}\right)\sin\xi + 2\frac{\Omega_\theta}{r}\frac{\alpha_\theta}{\alpha_r}\cos^2\xi + \frac{1}{2}r\frac{\Omega_r^2}{\Omega_\theta}\frac{\alpha_r}{\alpha_\theta}\sin^2\xi \,. \tag{9.107}$$

Now, recall that our *fundamental* assumption was that $\dot{\xi} = \Omega_r + O(\epsilon)$ where, as in the non-drifting, near-circle case, we define $\Omega_r^2 = (1/r^3)\partial(r^4\Omega_\theta^2)/\partial r$. Hence, we must force the term $\dot{\xi}_{-1} = 0$ and eliminate the ξ dependence from the $\dot{\xi}_0$ term. Setting the order ϵ^{-1} term to zero we recover our usual definition 1.2 of the betatron frequency

$$\Omega_\theta^2 = -\frac{q}{\gamma m}\frac{1}{r}\frac{\partial \psi}{\partial r} \,. \tag{9.108}$$

To eliminate the angular dependence of the order ϵ^0 term notice that the coefficient of $\sin\xi$ term vanishes of its own accord, since it is simply an angular

momentum balance

$$\frac{d}{dt}(\gamma m r^2 \Omega_\theta) = q\frac{\partial \psi}{\partial \theta} \ . \tag{9.109}$$

Since Ω_θ and ψ are known functions, we solve 9.109 for the radial drift velocity u_r

$$u_r = \frac{2}{r}\frac{\Omega_\theta}{\Omega_r^2}\left(\frac{q}{\gamma m}\frac{\partial \psi}{\partial \theta} - \beta c \frac{\partial}{\partial z}(r^2\Omega_\theta) - \Omega_\theta \frac{1}{r}\frac{\partial}{\partial \theta}(r^2\Omega_\theta)\right) \ . \tag{9.110}$$

All we need to do now is eliminate the $\cos^2 \xi$ and $\sin^2 \xi$ terms, but clearly this is achieved, non-trivially, if we set

$$\frac{2}{r}\frac{\Omega_\theta \alpha_\theta}{\Omega_r \alpha_r} = \frac{r}{2}\frac{\Omega_r \alpha_r}{\Omega_\theta \alpha_\theta} \ , \tag{9.111}$$

with the required result

$$\dot{\xi} = \Omega_r + O(\epsilon) \ . \tag{9.112}$$

Solving 9.111 for α_θ in terms of α_r we find the fundamental relation between α_r and α_θ

$$\alpha_\theta = \frac{1}{2} r \frac{\Omega_r}{\Omega_\theta}\alpha_r \ . \tag{9.113}$$

At this point in the development we have gotten u_r and Ω_θ as functions of the *known* pinch potential ψ . We have also related α_θ to α_r ; therefore, the only independent variables are α_r and ξ . The momenta p_r and p_θ are

$$p_r = \gamma m u_r + \gamma m \alpha_r \sin \xi \tag{9.114}$$

$$p_\theta = \gamma m r \Omega_\theta + \frac{1}{2}\gamma m \frac{\Omega_r}{\Omega_\theta}\alpha_r \cos \xi \tag{9.115}$$

therefore, the mathematical effect of our deliberations has been to replace the two momenta variables $(p_r, p_\theta) \rightarrow (\alpha_r, \xi)$. For future reference, we wish to point

out that (α_r^2, ξ) may well be thought of as the action and angle, respectively, of an oscillator.

It is important to note that our theory allows for two polarizations, that is, $\pm\Omega_\theta$, which correspond physically to the two senses of rotation which are required in an unpolarized (non-rotating) beam. For a non-rotating beam we must have an equal number of particles with $+\Omega_\theta$ and with $-\Omega_\theta$. The beam is a superposition of counter-rotating streams.

We have succeeded in recasting the single-particle transverse dynamics into the form of an aperiodic motion (the "spiral" $(u_r, r\Omega_\theta)$) and a one degree of freedom oscillation (the "elliptically polarized" oscillator (α_r, ξ)). In order to construct a drift-kinetic equation we may average the oscillation out of the problem, leaving only the spiral motion. Does this remove all the kinetics? The answer, of course, is no. We still have two counter-rotating streams of particles. In the fully fluid theory of Section 9.2 we didn't have even the angular drift (of two possible senses) left. Put another way, the azimuthal motion was fluidized along with the oscillation. Now we have the possibility of fluidizing only the oscillation.

In the sequel, dealing specifically with the hose instability, we will neglect the radial drift (due physically, perhaps, to Nordsiéck expansion of the beam, and therefore negligible on time scale of hose development) and concentrate upon the adiabatic evolution of the frequencies due only to the hosing motion. In this case we will think of the azimuthal motion Ω_θ as an oscillator. We therefore think of two oscillators: the "circular oscillator" and the "vortex oscillator". The

oscillator α_r, ξ is called the vortex oscillator by analogy with a fluid which has a macroscopic rotation (our Ω_θ) with smaller comoving vortices (our $\dot{\xi}$).

In Section 9.2 we discovered that for a monoenergetic, axially-cold ultra-relativistic electron beam, the covariant Vlasov equation reduced to a standard "two-space plus time" form, with the only proviso that the mass be replaced with the appropriate relativistic mass γm . Since we carefully delineated the approximations involved in the reduction in Section 9.2, here we shall simply start with the Vlasov equation (written for the particular slice under consideration) in a simple two-space plus time form. Therefore, in terms of the single-particle phase space distribution $f = f(r, \theta, J_r, \xi; z)$, where $\alpha_r^2 = 2\Omega_r J_r/\gamma m$ defines the action variable J_r , we have the Vlasov equation

$$\left(\beta c\frac{\partial}{\partial z} + \left(u_r + \sqrt{\frac{2\Omega_r J_r}{\gamma m}}\sin\xi\right)\frac{\partial}{\partial r} + \left(r\Omega_\theta + \frac{1}{2}\frac{\Omega_r}{\Omega_\theta}\sqrt{\frac{2\Omega_r J_r}{\gamma m}}\cos\xi\right)\frac{1}{r}\frac{\partial}{\partial\theta}\right. \tag{9.116}$$
$$\left. + \dot{J}_r\frac{\partial}{\partial J_r} + \dot{\xi}\frac{\partial}{\partial\xi}\right) f = 0$$

Now let us derive the drift-kinetic equation obeyed by our single-particle phase-space distribution $f(r, \theta, J_r, \xi; z)$. First, the particle density $n(r, \theta; z)$ is given by

$$n(r, \theta; z) = \int dp_r p_r dp_\theta f(r, \theta, p_r, p_\theta; z) \; . \tag{9.117}$$

From the results 9.114 and 9.115, for p_r and p_θ , in terms of J_r and ξ , we calculate the Jacobian of the transformation $(p_r, p_\theta) \rightarrow (J_r, \xi)$ and find $\mid \partial(p_r, p_\theta)/\partial(J_r, \xi) \mid = (1/2)(\gamma m)(\Omega_r^2/\Omega_\theta)$ therefore, the particle density in terms of our new distribution

(we use the same symbol f) is

$$n(r,\theta;z) = \frac{1}{2}\gamma m \frac{\Omega_r^2}{\Omega_\theta}\epsilon^2 \int dJ_r d\xi f(r,\theta,J_r,\xi;z) \tag{9.118}$$

where we have explicitly included the ordering parameter ϵ^2 associated with the factor J_r . Obviously, the particle density must be of order unity $n(r,\theta;z) \sim O(1)$; therefore, the correct expansion of the phase space distribution is $\epsilon^2 f = f_o + \epsilon f_1 + \epsilon^2 f_2 + \cdots$.

In terms of the action and angle variables (J_r, ξ) the transverse oscillatory Hamiltonian (drop the fluid motion contribution) is

$$H_\perp = u_r\sqrt{2\gamma m J_r \Omega_r}\sin\xi + \frac{1}{2}r\Omega_r\sqrt{2\gamma m J_r\Omega_r}\cos\xi + \Omega_r J_r \sin^2\xi + \frac{1}{2}r\frac{\Omega_r^2}{\Omega_\theta^2}\Omega_r J_r\cos^2\xi \ . \tag{9.119}$$

From this we calculate the time derivative $\dot{J}_r = -\partial H_\perp/\partial\xi$ and find that the angle average $\langle \dot{J}_r\rangle_\xi = 0$ (J_r is an adiabatic invariant) and that $\dot{J}_r = O(\epsilon^2)$. Upon substituting the distribution $\epsilon^2 f = f_o + \epsilon f_1 + \cdots$ into the Vlasov equation, and using that $\dot{J}_r = O(\epsilon^2)$ we get for the ϵ^0 order, the following equations

$$\frac{\partial f_o}{\partial \xi} = 0 \tag{9.120}$$

$$\left(\beta c\frac{\partial}{\partial z} + u_r\frac{\partial}{\partial r} + \Omega_\theta\frac{\partial}{\partial\theta}\right) f_o + \dot{\xi}\frac{\partial f_1}{\partial\xi} = 0 \ . \tag{9.121}$$

Therefore, upon averaging over the fast angle ξ , we have our drift- kinetic equation

$$\left(\beta c\frac{\partial}{\partial z} + u_r\frac{\partial}{\partial r} + \Omega_\theta\frac{\partial}{\partial\theta}\right) f_o = 0 \ . \tag{9.122}$$

The kinetic pressure is due to the thermal (non-fluid) components of the transverse momenta p_r and p_θ. Let us denote these by δp_r and δp_θ , respectively.

Explicitly, we have

$$\delta p_r = \sqrt{2\gamma m \Omega_r J_r}\sin\xi \tag{9.123}$$

$$\delta p_\theta = \frac{1}{2}\frac{\Omega_r}{\Omega_\theta}\sqrt{2\gamma m \Omega_r J_r}\cos\xi\ . \tag{9.124}$$

The pressure tensor components are: $P_{rr} = \langle \delta p_r \delta p_r \rangle$, $P_{r\theta} = P_{\theta r} = \langle \delta p_r \delta p_\theta \rangle$, and $P_{\theta\theta} = \langle \delta p_\theta \delta p_\theta \rangle$, where $\langle\rangle \equiv \frac{1}{2}\gamma m \frac{\Omega_r^2}{\Omega_\theta}\epsilon^2 \int dJ_r d\xi f_o(r,\theta,J_r,\xi;z)$. Working these out we find

$$P_{rr} = 2\gamma m \Omega_r \langle J_r \sin^2\xi \rangle \tag{9.125}$$

$$P_{r\theta} = P_{\theta r} = 0 \tag{9.126}$$

$$P_{\theta\theta} = \frac{1}{4}\frac{\Omega_r^2}{\Omega_\theta^2}P_{rr}\ . \tag{9.127}$$

It is interesting to determine under what conditions the beam is isothermal $P_{rr} = P_{\theta\theta}$. Setting $\Omega_r^2 = 4\Omega_\theta^2$ we find $\Omega_\theta^2 = 1$, or, in terms of the pinch potential, $\psi = -(\gamma m/2q)r^2$. Therefore, from the Ampère monopole equation, $J_b(r) = (\gamma m/q\beta)(c/2\pi)1/(1+f_m)$ which is a beam with uniform net current [11]. Such a beam has a harmonic potential. That is, the betatron frequency is independent or radial position ($\Omega_\theta^2 \equiv 1$) so there are no phase mixing effects.

Now that we have determined the pressure tensor in terms of the distribution $f(r,\theta,J_r,\xi;z)$ we may formulate the adiabatic fluid model of the beam. We use the exact continuity and momentum equations (exact in the monoenergetic, axially-cold beam) combined with the drift-kinetic equation, the EMPULSE field

[11] Recall that in Section 9.2 we determined that an isothermal beam $P_{rr} = P_{\theta\theta}$ has a Bennett profile net current $J_b(r) \sim (1+r^2)^{-2}(1+f_m)^{-1}$. This is a definite point of disagreement between the fluid and adiabatic theories, one which favors the fluid theory.

equations, and the conductivity equation

$$\beta c\frac{dN}{dz}+N\frac{1}{r}\frac{\partial}{\partial r}(ru_r)+N\frac{1}{r}\frac{\partial u_\theta}{\partial\theta}=0 \tag{9.128}$$

$$N\beta mc\gamma\frac{du_r}{dz}+\frac{\partial}{\partial r}(P_{rr})-\frac{1}{r}(P_{rr}-P_{\theta\theta})-\gamma mN\frac{u_\theta^2}{r}=qN\frac{\partial\psi}{\partial r} \tag{9.129}$$

$$N\beta mc\gamma\frac{d}{dz}(mu_\theta)+\frac{1}{r}\frac{\partial}{\partial\theta}P_{\theta\theta}+\gamma mN\frac{u_\theta u_r}{r}=qN\frac{1}{r}\frac{\partial\psi}{\partial\theta} \tag{9.130}$$

$$P_{\theta\theta}=\frac{1}{4}\frac{\Omega_r^2}{\Omega_\theta}P_{rr} \tag{9.131}$$

$$P_{rr}=(\gamma m)^2\frac{\Omega_r^3}{\Omega_\theta}\int dJ_rJ_rd\xi f_o\sin^2\xi \tag{9.132}$$

$$\left(\beta c\frac{\partial}{\partial z}+u_r\frac{\partial}{\partial r}+\Omega_\theta\frac{\partial}{\partial\theta}\right)f_o=0 \tag{9.133}$$

$$\Omega_\theta^2=-\frac{q}{\gamma m}\frac{1}{r}\frac{\partial\psi}{\partial r} \tag{9.134}$$

$$\Omega_r^2=\frac{1}{r^3}\frac{\partial}{\partial r}(r^4\Omega_\theta^2) \tag{9.135}$$

$$\frac{1}{r}\frac{\partial}{\partial r}r\frac{\partial}{\partial r}(\phi+\psi)+\frac{1}{r^2}\frac{\partial^2}{\partial\theta^2}(\psi+\phi)-\frac{4\pi}{c}\sigma\frac{\partial\psi}{\partial\varsigma}=-4\pi qN\beta \tag{9.136}$$

$$\frac{1}{r}\frac{\partial}{\partial r}r\frac{\partial}{\partial r}\frac{\partial\psi}{\partial\varsigma}+\frac{1}{r^2}\frac{\partial^2}{\partial\theta^2}\frac{\partial\psi}{\partial\varsigma}=\frac{4\pi}{c}\frac{\partial}{\partial r}\sigma\frac{\partial\phi}{\partial r}+\frac{4\pi}{c}\frac{1}{r^2}\frac{\partial}{\partial\theta}\sigma\frac{\partial\phi}{\partial\theta} \tag{9.137}$$

$$\frac{\partial\sigma}{\partial\varsigma}=\kappa qN\beta c\,. \tag{9.138}$$

This is a set of 11 equations to determine the 11 functions: N , u_r , u_θ , f_o , P_{rr} ,$P_{\theta\theta}$, Ω_θ , Ω_r , ψ , ϕ , and σ in the adiabatic beam theory.

9.4 Resonant Modification of Transverse Invariants

In Section 9.3 we developed an "adiabatic" theory describing an ultra-relativistic electron beam. Fundamentally, the theory rests firmly upon the existence of an adiabatic action invariant J_r which enables us to separate the vortex-gyration from the spiral drift motion of the transverse particle orbit.

We are, at this juncture, compelled to ask: just how *robust* is this action invariant? Clearly, the action is an adiabatic invariant for an axisymmetric, slowly expanding beam, but what happens in a nonaxisymmetric, linearly hosing beam? Does the invariant undergo a modification under these circumstances? It is to the resolution of these questions that we now address ourselves, indeed, it is the purpose of Section 9.4 to apply "modern" ideas of KAM theory [9.8] to the study of the adiabatic theory of a linearly hosing electron beam.

As mentioned in Section 9.3, for physical events which occur on the time scale (Ω_θ^{-1}) of the hose instability, we may neglect the radial drift motion u_r and reduce the spiral $(u_r, r\Omega_\theta)$ to the circle $r\Omega_\theta$. In this case, both motions are periodic, therefore, we have two oscillators: circle and vortex. Expanding the transverse Hamiltonian

$$H_\perp = \frac{1}{2\gamma m}(p_r^2 + p_\theta^2) - q\psi \tag{9.139}$$

about a reference circle orbit, with $r = r_o + \delta r$ and $p_r = \delta p_r$, we get a system of two linear oscillators for the circle and vortex degrees of freedom.

$$H_\perp = \Omega_\theta J_\theta + \epsilon^2 \Omega_r J_r + O(\epsilon^3) \tag{9.140}$$

where the action-angle variables (J_r, ξ) and (J_θ, θ) are defined by

$$\delta r = \epsilon \left(\frac{2}{\gamma m \Omega_r}\right)^{\frac{1}{2}} J_r^{\frac{1}{2}} \sin \xi \tag{9.141}$$

$$\delta p_r = \epsilon \left(2\gamma m \Omega_r\right)^{\frac{1}{2}} J_r^{\frac{1}{2}} \cos \xi \tag{9.142}$$

and $(J_\theta, \theta) = (P_\theta^2/(2\gamma m r_o^2 \Omega_\beta), \theta)$. As in Section 9.3, the frequencies are defined to be $\Omega_\theta^2 = -(q/\gamma m)(1/r_o)d\psi/dr_o$ and $\Omega_r^2 = (1/r_o^3)d(r_o^4\Omega_\theta^2)/dr_o$.

If we use the lowest order Hamiltonian 9.140, and perturb it with a linear hose perturbation, we get a nonlinear coupling of the two degrees of freedom which is, technically, very delicate to study since the "ground state" fails to satisfy the "sufficient nonlinearity" condition of the KAM theorem (about which we shall have more to say later) . This linearity of the ground state is not inherent in the physical system, but is a relic of the linearization (expansion to lowest order in noncircularity). In this work we are investigating the breakdown of adiabaticity and find it necessary to expand the ground state to higher order to expose the inherent nonlinearity. Expanding $H_\perp$ to *fourth* order in the noncircularity ϵ , in terms of the action-angle variables 9.141 and 9.142 for the linearized Hamiltonian, we find

$$H_\perp = \Omega_\theta J_\theta + \epsilon^2 \Omega_r J_r + \epsilon^3 \Omega_3 J_r^{\frac{3}{2}} \sin^3 \xi + \epsilon^4 \Omega_4 J_r^2 \sin^4 \xi + \cdots \tag{9.143}$$

where Ω_3 and Ω_4 are

$$\Omega_3 = -\left(\frac{2}{\gamma m \Omega_r}\right)^{\frac{3}{2}} \left(\frac{1}{6} q \frac{d^3\psi}{dr_o^3} + 2\gamma m \frac{\Omega_\theta^2}{r_o}\right) \tag{9.144}$$

$$\Omega_4 = -\left(\frac{1}{\gamma m \Omega_r}\right)^2 \left(\frac{1}{6} q \frac{d^4\psi}{dr_o^4} - 10\gamma m \frac{\Omega_\theta^2}{r_o^2}\right) . \tag{9.145}$$

Using the Hamiltonian 9.143 alleviates the problem of the weak nonlinearity, that is, the linear ground state, and results in fulfillment of the conditions of the KAM theorem in its strongest form. Note that the action-angle variables (J_r, ξ) are not really action -angle variables for the Hamiltonian to order ϵ^4 , only to order ϵ^2 . To get the action-angle variables to the requisite order we will employ Deprit's version [9.6] of canonical Lie transform perturbation theory [12].

The azimuthal contribution to the Hamiltonian $\Omega_\theta J_\theta$ is already in its exact action-angle variables. In what follows we shall only be concerned with the radial contribution

$$H_r = \epsilon^2 \Omega_r J_r + \epsilon^3 \Omega_3 J_r^{\frac{3}{2}} \sin^3 \xi + \epsilon^4 \Omega_4 J_r^2 \sin^4 \xi \, . \tag{9.146}$$

Before calculating the action-angle variables, let us say a few words about the method we are using. In the physical literature the operator that one calls a Lie transform is geometrically a "pullback by a flow". To carry out a Lie transform calculation in Hamiltonian mechanics involving a perturbation of some zeroth order H_o we need the flow of H_o , the pullback, and the pushout by the flow. The pullback is used to invert the inhomogeneous Liouville operator which occurs at each order of the perturbation calculation, on the orbits of the H_o flow. One selects, at each order, a function, whose vector field generates a flow, the pullback by which yields the new variables, from the old, at that order. This function is called the "Lie generating function ", and the pushout by its flow yields the

[12] Lie transforms operate directly upon the functions defined on the phase space manifold, and thereby avoid the well-known problem of the canonical Poincaré, Von-Zeipel perturbation theory, cf. [9.5], that is, mixing together the old and new variables.

new Hamiltonian, from the old. A general operator formalism was first used, in plasma physics [9.7], by Dewar, , but here we follow Fermi's dictum: "when in doubt...expand!, to get Deprit's version of the formalism, which in fact preceeded Dewar's more general treatment. To this end, we expand everything in sight in powers of ϵ .

Now we will present the essentials of the canonical perturbation theory for the time dependent generating function necessary to deal with a time dependent Hamiltonian. In terms of the generating function w the Lie derivative L is defined, in terms of the *canonical* Poisson bracket, as

$$L = \{w, \ \} = \frac{\partial w}{\partial q}\frac{\partial}{\partial p} - \frac{\partial w}{\partial p}\frac{\partial}{\partial q} \tag{9.147}$$

where $z = (p, q)$ are canonical momentum and coordinate variables. The derivative of the pullback T with respect to the parameter ϵ which labels the generating function w_ϵ , is

$$\frac{dT}{d\epsilon} = -TL \tag{9.148}$$

and the derivative of the pushout T^{-1} is

$$\frac{dT^{-1}}{d\epsilon} = LT \ . \tag{9.149}$$

Integrating the derivative of the pullback with respect to ϵ one arrives at the formal expression for the pullback

$$T(\epsilon) = \exp\left(-\int_0^\epsilon d\epsilon' L(w_\epsilon)\right) \tag{9.150}$$

where, we must think of this as an ϵ-ordered product, since the Lie derivatives do not necessarily commute at different values of ϵ . This result gives us the element

T in the Lie group of transformations as the exponential of the "generator" L in the Lie algebra. In terms of the pullback, the new variables $Z = (P, Q)$ are

$$Z = Tz \, . \tag{9.151}$$

The new Hamiltonian K is related to the old Hamiltonian H by the formula

$$K = T^{-1}H + T^{-1} \int_0^\epsilon d\epsilon' T(\epsilon') \frac{\partial w}{\partial t}(\epsilon', t) \, . \tag{9.152}$$

Deprit formulated a canonical perturbation theory, in 1969, in terms of Lie transforms in the case in which one has a small parameter in which one is able to expand. Dewar's treatment, in 1976, amounts to a generalization of Deprit's, to the case of possibly nonanalytic functions, that is, where series developments may not exist. We find it efficient to motivate things by going chronologically in reverse; therefore, we next expand all the objects K , H , L , T , and w in the small parameter ϵ . In terms of the expansion of the generating function w the derivative along the flow of w is

$$\frac{d}{d\epsilon} = -\sum_{n=0}^{n-1} \{w_n, \ \} = -\sum_{n=0}^{\infty} L_n \, . \tag{9.153}$$

Likewise, the formulae for the pullback and pushout are given recursively

$$T_n = -\frac{1}{n} \sum_{m=0}^{n-1} T_m L_{n-m} \tag{9.154}$$

$$T_n^{-1} = \frac{1}{n} \sum_{m=0}^{n-1} L_{n-m} T_m^{-1} \, . \tag{9.155}$$

Explicitly, the formulae we shall use in our calculation are

$$T_0^{-1} = I \tag{9.156}$$

$$T_1^{-1} = L_1 \tag{9.157}$$

$$T_2^{-1} = \frac{1}{2}L_2 + \frac{1}{2}L_1^2 \,. \tag{9.158}$$

At each order in the calculation the Lie generating function w_n is the solution of the following inhomogeneous Liouville equation

$$\left(\frac{\partial}{\partial t} - \{H_o, \}\right) w_n = n(K_n - H_n) - \sum_{m-1}^{n-1} \left(L_{n-m}K_m + mT_{n-m}^{-1}H_m\right) \tag{9.159}$$

where the new Hamiltonian K_n is chosen to eliminate secularities. Explicitly, the formulae we shall use in our calculation are

$$\left(\frac{\partial}{\partial t} - \{H_o, \}\right) w_1 = K_1 - H_1 \tag{9.160}$$

$$\left(\frac{\partial}{\partial t} - \{H_o, \}\right) w_2 = 2(K_2 - H_2) - L_1(K_1 + H_1) \,. \tag{9.161}$$

The differential operator of the left-hand-side is inverted by integrating along the flow lines of H_o . The explicit formula for this inversion, in terms of arbitrary phase-space functions f and g , is

$$\left(\frac{\partial}{\partial t} - \{H_o, \}\right) f = g \tag{9.162}$$

$$f = (F_t^*)^{-1} \int_{t_o}^{t} dt' F_{t'}^* g(t') + (F_t^*)^{-1} f(t_o) \,. \tag{9.163}$$

In 9.163 F_t^* is the pullback by the flow of H_o and, $(F_t^*)^{-1}$ is the pushout by the flow of H_o . The flow F_t of H_o, that is, the "time development mapping", is defined by its action upon phase-space coordinates (J_r, ξ) and, for our system, it is given by

$$F_t(J_r, \xi) = (J_r, \xi + \Omega_r t) \,. \tag{9.164}$$

The pullback F_t^* by the H_o flow, that is, the "time development operator", is defined by its action upon an arbitrary phase-space function f

$$F_t^* f(J_r, \xi) = f \circ F_t(J_r, \xi) = f(J_r, \xi + \Omega_r t) \,. \tag{9.165}$$

The first term of our generating function w is gotten from the equation 9.160 , which, upon inverting the Liouville operator yields

$$w_1 = \int^t dt' \left(K_1 \left(J_r, \xi + \Omega_r (t' - t) \right) - H_1 \left(J_r, \xi + \Omega_r (t' - t) \right) \right) \,. \tag{9.166}$$

To rid w_1 of secular terms we define K_1 to be the time average of H_1 on an H_o orbit

$$K_1 = \frac{\Omega_r}{2\pi} \int_0^{2\pi/\Omega_r} dt H_1(J_r, \xi + \Omega_r t) \,, \tag{9.167}$$

hence, to this order we have

$$K_1 = 0 \,. \tag{9.168}$$

$$w_1 = \frac{1}{12} \frac{\Omega_3}{\Omega_r} \bar{J}_r \left(9 \cos \bar{\xi} - \cos 3\bar{\xi} \right) \tag{9.169}$$

The old variables (J_r, ξ) in terms of the new $(\bar{J}_r, \bar{\xi})$ are

$$J_r = \bar{J}_r + \epsilon \{ w_1, \bar{J}_r \} \tag{9.170}$$

$$\xi = \bar{\xi} - \epsilon \{ w_1, \bar{\xi} \} \,. \tag{9.171}$$

We also compute the updated version of δr , in terms of the new action-angle variables, leaving out the computations we tabulate the results of the order ϵ perturbation

$$K = \epsilon^2 \Omega_r \bar{J}_r \tag{9.172}$$

$$w = 1 + \epsilon \frac{1}{12}\frac{\Omega_3}{\Omega_r}\bar{J}_r^{\frac{3}{2}}\left(9\cos\bar{\xi} - \cos 3\bar{\xi}\right) \tag{9.173}$$

$$J_r = \bar{J}_r + \epsilon \frac{1}{4}\frac{\Omega_3}{\Omega_r}\bar{J}_r^{\frac{3}{2}}\left(\sin 3\bar{\xi} - 3\sin\bar{\xi}\right) \tag{9.174}$$

$$\xi = \bar{\xi} + \epsilon \frac{1}{8}\frac{\Omega_3}{\Omega_r}\bar{J}_r^{\frac{1}{2}}\left(\sin 3\bar{\xi} - 9\sin\bar{\xi}\right) \tag{9.175}$$

$$\delta r = \left(\frac{2}{\gamma m \Omega_r}\right)^{\frac{1}{2}}\bar{J}_r^{\frac{1}{2}}\left(\sin\bar{\xi} - \epsilon\frac{1}{4}\frac{\Omega_3}{\Omega_r}\bar{J}_r^{\frac{1}{2}}\left(3 + \cos 2\bar{\xi}\right)\right) . \tag{9.176}$$

What is significant is that the Hamiltonian has not changed. Evidently, we need to go to higher order yet in order to expose the nonlinearity of the ground state.

The second order contribution to the generating function is given by equation 9.161 , which, in light of our previous results, reads

$$\left(\frac{\partial}{\partial t} - \{H_o, \}\right) w_2 = 2K_2 - \frac{1}{16}\bar{J}_r^2\left(4\Omega_4 + 3\frac{\Omega_3^2}{\Omega_r}\right)\cos 4\bar{\xi} \tag{9.177}$$

$$+\frac{1}{16}\bar{J}_r^2\left(16\Omega_4 - 12\frac{\Omega_3^2}{\Omega_r}\right)\cos 2\bar{\xi} - \frac{1}{16}\bar{J}_r^2\left(12\Omega_4 - 15\frac{\Omega_3^2}{\Omega_r}\right).$$

We choose K_2 to eliminate secularity, and invert the Liouville operator on the H_o flow, to arrive at

$$K_2 = \frac{3}{8}\bar{J}_r^2\left(\Omega_4 - \frac{5}{4}\frac{\Omega_3^2}{\Omega_r}\right) \tag{9.178}$$

$$w_2 = -\frac{1}{16}\bar{J}_r^2\left(\frac{\Omega_4}{\Omega_r} + \frac{3}{4}\frac{\Omega_3^2}{\Omega_r^2}\right)\sin 4\bar{\xi} + \frac{1}{16}\bar{J}_r^2\left(8\frac{\Omega_4}{\Omega_r} - 6\frac{\Omega_3^2}{\Omega_r^2}\right)\sin 2\bar{\xi} . \tag{9.179}$$

The second order contributions to the action-angle variables, in terms of the new variables, are computed from the formulae

$$J_2 = \frac{1}{2}\{w_1, \frac{\partial w_1}{\partial\bar{\xi}}\} + \frac{1}{2}\frac{\partial w_2}{\partial\bar{\xi}} \tag{9.180}$$

$$\xi_2 = -\frac{1}{2}\{w_1, \frac{\partial w_1}{\partial \bar{J}_r}\} - \frac{1}{2}\frac{\partial w_2}{\partial \bar{J}_r} \,. \tag{9.181}$$

After a fair amount of algebra, one arrives at the results

$$J_2 = \frac{1}{32}\bar{J}_r^2 \left(-\left(-4\frac{\Omega_4}{\Omega_r} + 6\frac{\Omega_3^2}{\Omega_r^2} \right) \cos 4\bar{\xi} + \left(16\frac{\Omega_4}{\Omega_r} - 24\frac{\Omega_3^2}{\Omega_r^2} \right) \cos 2\bar{\xi} + 15\frac{\Omega_3^2}{\Omega_r^2} \right) \tag{9.182}$$

$$\xi_2 = \frac{1}{128}\bar{J}_r \left(-\frac{\Omega_3^2}{\Omega_r^2}\sin 6\bar{\xi} + \left(8\frac{\Omega_4}{\Omega_r} + 18\frac{\Omega_3^2}{\Omega_r^2} \right) \sin 4\bar{\xi} + \left(-64\frac{\Omega_4}{\Omega_r} + 27\frac{\Omega_3^2}{\Omega_r^2} \right) \sin 2\bar{\xi} \right) \,. \tag{9.183}$$

Inserting the results for J_r and ξ into δr and expanding to order ϵ^2 we get the result for δr in terms of the second order correct action-angle variables

$$\begin{aligned} \delta r(\gamma m) \overset{\frac{1}{2}}{=} & \left(\frac{2}{\Omega_r}\right)^{\frac{1}{2}} J_r^{\frac{1}{2}} \sin\xi - \epsilon\frac{1}{4}\frac{\Omega_3}{\Omega_r}\left(\frac{2}{\Omega_r}\right)^{\frac{1}{2}} J_r \left(\cos 2\xi + 3\right) \\ & + \epsilon^2 \frac{1}{256}\left(\frac{2}{\Omega_r}\right)^{\frac{1}{2}} J_r^{\frac{3}{2}} \left(\frac{\Omega_3^2}{\Omega_r^2}\sin 7\xi - 19\frac{\Omega_3^2}{\Omega_r^2}\sin 5\xi + \left(-16\frac{\Omega_4}{\Omega_r} + 69\frac{\Omega^2}{\Omega_r^2} \right) \sin 3\xi \right) \\ & + \epsilon^2 \frac{1}{256}\left(\frac{2}{\Omega_r}\right)^{\frac{1}{2}} J_r^{\frac{3}{2}} \left(-96\frac{\Omega_4}{\Omega_r} + 189\frac{\Omega_3^2}{\Omega_r^2}\sin\xi \right) \end{aligned} \tag{9.184}$$

where we have now dropped the overbar from the new action-angle variables. The Hamiltonian, correct to fourth order, is

$$H_\perp = \Omega_\theta J_\theta + \epsilon^2 \Omega_r J_r + \epsilon^4 \Omega_2 J_r^2 \tag{9.185}$$

where we have defined a new "frequency" Ω_2 by

$$\Omega_2 = \frac{3}{8}\Omega_4 - \frac{15}{32}\frac{\Omega_3^2}{\Omega_r} \,. \tag{9.186}$$

The Hamiltonian 9.185 is in a form which is very convenient for carrying out theoretical investigations. This Hamiltonian is that of two *uncoupled* oscillators, one which is linear $\Omega_\theta J_\theta$ and one which is nonlinear $\epsilon^2\Omega_\theta J_r + \epsilon^4\Omega_2 J_r^2$. Time

evolution of two-degree of freedom dynamical systems may be described as a toral flow, on a two-torus whose major and minor radii are actions and whose toroidal and poloidal angles are the corresponding angles [13]. When one considers the collection of tori, parameterized by the ranges of actions consistent with the total energy, one arrives at a family of nested two-tori [14]. It is interesting that the behavior of the phase space orbits in this family of tori is perfectly analogous to the behavior of magnetic field lines in a tokamak. This is because one may, in fact, arrive at a description of field line behavior as a two-degree of freedom Hamiltonian system [9.8].

Prior to looking at the beam system from the point of view of Hamiltonian systems, let us indulge in a brief, and necessarily sketchy, historical interlude. Toral flows have been investigated since the time of Jacobi, who, in 1835, proved that orbits with irrational winding numbers densely cover the torus [9.9]. The modern "qualitative" period of dynamics was initiated by Poincaré in the late 1880's. This work continued with developments by Birkhoff and others, including Kolmogorov, whose fundamental paper of 1954 [9.10], followed by work of Arnold [9.11], and Moser [9.12], in the early 1960's resulted in KAM theory. This theory resolved the long-standing problem of small denominators, which had plagued celestial mechanics ever since Poincaré had pointed it out, nearly one hundred years earlier. Chirikov [9.13], and others, began introducing these ideas into plasma physics in the late 1950's. In 1966, a paper appeared in which these ideas

[13] cf., Fig. 9.1.

[14] An idea which, apparently, may be traced back to Lagrange in 1762 [9.14].

were applied directly to the physics of tokamaks [15] [9.8].

With this brief bit of lore behind us, we move on to describe the tori of the classical Bennett "ground state". It is nice to introduce some dimensionless variables at this point in our work. We may easily non-dimensionalize the problem, and by so doing scale away any mention of the transverse temperature T and the Bennett radius a . To this end, we shall measure action in units of $a\sqrt{T}$, frequency in units of T/a^2 , energy in units of T , and length in units of a . The scaling of frequency, energy, and action, is therefore

$$\Omega' = \frac{T}{T'}\left(\frac{a}{a'}\right)^{\frac{1}{2}}\Omega \tag{9.187}$$

$$E' = \frac{T'}{T}E \tag{9.188}$$

$$J' = \frac{a'}{a}\left(\frac{T'}{T}\right)^{\frac{1}{2}}J \tag{9.189}$$

We therefore have the near-circle Hamiltonian

$$H_\perp = \Omega_\theta J_\theta + \epsilon^2\Omega_\rho J_\rho + \epsilon^4\Omega_2 J_\rho^2 \tag{9.190}$$

where the various quantities have the same meaning as before, but are now pure numbers.

For the Bennett equilibrium, we may explicitly work out the various frequencies, with the result being

$$\Omega_\theta^2 = 4\frac{1}{1+\rho_o^2} \tag{9.191}$$

[15] These ideas must have seemed all the more compelling for tokamak physicists, in light of the direct analogy between the toral flow and the field lines in a tokamak. In fact, one might look at this aspect of tokamak physics as a particularly beautiful physical manifestation of an otherwise abstract concept, that is, Hamiltonian systems as toral flows!

$$\Omega_\rho^2 = 8\frac{2+\rho_o^2}{(1+\rho_o^2)^2} \tag{9.192}$$

$$\Omega_2 = -\frac{1}{96}\Omega_\rho^2\frac{11\rho_o^6+66\rho_o^4+129\rho_o^2+72}{(2+\rho_o^2)^2}\ . \tag{9.193}$$

Since Ω_2 is manifestly negative, the ground state system is of the "weak spring" type, that is, $\partial^2 H_\perp/\partial J_\rho^2 \leq 0$, so that the "twist mapping" in the (J_ρ, ξ) plane is such that larger actions revolve more slowly than smaller actions. The fact that the ground state Hamiltonian depends linearly upon J_θ is of some consequence, resulting in primary resonances that are separated by a frequency interval which is independent of the action, and therefore the same for *all* adjacent pairs of primary (integer) resonances. Of course, one only considers primary resonances which actually *exist* , and in general there are only finitely many primary resonances consistent with allowable winding numbers.

For the Bennett beam, in the ground state, the actions and winding number of a given torus are explicitly given by

$$J_\theta(\rho_o) = \frac{1}{2}\rho_o^2\Omega_\theta(\rho_o) \tag{9.194}$$

$$J_\rho(\rho_o, H_\perp) = -\frac{1}{2}\frac{\Omega_\rho}{\Omega_2}\left(1-\left(1-4\frac{\Omega_2}{\Omega_\rho^2}\left(H_\perp-\frac{1}{2}\rho_o^2\Omega_\theta^2\right)\right)^{\frac{1}{2}}\right) \tag{9.195}$$

$$w(\rho_o, H_\perp) = \frac{\Omega_\rho}{\Omega_\theta}\left(1-4\frac{\Omega_2}{\Omega_\rho^2}\left(H_\perp-\frac{1}{2}\rho_o^2\Omega_\theta^2\right)\right)^{\frac{1}{2}} \tag{9.196}$$

where, in deriving J_ρ we have selected the branch which goes to zero as the radial energy goes to zero: $H_\perp \to \frac{1}{2}\rho_o^2\Omega_\theta^2$. The winding numbers are bounded above by a ρ_o dependent maximum $\Omega_\rho/\Omega_\theta$, and this upper-bound itself is constrained to

fall within the range $\sqrt{2} \leq \Omega_\rho/\Omega_\theta \leq 2$. This restricts the primary resonances to $w = 1, 2$ which are equally separated from one another.

At any *finite* radius, the only resonance of importance is the $w = 1$ resonance. The "sidebands" of secondary resonances ranging on either side of $w = 1$ are $w = 1 \pm m/n$ where $m < n$, so the sidebands form a dense set of resonances.

When we look at coupling resonances, driven by linear hose instability, we shall be interested in whether or not the islands associated with the secondary resonances "overlap" one another. Technically, the "smoothness" condition of the KAM theorem requires good separation of these islands if invariant tori are to persist despite the perturbation.

If the radial action J_ρ ceases to be a good invariant, due to any coupling resonance overlaps, then the particle orbits will "diffuse" to other reference radii. This is because there is a one-to-one relationship between the reference radius and the azimuthal action J_θ . In fact, we could think of (ρ_o, J_ρ) as the invariants of the ground state system, as well as (J_θ, J_ρ) , so that diffusion in action is equivalent to radial diffusion.

Inverting the winding number resonance condition 9.196 yields the resonant energy spectrum

$$E_{pq} = \frac{1}{2}\rho_o^2\Omega_\theta^2 + \frac{1}{4}\frac{\Omega_\theta^2}{\Omega_2}\left(\frac{\Omega_\rho^2}{\Omega_\theta^2} - \frac{p^2}{q^2}\right) \tag{9.197}$$

where p and q are integers, and their ratio is of the form unity plus or minus a fraction less than unity. We naturally speak of such an energy spectrum as there are many particles at any reference radius, and these particles have a distribution in energy; the Bennett equilibrium is characterized by a transverse temperature

[16]. Changing our point of view, any particle with a given fixed energy has a nested tori family as orbit space. A torus in this family may be thought of as being parameterized by radius of the orbit.

For the two degree of freedom system, as with all such systems, resonant tori are densely distributed in the energetically accessible region of action space. We have a dense distribution in radius, at fixed energy, of resonant tori, or a dense distribution in energy at a fixed radius.

Resonance structure in action-space tends to enhance the diffusive effects of weak, extrinsic random noise. We are not explicitly considering the effects of extrinsic diffusion, such as caused by elastic collisions of beam electrons with plasma ions, which tend to cause radial diffusion (by changing the balance of p_r and p_θ). Collisions can remove a phase point from a nonresonant torus and place it on a resonant torus or "island". Such resonant diffusion, taking place in the absence of intrinsic resonant island-island interaction, amounts to an enhancement over the nonresonant extrinsic diffusion, since the islands provide "stepping stones" for a phase point to random walk about phase space, propelled from island to island by the collisions. Even KAM tori cannot prevent such diffusion: the particle is able to "hop over" the tori. In this work, for ultra-relativistic electron beams,

[16] Introducing the transverse energy spread described by T into our considerations, we have a one parameter family of nested tori families, a so-called "VAK nest" (for "Vague Attracter of Kolmogorov") [9.14]. The true dynamical system is the four-manifold and a nested tori family corresponding to an energy level submanifold is a "slice" of the four-manifold. For a description of the bewildering variety of bifurcational processes which may occur as one varies the energy parameter in such a system, we refer the reader to [9.14].

we may neglect extrinsic diffusion and concentrate only upon intrinsic diffusion driven by interaction of neighboring islands.

The KAM theorem establishes the fact that "most" of the tori bearing incommensurate frequencies [17] (irrational winding numbers) survive with only a small distortion, a small nonintegrable perturbation. By a "small distortion", we mean one without any ripping or topological changes. That is, we end up with a deformed manifold which is topologically a torus. One the other hand, tori bearing periodic orbits, or nearly periodic orbits, that is, incommensurate but with winding number approximated extremely well by n/m (where n and m are relatively small integers) are grossly, that is to say, topologically deformed.

Now let us consider the effect of a linear hose instability upon the Bennett equilibrium. In the rest frame of a slice of the beam, the passage of a hose instability, propagating from the head to the tail of the beam, results in a nonaxisymmetric perturbation with sinusoidal time dependence. For the approximately autonomous case $\Omega \ll \Omega_\theta(\rho_o)$, where Ω is the Doppler shifted hose frequency, we

[17] Ultimately, the distinction between rational and irrational winding numbers is meaningful only in a time asymptotic sense and has no *physical* significance for finite times. Mathematically, one distinguishes between the concepts of an *orbit* and a *trajectory* . An orbit is a geometrical concept, independent of time. An orbit is the set of phase space points which may be gottne from one another by action of the flow map or its inverse. A trajectory is the *act* of evolution along an orbit. Periodic orbits whose winding numbers are the ratios of very large, relatively prime numbers, tend to look very much like irrational orbits, that is, tend to cover the torus very well and close upon themselves only after a very great, but finite path length [9.15].

shall prove that the perturbation is of the form

$$\delta H = \sum_{lm} \delta H^c_{lm} \cos(l\xi - m\theta) + \sum_{lm} \delta H^s_{lm} \sin(l\xi - m\theta) \; . \tag{9.198}$$

In this Hamiltonian, the angle θ is that of circular-drift, and the angle ξ is that of vortex-gyration. It is seen that the linear hose instability couples these two oscillators nonlinearly. Before deriving the detailed form of δH^c_{lm} and δH^s_{lm} let us discuss the problem of resonance from a general point of view, based upon our perturbed Hamiltonian 9.198.

The unperturbed Hamiltonian 9.190 is "integrable". Will the perturbed Hamiltonian $H = H_\perp + \delta H$ also be integrable? Poincaré and Birkhoff realized that very few two degree of freedom Hamiltonian systems possess two independent invariants (for $H_\perp$ they are J_θ and J_ρ); that is, classical Hamilton-Jacobi theory [9.16] fails for *most* systems. Therefore, nonintegrable systems are properly thought of as "garden-variety" systems. This means that one may write down any Hamiltonian involving only actions, and perturb it with any perturbation involving angles, at random, so to speak, and be *reasonably* certain that the combined system is nonintegrable [18].

On the one hand, for "garden-variety" perturbations of integrable systems, one has the celebrated theorems of Kolmogorov, Arnold, and Moser to fall back

[18] In fact, physicists are rather astounded if it turns out to be integrable, as in the case of the Toda lattice [9.17] which suprized Ford *et al.* [9.18] when they numerically found evidence of its integrability, which was analytically verified by Henon [9.19] who, inspired by Ford's work, sought and found n independent invariants for the n particle lattice, showing that the Toda lattice is indeed, to quote Ford, "a jewel in physics".

upon. The existence of invariant tori enables one to effectively study a wide class of otherwise intractable systems. These systems may be thought of as those for which perturbation theory succeeds, if done correctly. On the other hand, as one moves a system further and further from an integrable system, the KAM tori begin to disintegrate; that is, perturbation theory fails outright. If one pushes a system far enough in this direction, one may fall back upon essentially statistical methods [9.5].

Of particular interest is the behavior of a system undergoing *transition* between near-integrability and non-integrability. For two degree of freedom systems, such as the one we are studying, the computation of the threshold of stochasticity involves determination of the critical perturbation strength at which all the KAM tori disintegrate. The breakup and dissappearance of the last KAM torus triggers "global stochasticity" [19].

In the late 1950's Chirikov [9.13] began formulating a practical method of discerning and quantifying the point at which the last KAM torus between two fundamental resonances is destroyed, the "overlap criteria". Although the overlap criterion is neither necessary, nor sufficient [9.5] for destruction of the torus, it is easy to apply and has great intuitive appeal [9.13].

At "resonance" between the two oscillators the frequencies of the resonant

[19] Even after the destruction of the KAM tori there are structures which appear to provide resistance to global diffusion; invariant Cantor sets, the "Cantori", stubborn remnants of KAM tori which impede global diffusion of actions and result in a divided or clumpy phase space. These partial barriers to diffusion are of considerable current interest in plasma physics [9.20].

term are related in such a fashion that the phase is stationary. All other terms have rapidly varying phases when the actions (J_θ, J_ρ) yield a stationary phase of a given term, so they tend to average away as high-frequency perturbations. Mathematically, therefore, the condition of "coupling resonance" is

$$\frac{d}{dt}(n\xi - s\theta) \approx 0 \,. \tag{9.199}$$

Since the resonant term dominates when (J_ρ, J_θ) are such that $n\dot{\xi} - s\dot{\theta} = 0$, where $\dot{\xi} = \partial H_\perp / \partial J_\rho$ and $\dot{\theta} = \partial H_\perp / \partial J_\theta$, with $H_\perp = \Omega_\theta J_\theta + \epsilon^2 \Omega_\rho J_\rho + \epsilon^4 \Omega_2 J_\rho^2$. Let us look only at the resonant term δH_{ns} . Without loss of generality, for this discussion, let us suppose that $\delta H_{ns}^s = 0$, then

$$H = H_\perp + \delta H_{ns}^c \cos(n\xi - s\theta) \,. \tag{9.200}$$

If this Hamiltonian is nearly integrable we should be able to construct a canonical near-identity transformation which eliminates the angular dependence to lowest order. Supposing this to be possible, we use the near-identity generator

$$S = \hat{J}_\rho \xi + \hat{J}_\theta \theta + S_{ns}(\hat{J}_\rho, \hat{J}_\theta) \sin(n\xi - s\theta) \tag{9.201}$$

where S_{ns} is to be determined by forcing angular terms in the new Hamiltonian $\hat{H}$ to vanish. The new Hamiltonian is computed to be

$$\hat{H} = H_\perp(\hat{J}_\rho, \hat{J}_\theta) + \left(\left(n \frac{\partial H_\perp}{\partial \hat{J}_\rho} - s \frac{\partial H_\perp}{\partial \hat{J}_\theta} \right) S_{ns}(\hat{J}_\rho, \hat{J}_\theta) + \delta H_{ns}^c(\hat{J}_\rho, \hat{J}_\theta) \right) \cos(n\xi - s\theta) \,. \tag{9.202}$$

Therefore, the angle dependent term vanishes if we define

$$S_{ns}(\hat{J}_\rho, \hat{J}_\theta) = -\delta H_{ns}^c(\hat{J}_\rho, \hat{J}_\theta) \left(n \frac{\partial H_\perp}{\partial \hat{J}_\rho} - s \frac{\partial H_\perp}{\partial \hat{J}_\theta} \right)^{-1} \,. \tag{9.203}$$

provided the denominator is not vanishingly small compared to the numerator. Immediately we realize that this perturbation method fails near resonance. Physically, this means that near resonance the motion is greatly perturbed away from the unperturbed motion. This is true even if the perturbation is very small. Mathematically, that the motion is grossly perturbed even by a small δH is indicated by the fact that, near resonance, the transformation S is *not* near-identity.

In order to study the motion near resonance we must use a different approach. To proceed near resonance we must transform to "island-variables" which "resolve" the resonance. In island-variables we will demonstrate that the near-resonance Hamiltonian is approximately integrable. Let us begin with the hose Hamiltonian 9.198 and transform to island-variables. Introducing the near-identity generating function

$$S = (n\xi - s\theta)\hat{J}_\rho + \theta\hat{J}_\theta \tag{9.204}$$

we may eliminate one of the actions and resolve the resonance. In terms of this S the new and old variables are related by

$$J_\rho = \frac{\partial S}{\partial \xi} = n\hat{J}_\rho \tag{9.205}$$

$$J_\theta = \frac{\partial S}{\partial \theta} = \hat{J}_\theta - s\hat{J}_\rho \tag{9.206}$$

$$\hat{\xi} = \frac{\partial S}{\partial \hat{J}_\rho} = n\xi - s\theta \tag{9.207}$$

$$\hat{\theta} = \frac{\partial S}{\partial \hat{J}_\theta} = \theta\,. \tag{9.208}$$

Substituting for the old variables in 9.198 we find

$$\delta H = \sum_{lm} \delta H^c_{lm} \cos\left(\frac{l}{n}\hat{\xi} + \left(l\frac{s}{n} - m\right)\hat{\theta}\right) + \sum_{lm} \delta H^s_{lm} \sin\left(\frac{l}{n}\hat{\xi} + \left(l\frac{s}{n} - m\right)\hat{\theta}\right) . \tag{9.209}$$

We want to average over $\hat{\theta}$ since it is now the fast angle (before the variable transformation θ was the slow variable). Expanding the sine and cosine by means of the multiple angle formulae, we see that upon averaging over $\hat{\theta}$ only terms for which $ls - mn = 0$ survive. Since for the surviving terms $ls - mn = 0$ let us define $p = l/n$, then $m = sp$ and $l = np$. The angle-averaged Hamiltonian δH becomes, near the (n, s) resonance

$$\delta \hat{H}_{ns} = \sum_{p=1} \delta H^c_{np,sp} \cos p\hat{\xi}_{ns} + \sum_{p=1} \delta H^s_{np,sp} \sin p\hat{\xi}_{ns} \tag{9.210}$$

where $\hat{\xi}_{ns} = n\xi - s\theta$.

The Hamiltonian $\hat{H} = H_\perp(\hat{J}_\rho, \hat{J}_\theta) + \delta \hat{H}_{ns}$ has a second (besides $\hat{H}$ itself) invariant. To see this we compute $\dot{J}_\rho = -\partial \hat{H}/\partial \xi$ and $\dot{J}_\theta = -\partial \hat{H}/\partial \theta$. This yields $s\dot{J}_\rho = -n\dot{J}_\theta$ hence $I = sJ_\rho + nJ_\theta$ is the second invariant. This demonstrates the integrability of the isolated resonance.

If one considers a region in action-space, in which there is a resonance between two degrees of freedom, with no other resonances nearby, then all terms, save the resonant term, have rapidly varying phases and so tend to average away on the time scale of the resonant term. Such an "isolated resonance" is in fact integrable (approximately), that is, an invariant besides the energy exists, enabling one to easily study the properties of the given isolated coupling resonance betwen the two degrees of freedom.

If we examine the perturbed Hamiltonian 9.198, we immediately realize that there will be many pairs of interacting, that is, "overlapping" [20], coupling resonances, when the hose perturbation exceeds a certain strength. Can one hope to retain good invariants in such a situation? It is to the study of these resonances that we shall turn our attention in the sequel.

In order to study the effects of the coupling resonances, we will numerically integrate the Hamiltonian equations of motion, following a trajectory around the two-torus. Our basic method is to look at the "punch plot", that is, the Poincaré section map induced by the flow on the energy level torus as it intersects a $\theta =$ constant cross-section. For a given point on the section, the Poincaré map is the "first return map", which takes the point of intersection at one time to the point of intersection one unit of time later (the frequencies are suitably normalized to accomplish this). If the winding number on a torus is irrational, the images of a single point will densely cover the circle of intersection of the torus with the section as one iterates the map infinitely many times. For intersections with rational tori, the images of a single point will repeat themselves eventually.

In order to calculate, and investigate the effect of the hose instability upon, the orbits, we must compute the explicit form of δH . The passage of a lateral displacement manifests itself, as far as a beam slice is concerned, by the appearance of a factor

$$\delta\psi(\rho,\theta) \sim \delta\psi(\rho)\exp i\theta \tag{9.211}$$

in the pinch potential. This is only correct for a low frequency perturbation,

[20] Resonances never literally "overlap" (private communication J.D.Meiss)

where $\Omega \ll \Omega_{\beta o}$. For a high frequency $\Omega \sim \Omega_{\beta o}$ perturbation there is explicit time dependence.

Let us now consider the effect, of a rigid lateral displacement of a beam slice, upon the near-circle orbits. When we carried out the calculations which follow, we used the convention (which will be maintained in this presentation) that the mass factor γm (without loss of any physics) is set to unity [21]. We denote by $\rho = \rho_o + \delta\rho$ the (dimensionless) radius of a near-circle orbit with respect to the center of the *displaced* beam, where $\delta\rho$ is given by 9.212, and by $\rho' = \rho_o + \delta\rho'$ the (dimensionless) radial position with respect to the center of the unperturbed beam. In order to compute the perturbed Hamiltonian for a weakly hosing, near-circle beam, we need to relate $\delta\rho$ to $\delta\rho'$. The geometry of the situation is depicted in Fig. 9.4. If we denote by δx the (dimensionless) amplitude of the lateral displacement, in the x-direction, then using the law of cosines $\rho'^2 = \rho^2 + \delta x^2 + 2\rho\delta x\cos\theta$ we have, after expanding to order δx^4, the result

$$\begin{aligned}\rho' \quad &= -\frac{5}{64}\frac{\delta x^4}{\rho^3}\cos 4\theta + \frac{1}{8}\frac{\delta x^3}{\rho^2}\cos 3\theta + \frac{1}{16}\frac{\delta x^4}{\rho^3}\cos 2\theta - \frac{1}{4}\frac{\delta x^2}{\rho}\cos 2\theta \\ &\quad -\frac{1}{8}\frac{\delta x^3}{\rho^2}\cos\theta + \delta x\cos\theta + \frac{1}{64}\frac{\delta x^4}{\rho^3} + \frac{1}{4}\frac{\delta x^2}{\rho} + \cdots \end{aligned} \tag{9.212}$$

Next, we insert $\rho = \rho_o + \delta\rho$, expand ρ' to order $\delta\rho^2$, and set $\delta\rho' = \rho' - \rho_o$ to get

$$\delta\rho' = \frac{1}{4\rho_o^3}\delta x^2\left(\delta x\delta\rho\cos\theta + \left(\rho_o\delta\rho - \delta\rho^2\right)\cos 2\theta - \delta x\delta\rho\cos 3\theta + \cdots\right) . \tag{9.213}$$

[21] It is easy enough to trace through and replace the factors of γm if desired.

We shall also need $\delta\rho'^2$ which works out to be

$$\delta\rho'^2 = \frac{1}{2\rho_o^2}\delta x\delta\rho\left(\left(4\rho_o^2 - \delta x^2\right)\cos\theta + (\delta x\delta\rho - \delta x\rho_o)\cos 2\theta + \delta x^2\cos 3\theta + \cdots\right) \tag{9.214}$$

where ellipses denote terms of higher order, and terms with no ξ dependence.

The hose perturbation of the Hamiltonian works out to be

$$\delta H = \rho_o\Omega_\theta^2\delta\rho' + \frac{1}{2}\left(\Omega_\rho^2 - 3\Omega_\theta^2\right)\delta\rho'^2 + \cdots . \tag{9.215}$$

If we substitute our expressions for $\delta\rho'$ and $\delta\rho'^2$ into δH , we get the double Fourier expansion 9.198 in harmonics of ξ and θ , after quite a considerable amount of algebra

$$\delta H_{11} = 4h_1 J_\rho^{\frac{1}{2}}\sin(\theta - \xi) + \epsilon^2 h_1\left(3\frac{\Omega_3^2}{\Omega_\rho^2} - \frac{3}{2}\frac{\Omega_4}{\Omega_\rho}\right)J_\rho^{\frac{3}{2}}\sin(\theta - \xi) \tag{9.216}$$

$$\delta H_{12} = -\epsilon h_1\frac{\Omega_3}{\Omega_\rho}J_\rho\cos(\theta - 2\xi) + \frac{1}{4}\epsilon^2 h_1\frac{\Omega_4^2}{\Omega_\rho^2}J_\rho^{\frac{3}{2}}\sin(\theta - 2\xi) \tag{9.217}$$

$$\delta H_{13} = \epsilon^2 h_1\frac{\Omega_4^2}{\Omega_\rho^2}J_\rho^{\frac{3}{2}}\sin(\theta - 3\xi) \tag{9.218}$$

$$\delta H_{22} = \left(-h_2\frac{4}{\Omega_\rho} + \epsilon h_2\rho_o\frac{\Omega_3}{\Omega_\rho}\left(\frac{2}{\Omega_\rho}\right)^{\frac{1}{2}}\right)J_\rho\cos(2\theta - 2\xi) - \epsilon^2\frac{3}{4}h_2\frac{\Omega_3}{\Omega_\rho^2}J_\rho^{\frac{3}{2}}\cos(2\theta - 2\xi) \tag{9.219}$$

$$+ \epsilon^2 3h_2\frac{\Omega_4}{\Omega_\rho^2}J_\rho^2\cos(2\theta - 2\xi) - \epsilon^2\frac{1}{4}h_2\rho_o\frac{\Omega_4}{\Omega_\rho}\left(\frac{2}{\Omega_\rho}\right)^{\frac{1}{2}}J_\rho^{\frac{3}{2}}\sin(2\theta - 2\xi)$$

$$\delta H_{23} = \left(\epsilon 4h_2\frac{\Omega_3}{\Omega_\rho} + \epsilon^2 h_2\rho_o\frac{\Omega_3^2}{\Omega_\rho^2}\left(\frac{2}{\Omega_\rho}\right)^{\frac{1}{2}}\right)J_\rho^{\frac{3}{2}}\sin(2\theta - 3\xi) + \epsilon^2\frac{1}{2}h_2\frac{\Omega_4}{\Omega_\rho^2}J_\rho^2\cos(2\theta - 3\xi) \tag{9.220}$$

$$\delta H_{32} = -\epsilon h_3 \frac{\Omega_3}{\Omega_\rho}\left(\frac{2}{\Omega_\rho}\right)^{\frac{1}{2}} J_\rho \cos(3\theta - 2\xi) + \epsilon^2 \frac{1}{4} h_3 \frac{\Omega_4}{\Omega_\rho}\left(\frac{2}{\Omega_\rho}\right)^{\frac{1}{2}} J_\rho \sin(3\theta - 2\xi) \tag{9.221}$$

where $s = \delta x/\rho_o$ is the "hose strength", and h_1 , h_2 , and h_3 are defined as

$$h_1 = \frac{1}{8}\rho_o \left(\Omega_\rho^2 - 4\Omega_\theta^2\right)\left(\frac{2}{\Omega_\rho}\right)^{\frac{1}{2}}\left(s - \frac{1}{4}s^3\right) \tag{9.222}$$

$$h_2 = \frac{1}{32}s^2\left(\Omega_\rho^2 - 4\Omega_\theta^2\right) \tag{9.223}$$

$$h_3 = \rho_o s h_2 \, . \tag{9.224}$$

Having derived the hose perturbations, it is a matter of numerical integration to solve Hamilton's equations of motion for the orbit. Explicitly, we have $\dot{J}_\rho = -H_\xi$, $\dot{\xi} = H_{J_\rho}$, $\dot{J}_\theta = -H_\theta$, and $\dot{\theta} = H_{J_\theta}$, where H_f denotes the partial derivative $\partial H/\partial f$. It is favorable that $\dot{\theta}$ turns out to be independent of J_ρ , J_θ , and ξ . For the Hamiltonian $H = H_\perp + \delta H$, with $H_\perp = \Omega_\theta J_\theta + \epsilon^2 \Omega_\rho J_\rho + \epsilon^4 \Omega_2 J_\rho^2$, and δH the sum of the perturbations δH_{nm} listed above, we have numerically investigated the coupling resonances and their overlaps. As mentioned previously, the method consists in following a given trajectory as it winds around the torus and recording where it "punches" through a given cross-section. Since the angle θ evolves at a uniform rate (the frequency is constant), it is convenient to use θ as the "toroidal" angle and to define a Poincaré section to be θ = constant. We chose $\theta = 0$ for convenience, a different choice simply rotates the pictures (since the island "filaments" themselves wind around the torus).

To numerically integrate the equations of motion, a simple fourth order Runga-Kutta scheme was employed, the details of which we shall not even mention. It

was found that the higher harmonic contributions were negligible (as theoretically predicted) compared to the lower harmonics. Precisely, only the following harmonics were important: δH_{11} , δH_{12} , and δH_{13} . Therefore, only the θ fundamental and the fundamental and first two harmonics of ξ were included.

In the numerical calculations, nine orbits were launched for each case studied. Each of the *isolated* resonances δH_{11} , δH_{12} , and δH_{13} were plotted separately (to look at the isolated coupling resonance) for various values of reference radius ρ_o and various hose strengths s . Then the isolated coupling resonances were combined pairwise: $\delta H_{11} + \delta H_{12}$, $\delta H_{11} + \delta H_{13}$, and $\delta H_{12} + \delta H_{13}$ to determine the pairwise interactions. Finally, all three were included together: $\delta H_{11} + \delta H_{12} + \delta H_{13}$.

The numerical results are depicted in a series of figures. Rather than describe the individual results here we refer to the figure captions wherein a "running commentary" is presented.

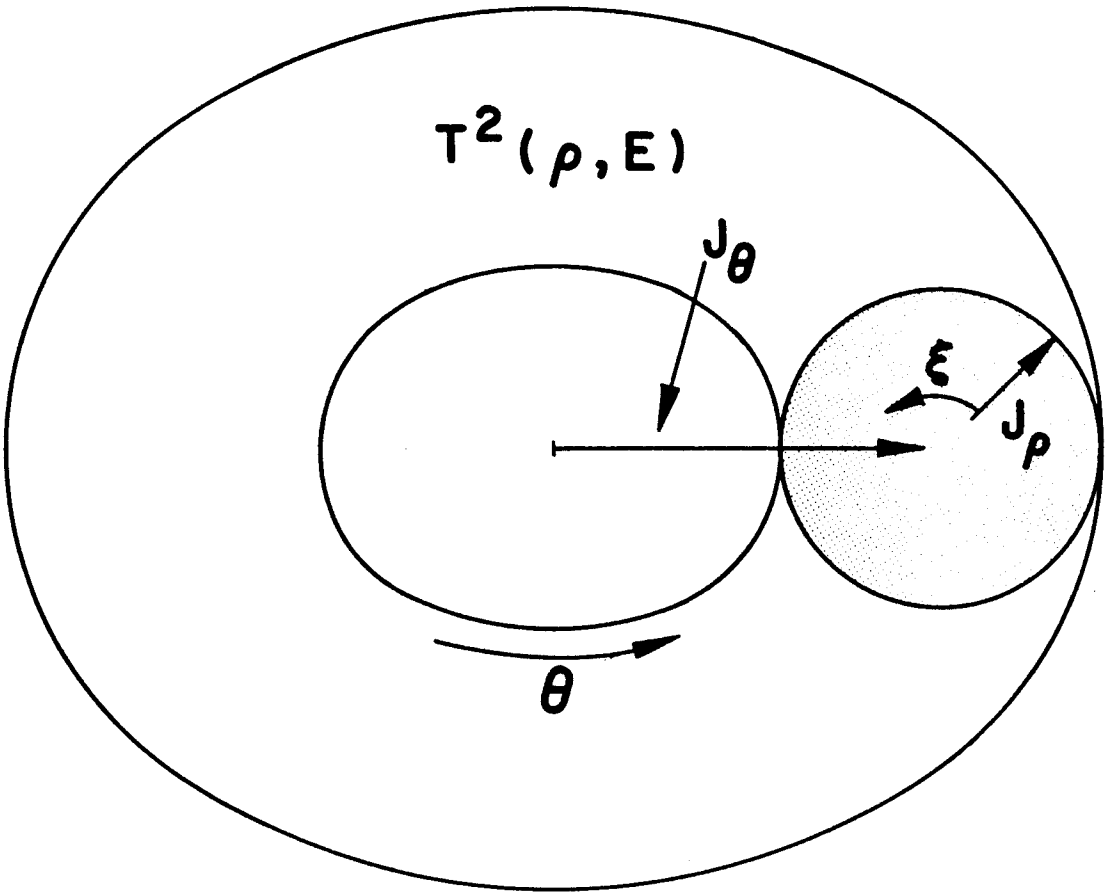

Figure 9.1: The orbit-space of the transverse dynamics in the equilibrium beam consists of a collection of nested tori. The action-angle variables form a set of coordinates for the tori.

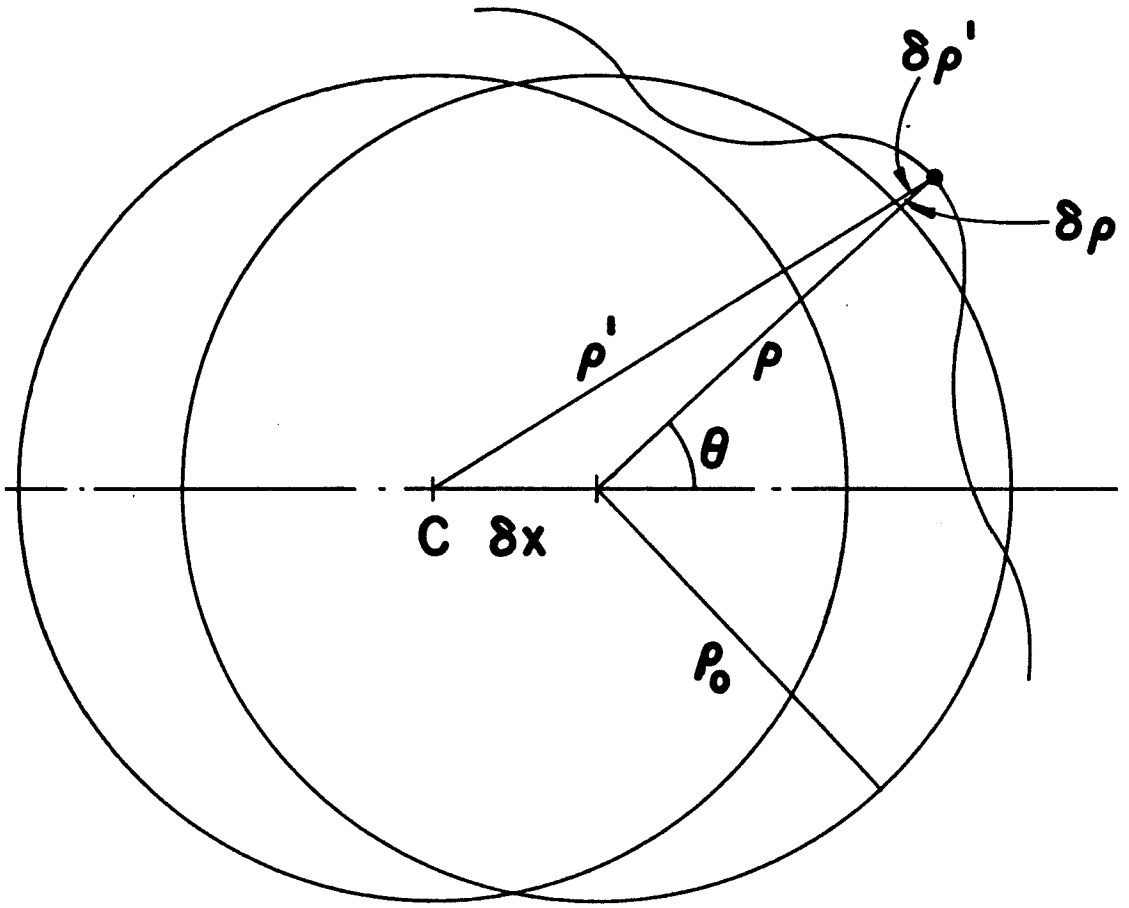

Figure 9.2: Geometry of the effect of a lateral displacement of a beam slice upon the near-circle orbits. C denotes the center of the undisplaced beam and δx is the amplitude of the lateral displacement.

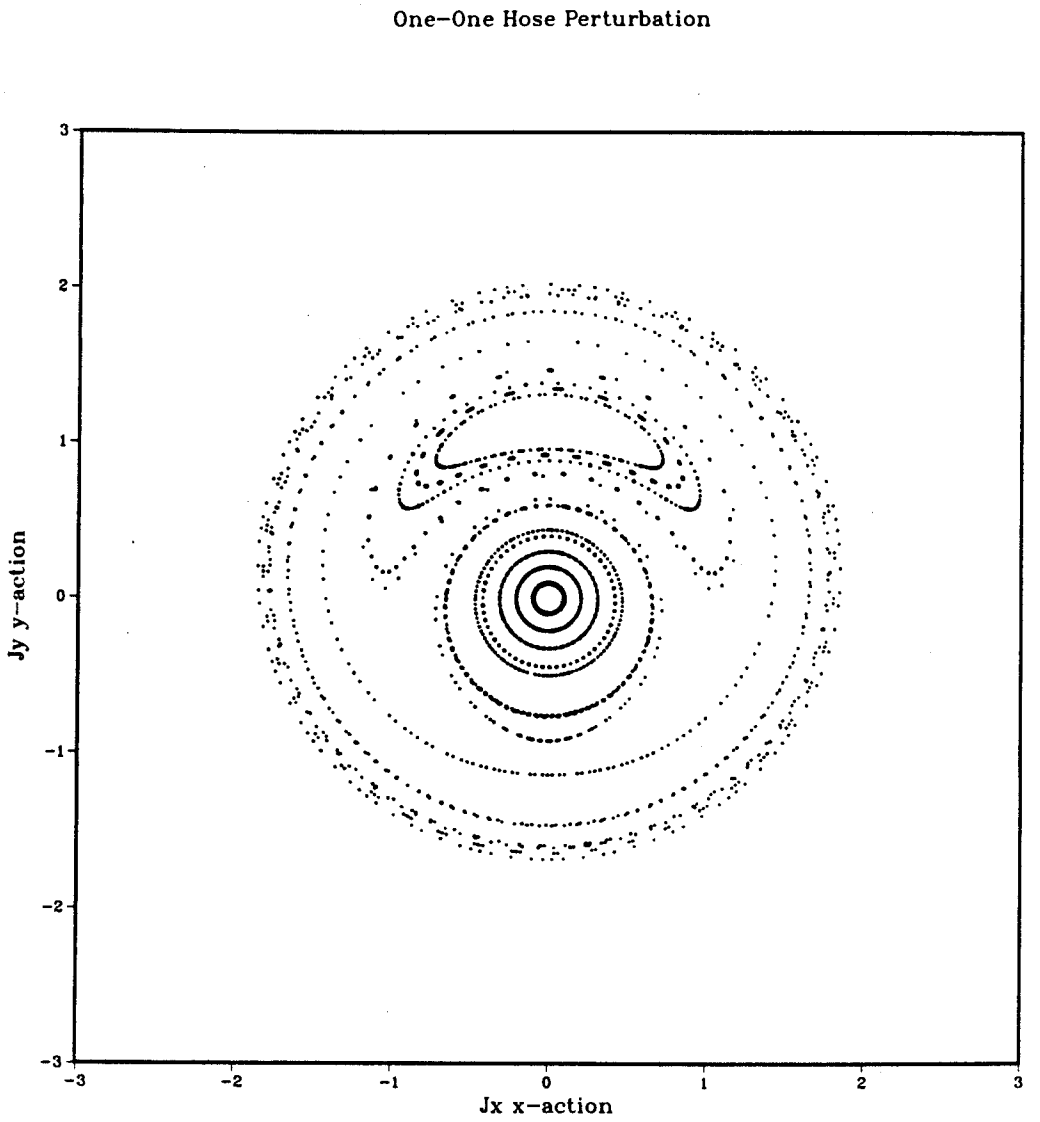

Figure 9.3: Depicting the growth of a primary island with elliptic point at $\xi = \pi/2$ and hyperbolic point at $\xi = -3\pi/2$. The actual separatrix orbit is not shown. For this plot the hose strength is $s = 0.01$ and the reference radius is $\rho_o = 0.5$.

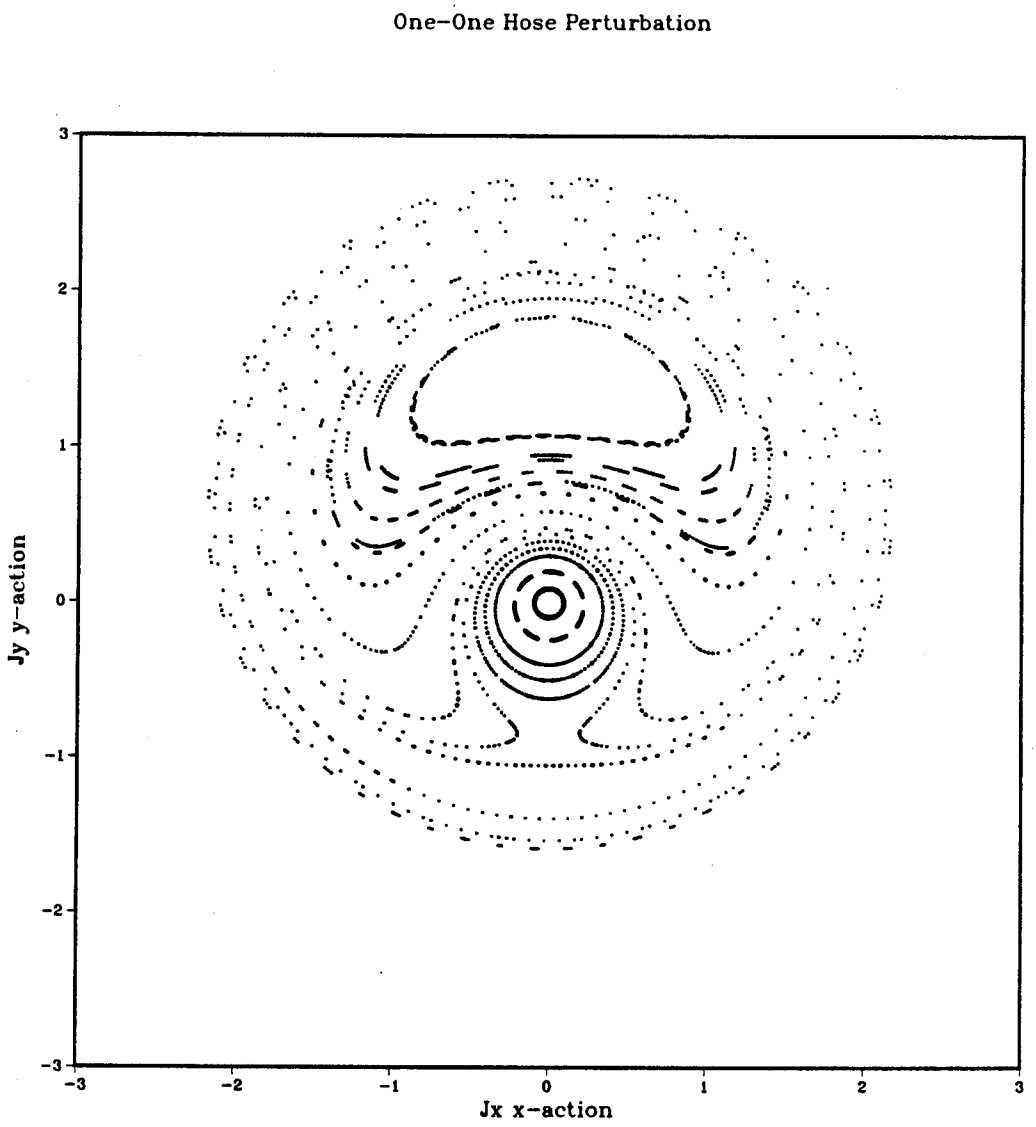

Figure 9.4: Depicting the growth of a primary island with elliptic point at $\xi = \pi/2$ and hyperbolic point at $\xi = -3\pi/2$. The actual separatrix orbit is not shown. For this plot the hose strength is $s = 0.01$ and the reference radius is $\rho_o = 1.0$, cf. Fig. 9.3.

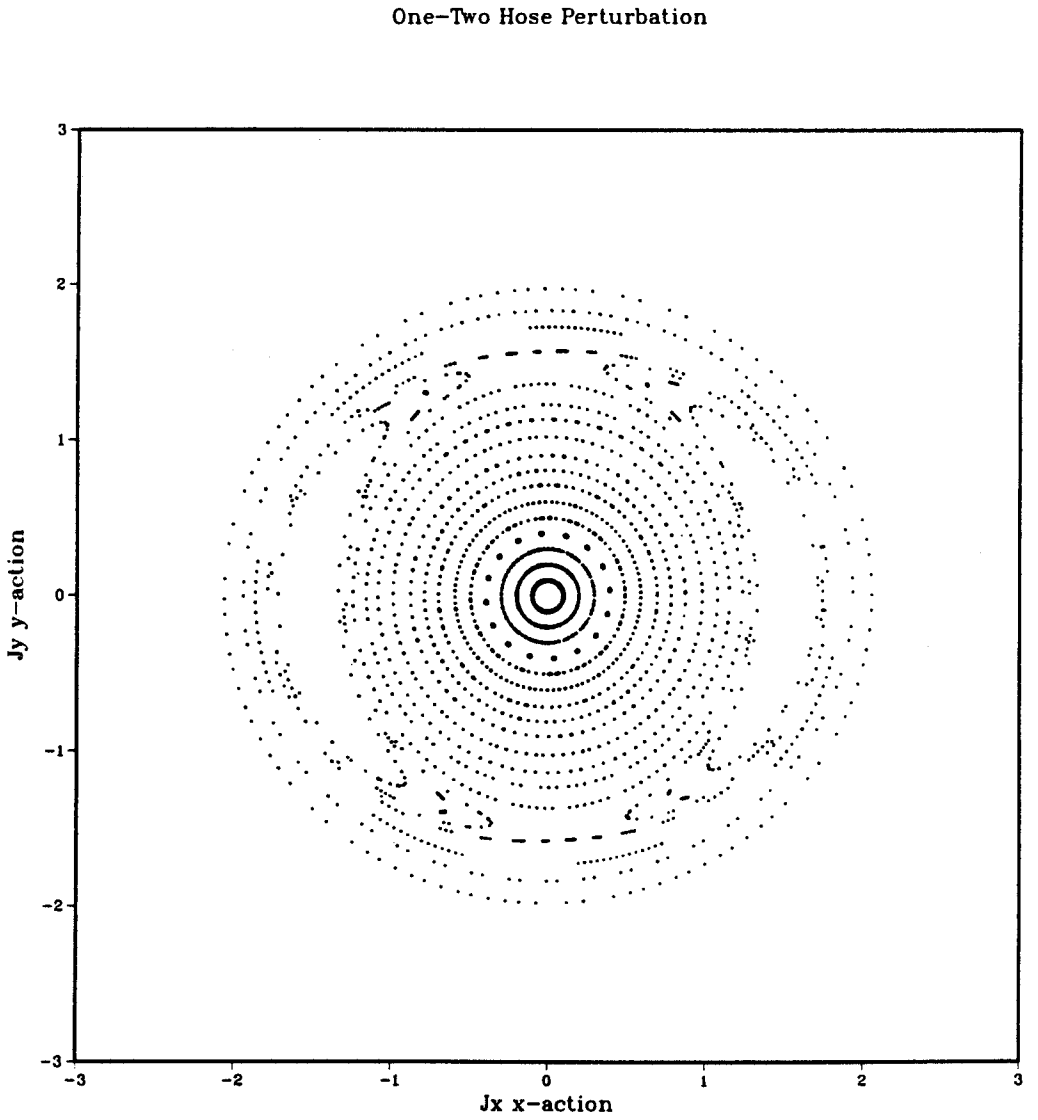

Figure 9.5: Depicting the islands of the δH_{12} isolated resonance. In this result the reference radius is $\rho_o = 1.0$ and the hose strength is $s = 0.01$.

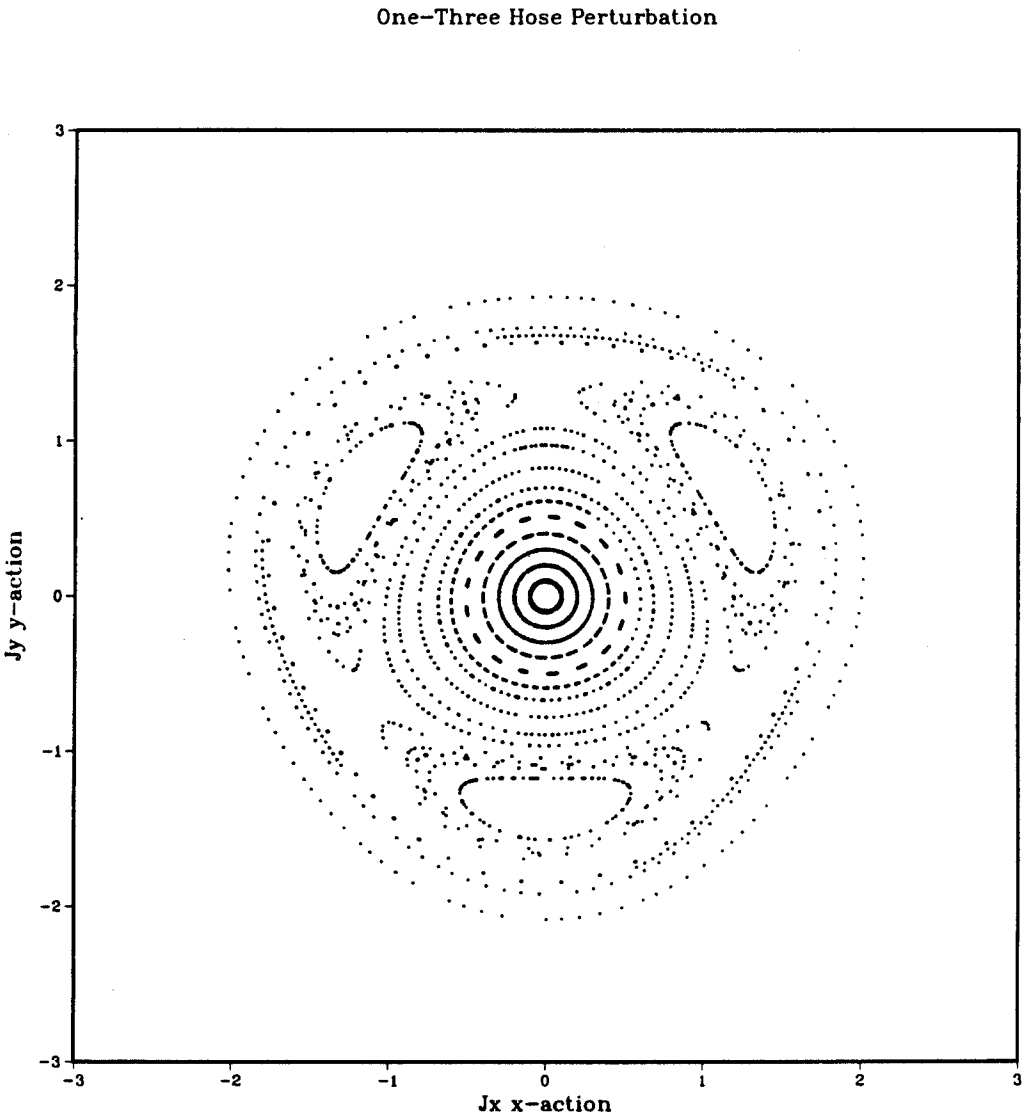

Figure 9.6: Depicting the islands of the δH_{13} isolated resonance. In this result the reference radius is $\rho_o = 0.5$ and the hose strength is $s = 0.01$.

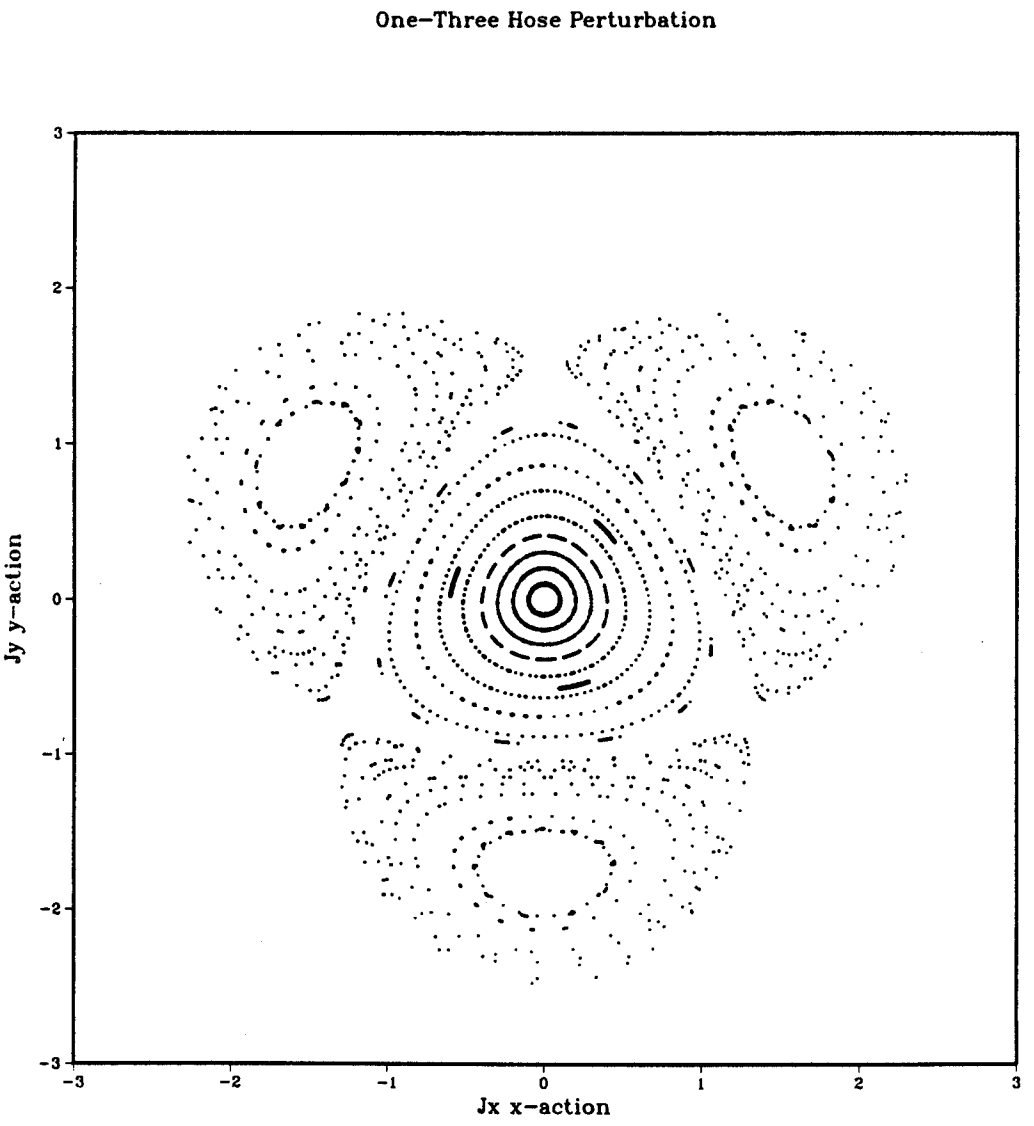

Figure 9.7: Depicting, again, the islands of the δH_{13} isolated coupling resonance. In this result the reference radius is $\rho_o = 1.0$ and the hose strength is $s = 0.01$. Comparing with Fig. 9.6, the resonance is stronger at larger radii.

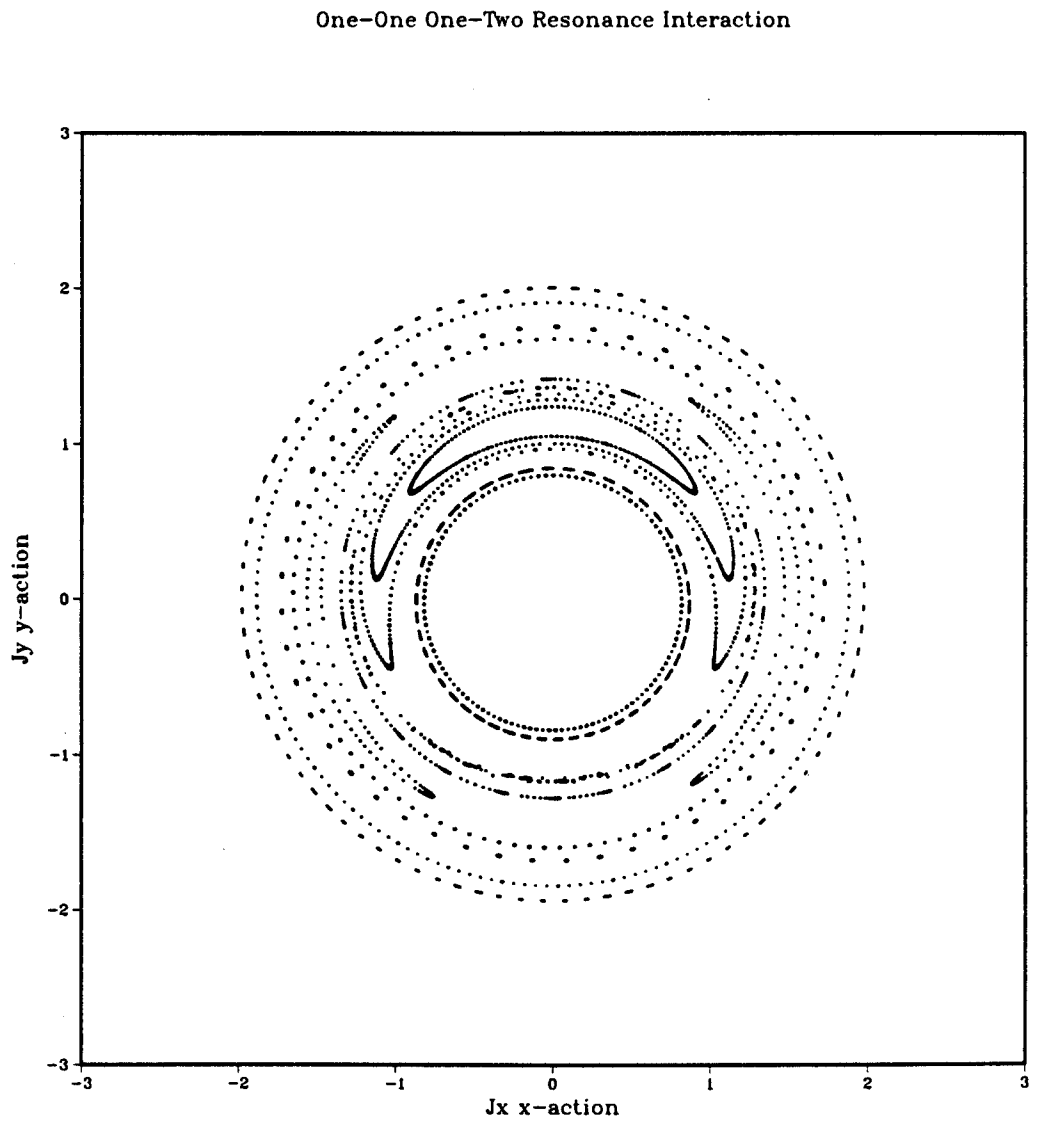

Figure 9.8: Depicting the interaction of the δH_{11} and δH_{12} coupling resonances. In this result $\rho_o = 1.0$ and $s = 0.0005$. A thin stochastic layer around the unstable hyperbolic point is emerging.

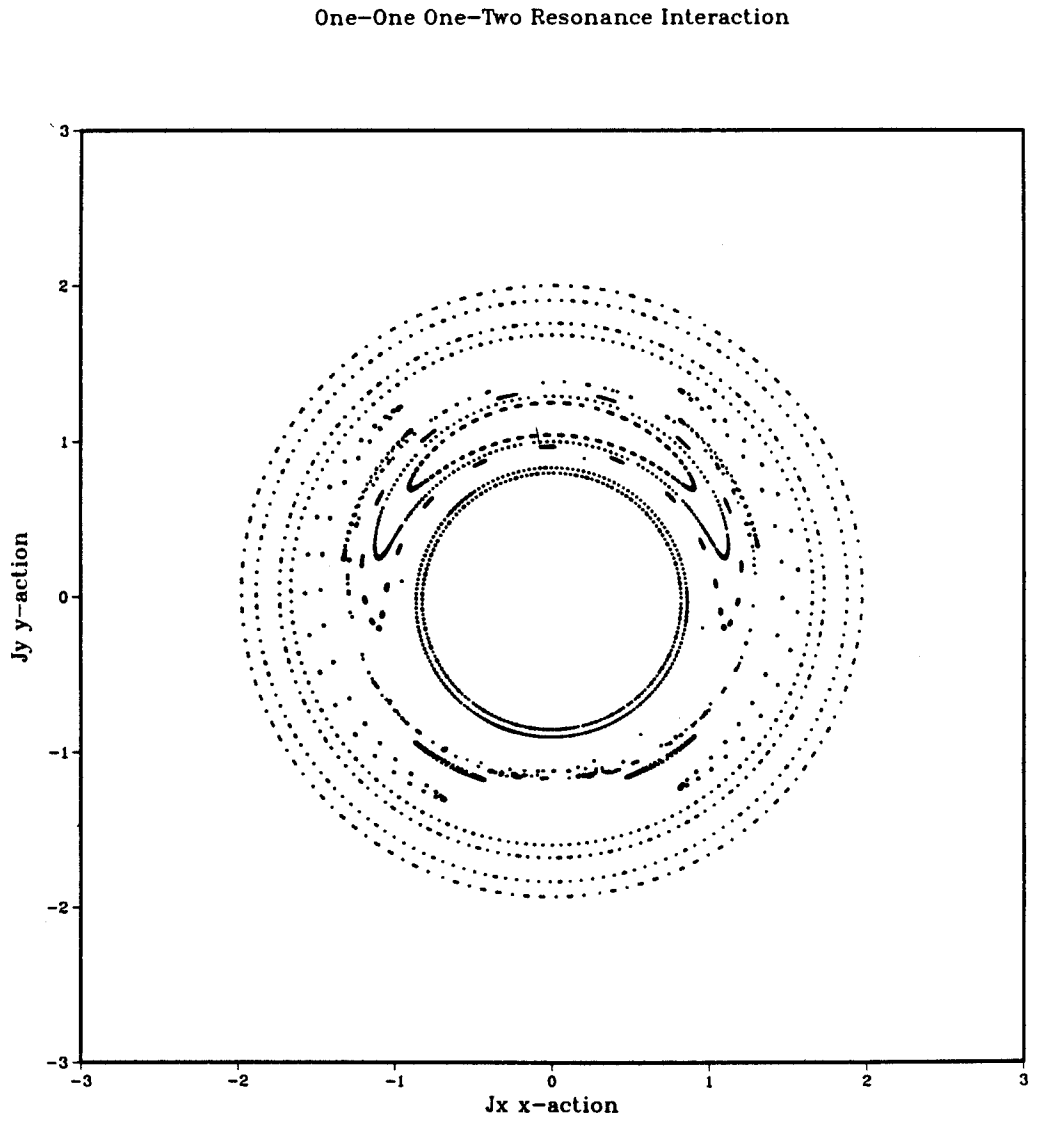

Figure 9.9: Depicting the δH_{11} and δH_{12} resonance interaction. In this result $\rho_o = 1.0$ and $s = 0.0006$. Island interaction has generated visible satellite islands and the island width has increased compared with Fig. 9.8.

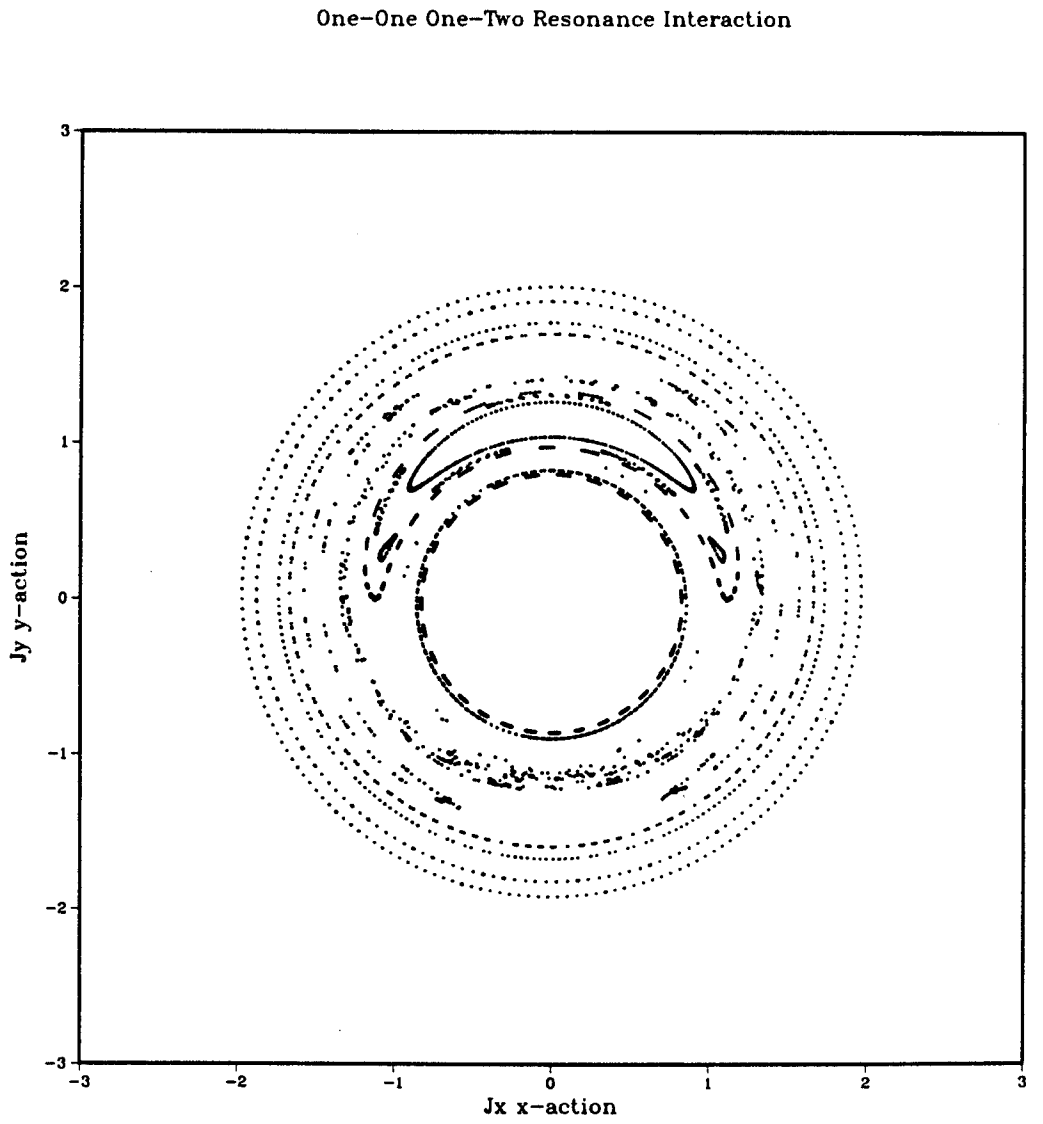

Figure 9.10: Depicting the δH_{11} and δH_{12} resonance interaction. In this result $\rho_o = 1.0$ and $s = 0.0007$. Further widening of the stochastic layer is apparent, and more satellite stucture is visible.

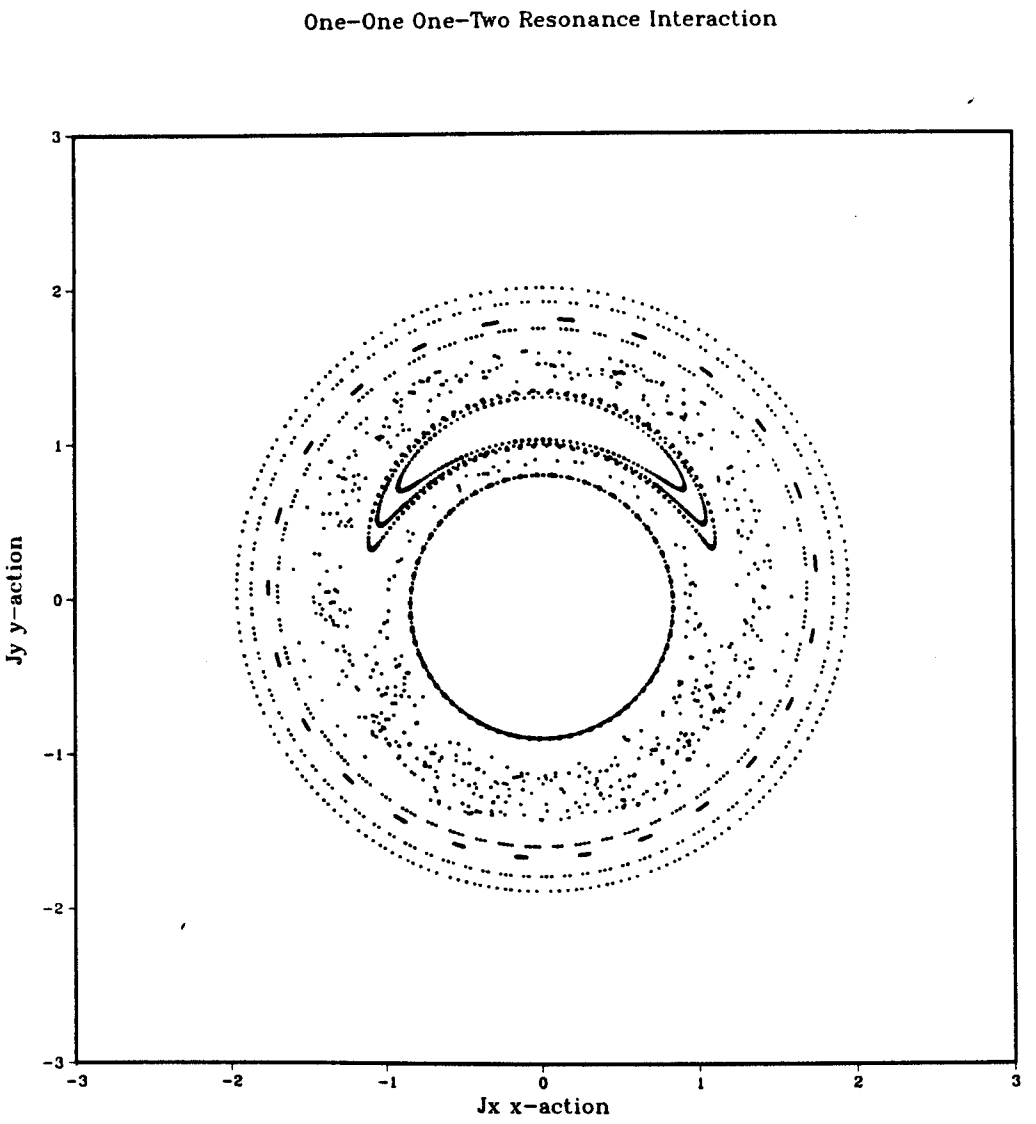

Figure 9.11: Depicting the δH_{11} and δH_{12} resonance interaction. In this result $\rho_o = 1.0$ and $s = 0.001$. The one-two islands have shrunken out of visibility, a wide stochastic layer surrounds the one-one island, but the layer is still well bounded by KAM tori.

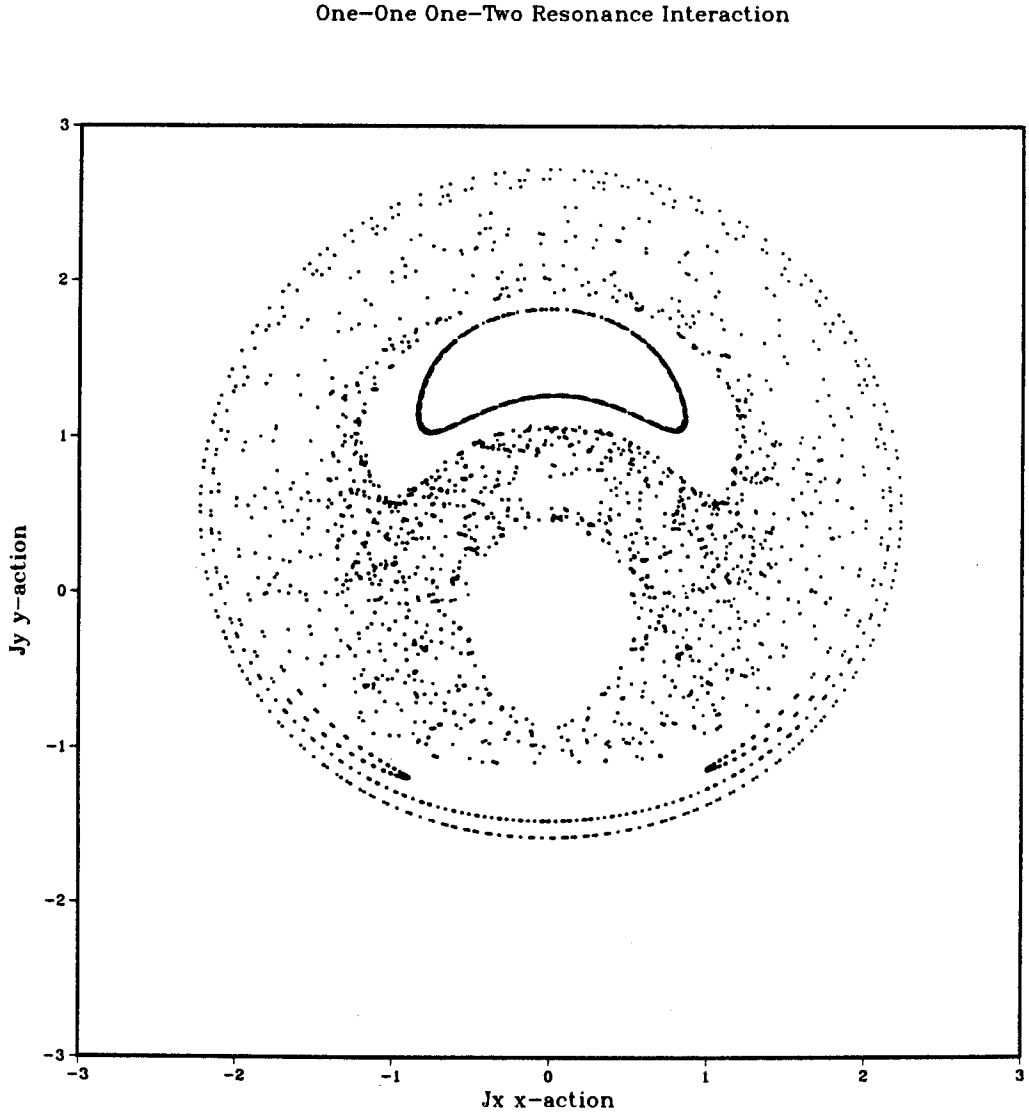

Figure 9.12: Depicting the δH_{11} and δH_{12} resonance interaction. In this result $\rho_o = 1.0$ and $s = 0.01$. The inner tori are shrinking as the stochastic region encompasses more, and more of the section. One can see very thin remnants of the one-two islands.

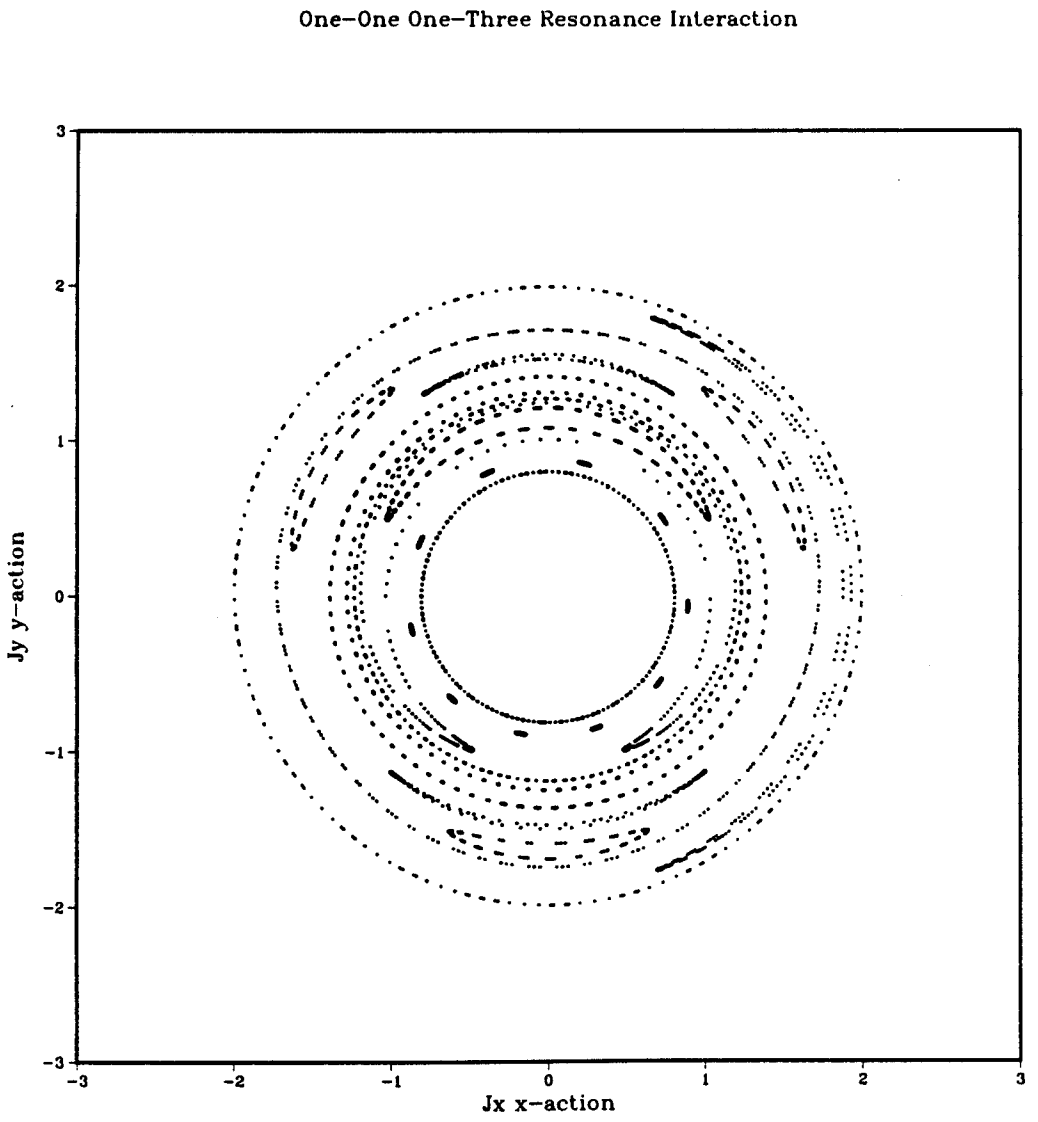

Figure 9.13: Depicting the δH_{11} and δH_{13} resonance interaction. In this result $\rho_o = 1.0$ and $s = 0.0003$. One can see some instability around the separatrices of the one-three island chain, bounded as yet by unaffected tori.

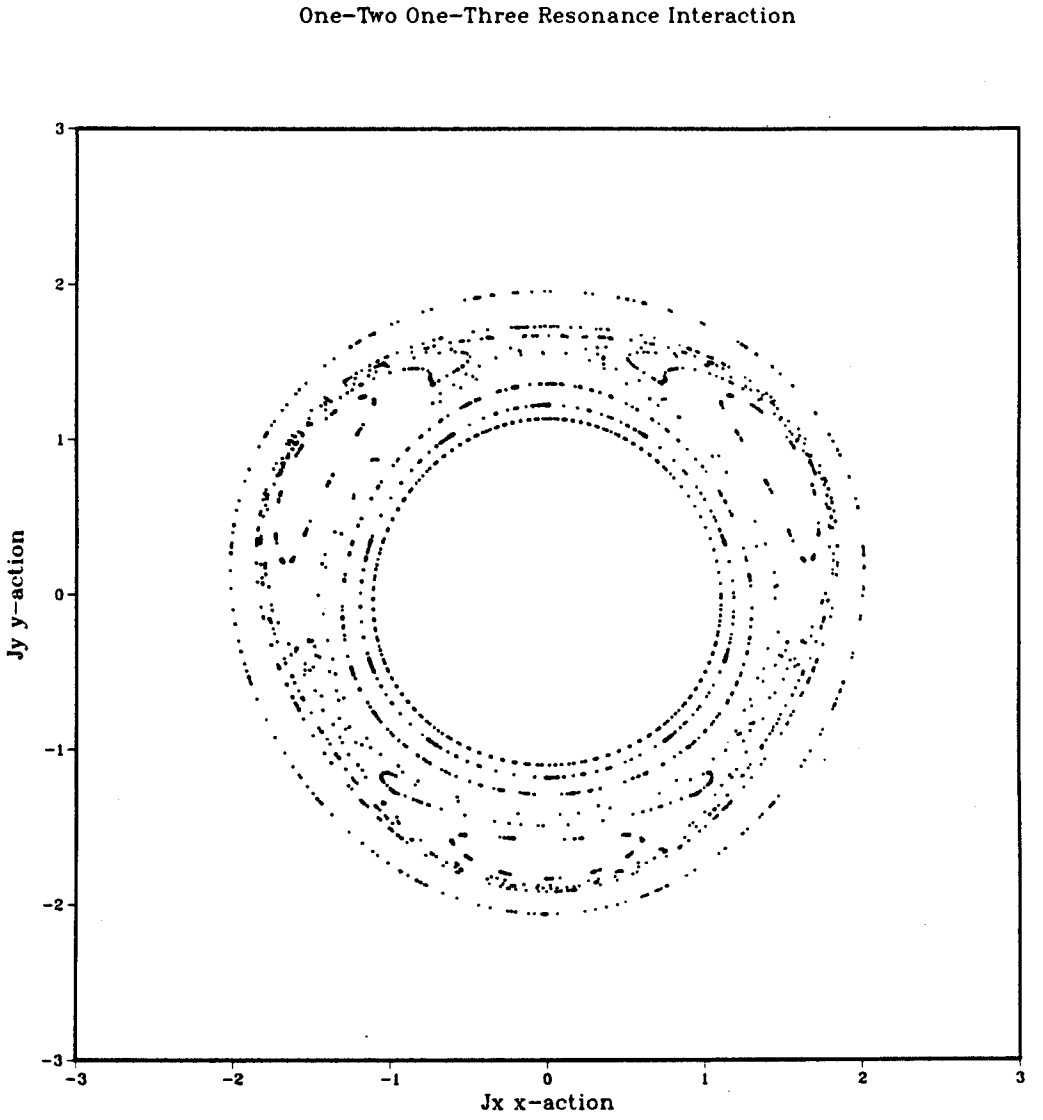

Figure 9.14: Depicting the δH_{11} and δH_{13} resonance interaction. In this result $\rho_o = 1.0$ and $s = 0.001$. Interaction has generated satellites but there is no apparent instability yet. The resonance interaction is weaker than for the one-one, one-two interaction, since the harmonic is higher.

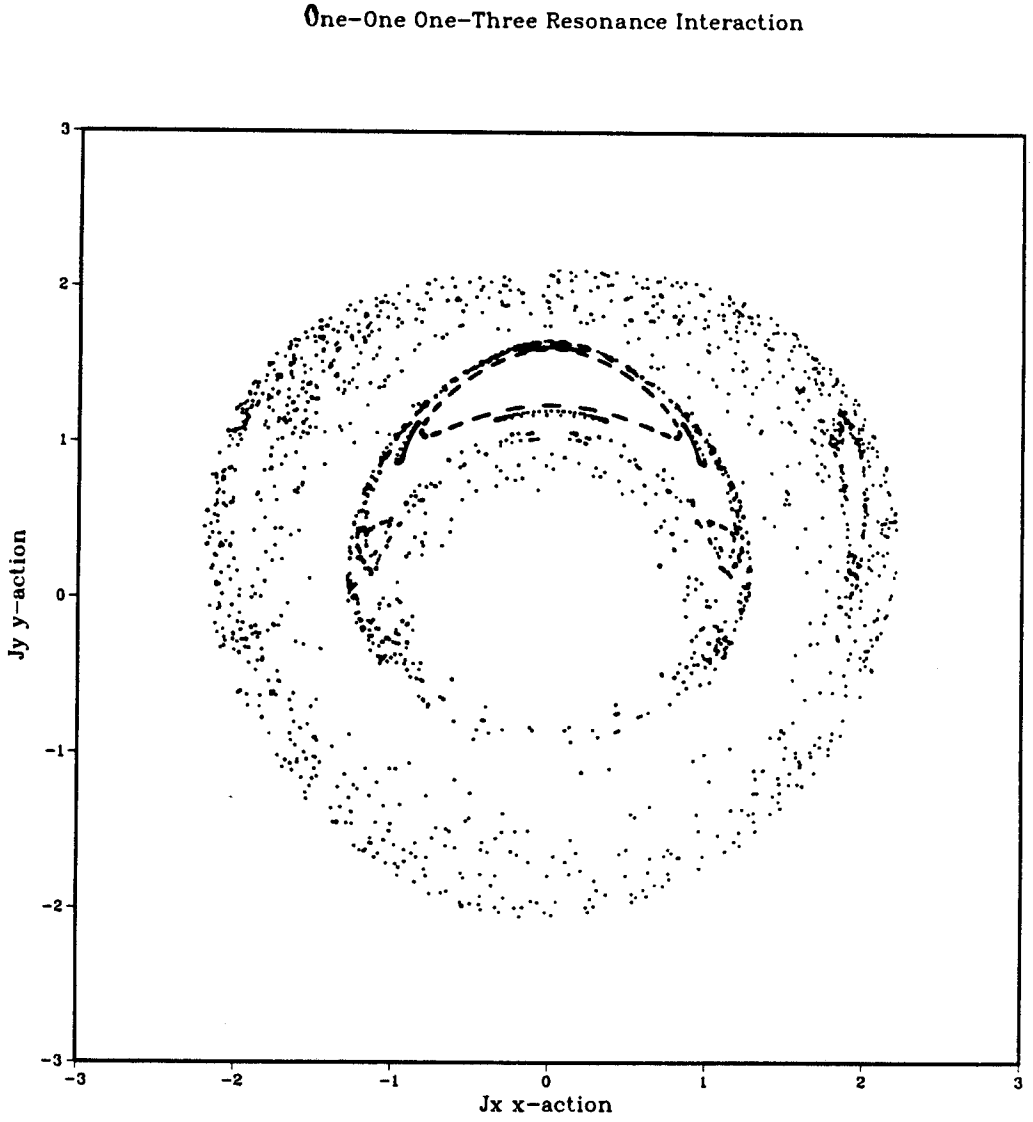

Figure 9.15: Depicting the δH_{11} and δH_{13} resonance interaction. In this result $\rho_o = 1.0$ and $s = 0.01$. Here, compared with Fig. 9.14, the situation has changed dramatically, although good tori are still bounding the action quite effectively.

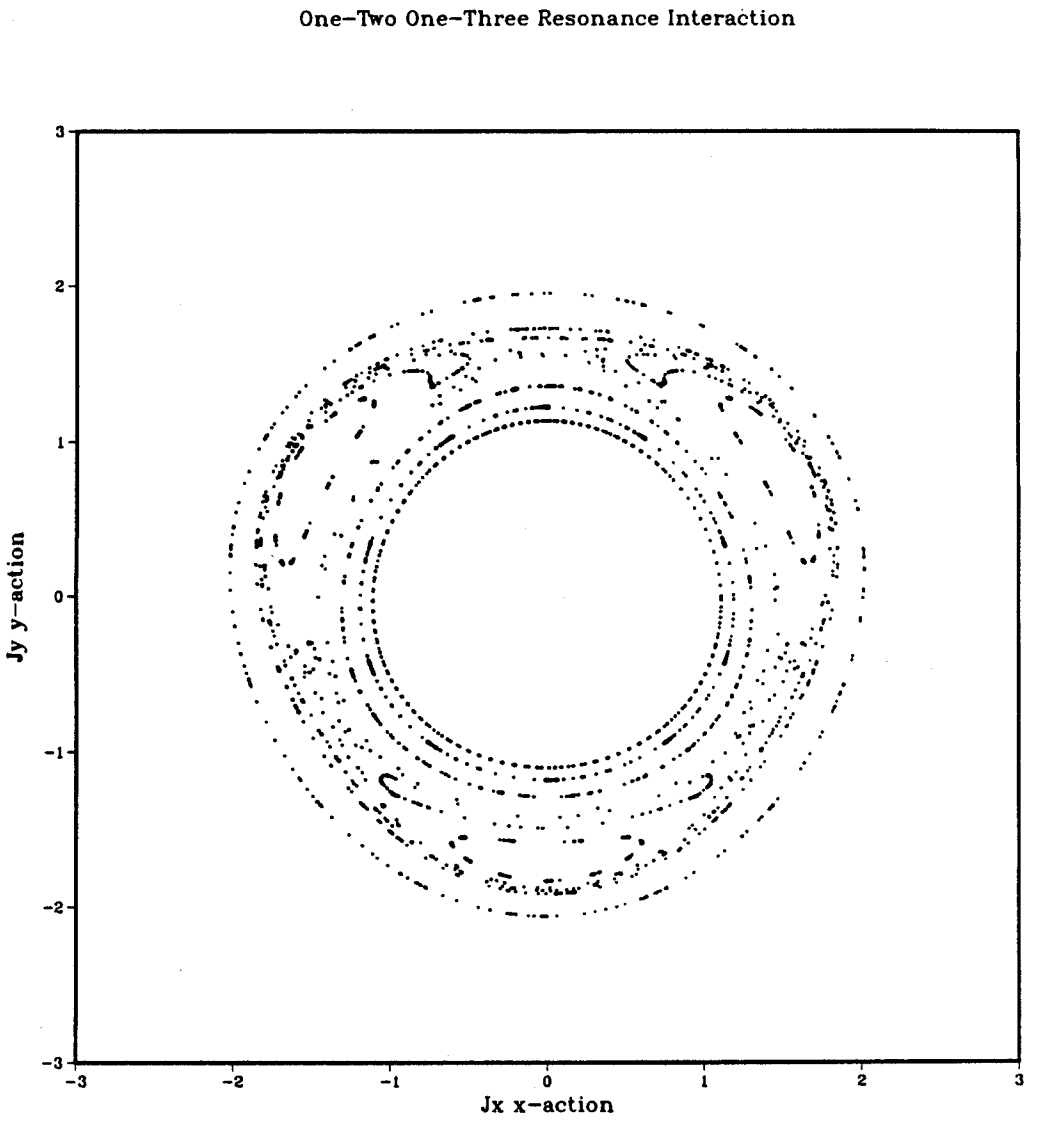

Figure 9.16: Depicting the δH_{12} and δH_{13} resonance interaction. In this result $\rho_o = 1.0$ and $s = 0.007$.

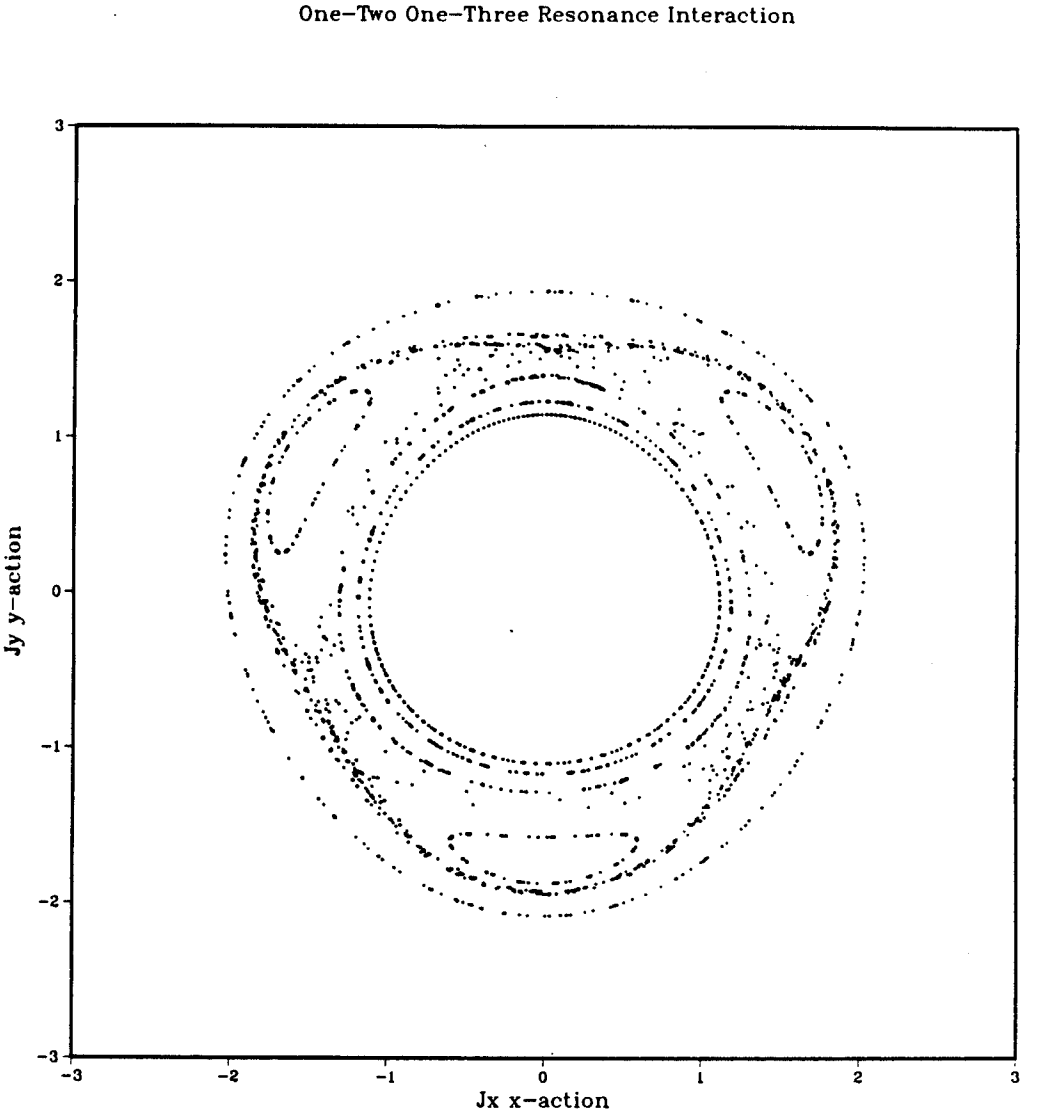

Figure 9.17: Depicting the δH_{12} and δH_{13} resonance interaction. In this result $\rho_o = 1.0$ and $s = 0.01$. The one-two islands are not yet even visible, there is some instability near the separatrices of the one-three islands.

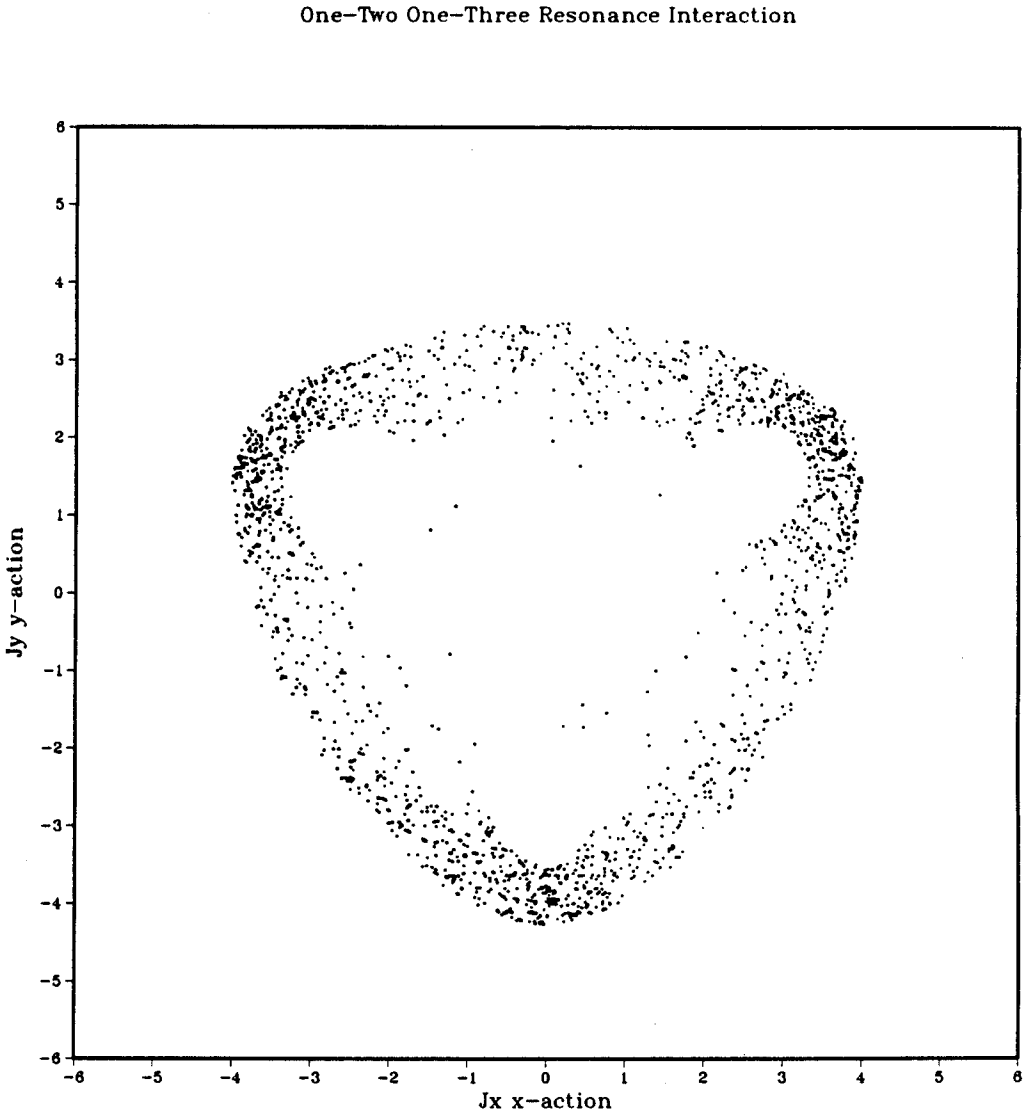

Figure 9.18: Depicting the δH_{12} and δH_{13} resonance interaction. In this result $\rho_o = 1.0$ and $s = 0.1$. The nine orbits are very unstable, but, and this is the significant point, are still bounded within a region of action-space.

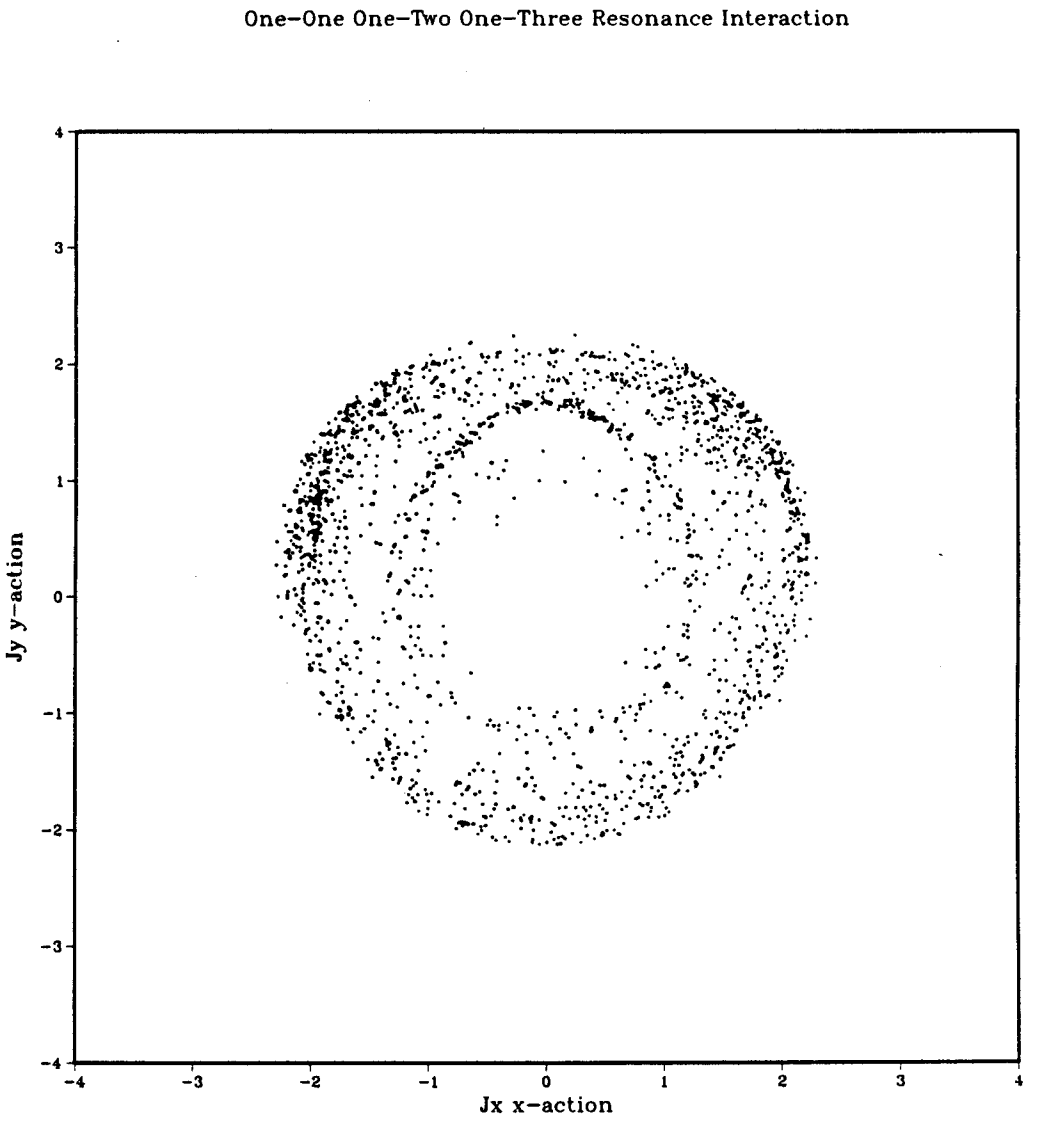

Figure 9.19: Depicting the δH_{11} , δH_{12} , and δH_{13} resonance interactions. In this result $\rho_o = 1.0$ and $s = 0.01$. The orbits are *very* unstable, but are *still* bounded by good tori.

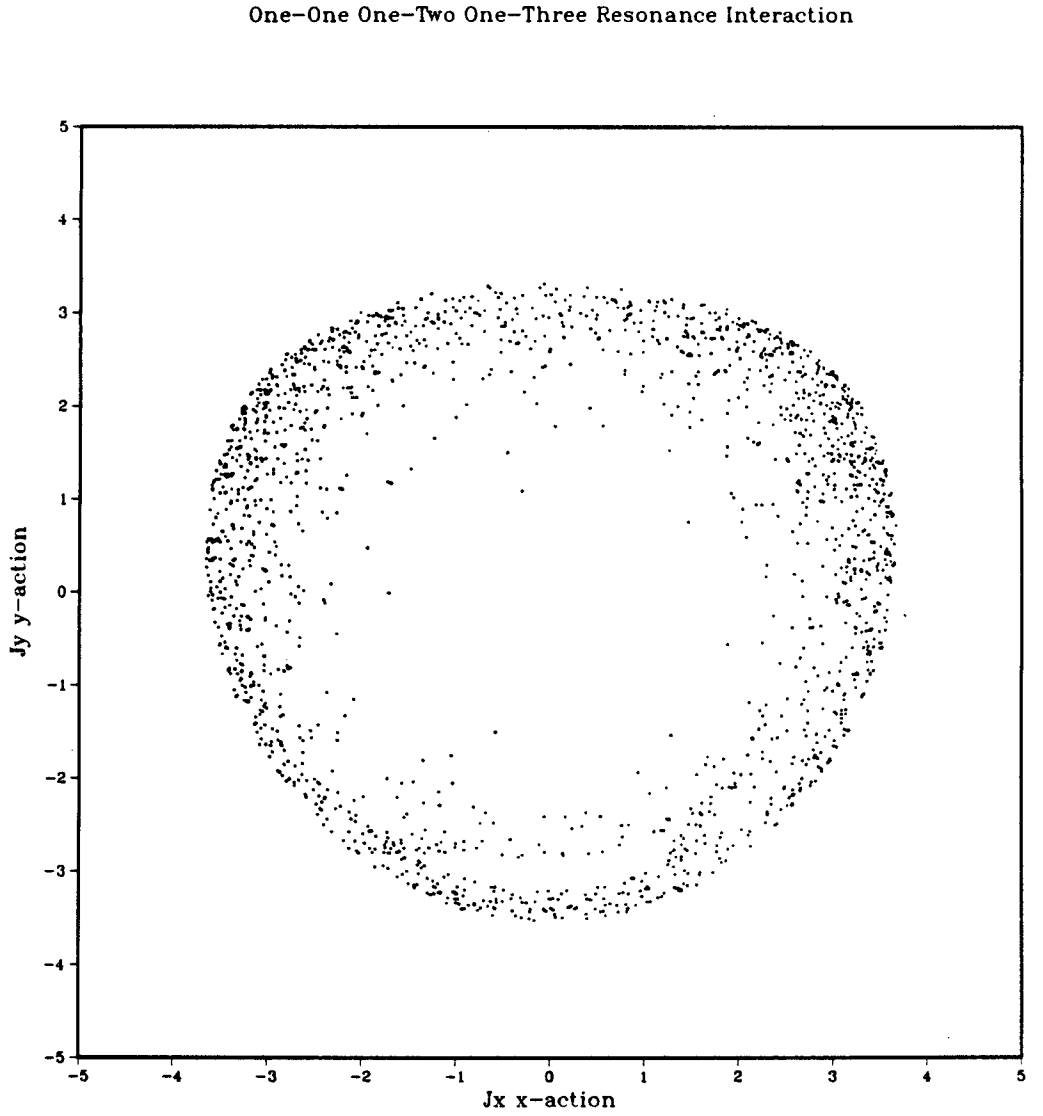

Figure 9.20: Depicting the δH_{11} , δH_{12} , and δH_{13} resonance interactions. In this result $\rho_o = 1.0$ and $s = 0.03$. The outer tori are expanding, indicating increasing transfer of energy from the azimuthal to the radial motion. We have found that this continues as the lateral displacement increases.

9.5 References

9.1 J.L.Lopes, Gauge Field Theories , Pergamon Press (1981)

9.2 G.F.Chew, M.L.Goldberger, F.E.Low, "Los Alamos Lecture Notes of the Physics of Ionized Gases", LA-2055 (1955)

9.3 J.Mark, "Plasma in Particle Accelerators: Adiabatic Theories for Bunched Beams", SIAM J. Appl. Math. **4**, 914 (1982)

9.4 during discussion at the 1911 Solvay Conference, cf. [9.5]

9.5 A.J.Lichtenberg, M.A.Lieberman, Regular and Stochastic Motion , Springer-Verlag (1983)

9.6 A.Deprit, "Canonical Transformations Depending Upon a Small Parameter", Cel. Mech. **1**, 12 (1969)

9.7 R.L.Dewar, "Renormalized Canonical Perturbation Theory for Stochastic Propagators", J. Phys. **A9**, 2043 (1976)

9.8 M.M.Rosenbluth, R.Z.Sagdeev, J.B.Taylor, G.M.Zaslavskii, "Destruction of Magnetic Surfaces by Magnetic Field Irregularities", Nucl. Fusion **6**, 207 (1966)

9.9 V.I.Arnold, A.Avez, Ergodic Problems in Classical Mechanics , W.A. Benjamin (1963)

9.10 A.N.Kolmogorov, "On Conservation of Conditionally Periodic Motion Under Periodic Perturbations of the Hamiltonian", Dokl. Akad. Nauk. SS7 (1954); reprinted in English in [9.14]

9.11 V.I.Arnold, "Proof of A.N.Kolmogorov's Theorem on the Preservation of Quasiperiodic Motions Under Small Perturbations of the Hamiltonian", Russ. Math. Surv. **18**, 9 (1963)

9.12 J.Moser, "On Invariant Curves of Area-Preserving Mappings of an Annulus", Nachr. Akad. Wiss., Gottingen, Math. Phys. K1 **2**, 1 (1962)

9.13 cf. B.V.Chirikov, "A Universal Instability of Many Dimensional Oscillator Systems", Phys. Reps. **52**, 263 (1979)

9.14 R.H.Abraham, J.E.Marsden, Foundations of Classical Mechanics , Benjamin/Cummings (1978)

9.15 J.M.Greene, "Behavior of Orbits of Two Coupled Oscillators", invited paper, Proc. 1984 Intl. Conf. Plasma Phys., Lausanne Switzerland

9.16 H.Goldstein, Classical Mechanics , Addison-Wesely Publishing Company (1950)

9.17 M.Toda, "Waves in Nonlinear Lattice", Prog. Theor. Phys. Suppl. **45**, 174 (1970)

9.18 J.Ford, S.D.Stoddard, J.S.Turner, "On the Integrability of Toda Lattice", Prog. Theor. Phys. **50**, 1547 (1973)

9.19 M.Henon, "Integrals of the Toda Lattice", Phys. Rev. **B9**, 1921 (1974)

9.20 R.S.MacKay, J.D.Meiss, I.C.Percival, "Transport in Hamiltonian Systems", University of Texas Inst. for Fusion Studies Report IFSR-109 (1983)

Chapter 10

Conclusions and Future Work

This thesis documents our theoretical investigations of the linear hose instability of an ultra-relativistic electron beam propagating in resistive plasma. Linear hose instability has been long recognized and studied by plasma physicists. The purpose of Chapter 10 is to summarize our contributions to this ongoing process of theoretical illumination, clarification, and refinement. Also, several intriguing avenues of future research which have been revealed by our work will be marked. Some of our work has wider ramifications, than just the linear hose instability, impinging upon the general problem of numerical simulation of electron beams propagating over many betatron wavelengths. In this regard, our introduction of modern Hamiltonian system theory, to the study of electron beam problems, is a new and hopefully fruitfull development.

The primary observations, and, conclusions which we have drawn during the course of our inquiry, are as follows:

1. The theoretical significance of the circle-orbits far transcends any previous realization of their importance. We have discovered that

   1.1 The circle-limit of the general Vlasov theory is the same as the cold Vlasov theory.

   1.2 The cold Vlasov theory results in the same dispersion relation as the spread-mass model.

   1.3 The energy-group model results in the same dispersion relation as the spread-mass model.

   1.4 Circle-orbits (a circular-helix beam) *do* yield phase-mix damping. Moreover, a circular-helix beam is tantamount to a spread-mass beam.

   1.5 An orbit-perturbation calculation, which builds up the perturbed current in the mathematical form of an integral over initial conditions which launch particles which arrive at a given space point, at a given time, on the *linearly perturbed* orbits, predicts quite a different result than any of the equivalent circle-orbit Vlasov theories or multiple-oscillator models.

2. A general elliptical-helix beam theory, including linear orbit perturbation effects, can be developed. This calculation will involve a nontrivial unperturbed orbit, as opposed to the circular-helix beam, wherein the unperturbed orbits are easily specified analytically.

3. The spread-mass, and energy-group models are *operationally* perfectly equivalent. Only the underlying, but calculationally irrelevent, interpretation as

to the *meaning* of the models differ.

4. Stronger than Item 3, *only* the choice of oscillator-component radial profile distinguishes, operationally, between the multiple-oscillator models. We discovered this by means of our formulation of the general multiple-oscillator equations.

5. It is possible, starting from the coupled covariant Vlasov and Maxwell equations, to construct a fluid moment hierarchy. Truncating the hierarchy at third order, by means of a third order cumulant discard, a series of four *natural* approximations strips away all but a beamlike character from the system. A fully self-consistent set of 8 coupled, nonlinear partial differential equations describing a relativistic, fluid electron beam propagating in resistive plasma results.

6. Apparently, the fluid and adiabatic theories disagree as to the physical condition under which a beam is isothermal $P_{rr} = P_{\theta\theta}$ in the transverse plane. The fluid model predicts a Bennett profile, while the adiabatic model predicts a uniform profile.

7. Low frequency linear hose instability results in a nonaxisymmetric pinch potential which couples the circular-drift and vortex-gyration oscillators. The coupling of these oscillators results in coupling resonances. Modification of the transverse adiabatic action invariant (diffusion in action-space) results. Using methods of KAM theory we have determined that the action invariant upon which adiabatic beam theory is built holds up quite well for

lateral displacements of the order $\delta y/d \sim 10^{-6} - 10^{-4}$ typically considered in linear theory. We view this as justification for the adiabatic theory in the linear regime.

8. In the nonlinear regime, adiabatic theory will not work.

During the course of our work we have come upon several areas which could yield interesting results, pending further work:

1. The elliptical-helix beam undergoing hose instability: A calculation of the perturbed current including orbit perturbation effects would be quite interesting. Also, the resulting eigenvalue problem should be compared with numerical results of the multicomponent model, which also deals with the elliptical-helix beam.

2. It was never our intention to numerically implement the fluid or adiabatic models, however, there is no gainsaying that such a program is advisable. The systems of equations we have carefully derived and motivated form the basis for rigorous numerical investigations of beam propagation over long distances.

3. It would be instructive to extend the low-frequency results concerning the modification of the transverse invariant, to higher hose frequencies. This would result in a time dependent Hamiltonian system of 5/2 degrees of freedom. KAM theory is capable of dealing with such a nonautonomous case.